Electrochemical Society

Ottawa Meeting Program Issue

Quiet, please—skill at work!

The quiet efficiency of a skillfully operated cell room has the rewarding effect of extra returns.

The technical know-how of the man on the job contributes greatly to a profitable operation. Equally important is the superior performance of **GLC anodes,** which are "custom-made" to individual cell requirements.

FREE – *This illustration of anode adjustment has been handsomely reproduced with no advertising text. We will be pleased to send you one of these reproductions with our compliments. Simply write to Dept. J-8.*

ELECTRODE
GLC
DIVISION

GREAT LAKES CARBON CORPORATION

18 EAST 48TH STREET, NEW YORK 17, N.Y. OFFICES IN PRINCIPAL CITIES

EDITORIAL STAFF

R. J. McKay, Chairman, Publication Committee

Cecil V. King, Editor

Norman Hackerman, Technical Editor

Ruth G. Sterns, Managing Editor

U. B. Thomas, News Editor

H. W. Salzberg, Book Review Editor

Natalie Michalski, Assistant Editor

DIVISIONAL EDITORS

W. C. Vosburgh, Battery

Milton Stern, Corrosion, I

R. T. Foley, Corrosion, II

T. C. Callinan, Electric Insulation

Abner Brenner, Electrodeposition

H. C. Froelich, Electronics

D. H. Baird, Electronics—Semiconductors

Sherlock Swann, Jr., Electro-Organic, I

Stanley Wawzonek, Electro-Organic, II

John M. Blocher, Jr., Electrothermics and Metallurgy, I

A. U. Seybolt, Electrothermics and Metallurgy, II

W. C. Gardiner, Industrial Electrolytic

C. W. Tobias, Theoretical Electrochemistry, I

A. J. de Bethune, Theoretical Electrochemistry, II

REGIONAL EDITORS

Howard T. Francis, Chicago

Joseph Schulein, Pacific Northwest

J. C. Schumacher, Los Angeles

G. W. Heise, Cleveland

G. H. Fetterley, Niagara Falls

Oliver Osborn, Houston

Earl A. Gulbransen, Pittsburgh

A. C. Holm, Canada

J. W. Cuthbertson, Great Britain

T. L. Rama Char, India

ADVERTISING OFFICE

ECS
1860 Broadway, New York 23, N. Y.

ECS OFFICERS

Sherlock Swann, Jr., President
University of Illinois, Urbana, Ill.

W. C. Gardiner, Vice-President
Olin Mathieson Chemical Corp., Niagara Falls, N. Y.

R. A. Schaefer, Vice-President
Cleveland Graphite Bronze Div., Clevite Corp., Cleveland, Ohio

Henry B. Linford, Vice-President and Interim Secretary
Columbia University, New York, N. Y.

Lyle I. Gilbertson, Treasurer
Air Reduction Co., Murray Hill, N. J.

Robert K. Shannon, Executive Secretary
National Headquarters, The ECS, 1860 Broadway, New York 23, N. Y.

Journal of the Electrochemical Society

AUGUST 1958 **VOL. 105 • NO. 8**

CONTENTS

Editorial

Good Campers. *W. C. Gardiner* 143C

Technical Papers

A New Zinc-Iodate Primary Battery. *J. L. Jones and A. B. Arranaga* 435

Halogen-Activated Solid Electrolyte Cell. *J. L. Weininger* 439

The Microtopography of Oxide Films on Niobium. *J. V. Cathcart, J. J. Campbell, and G. P. Smith* 442

Higher Oxides of Silver. *W. S. Graff and H. H. Stadelmaier* 446

Protection of Molybdenum from Oxidation at Elevated Temperatures. *D. E. Couch, H. Shapiro, J. K. Taylor, and A. Brenner* 450

Temperature Dependence of Fluorescence of Tin-Activated Orthophosphates. *R. W. Mooney* 456

Electron Traps and the Electroluminescence Brightness and Brightness Waveform. *F. F. Morehead, Jr.* 461

Selective Electrolytic Etching of Germanium and Silicon Junction Transistor Structures. *I. A. Lesk and R. E. Gonzalez* 469

Preparation and Identification of the Thorium Germanides. *A. G. Tharp, A. W. Searcy, and H. Nowotny* 473

The Mobilities of the Ions in Fused KNO_3-$AgNO_3$ Mixtures. *F. R. Duke and B. Owens* 476

Mechanism of Anode Thermal Reaction in Aluminum Reduction Cells. *H. Stern and G. T. Holmes* 478

Technical Notes

The Effect of Gamma Irradiation on the Potential Behavior of Platinum and Stainless Steel Electrodes. *W. E. Clark* 483

The Use of Nickel-Aluminum Alloy Coatings for the Protection of Molybdenum from Oxidation. *D. E. Couch, H. Shapiro, and A. Brenner* 485

Current Affairs

Complete Ottawa Meeting Program 145C
Candidates for Society Offices 171C
William J. Kroll Chosen Acheson Medalist 174C
Division News 173C
News Items 174C
New Members 176C
ECS Membership Statistics 176C
Section News 177C
Personals 177C
Letters to the Editor 179C
Employment Situation 179C
ECS Future Meeting Dates 170C

Published monthly by The Electrochemical Society, Inc., from Manchester, N. H., **Executive Offices, Editorial Office** and **Circulation Dept.,** and **Advertising Office** at 1860 Broadway, New York 23, N. Y., combining the JOURNAL and TRANSACTIONS OF THE ELECTROCHEMICAL SOCIETY. Statements and opinions given in articles and papers in the JOURNAL OF THE ELECTROCHEMICAL SOCIETY are those of the contributors, and The Electrochemical Society assumes no responsibility for them. Nondeductible subscription to members $5.00; subscription to nonmembers $18.00. Single copies $1.25 to members, $1.75 to nonmembers.

Copyright 1958 by The Electrochemical Society, Inc.

Entered as second-class matter at the Post Office at Manchester, N. H., under the act of August 24, 1912.

NOW!

AUTOMATIC Spectrophotometric and Electrometric Titrations with the

NEW SARGENT-MALMSTADT AUTOMATIC SPECTRO-ELECTRO TITRATOR

Designed and manufactured by
E. H. SARGENT & CO.
Patents Pending

S-29700 Spectro-Electrometric Titration Apparatus—Model SE, SARGENT-MALMSTADT.....$690.00

For SPECTROPHOTOMETRIC TITRATIONS

Provides direct automation of most titrations now being performed which inherently or in conjunction with an indicator provide a spectrophotometric end point. These include acid-base, oxidation-reduction, complex formation and some precipitation reactions, indicators being available for most of the titrations currently performed by manual methods.

For ELECTROMETRIC TITRATIONS

Provides new and better facilities to perform automatic derivative potentiometric titrations as performed by the S-29690 SARGENT-MALMSTADT potentiometric titrator. Provision is made for the convenient connection of simple circuits for constant current potentiometric, "polarized electrode " and similar titrations.

For complete information contact your nearest Sargent Division or write: Dept. SE, Chicago, Illinois

SARGENT *SCIENTIFIC LABORATORY INSTRUMENTS • APPARATUS • SUPPLIES • CHEMICALS*

E. H. SARGENT CO., 4647 W. FOSTER, CHICAGO 30, ILL.
DETROIT 4, MICHIGAN • DALLAS 35, TEXAS • BIRMINGHAM 4, ALA.

Editorial

Good Campers

WE *HOPE* that President Sherlock Swann is back to normal health again and able to assume the presidential duties before this appears in print. Meanwhile, we carry on as Acting President and will do our best with the able assistance and momentum of the organization. We learned early in life that no man is indispensable. Life must go on! The better the organization, the better is it able to carry on if, or when, an individual must be absent.

However, we cannot disregard the character given to an organization by an individual. One of our hobbies is camping and we always appreciate the thoughtfulness of the good camper ahead of us. He would leave some ready firewood and improve the campsite a little. We took office with much of the preliminary work done by our predecessor so that the initial shock was not too great. We hope that we can make our contribution toward building a stronger Society.

The Society has never been in a sounder position. The Treasurer has been able to report that the Society Reserve Fund is building up faster than planned. This is due partly to operating economies and partly to increased income from members. It is hoped that the present economic trend will not endanger our financial position. At this time, there is no indication that it will, possibly due to the popular concern over the need for science and engineering in our country. The increasing attendance at our conventions and an increase of eleven per cent in our membership last year are measures of the soundness of our Society and an indication that we are fulfilling a useful purpose in the scientific community.

The founding and growth of the Theoretical Electrochemistry Division insures the growth of electrochemistry from the "grass roots." Stimulation of theoretical electrochemistry is the best insurance for the future of applied electrochemistry. We are pleased to note that foreign scientists are happy to contribute to the symposia of the Theoretical Division, and many of our members have been able to participate in foreign scientific congresses.

This issue of the JOURNAL contains the complete program for our Fall Meeting to be held in Ottawa, Canada, September 28th to October 2nd. The various Divisions of our Society, as you will see, have arranged an exceptionally fine program of papers.

John Convey, General Chairman of our Ottawa Meeting Committee, and his associates have scheduled a splendid program of events which we know will be thoroughly enjoyed by the members and guests who will attend this meeting. Special attention has been devoted to entertaining the ladies and we are sure that they, too, will have an enjoyable time.

Ottawa, being the national capital of Canada, offers you the opportunity of viewing many outstanding tourist attractions. We know that your attendance at this meeting will be a memorable experience for you.

—W. C. GARDINER

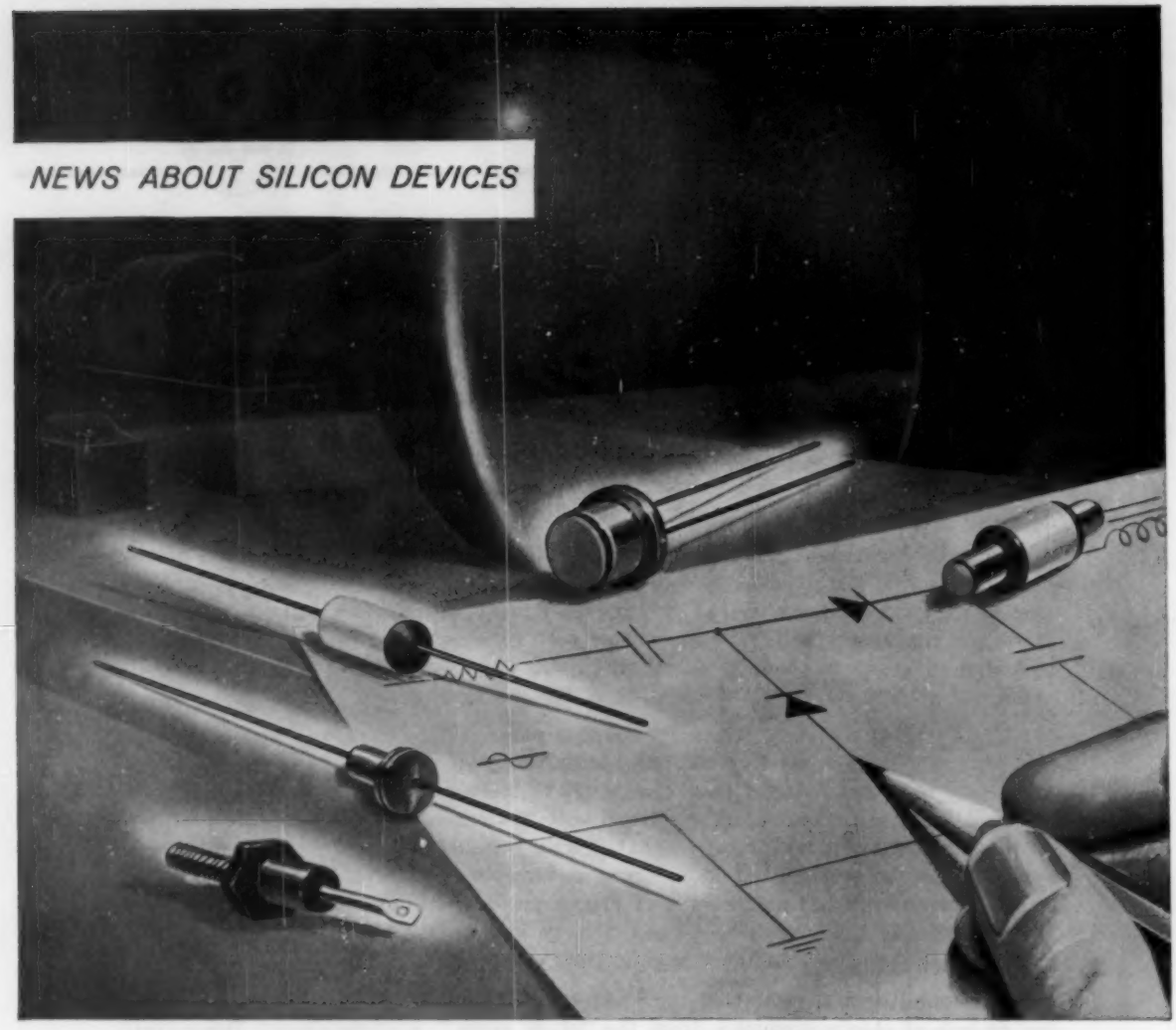

Reverse current: 10^{-7} amp. Rectification ratio: 10,000,000:1

Now... new efficiency for TV power supplies with dependable diodes of Du Pont Hyperpure Silicon

More efficient power supplies . . . savings in space and weight . . . important reasons why TV manufacturers are replacing conventional rectifying systems with silicon diodes. Today, several types of silicon diodes and rectifiers are readily available for TV circuits. TV manufacturers have tested silicon rectifiers and report no noticeable change in output voltage under continuous load conditions over long periods of time. Silicon components can operate in ambients from −65° to 150° C. They maintain excellent electrical stability and resist aging.

Silicon components have high shock and vibration limits. They are up to 99% efficient in units operated at 60 cps. and require little maintenance. Silicon cells permit a rectification ratio as high as 10 million to 1—almost negligible reverse conductance. Silicon bridges are available with ratings from 1 to 1,000 amperes and more than 600 volts rms.

Note to device manufacturers: You can produce silicon transistors, rectifiers and diodes of the highest quality with Du Pont Hyperpure Silicon. It's now available in three grades for maximum efficiency and ease of use . . . with a purity range of 3 to 11 atoms of boron per billion. Technical information on crystal growing is available from Du Pont . . . pioneer producer of semiconductor-grade silicon.

NEW BOOKLET ON DU PONT HYPERPURE SILICON

You'll find our new, illustrated booklet about Hyperpure Silicon helpful and interesting—it describes the manufacture, properties and uses of Du Pont Hyperpure Silicon. Just drop us a card for your copy. E. I. du Pont de Nemours & Co. (Inc.), Pigments Department, Silicon Development Group, Wilmington 98, Delaware. (This offer limited to United States and Canada.)

PIGMENTS DEPARTMENT

DU PONT HYPERPURE SILICON

BETTER THINGS FOR BETTER LIVING
. . . THROUGH CHEMISTRY

A New Zinc-Iodate Primary Battery

J. L. Jones and A. B. Arranaga

U. S. Naval Ordnance Test Station, Pasadena Annex, Pasadena, California

ABSTRACT

A new primary battery has been developed comprising a zinc anode, a potassium iodate cathodic reactant, and an electrolyte consisting substantially of sulfuric acid. A reserve battery of this type is capable of comparatively high current drain rates, typically 0.092 amp/cm^2 (0.6 amp/in.^{2}) at a discharge potential of 1.6 v for 7 min. A typically self-contained battery capable of operating at the above performance level has an energy output of 2.32 watt min/cm^3 and watt min/g output of 1.88. Procedures have been developed for manufacturing low cost cells in a simplified type of mechanical battery construction. Prototype batteries have been constructed and experimental data are given on their performance.

An experimental program has been carried out at the U. S. Naval Ordnance Test Station to develop new high drain rate primary batteries for ordnance applications. As a result of this investigation, a new electrochemical couple has been developed to a practical stage for primary battery application.

The couple consists of potassium iodate as the cathodic reactant, and zinc metal as the anodic reactant in the presence of sulfuric acid as the electrolyte. Two possible equations for the reaction may be written as follows:

$$5Zn + 2KIO_3 + 6H_2SO_4 \rightarrow 5ZnSO_4 + I_2 + K_2SO_4 + 6H_2O \quad [1]$$

$$3Zn + KIO_3 + 3H_2SO_4 \rightarrow 3ZnSO_4 + KI + 3H_2O \quad [2]$$

The standard half-cell reactions of the zinc anode, reaction [3], and the iodate cathode, reaction [4], as combined below in acid solution yield a standard open cell potential of 1.958 v, reaction [5] (1).

$$Zn \rightarrow Zn^{++} + 2e \qquad E^\circ = 0.763 \text{ v} \quad [3]$$

$$IO_3^- + 6H^+ + 5e \rightarrow 1/2I_2 + 3H_2O \qquad E^\circ = 1.195 \text{ v} \quad [4]$$

$$5Zn + 2IO_3^- + 12H^+ \rightarrow 5Zn^{++} + I_2 + 6H_2O \qquad E^\circ = 1.958 \text{ v} \quad [5]$$

Analytical results on the nature of actual cell reactions clearly indicate that both reactions [1] and [2] occur, reaction [1] being the dominant cell reaction at room temperature and higher, while reaction [2] becomes more important at temperatures down to 0°C. It is interesting to note that the experimental cell develops approximately 1.6 v at high current drains, e.g., 0.092 amp/cm^2 (0.6 amp/in.^{2}) as compared to the standard open-circuit voltage of 1.958 v.

A review of the literature indicates that there has been no systematic cell investigation of the zinc-iodate couple. A passing reference in a British patent of 1884 mentions the use of iodate solutions in galvanic batteries as a depolarizing agent (2). A patent application is pending on the now developed zinc-iodate battery (3).

The battery developed from the above cell reaction has been of interest for ordnance application problems in view of its high available current drain rates for limited periods of time. The zinc-iodate battery, as it has been developed mechanically, is a reserve type of primary battery in which the electrolyte is rapidly forced into the dry cell structure by compressed carbon dioxide gas, aided by a partial vacuum previously created in the dry plate structure.

Early work in this experimental program also applied the bromate ion as a cathodic reactant. Cells containing bromate ion cathodes tended to yield cell voltage vs. discharge time curves considerably less flat than cells utilizing the iodate cathodes. Bromate and iodate cathodes produced cells capable of discharging at comparable current density; however, the bromate cells tended to produce more hydrogen gas. As a result of the deficiencies of the bromate cathode as compared to the iodate cathode, a decision was made to develop the iodate cell.

Experimental

The Zinc-Iodate Cell

The basic element in the cell construction is an electrode, approximately 0.10 cm (0.04 in.) thick, which has the following structure: A zinc sheet, 0.020 cm (0.008 in.) thick, is coated on one side with a silver pigmented paint, approximately 0.002 cm (0.0007 in.) thick. Bonded to the silver layer is a cathodic reactant mix in which potassium iodate is the active ingredient, made electrically conducting by the addition of graphite and acetylene black. In principle, the electrodes can be stacked, the anode side of one electrode facing the cathode side of the next electrode, separated by a 0.10 cm (0.04 in.) gasket and round spacers to provide room for the electrolyte (*see* Fig. 1). The battery is activated and made electrically conducting by introducing the electrolyte rapidly into the dry cell plate structure of the battery. All of the experimental program has been designed to produce a cell capable of discharging within a second or less at high drain rate after introducing the electrolyte.

Fig 1. Exploded view of eleven-cell battery

The cathode dry mixture consists of the following [for 645 cm² (100 in.²) surface]:

	Grams	Per cent
Potassium iodate (−120 mesh)	29.5	57.1
Graphite (Acheson No. 38)	21.1	40.8
Acetylene black, 50% compression	1.1	2.1
	51.7	100.0

The dry mixture was blended for 1 hr in a rotary mixer and then blended for approximately 5 min with a prescribed amount of polyvinyl acetate binder. In a typical cell construction, the thickness of the cathodic reactant [0.080 cm (1/32 in.)] thick was easily regulated by cementing on a rubber gasket of the proper thickness to the periphery of the zinc sheet (Fig. 1), providing an interior area which was covered with the pasty cathode mix to the top level of the gasket. After air drying for ½ hr, the wet cathode was baked for 1 hr at 105°C. The proportion of dry cathode mix ingredients of graphite and acetylene black were arrived at experimentally to provide a mixture of proper electrical conductivity for the cathode plate structure. The function of the silver surface coating is to provide an electrically conducting layer which physically and chemically separates the zinc anode and the potassium iodate cathode and prevents their direct reaction in the presence of the sulfuric acid electrolyte. The electrolyte volume was provided by cementing typically 0.119 cm (3/64 in.) thick neoprene rubber gaskets and spacers to the clear zinc surface of the electrode.

The dry plate structure of a battery was simply completed by cementing the zinc anode face of one electrode, fitted with an electrolyte gasket and spacers, to the iodate cathode face of an adjacent electrode. The cell formed was nominally 0.203 cm (0.080 in.) thick. Cell structure thus assembled into packs formed electrical series of cells when filled with electrolyte. The power was withdrawn from tabs on the end plates. The maximum number of cells placed in series to date is 25, but there is no reason the number cannot be much larger.

The electrolyte consisted of 8.0*N* H_2SO_4 + 0.5*N* HCl + 2% $HgCl_2$. It was found that mercuric chloride was very effective in reducing the formation of hydrogen gas to a low level. The use of 0.5*N* HCl in conjunction with 8.0*N* H_2SO_4 increased the voltage of the battery at low temperature, i.e., 0°C.

The Cell Reaction

Cells of the following construction were discharged at various temperatures from 0°-65°C:

Zinc/8*N* H_2SO_4 + 0.5*N* HCl + 3% $HgCl_2$/KIO_3

The cells were discharged at constant external resistance to a 1-v cut-off at current densities of approximately 0.0853 amp/cm² (0.55 amp/in.²). The average voltages produced were approximately 1.5 v, except for the 0° discharge, which produced an average 1.16 v.

The spent electrolyte was removed and saved and the cell rinsed thoroughly with distilled water. The electrolyte with rinsings was analyzed for total hydrogen ion, iodine, iodide ion, chloride ion, and zinc ion. A 1.3 × 15 cm (½ × 6-in.) strip was cut vertically from the center portion of the cathode [originally 15 × 15 cm (6 × 6 in.)] and the cathode material scraped from the zinc and extracted with water. The extract and rinsings were analyzed for iodine and iodate.

In both the electrolyte and cathode analyses, iodine was extracted with carbon tetrachloride and determined by titration with standard sodium thiosulfate. To determine the quantity of iodate present, an aliquot portion of the solution obtained in the cathode extractions was treated with an excess of KI and titrated with standard sodium thiosulfate.

The total activity was measured potentiometrically by titration with standard sodium hydroxide solution.

Iodide and chloride were analyzed together volumetrically and gravimetrically by precipitation with silver nitrate. In the volumetric analysis an excess of standard silver nitrate was added and the excess back-titrated with standard potassium thiocyanate solution. The results of the volumetric and gravimetric analyses were expressed in the form of two equations which were solved simultaneously for the quantities of the halides.

Zinc was determined gravimetrically by treatment of aliquot portions of the spent electrolyte with diammonium hydrogen phosphate and weighing as the pyrophosphate.

According to Table I less that 10% of the zinc consumed entered into side reactions. This indicates that the predominant side reactions do not involve zinc.

The values in Table I indicate that, except for the 0° discharge, the unused acid remaining after the discharge was 16-29% of the original. The 46.1% acid remaining at 0° is indicative of the slowness of the cell reaction at this temperature. The hydrogen ion consumed in side reactions varied between 14-41%, depending on which current-producing reaction is postulated, being greater at 40°, 55°, and 65° than at 26° and 0°C.

The results in Table I show that, except for the 0° discharge, the amount of potassium iodate remaining unreacted in the cell was 14-29% of the original amount. All cells were discharged to the 1-v end point. In the 0° discharge the unreacted iodate was approximately one-half of the original. The percentage of potassium iodate consumed in the production of current also represents the electrical efficiency of the cell. The efficiency is greatest at room temperature (26°C), and becomes less as the ambient temperature rises toward 65°C, or falls toward 0°C. The

Table I. Distribution of reactant consumption
(Per cent of original cell reactants)

Exp.	Temp, °C	Zn consumed in side reaction	Reaction [1]		Reaction [2]		Unreacted KIO_3 in cathode	KIO_3 used in producing current	KIO_3 unaccounted for
			H^+ used in cell react.	H^+ used in side react.	H^+ used in cell react.	H^+ used in side react.			
1	65		45.5	32.9	37.9	40.5	14.3	38.4	47.3
2	55	9.7	55.0	28.4	45.8	37.6	25.8	40.6	33.6
3	40	5.5	51.8	19.5	43.1	28.2	23.5	40.6	35.9
4	26		60.1	14.9	50.0	25.0	29.0	57.6	13.4
5	0	5.1	39.9	14.0	33.2	20.6	51.5	36.1	12.4

tendency of the cathodic reactant to engage in side reactions increases as the temperature rises. The most favorable ambient temperature for discharge appears to be about 26°C.

From Table I the quantity of potassium iodate unreacted in the cell discharge is known, and this value subtracted from the amount originally present gives the amount of potassium iodate consumed. The quantity of potassium iodate consumed may also be calculated from the iodide and iodine found by chemical analysis, provided the recovery is 100%.

Iodide ion and iodine were probably partially unrecovered for several reasons. Mercuric chloride, present in the electrolyte, can react with iodide or iodine.

Although the quantities of iodine and iodide recovered in the chemical analyses did not approach the theoretical values, the quantities of iodine determined were fairly consistent with each other at the various temperatures. However, the values for iodide ion at 0° and 26°C were considerably greater than those at the higher discharge temperatures. This seems to indicate that at the lower temperatures the current-producing reaction tends more toward the formation of iodide ion rather than iodine, that is, Eq. [2] rather than Eq. [1].

Power Output of the Cell

The power output of the cell is shown in Fig. 2, which illustrates a typical discharge for a 232 cm^2 (36 $in.^2$) cell. The zinc-iodate cell had a typical current density of 0.104 amp/cm^2 (0.67 amp/$in.^2$); however, current densities as high as 0.155 amp/cm^2 (1.0 amp/$in.^2$) could be obtained for short periods of time. The flat voltage characteristics of the cell discharge is particularly desirable for operation of electronic equipment. For design purposes in testing the cell, power was usually withdrawn from the cell until there was a 15% voltage drop.

Although the development work was directed primarily toward high discharge rates for short intervals of time, sufficient information was gathered to indicate that the battery is probably capable of discharging over periods of several hours. Figure 3 illustrates the typically developed cell voltage as a function of current density for varying discharge periods of time. As would be expected, the average cell voltage is higher for the longer discharge time. In these cells the zinc anode was 0.013 cm (0.005 in.) thick and the iodate cathode was 0.080 cm (1/32 in.) thick. The electrode spacing for the electrolyte is as indicated in Fig. 3.

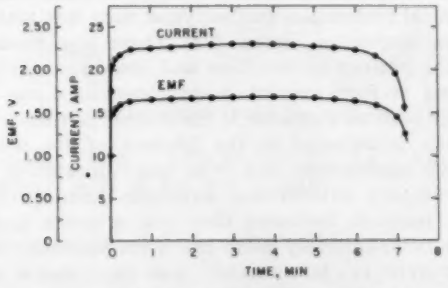

Fig. 2. Discharge of zinc-iodate cell at 28°C

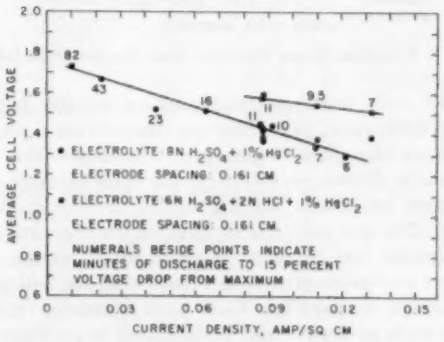
AVERAGE CELL VOLTAGE
CURRENT DENSITY, AMP/SQ. CM
ELECTROLYTE 8N H_2SO_4 + 1% $HgCl_2$
ELECTRODE SPACING: 0.161 CM.
ELECTROLYTE 6N H_2SO_4 + 2N HCl + 1% $HgCl_2$
ELECTRODE SPACING: 0.161 CM.
NUMERALS BESIDE POINTS INDICATE MINUTES OF DISCHARGE TO 15 PERCENT VOLTAGE DROP FROM MAXIMUM

Fig. 3. Cell voltage vs. current density

A Prototype Battery

A zinc-iodate primary battery for a military application was designed to the following specifications:

Average emf, v	26.5 ± 1
Average current, amp	135 ± 2
Discharge time, min	8
Weight, kg	14.1 (31 lb)
Length, cm	27.2 (10.7 in.)
Diameter, cm	23.1 (9.1 in.)

The battery consists of a dry-plate section (Fig. 4, lower) and an electrolyte chamber (Fig. 4, upper). The battery case is made of 0.025 cm (0.010 in.) steel sheet. The electrolyte, consisting of 8*N* H_2SO_4 + 0.5*N* HCl + 2% $HgCl_2$, is contained in a rubber bag. The dry-plate structure is housed in an electrically insulated and vacuum-sealed container. The power terminals are located beneath the plate structure and are brought out of the case through glass-insulated connectors. The electrolyte bag is connected to the lower half of the battery through an assembly consisting of an acid-resistant fitting, an O-ring seal, and a plastic diaphragm which is in-

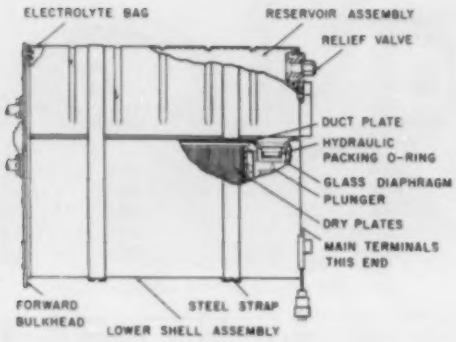

Fig. 4. Partial sectional elevation view of a prototype battery

tegral with the evacuated section of the battery. Upon activation, gas under pressure forces a plunger to break the glass diaphragm, whereupon the electrolyte is drawn rapidly into the cells through a set of ducts located at the top of the cells. Simultaneously, CO_2 gas pressure is exerted on the outside of the rubber bag to assist in rapid filling of the cells.

The dry-plate structure consists of six cell packs connected in parallel. Each pack consists, in turn, of 17 cells in series, and is designed to produce 22.5 amp at 26.5 v. A pack is fabricated as a unit by first assembling the cell bipole plates, using rubber O-ring stock for spacing and insulation purposes, then potting the assembly with resin. The top is left open. Six packs are potted together in a mold to form a block and the duct plate is cemented to the open side of the cell block. Next, the bus bars are attached to the bottom of the cell block and the whole assembly inserted into the battery case. Remaining operations consist of attaching fittings, filling dead space with resin, sealing the can, and attaching heating units and the electrolyte section. The electrolyte bag is filled in the field just before field-check of the torpedo.

A feature not incorporated in the design of the battery was a means which has been devised for leveling the electrolyte in a cell pack should some of the cells not fill completely. However, there is at present no reason to believe that the cells will not fill completely. A slight excess of electrolyte will insure this fact. Figure 5 shows a typical battery discharge of the construction illustrated in Fig. 4. A well-constructed battery of the type described discharged for 7.3 min to a 23-v end point. The average potential of the discharge was 26.9 v and the average current was 134.2 amp. These values compare favorably with the specification requirement for a

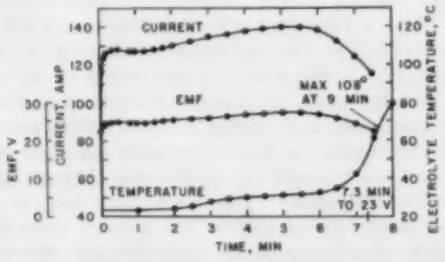

Fig. 5. Discharge of a zinc-iodate battery

potential of 26.5 ± 1 v and a current of 135 ± 2 amp. The discharge time of the battery favorably approached the 8-min discharge time design limit. The activation time of the battery was 2.1 sec to a rising transient 20-v discharge potential under load, well within the specification requirements of 5 sec. It is expected that some further improvement can be made in the performance of the battery by further changes in design.

Discussion

A typical type of battery design has been illustrated in the previous discussion, being cylindrical in general configuration. There is little doubt that this battery can be constructed inexpensively in a variety of sizes and shapes to meet varying military and commercial requirements. The mechanical design of the battery can be made far more flexible than the typical rectangular shape of commercial batteries. The rapid activation time under load of the battery is another distinct advantage, being of the magnitude of 1-2 sec, to a voltage approximating the working level. The battery is of the primary type and was designed for high-current drain applications. A typical reserve battery of this type is capable of producing a discharge potential of 1.6 v, for 7 min, at a current drain rate of 0.092 amp/cm^2 (0.6 amp/in.^{2}). A self-contained battery of this type, operated at the above performance level, has an energy output of 2.32 watt min/cm^3 and a watt min/g output of 1.88. The battery has been operated at current drains of as high as 0.140 amp/cm^2 (0.9 amp/in.^{2}). Considering a single cell structure alone, composed of a zinc anode, a typical iodate cathode (without a zinc sheet backing), and sulfuric acid electrolyte, the energy output of a single cell without auxiliary mechanical structures is 5.38 watt min/cm^3 and 2.61 watt min/g for a typical discharge time of 7 min. The inexpensive chemicals used in this battery are important for basic over-all low battery costs. The inexpensive tin can type of mechanical battery construction is also important for rapid manufacture of low-cost batteries.

There are indications that the battery can be adjusted to different environmental temperature conditions by changing the composition of the electrolyte. Sulfuric acid electrolyte is suitable at high temperature applications. Increasing amounts of hydrochloric acid should be added to the electrolyte as the environmental operating temperature drops toward 0°C.

There are, of course, limitations in the applications of the battery. This battery, like other electrochemical systems, is ineffective at very low ambient temperatures, i.e., below 0°C. There is a tendency for the battery to overheat and lose electrolyte by boiling at high current drain rates. In a one-shot device such as a missile, if the discharge time of the battery is adjusted to the lifetime of the desired missile application, this is of less importance. The fragmentary information available from preliminary research indicates that this primary battery has a comparatively short life after activation with electrolyte, i.e., hours rather than days, due to self-discharge.

As far as the writers are aware, this battery represents the first practical demonstration of this electrochemical couple. On this same type of technical basis, the performance of the zinc-bromate couple should also be studied.

Manuscript received Jan. 3, 1958.
Any discussion of this paper will appear in a Discussion Section to be published in the June 1959 JOURNAL.

REFERENCES

1. W. M. Latimer "Oxidation Potentials," Prentice-Hall, Inc., New York (1952).
2. John Rapieff, British Pat. 5922, Jan. 5, 1884.
3. J. L. Jones, U. S. Patent Application, Serial No. 342,761, March 16, 1953.

Halogen-Activated Solid Electrolyte Cell

J. L. Weininger

Research Laboratory, General Electric Company, Schenectady, New York

ABSTRACT

A new type of silver halide solid electrolyte cell consists of a small bead of silver halide with tantalum and silver wires, cathode and anode, respectively. The mechanism of the electrochemical reaction of this cell has been determined. When the cell is exposed to bromine or iodine vapor, it is a promising primary cell for elevated temperatures. With silver iodide as electrolyte, the cell can be recharged several times.

Historically, electrochemical cells with solid electrolytes were first used by Reinhold (1). He studied thermocells as an outgrowth of his work on chemical equilibria between solid salts. Likewise Wagner used solid electrolytes in galvanic cells in his study of the conductance of solids (2). These cells have come into prominence recently because of the development of electronic equipment, such as ion chambers, scintillation counters, or photomultiplier tubes, which requires high voltages and very small currents.

Generally, solid electrolyte cells, as distinguished from cells with liquid electrolytes, have the advantage of simpler construction. By reducing their weight and size, batteries can be miniaturized. Their disadvantage is that the solid electrolyte has a high internal impedance, which results in short-circuit currents or flash currents of the order of a few microamperes at room temperature.

Cells with Silver Halide Electrolytes

The solid electrolytes of the present work are silver halides, because they have relatively large ionic conductivities. Their use in solid-state cells has been described by Lehovec and Broder (3) and van der Grinten (4). The cells developed by van der Grinten consist of the following:

⊕	ELECTROLYTE	⊖
CATHODE	AgBr	ANODE
$CuBr_2 + C$		Ag

The reactions as postulated by van der Grinten are:

Electrode reactions: $CuBr_2 \rightarrow \frac{1}{2}Cu_2Br_2 + \frac{1}{2}Br_2$ $Ag \rightarrow Ag^+ + e^-$
$\frac{1}{2}Br_2 + Ag^+ + e^- \rightarrow AgBr$

Cell reaction: $\frac{1}{2}Br_2 + Ag \rightarrow AgBr$

Over-all reaction: $CuBr_2 + Ag \rightarrow \frac{1}{2}Cu_2Br_2 + AgBr$

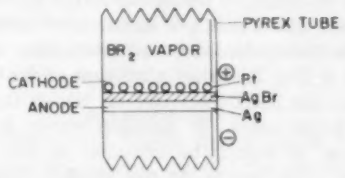

Fig. 1. Basic cell

In this cell it is possible to replace the cathode mix, the source of bromine vapor, with an inert metallic conductor, at which the halogen vapor reacts directly, e.g., in the cell

$$\oplus \text{Pt (or Ta)} + Br_2 / AgBr / Ag \ominus$$

Figure 1 indicates the basic structure of such a cell, which is in the form of a thin disk. A brominated silver foil (anode and electrolyte) is placed against a platinum screen (cathode). A simple stack of these cells could be assembled to form a battery, but firm electrical contact between the silver foil of one cell and the platinum screen of the next would have to be maintained. It is also convenient to use a bimetallic strip of silver and tantalum in which tantalum provides very satisfactory protection from thermal tarnishing of silver as contrasted to the desirable electrochemical consumption of silver in the cell reaction.

Bead Cell

Construction and mechanism.—More recently "bead" cells have been constructed in order to elucidate the mechanism of these solid electrolyte cells. Figure 2 shows the basic structure and explains the name. Beads with diameters ranging in size from 0.075 to 0.15 cm are formed by melting the chemically pure halide in a stream of dry nitrogen. The electrodes are inserted into the solid beads by heat-

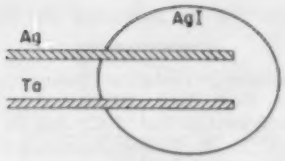

Fig. 2. Halide "bead" cell

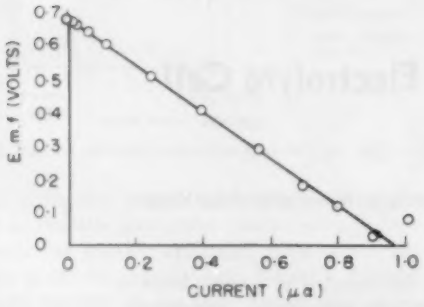

Fig. 3. Current-voltage plot of a silver iodide bead cell at room temperature.

ing the wires (0.012 to 0.05 cm diameter) while they are touching the beads. This melts the electrolyte at the point of entry of the wires only. By continuing this process the wires are submerged substantially in the bead and should be situated side by side as indicated in Fig. 2. Either platinum or tantalum can be used as the inert electrode on which the cathode reaction takes place. If halogen vapor is present, e.g., iodine, it would be reduced at the cathode: $\frac{1}{2}\ I_2 + e^- = I^-$, while, at the anode, silver is oxidized: $Ag = Ag^+ + e^-$. Thus, the over-all cell reaction is the formation of more electrolyte: $Ag + \frac{1}{2}\ I_2 = AgI$. The same cell can be used as a secondary cell in the absence of halogen. The cell is charged by application of an external voltage larger than the decomposition potential of the halide. In the case of silver iodide at room temperature this is 0.685 v. Silver is plated out on the cathode and iodine vapor is produced at the anode. Removal of the externally applied voltage leaves the cell in a charged condition. On discharge, the reaction will be the reverse of the original decomposition reaction.

Bead cell as primary cell.—Figure 3 is a typical current-voltage plot of the silver iodide bead cell at room temperature. The open cell voltage corresponds to the theoretical voltage derived from the thermodynamic free energy of formation of silver iodide. Application of Ohm's law gives an impedance of 700KΩ. The straight line indicates that at room temperature the internal impedance of the cell is so large that the *IR* drop overshadows all other polarization phenomena.

A similar cell was maintained at open cell voltage for 47 days at room temperature. The impedance of this cell increased to about 5MΩ and then remained constant. This is shown by the current-voltage diagrams of Fig. 4. After 50 days the cell broke down because the protruding silver anode had been severely attacked by the iodine vapor. The cell design of Fig. 5 illustrates, however, one method of eliminating the thermal attack on the silver wire.

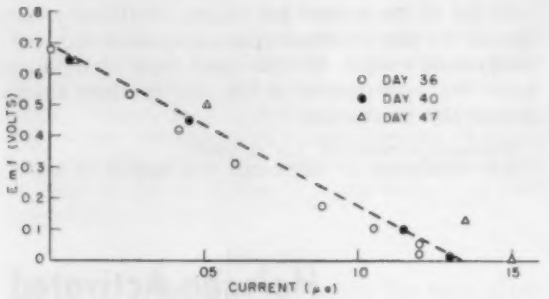

Fig. 4. Current-voltage measurements during life test of a silver iodide bead cell. Cell was stored at 80°C, measured at room temperature.

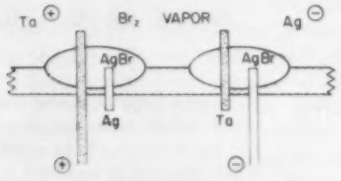

Fig. 5. Series connection of bead cells

In this battery the halogen vapor again activates the tantalum cathode, but it is physically separated from the silver anode by an insulating Pyrex sheet. Individual cells are connected in series as shown. They have very long lifetimes. Thus, one iodine cell retained theoretical voltage at 75°C for one year. Another cell, tested at room temperature with 1 MΩ load, yielded 0.145 coulombs over a period of 32 days.

More favorable results are obtained with bead cells at elevated temperatures because the conductivity of silver iodide increases rapidly with temperature. Figure 6 illustrates the improved cell output with increased temperature. The dashed line is the room temperature long-life behavior of Fig. 4. As the temperature increases, the internal impedance of the electrolyte decreases and correspondingly larger currents are obtained. Whereas at room temperature the cells exhibit only resistance polarization as described above, below 120°C they are subject to another type of polarization, presumably concentration polarization. This, in turn, disappears at 120°C with the first of two phase transformations of AgI. Due to changes of crystal structure at 120° and 145°C the conductivity of silver iodide, which is only slightly larger than those of other silver halides at room temperature, in-

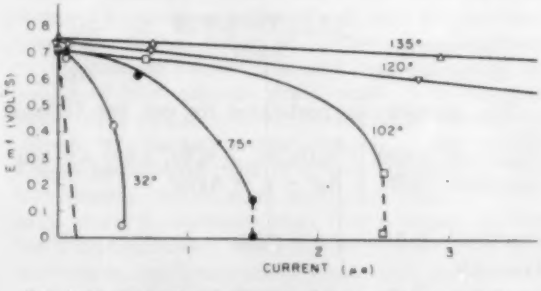

Fig. 6. Current-voltage curves as function of temperature

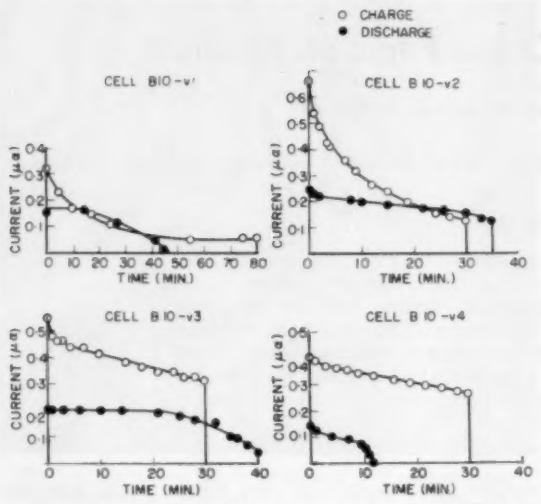

Fig. 7. First charge-discharge cycles of AgI cells at different temperatures and periods of storage. B10-v1, no storage, 73% of charge recovered; B10-v2, B10-v3, and B10-v4 stored 90 min each at −210°, 0°, and 25°C, after which 73, 63, and 15% of charge recovered, respectively. Open circle, charge; solid circle, discharge.

creases very rapidly, first at 120°, from an order of 10^{-6} to 10^{-4} ohm^{-1}-cm^{-1}, then to 1 ohm^{-1}-cm^{-1} at 145° (5,6). In fact, at the melting point, 552°, the conductivity is larger in the solid phase than in the melt. This is explained by the crystal structure, which is cubic in the high temperature alpha-modification (7). The large iodine ions form the big building blocks among which the smaller silver ions move freely. The application of the bead cell to higher temperature, therefore, became obvious. This work is still in progress.

Bead cells as secondary cells.—Bead cells could be charged to the theoretical open cell voltage and discharged several times without deterioration. Better yields were obtained with the iodine system than with the comparable bromine system; data obtained with four identical silver iodide cells in their first cycle are shown in Fig. 7. The cells were charged and discharged at 0°C. Duration and temperature of storage, before discharge, was varied. Charge was best retained at the lowest temperature and is lost on storage at room temperature.

These observations are consistent with the hypothesis that diffusion of iodine to the surface of the electrolyte bead determines the loss of charges in the bead. However, the published diffusion data indicate that anion diffusion through the ionic lattice is very slow. Thus, Teltow (8) estimates a diffusion coefficient of bromine in silver bromide of the order of 10^{-20} cm^2/sec at 20°C. This implies that the anions are immobile because the diffusion path per day would be less than one lattice parameter. Jordan and Pochon (9) have given an upper limit of 10^{-13} cm^2/sec for the diffusion coefficient of iodine at 20°C in either of the two modifications of silver iodide that are stable at room temperature. This would also be too slow to account for loss of charge in the present experiments. But the magnitude of diffusion clearly depends on the structure of the halide. By analogy, in the case of conductivity of silver bromide it is known that in single crystals in the absence of bromine the conductivity is electronic (10), but when the pure single crystal is exposed to bromine, or dislocations are introduced, silver ion conduction will completely account for charge transport. In the present cells the diffusion path of iodine to the surface of the electrolyte is open to speculation. It may be along dislocations at grain boundaries or gross faults in the bead; or, since about 0.5 μg of iodine is formed in charging the bead cell, it has been suggested (11) that solid iodine is produced at the cathode to a thickness of about 100 atomic layers, and that in the process of depositing iodine some free space develops at the cathode. Thus, an alternative diffusion path lies along the tantalum wire cathode. No explanation is offered why only 73% charge was recovered with zero storage time. Although some energy losses in overcoming cell impedance and in the cathode reaction are feasible the possibility of submicroscopic leaks seems more likely. As in the discussion of diffusion paths this again emphasizes the importance of the solid electrolyte structure.

Acknowledgment

The author would like to thank Dr. W. T. Grubb for valuable discussions during the course of this work.

Manuscript received Dec. 18, 1957. This paper was prepared for delivery before the Buffalo Meeting, Oct. 6-10, 1957.

Any discussion of this paper will appear in a Discussion Section to be published in the June 1959 JOURNAL.

REFERENCES

1. H. Reinhold, *Z. anorg. u. allgem. Chem.*, **171**, 181 (1928); H. Reinhold and A. Blachny, *Z. Elektrochem.*, **39**, 290 (1933).
2. C. Wagner, *Z. physik. Chem.*, **B21**, 25 (1933); *Z. Elektrochem.*, **60**, 4 (1956).
3. K. Lehovec and J. Broder, *This Journal*, **101**, 208 (1954); K. Lehovec, Proc. 10th Annual U.S.A. Signal Corp. R. & D. Conf., Asbury Park, May 1956.
4. W. J. van der Grinten, *This Journal*, **103**, 201C, (1956).
5. C. Tubandt and E. Lorenz, *Z. physik. Chem.*, **87**, 513 (1914).
6. K. H. Lieser, *Z. physik. Chem. (n.F.)*, **9**, 216, 302 (1956).
7. L. W. Strock, *Z. physik. Chem.*, **B25**, 441 (1934).
8. J. Teltow, *Z. Elektrochem.*, **56**, 767 (1952).
9. P. Jordan and M. Pochon, *Helv. Phys. Acta*, **30**, 33 (1957).
10. I. Pfeiffer, K. Hauffe, and W. Jaenicke, *Z. Elektrochem.*, **56**, 728 (1952).
11. A. F. Daniel, Private communications.

The Microtopography of Oxide Films on Niobium

J. V. Cathcart, J. J. Campbell, and G. P. Smith

Metallurgy Division, Oak Ridge National Laboratory, Union Carbide Nuclear Company, Oak Ridge, Tennessee

ABSTRACT

An electron microscopic study of the oxide films formed on niobium permits the apparently anomalous oxidation rate behavior of niobium to be explained in terms of the formation of small, blister-like cracks in the oxide film. An oxidation model, based on the idea that an oxidation process which is maintained by interstitial-anion or anion-vacancy diffusion leads to the generation of stresses in the oxide film, is proposed to account for these results. The observation of similar blister-like cracks in oxide films on tantalum is also reported.

This paper is a report of an electron optical investigation of the microtopography of oxide films formed on niobium at temperatures ranging from 325° to 450°C. It was found that small, blister-like cracks tended to form in the oxide while the film was still relatively thin and that the onset of this blistering could be correlated with an increase in the oxidation rate. A similar phenomenon was observed in oxide films on tantalum.

As a preliminary to the main study, a series of rate measurements was made on niobium at temperatures in the vicinity of 400°C. A typical result is shown in Fig. 1. Characteristically, these oxidation rate curves showed an initial protective stage of oxidation followed by a transition period in which the oxidation rate increased. Finally, a nonprotective stage of oxidation ensued in which the oxidation rate became essentially constant. A manometric technique similar to that used in a previous study of the oxidation of alkali metals (1) was utilized for these rate measurements.

The above results are in general agreement with the data of Inouye (2) and of Gulbransen and Andrew (3). The latter authors reported that protective oxidation continued for at least 7 hr at 375°C. At higher temperatures, however, their rate curves had the same qualitative form as that shown in Fig. 1, the protective stage of oxidation becoming shorter and shorter as the temperature was increased to 500°C. At 600°C and above, Inouye reported the existence of linear rate curves throughout his experiments.

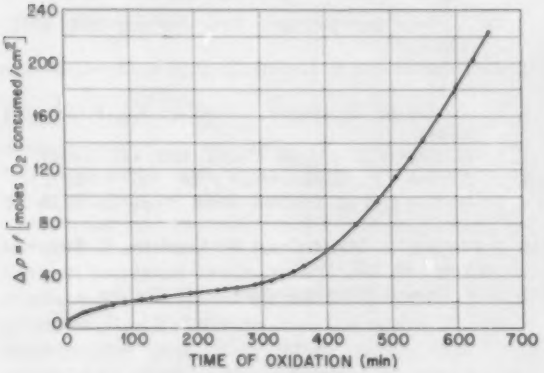

Fig. 1. Oxidation rate curve for niobium at 400°C

Procedure and Results

Electron microscope specimens were prepared from niobium[1] coupons 1 x 2 cm on a side and 0.05 cm thick. The coupons were hand ground through 4/0 emery, polished with 0.3-micron levigated alumina, and electrolytically polished in a 90% H_2SO_4 –10% HF solution. Prior to oxidation the polished specimens were annealed in a Pyrex glass apparatus overnight at the oxidation temperature under a pressure of approximately 10^{-6} mm Hg. All specimens were oxidized in purified O_2 at 1 atm pressure. Carbon replicas, preshadowed with a gold-Manganin alloy, were then made of the surfaces of most of the oxidized specimens, but in a few instances Formvar replicas were prepared.

Several additional specimen pretreatments were also tested. For example, some specimens were mechanically polished only, and these along with electropolished specimens were oxidized both with and without prior vacuum annealing. In a few instances specimens were annealed at 1000°C at a pressure of 1 x 10^{-6} mm Hg before oxidation at 400°C. Speci-

[1] Chemical analysis of Nb specimens: C, 0.007%; Si, 0.10%; Ti, 0.025%; Fe, less than 0.005%; Ta, less than 0.16%; H_2, 0.002%; O_2, 0.010%; N_2, 0.017%.

Fig. 2a. Carbon replica, preshadowed with gold-Manganin, of Nb specimen oxidized for 30 min at 140°C. Magnification 12,000X before reduction for publication.

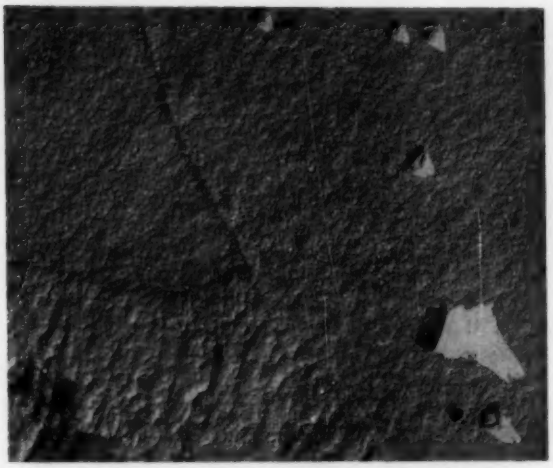

Fig. 2b. Carbon replica, preshadowed with gold-Manganin, of Nb specimen oxidized for 120 min at 400°C. The irregular white area in the lower right hand corner is a tear in the replica produced when the replica was removed from the specimen. Note that the shadowing indicates that a blister had formed at this point in the oxide. Magnification 22,700X before reduction for publication.

Fig. 2c. Formvar replica, shadowed with gold-Manganin, of Nb specimen oxidized for 210 min at 400°C. Magnification 5,000X before reduction for publication.

mens prepared by these different methods all exhibited essentially the same oxidation behavior; however, the method described in the preceding paragraph gave the most consistently reproducible results and, therefore, was adopted as a standard procedure.

The changes in oxide topography as a function of time at a constant oxidation temperature are illustrated in Fig. 2a, b, and c. These electron micrographs show the surface topography of the oxide film after times ranging from 30 to 210 min for oxidation at 400°C. Optical examination of the specimen which had been oxidized for 30 min, corresponding to the protective stage of oxidation, revealed only the presence of the oxide interference colors usually associated with protective oxide films. In the related electron micrograph (Fig. 2a), the oxide film appeared to be essentially smooth and coherent; no cracks could be observed in the film. The most striking feature of the specimen was the variation of oxidation rate with crystal plane as was shown by the different thicknesses of oxide over different grains in the metal.

The 120-min specimen corresponded to the beginning of the transition zone in the oxidation rate curve. Again optical examination showed only interference colors in the oxide film. However, a few blister-like cracks were apparent in the electron micrograph, Fig. 2b, although most of the oxide still appeared to be quite coherent.

The approximate center of the transition zone in the oxidation rate curve was reached with the 210-min specimen. Optical examination of this specimen revealed areas of oxide interference colors interspersed with small rough areas of white oxide. Electron micrographs (*see* Fig. 2c) showed that these white areas were regions of the oxide in which a large increase in blister density had occurred.

When oxidation was continued until the linear portion of the oxidation rate curve had been reached, the entire specimen surface became covered with a rough white oxide. These surfaces were too rough to permit replication, since particles of oxide adhered to the replica. For this reason, the electron optical portion of this study had to be limited to cases where the oxidation of the specimens had not proceeded beyond the approximate center of the transition zone of the rate curves.

The surface topography of the niobium-oxide films also reflected the decrease, reported by Gulbransen and Andrew (3), in the duration of the initial, protective stage of oxidation with increasing temperature. As judged on the basis of blister density, the transition region between the protective and nonprotective stages of oxidation occurred after 10, 60, 240, 480, and 2900 min for oxidation temperatures of 450°, 420°, 400°, 380°, and 350°C, respectively. A typical result from these experiments is illustrated in Fig. 3 which shows the surface topography of the oxide film formed in 480 min at 380°C. At 325°C no blisters were seen in the oxide films in experiments lasting up to 144 hr (*see* Fig. 4).

It was also observed that, as the oxide films thickened, their surfaces tended to become rougher. This phenomenon occurred at all temperatures investi-

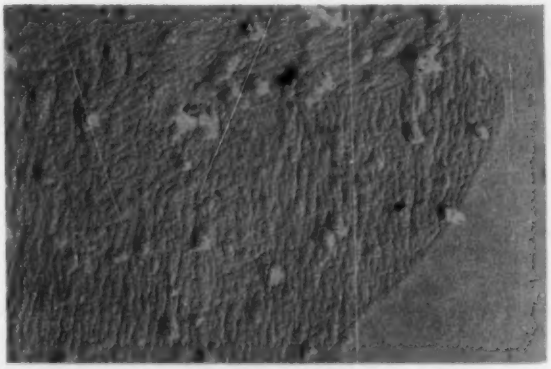

Fig. 3. Carbon replica, preshadowed with gold-Manganin, of Nb specimen oxidized for 480 min at 380°C. Magnification 7,500X before reduction for publication.

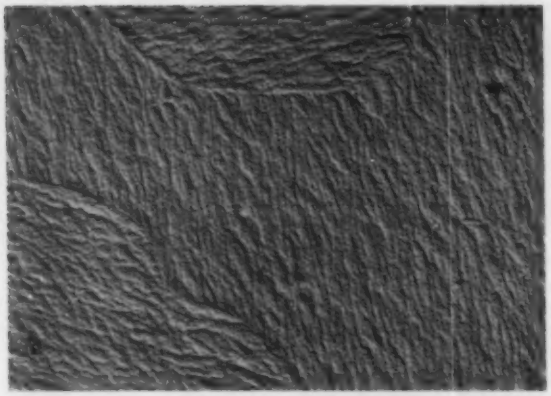

Fig. 4. Carbon replica, preshadowed with gold-Manganin, of Nb specimen oxidized 48 hr at 380°C. Magnification 12,000X before reduction for publication.

gated, but it can be seen most clearly in Fig. 3 and 4. The oxide surface had a "rippled" texture, the direction of the "ripples" varying with crystallographic direction. As discussed below, it is thought that this effect may be related to plastic deformation of the oxide film.

The oxide films formed on niobium were studied both by x-ray and electron diffraction methods. Only the low temperature form of Nb_2O_5 was detected. However, this result does not preclude the presence of one of the lower oxides of niobium, especially if such an oxide were present as a thin layer at the oxide-metal interface.

Discussion

A clear correlation appeared to exist between oxide topography and the oxidation rate curves (cf., Fig. 1 and 2). Both the rate curves and the electron micrographs showed that in the initial stages the oxide film was nonporous and protective. After a period of time which depended inversely on the temperature of oxidation, blister-like cracks formed in the oxide, and the film became less protective. Further increase in blister density produced a corresponding increase in oxidation rate until finally a steady-state condition was attained in which the rate curve was linear. Thus, it is evident that blister formation was related to an increase in the porosity of the oxide film, and in the latter stages where a linear rate curve was observed, the oxidation was either an interface-controlled process or else the rate of oxidation was determined by diffusion across a thin layer of oxide which statistically maintained a constant thickness.

While it is plain that the nonprotective stage of the oxidation of niobium is related to the formation of blister-like cracks in the oxide, the source of the stress which leads to such blister formation is much less obvious. The oxide-to-metal volume ratio for Nb_2O_5/Nb is high (2.7), but it is to be expected that any stresses produced in the oxide on account of its epitaxial misfit with the substrate metal should be confined to a very thin layer at the oxide-metal interface as a result of the formation of an array of dislocations or other lattice defects at this interface. If such be the case, differences in volume of equivalent amounts of oxide and parent metal cannot, *per se*, produce a significant stress in any but the thinnest oxide films.

Blister formation could, perhaps, be accounted for in terms of the recrystallization of the oxide films in accord with the mechanism proposed by Vermilyea (4) to explain crack formation during the early stages of the "field crystallization" of anodically formed, amorphous tantalum oxide films. This mechanism does not, however, appear to explain the continued linearity of the oxidation rate curves for niobium after long periods of oxidation (2), nor does it account for the "rippled surface texture" (*see* above) which developed as the niobium oxide films thickened.

A possible alternative explanation, somewhat similar to that proposed by Jenkins (5) for the oxidation of titanium, of the results observed is provided by a consideration of the diffusion mechanism associated with the oxidation of niobium. A marker experiment was performed in which a fine platinum wire was tied around a 0.25-in. diameter niobium rod, and the rod was oxidized for 4 hr at 450°C. The specimen was then sectioned and examined metallographically. The platinum wire was found at the oxide-gas interface while the oxide-metal interface had receded from the wire, indicating that oxidation has proceeded by either anion-vacancy or anion-interstitial diffusion. This result was consistent with the known electrical properties of Nb_2O_5 (6) and with the fact that thick oxide films on Nb exhibit re-entrant edges and corners (2). It was concluded, therefore, that new oxide was formed at the oxide-metal interface rather than at the oxide-gas interface.

On the basis of this observation, a model for the oxidation of Nb has been devised. The basic assumption made is that cation diffusion within the oxide film is insignificant compared to anion diffusion. It follows then that new oxide must be formed at the oxide-metal interface. When a segment of the metal lattice at this interface is converted to oxide, a three-dimensional expansion of the metal lattice is required to bring the metal ions into their new positions in the oxide. This expansion is resisted by the overlying layer of previously formed oxide and can occur only through the deformation of this layer. Thus, an important conclusion of the above argument is that, in an oxidation reaction where new oxide is formed at the oxide-metal interface, the oxidation process itself continually produces stresses in the oxide film.

The observed increase in surface roughness of the oxide with film thickness may be cited in support of this argument. The surface topography of the niobium-oxide films (*see* especially Fig. 3 and 4) resembles in many respects the type of surface texture which might be expected for a highly deformed film.

Sufficient plastic deformation would, of course, eventually lead to fracturing of the oxide. However, the blister-like nature of the cracks actually observed suggests that the stresses producing them were much more highly localized than the stresses discussed in connection with the plastic deformation of the entire oxide film. The development of a

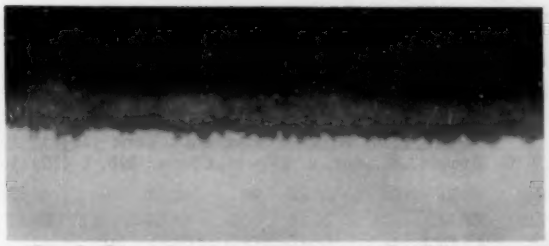

Fig. 5. Edge of a transverse section of a Nb specimen oxidized 4 hr at 400°C. Magnification 2000X.

locally highly stressed region leading ultimately to blister formation can be rationalized in terms of any mechanism which would produce a localized acceleration of oxidation. Such a condition would lead to the formation of a pit in the metal at the metal-oxide interface. Then, because of the volume difference between equivalent amounts of oxide and metal, the oxide produced in forming the pit would exert a substantial force normal to the surface of the oxide film. When the stress so generated exceeded the fracture strength of the oxide, a blister-like crack would form. It should also be noted that, once the surface of the metal becomes pitted, this same mechanism would permit continued crack formation in newly formed oxide. If the breakdown of the new film occurred at different moments at different sites over the specimen surface, the various "rate curves" for each such microscopic area must blend into a straight line, thus accounting for the linear portion of the macroscopic rate curve.

Figure 5 shows an optical micrograph of the edge of a transverse section through a niobium specimen which had been oxidized for 4 hr at 400°C. The white area at the bottom of the photograph is a portion of the unoxidized part of the metal specimen, while a cross section through a heavily blistered region of the oxide film appears as a narrow, slightly irregular band of gray just above the metal. As may be seen, the metal surface under this blistered area was badly pitted, in agreement with the mechanism outlined above.

It is realized that much of the argument presented above is speculative, and the authors regard this oxidation model only as a working hypothesis. It is an hypothesis which has, nevertheless, proved very helpful in suggesting a new approach to the problem of determining the factors which produce non-protective oxide formation on many metals. Thus, the model requires that any metal for which oxidation is maintained primarily by some form of anion diffusion should exhibit a tendency toward non-protective oxidation, especially if its oxide-to-metal volume ratio is significantly different from unity.

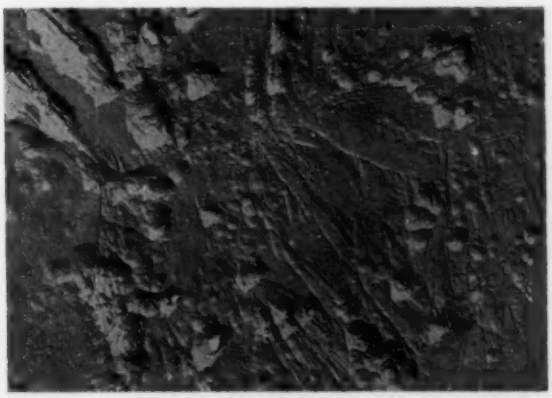

Fig. 6. Carbon replica, preshadowed with gold-Manganin, of Ta specimen oxidized for 4 hr at 500°C. Magnification 7,500X before reduction for publication.

The selection of another oxide-metal system with which to test this postulate is difficult because very little unequivocable information is available concerning the mode of diffusion in metallic oxides. For example, Ta_2O_5 has been shown to contain an excess of metallic ions (7), but it is not known whether this fact is attributable to the presence of interstitial cations on anion vacancies. However, from the point of view of its oxidation rate behavior (8), the structure and composition of its oxides (9), and its general chemical and physical properties, tantalum is similar to niobium. The oxide-to-metal volume ratio for Ta_2O_5/Ta is also large (2.5). Preliminary studies of the microtopography of oxide films on tantalum have shown results in many respects like those observed for niobium oxide. Figure 6 is an electron micrograph of the surface of a tantalum specimen oxidized for 4 hr at 500°C. Blister-like cracks, similar to those observed in niobium oxide, are clearly evident. Thus, it is to be expected that the oxidation mechanisms of the two metals are analogous and involve anion-vacancy diffusion. Moreover, the oxidation results obtained with tantalum appear to be explainable in terms of the oxidation model devised for Nb.

Summary

Previous measurements of the oxidation rates of niobium in a temperature range from about 350° to 500°C indicated that the oxidation process consisted of an initial stage in which protective oxidation occurred, a transition period marked by a gradual increase in the oxidation rate, and finally, a non-protective stage in which the oxidation rate was constant. An electron microscopic study of oxide films on niobium has permitted these rate changes to be correlated with the formation of small, blister-like cracks in the oxide film. An oxidation model, based primarily on the idea that an oxidation process which is maintained by interstitial-anion or anion-vacancy diffusion leads to the generation of stresses in the oxide film, was proposed to explain the experimental results obtained with niobium. The formation of similar blister-like cracks in oxide films on tantalum was cited as an example of a second case explainable in terms of this model.

Acknowledgment

The authors gratefully acknowledge the assistance rendered in this research by E. L. Long and W. H. Bridges of the Electron Microscopy Section of the Metallurgy Division at the Oak Ridge National Laboratory.

Manuscript received Oct. 18, 1957.

Any discussion of this paper will appear in a Discussion Section to be published in the June 1959 JOURNAL.

REFERENCES
1. J. V. Cathcart, L. L. Hall, and G. P. Smith, *Acta Met.*, **5**, 245 (1957).
2. H. Inouye, "Scaling of Niobium in Air," ORNL-1565 (1953).
3. E. A. Gulbransen and K. F. Andrew, To be published.
4. D. A. Vermilyea, *This Journal*, **102**, 207, (1955); *ibid.*, **104**, 537 (1957).
5. A. E. Jenkins, *J. Inst. Met.*, **82**, 215 (1953-54).
6. K. Hauffe, "Oxydation von Metallen und Metallegierungen," pp. 200-204, Springer-Berlin (1956).
7. W. Hartmann, *J. Physik.*, **102**, 709 (1936).
8. W. McKewan and W. M. Fassel, Jr., AECU, 1918; "Corrosion Handbook," H. H. Uhlig, Editor, pp. 720-721, John Wiley & Sons, New York (1948).
9. G. Brauer, *Z. anor. u. allgem. Chem.*, **248**, 1 (1941).

Higher Oxides of Silver

William S. Graff[1]

American Machine & Foundry Company, Raleigh, North Carolina

and

Hans H. Stadelmaier

Department of Engineering Research, North Carolina State College, Raleigh, North Carolina

ABSTRACT

Samples of higher oxides of silver were prepared by several chemical and electrochemical procedures. Two distinct higher oxides were produced. The first, argentic oxide, AgO, is a black powder and has a monoclinic structure for which lattice constants are derived. There is no evidence of the existence of other crystalline forms of AgO. The second oxide, with silver in a valence state higher than plus two, is present in some preparations along with AgO. The stoichiometry was not determined. It is also black and has a face-centered cubic lattice. It decomposed to AgO gradually over a period of months.

The only commonly recognized silver oxide is Ag_2O. Its existence and crystal structure have been definitely established.

The existence of a higher oxide with silver in the plus two state appears to be definitely established (1-10). Silver oxide with silver in the plus two state is sold to the battery industry by Merck and Company under the trade name of "Divasil." The structure of the divalent oxide has not been established conclusively. McMillan (11) reported AgO to be monoclinic and isomorphous with Tenorite (CuO), and he proposed lattice constants based on powder analysis. On the other hand Conn (12) reported that AgO exhibited three crystalline modifications: cubic, face-centered cubic, and orthorhombic.

The existence of even higher oxides of silver, notably Ag_2O_3, has been reported (10, 13-22). The only structure information is that reported by Braekken (23), who claimed that Ag_2O_3 is face-centered cubic and reported lattice constants for preparations from several silver salts. However, this information is clouded by the reports of Zvonkova and Zdanov (24) and Swanson, Fuyat, and Ugrinic (25) who claim that preparations yielding diffraction data indentical with Braekken's are silver peroxynitrate (Ag_2NO_{11}).

Experimental

Samples of higher silver oxides were prepared by the following methods:

1. *Reaction of potassium peroxydisulfate with silver nitrate.*—The procedure essentially duplicates that described by deBoer (18) and Jirsa (20) except that the reaction was carried out between 80°-90°C.

2. *Anodic oxidation of silver perchlorate-perchloric acid solution.*—A spiraled platinum wire anode and cathode were used. The anode was rotated at 60 rpm. A plastic bucket was installed underneath the anode to catch the sample. The cathode was surrounded by a Coors porous porcelain cup to prevent silver from treeing to the anode. Ranges of bath concentrations (from 0.4 to 5.3*N* $AgClO_4$ and from 0.005 to 4.7*N* $HClO_4$), anode current densities (from 0.6 to 185 amp/dm^2), and bath temperatures (from 2° to 28°C) were investigated in an unsuccessful attempt to grow large single crystals. Only fine black powder samples (minus 150 mesh) could be formed. The samples were washed in 25°C water followed by air drying at 55°C for 1 hr. During initial washing the samples gave off some gas with a faint chlorine odor but presumably consisting mainly of adsorbed oxygen.

3. *Anodic oxidation of silver fluoride-hydrofluoric acid solution.*—The apparatus described above was used except that a sheet polyethylene shield was used instead of the Coors cup. The samples contained considerably coarser particles than those formed with the perchlorate bath. The coarsest particles were obtained with a bath concentration of 9.0*N* AgF and 0.75*N* HF, an anode current density of 1 amp/dm^2, and a bath temperature of 29°C. Microscopic examination evidenced a fraction of larger crystals (up to 0.8 mm) with octagonal symmetry plus a fraction of fine black powder. In some cases the larger crystals were joined together to build up dendritic structures. The dendrite branches always formed at 90° to the stem with a fourfold symmetry

[1] Present address: International Business Machines Corporation, Poughkeepsie, New York.

Table I. Argentic oxide samples powder diffraction data

Reaction of $K_2S_2O_8 + AgNO_3$		Anodic oxidation of perchlorate bath		Boiled sample from anodic oxidation nitrate bath		Surface of overcharged silver plaque		Merck & Co. "Divasil"		Accepted values			Observed	Calculated	
2θ	I/I_o	2θ	I/I_o	2θ	I/I_o	2θ	I/I_o	2θ	I/I_o	2θ	d	I/I_o	$\sin^2\theta$†	$\sin^2\theta$†	hkl
30.30°	3	—	—	—	—	30.30°	3	—	—	30.30°	2.950	3	0.0682	0.0681	110
32.15	52	32.30°	80	32.15°	60	32.10	49	32.15°	60	32.15	2.783	65	0.0765	0.0764	200
32.40	100	32.45	100	32.30	100	32.35	100	32.35	100	32.35	2.768	100	0.0775	0.0776	$\bar{1}11$
34.25	34	34.40	41	34.25	31	34.25	46	34.30	35	34.25	2.618	32	0.0866	0.0866	002
37.30	80	37.30	77	37.25	65	37.25	75	37.30	88	37.25	2.414	80	0.1018	0.1020	111
39.55	29	39.60	22	39.45	29	39.50	47	39.50	35	39.50	2.281	32	0.1140	0.1142	$\bar{2}02$
52.55*	10	52.75	8	52.55	6	52.65	9	52.55*	7	52.55*	1.740	8	0.1960	0.1960	020
54.05	19	54.00	21	53.95*	17	54.00	16	53.95*	20	53.95*	1.698	20	0.2058	0.2060	$\bar{3}11$
54.80	11	54.80	8	54.80*	8	54.85	10	54.80*	11	54.80*	1.673	10	0.2118	0.2118	202
56.75*	19	56.80	22	56.80*	16	56.85	21	56.75*	17	56.80*	1.621	18	0.2268	0.2264	$\bar{1}13$
62.95*	11	62.90*	18	62.90*	9	62.90	9	62.95	11	62.90*	1.476	11	0.2722	0.2724	220
63.80*	11	63.60*	16	63.80	7	63.90	11	63.75*	10	63.75*	1.459	12	0.2789	0.2792	311
64.20*	11	64.20*	18	64.20*	8	64.30	8	64.20*	9	64.20*	1.449	9	0.2824	0.2826	022
65.65	4	65.90	11	65.70*	3	———		65.80*	6	65.80*	1.418	7	0.2950	0.2946	$\bar{4}02$
66.40	8	66.40	11	———				66.30*	7	66.35*	1.408	7	0.2994	0.2996	113
67.05	10	67.05	11					67.05*	14	67.05*	1.395	14	0.3050	0.3056	400
67.70	6	67.80	14					67.60*	9	67.65*	1.384	8	0.3099	0.3102	$\bar{2}22$
69.45*	4	69.50*	8					69.50*	3	69.50*	1.351	4	0.3249	0.3252	$\bar{2}04$
72.15	4	———						72.20	4	72.10*	1.309	4	0.3463	0.3464	004
79.50	3							79.40*	4	79.40*	1.206	4	0.4080	0.4078	222
86.50	3							86.40*	3	86.45*	1.125	3	0.4690	0.4696	$\bar{1}31$

Notes:
* Cu $K\alpha_1$ lines. † All positions converted to Cu $K\alpha_1$.

around the stem. The samples were washed in 25°C water followed by air drying at 55°C for 1 hr. During initial washing most samples gave off a small amount of odorless gas, presumably adsorbed oxygen.

4. *Anodic oxidation of silver nitrate-nitric acid solutions.*—The apparatus described in 2 above was used. The electrolyte used for the first preparation was that given by Noyes (10) (1.5*N* $AgNO_3$ and 1.5*N* HNO_3). The largest crystals were obtained with the HNO_3 reduced to 0.75*N*, an anode current density of 0.4 amp/dm², and a bath temperature of 2°C. Samples were washed in 25°C water followed by drying over P_2O_5. Microscopic examination indicated the same type of crystal formations as obtained from the fluoride bath except that the dendritic growth did not have simple 90° symmetry. A portion of one sample was heated in a water bath for 2 hr at 98°-100°C to attempt the decomposition to AgO reported in the literature (1, 2, 10). The sample remained black. Under the microscope, however, it was observed that the once hard single crystals, while still in the same shape, had transformed to fine powder easily broken apart.

5. *Anodic oxidation of porous sintered silver in potassium hydroxide solution.*—Three porous sintered silver plaques were prepared by pasting a mixture of Ag_2O and water on a silver screen and firing in air at 425°C for 20 min followed by pressing. The resultant plaques were 24.2 cm² x 0.61 mm thick and contained 4.15-4.19 g of porous sintered silver. The plaques were anodized in 5% KOH at 0.14 amp for 22 hr. They were then discharged at 25°C in 32% KOH at 1.00 amp to a cut-out at 1.00 v taken against a zinc reference electrode. Recharging followed at 0.10 amp. Two plaques were charged for 16.50 and 15.25 hr to 2.00 v. The third plaque was overcharged for a total of 27.75 hr to a charge voltage of 2.17 v. One of the plaques charged to 2.00 v was discharged again at 27°C in 32% KOH at 0.20 amp and delivered 1.66 amp-hr to a cut-out at 1.00 v. The other two were washed and dried over P_2O_5.

The samples were analyzed for total oxygen and total silver by thermally decomposing the oxide at 480°C to silver and determining oxygen by weight change. Samples were dried to constant weight over P_2O_5. It is to be noted that this procedure does not necessarily constitute a complete and accurate analysis since additional analyses for other possible constituents (e.g., nitrogen or fluorine) were not included.

X-ray diffraction powder patterns and, where possible, single crystal rotation patterns were obtained using nickel filtered copper radiation.

Results and Discussion

Argentic oxide, AgO.—Preparations 1, 2, 4 (after boiling in water for 2 hr), and 5 gave an identical and unique powder diffraction pattern. Merck and Company's "Divasil" also gave the same powder pattern.

No Ag_2O lines were present in any of the patterns. The sintered silver plaque charged to 2.00 v contained some weak silver lines; the plaque charged to 2.17 v evidenced a pure pattern of the oxide.

The relative line intensities for all the samples appear to be in good agreement (*see* Table I). Therefore, it is considered that the pattern is singular and is not a mixture of two or more individual oxides. It is to be noted that three extra trace lines appeared at 19.2°, 29.2°, and 33.7° 2θ for some of the samples. These lines can be accounted for by postulating the

Table II. Higher silver oxide powder diffraction data

Anodic oxidation of fluoride bath			Anodic oxidation of nitrate bath			Swanson, *et al.* (25) data Anodic oxidation of nitrate bath			
Obs. *d*	Calc. *a*	I/I_o	Obs. *d*	Calc. *a*	I/I_o	Obs. *d*	Calc. *a*	I/I_o	Assigned hkl
Å	Å		Å	Å		Å	Å		
5.66	9.80	31	5.70	9.87	10	5.73	9.92	10	111
4.90	9.80	16	4.94	9.88	3	4.96	9.92	6	200
3.47	9.80	25	3.49	9.86	3	3.498	9.894	4	220
2.96	9.80	6	—		—	2.980	9.884	2	311
2.836	9.824	100	2.815	9.890	100	2.856	9.893	100	222
2.457	9.828	80	2.472	9.888	32	2.474	9.896	45	400
2.254	9.825	20	2.27		12	2.270	9.895	12	331
2.19		3	—		—	2.213	9.897	4	420
2.00		3	2.02		3	2.019	9.891	3	422
1.90		2	—		—	1.903	9.888	2	511, 333
1.740	9.843	89	1.747	9.883	30	1.749	9.894	42	440
1.66		5	—		—	1.672	9.892	4	531
1.641	9.846	5	—		—	1.649	9.894	4	600, 442
1.56		2	1.56		1	1.564	9.892	1	620
1.50		1	1.50		5	1.508	9.892	1	533
1.483	9.837	66	1.491	9.900	14	1.491	9.890	37	622
1.42		2				1.428	9.893	15	444
1.378	9.841	6				1.385	9.891	2	711, 551
1.36		3				1.372	9.894	2	640
1.32		2				1.322	9.893	1	642
1.28		2				1.288	9.892	3	731, 553
1.230	9.840	5				1.237	9.896	7	800
1.20		3				1.209	9.896	2	733
1.19		3				—		—	820, 644
1.159	9.834	3				—		—	822, 660
1.13		30				1.1425	9.894	1	751
1.1261	9.817	20				1.1348	9.893	14	662
1.0988	9.837	20				1.1062	9.894	9	840
Av lattice spacing, *a*	9.834±0.009			9.890±0.006			9.893±0.003		

formation of a trace surface film of Ag_2CO_3 during air drying.

It was not possible to index the pattern as tetragonal, hexagonal, or orthorhombic (using the Lipson method). The pattern was indexed by trial and error using the monoclinic structure of Tenorite (CuO) as a starting point. The observed and calculated $\sin^2\theta$ values are compared in Table I. Their agreement is excellent with most differences less than 0.0002 and with no greater difference than 0.0006. The calculated line positions establish the following monoclinic lattice constants for the oxide:

$$a = 5.842\text{Å} \qquad c = 5.487\text{Å}$$
$$b = 3.480\text{Å} \qquad \beta = 107^\circ\ 27'$$

This indexing confirms that of McMillan (11).

The chemical analyses for total oxygen in the samples are as follows: boiled sample from anodic oxidation of nitrate bath, $AgO_{1.00}$; anodic oxidation of perchlorate bath, $AgO_{1.10}$, $AgO_{1.19}$; reaction of $K_2S_2O_8$ and $AgNO_3$, $AgO_{1.00}$; Merck and Co. "Divasil", $AgO_{1.00}$, $AgO_{1.01}$. These results indicate fairly close agreement with the formula AgO. The excess above the stoichiometric ratio could be due to absorbed salts, excess oxygen in the lattice, and/or a small amount of higher silver oxide that did not show up in the diffraction pattern.

This compound has variously been referred to as an oxide and a peroxide. Yost (14) reported that the structure was not a peroxide since it did not give a hydrogen peroxide reaction when dissolved in acid. It can be added to this evidence that the electrical capacity of the charged sintered silver plaque (1.66 amp-hr for 4.17 g of Ag) is equivalent to 80% of the theoretical capacity based on a plus two valence state. Hence, the plus one state is impossible, and the compound cannot be a peroxide. The oxide, therefore, is AgO, argentic oxide, and not Ag_2O_2, silver peroxide, as it has often been referred to in the literature.

Higher silver oxide.—Preparations from the anodic oxidation of the silver fluoride and silver nitrate baths gave powder diffraction patterns that were mixtures of the AgO pattern and another pattern which will be tentatively referred to as a higher silver oxide.

Rotation patterns of the large crystals described above were identical for rotations in three mutually perpendicular axes, thus establishing cubic symmetry. The first and third layer lines were very weak. The extra pattern in the powder samples was then readily indexed as face-centered cubic. Table II summarizes our powder data for this higher oxide. The data is identical with that reported by Braekken (23) for Ag_2O_3, and with that reported by Zvonkova (24) and Swanson (25) for Ag_7NO_{11}.

Three points should now be considered. First, Braekken's work and our work present evidence that the same structure is obtained regardless of the salt contained in the anodizing bath, i.e., whether or not nitrogen compounds are present. Second, the powder diffraction pattern for a sample prepared from the nitrate bath evidenced a small but definite amount of separately crystallized $AgNO_3$. Third, Noyes (10)

established by solubility measurements that a complex of silver oxide and silver nitrate (e.g., Ag_7NO_{11}) existed in solution; however, this should not be considered to establish the fact that the same complex or compound exists after precipitation and drying. Both Zvonkova (24) and Swanson (25) did not perform chemical analysis of their samples, but followed Noyes (10) preparation and assumed his analysis to hold for their precipitates. On the basis of these considerations it is postulated that on formation at the anode, and/or on drying, the anode product is converted to a higher silver oxide, and that in the case of the nitrate bath, as a consequence of the intermediate nitrate complex, a measurable amount of $AgNO_3$ is absorbed.

A series of powder diffraction patterns was obtained for these samples to investigate aging effects. The data are often inconsistent because the large crystal size of the higher oxide fraction presented preferred orientation difficulties. The samples were not ground to a smaller particle size because it was thought that the higher oxide, and possibly AgO, would suffer some decomposition. It can be stated qualitatively that over a five month period of storage at 22°-30°C the higher oxide decomposed to some extent with a resultant increase in AgO. As mentioned above, there was complete decomposition to AgO after 2 hr of heating in water at 98°-100°C. There was no evidence of line shifting in either the higher oxide or the AgO patterns with aging, indicating no range of solid solubility of oxygen in the lattices.

It is now of interest to consider the stoichiometry of this higher oxide. This task is made difficult by the fact that AgO was present in all the samples regardless of variations in bath composition and concentration, temperature, and current density. Jirsa (3) reported the same difficulty. The total oxygen analyses for the preparations ranged between $AgO_{1.32-1.67}$ for aging up to one month, and $AgO_{1.33-1.33}$ for aging between 4½ to 5½ months. Therefore, even though the stoichiometry of the higher oxide cannot be determined, it appears that the silver is in a higher valence state than plus two.

Summary

Argentic oxide, AgO, was prepared by several different procedures resulting in all cases in a black powder that gave a unique powder diffraction pattern. This pattern was indexed to establish monoclinic symmetry and cell dimensions. These results confirm the work of McMillan and tend to reject the possibility that AgO exists in other crystalline modifications. Crystals of AgO suitable for single crystal diffraction studies could not be prepared.

The anodic oxidation of both silver fluoride and silver nitrate baths gave samples that were a mixture of AgO and another substance, sometimes present as fairly large (0.8 mm) single crystals. This other substance has a face-centered cubic lattice with very weak first and third layer lines. It is concluded that the substance is a higher silver oxide with silver in a valence state higher than plus two. Unfortunately the exact stoichiometry could not be determined. The substance is evidently not Ag_7NO_{11} as proposed by other investigators (24, 25) since it can also be prepared from a silver fluoride bath. This oxide decomposes to AgO slowly (longer than five months) at normal temperatures but within 2 hr in 98°-100°C water.

Acknowledgment

One of the authors (W. S. Graff) wishes to thank Professor R. Maddin, Acting Director of the School of Metallurgical Engineering of the University of Pennsylvania, for his guidance and encouragement; Mr. H. F. Bauman, associated at present with Armour Research Foundation, for his advice concerning the chemical preparations; and the Raleigh Laboratory of the American Machine and Foundry Company for making available laboratory facilities for portions of this work.

Manuscript received Sept. 25, 1957. This paper is based on a thesis submitted by W. S. Graff to the Faculty of the School of Metallurgical Engineering of the University of Pennsylvania in partial fulfillment of the requirements for the M.S. degree in metallurgical engineering.

Any discussion of this paper will appear in a Discussion Section to be published in the June 1959 issue of the JOURNAL.

REFERENCES

1. O. Sulc, *Z. anorg. Chem.*, **12**, 89 (1896).
2. E. R. Watson, *J. Chem. Soc.*, **89**, 578 (1906).
3. F. Jirsa, *Chem. Listy*, **19**, 3 (1925).
4. F. Jirsa, *Z. anorg. u. allgem. Chem.*, **158**, 33 (1926).
5. F. Jirsa and J. Jelinck, *ibid.*, **158**, 61 (1926).
6. A. A. Noyes, *et al.*, *J. Am. Chem. Soc.*, **57**, 1221 (1935).
7. A. A. Noyes, *et al.*, *ibid.*, **57**, 1229 (1935).
8. A. A. Noyes, *et al.*, *ibid.*, **57**, 1238 (1935).
9. A. A. Noyes, *et al.*, *ibid.*, **59**, 1316 (1937).
10. A. A. Noyes, *et al.*, *ibid.*, **59**, 1326 (1937).
11. J. A. McMillan, *Acta Cryst.* (abstract), **7**, 640 (1954).
12. J. B. Conn, Abstracts, 8th Annual Battery Research and Development Conference (Signal Corps Engineers Labs.) Asbury Park, N. J. (1954).
13. P. C. Austin, *J. Chem. Soc. Trans.*, **99**, 262 (1911).
14. D. M. Yost, *J. Am. Chem. Soc.*, **48**, 152 (1926).
15. G. A. Barbieri, *Ber.*, **60B**, 2427 (1927).
16. G. A. Barbieri, *Atti accad. Lincei*, **13**, 882 (1931).
17. P. C. Carman, *Trans. Faraday Soc.*, **30**, 574 (1934).
18. J. H. deBoer and J. Van Ormondt, British Pat. 579, 817, Aug. 16, 1946.
19. F. Jirsa, *Chemie (Prague)*, **3**, 4 (1947).
20. F. Jirsa, *Czech. Chem. Communs.*, **14**, 445 (1949).
21. G. A. Barbieri and A. Malaguti, *Atti accad. nazl. Lincei*, **8**, 619 (1950).
22. A. Malaguti, *Ann. chim.*, **41**, 241 (1951).
23. H. Braekken, *Kgl. Norske Videnskab. Selskabs Forh.*, **7**, 143 (1935).
24. Z. V. Zvonkova and G. S. Zdanov, *Zhur. Fiz. Khim*, **22**, 1284 (1948).
25. H. E. Swanson, R. K. Fuyat, and G. M. Ugrinic, *Nat. Bur. Standards Circ. 539*, Vol. IV (1955).

Protection of Molybdenum from Oxidation at Elevated Temperatures

Dwight E. Couch, Harold Shapiro, John K. Taylor, and Abner Brenner

National Bureau of Standards, Washington, D. C.

ABSTRACT

Molybdenum may be protected against oxidation at 1100°C by composite coatings of chromium and nickel. Adhesion of chromium to molybdenum was obtained by anodically etching the molybdenum in a solution of sulfuric and phosphoric acids (1:1 by volume) before plating.

Chromium was deposited from a conventional chromic acid bath operated at 75°-80°C and at a current density of 120 amp/dm². A coating consisting of 0.001 in. of chromium followed by 0.007 in. of nickel protected molybdenum at 980°, 1100°, and 1200°C for 1200, 500, and 100 hr, respectively. Shot peening and ball milling of the coatings did not increase their life. Oxidation and diffusion phenomena were studied to explain ultimate failure of the coatings, and both mechanisms are shown to be contributing causes.

The engineer and metallurgist have in molybdenum a material possessing high strength at elevated temperatures. The chemical nature of this metal, however, precludes its use under oxidizing conditions. The work reported here was an attempt to protect molybdenum from oxidation by electroplating it with composite coatings of chromium and nickel.

Alloys of molybdenum with nickel or cobalt (1) form protective coatings of molybdates when oxidized at 900°-1000°C. However, these alloys are not satisfactory when thermocycling is necessary because of severe spalling of the molybdates. The addition of nickel or cobalt to molybdenum in percentages large enough to prevent oxidation also causes a loss in the hot strength of molybdenum. Molybdenum-chromium alloys with as much as 36% chromium have been studied (2) but were not recommended for use above 980°C because of rapid oxidation. Cladding of molybdenum with nickel and nickel alloys was investigated by Bruckhart and Jaffee (3).

Korbelak (4) used chromium as an initial deposit and electrodeposited other metals on the chromium strike. Brenner (5) obtained adhesion by using a brass strike. Vaaler (6) reported that adhesion of the chromium to molybdenum was improved through the use of Murakami's etching solution (7). Whitfield (8) electrodeposited several metals on molybdenum but gave no procedure or indication of the degree of adhesion he obtained. Runck (9) has published a metallographic study of chromium-plated molybdenum.

Experimental Methods

Sample preparation.—Fastening electrical leads to the molybdenum samples presented some difficulty since the sample failed at the point where the lead joined the molybdenum because of access of oxygen at these points. This difficulty was overcome by welding a nickel wire to a sharp tip of the molybdenum piece with Colmonoy[1] (*see* Fig. 1). The welded area was ground to give a smooth continuous metal surface so that subsequent plating operations completely covered this area with coating. The sharp edges of molybdenum left by shearing or machining operations were ground smooth to prevent treeing and edge buildup during plating. These samples were then degreased and the scale removed by anodic treatment in 70% sulfuric acid.

Plating and adhesion.—Preliminary studies showed that good adhesion of chromium to molybdenum could be obtained fairly consistently by the use of Murakami's etching solution. The etching time in this solution required rather careful control. If insufficiently etched, poor adhesion was obtained; however, if etching were extended to 10 min, a brown film formed on the molybdenum which prevented adhesion. Murakami's etching reagent was also prepared in a more dilute solution containing 100 g of potassium ferricyanide and 100 g of sodium

[1] Hard facing alloy purchasable from Wall Colmonoy Corp., 19345 John R St., Detroit, Mich.

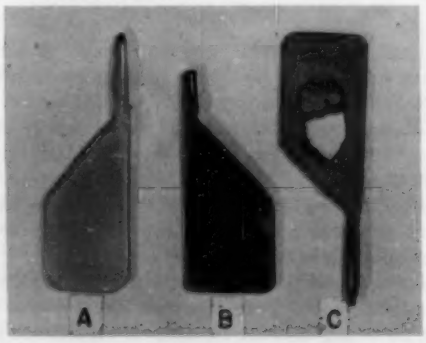

Fig. 1. Typical test panels of chromium-nickel plated molybdenum. A, as plated; B, after 300 hr, oxidation 1100°C; C, after 300 hr, oxidation 1100°C. The difference between B and C shows the variations in samples prepared under identical conditions. Magnification ¾X before reduction for publication.

hydroxide per liter and used at 80°-90°C. Agitation of the samples during the etching process tended to prevent formation of the brown films mentioned above and gave a clean, etched surface on the molybdenum. This solution was not satisfactory for cleaning alloys containing titanium because they formed more tenacious films when etched. After being etched, the samples were rinsed and plated with chromium.

A second method of preparation consisted of treating the samples anodically at 20-40 amp/dm² in 70% sulfuric acid for about 2-3 min. However, a blue film sometimes formed during rinsing which caused poor adhesion. Higher current densities in the anodic treatment usually prevented the formation of these films.

A third etching reagent that worked very well, even with alloys containing titanium, was prepared by using equal volumes of concentrated sulfuric and phosphoric acid. This solution gave a very satisfactory etch when samples were treated anodically in it at 2-10 amp/dm² for 2 to 3 min.

After etching by one of the procedures previously described, the samples were rinsed and plated with 25μ (1 mil) of chromium from a bath containing 250 g of CrO_3 and 2.5 g of sulfuric acid per liter. The chromium was electrodeposited under three different conditions. Low contraction chromium (10), plated at 80-120 amp/dm², at a temperature of 85°-95°C, gave excellent adhesion. Satisfactory adhesion was also obtained by plating bright chromium at 20-30 amp/dm², and at a temperature of 50°C. However, the chromium plated at low temperatures (25°C) gave poor coverage, and the adhesion was not satisfactory. Deposits made under these conditions tended to crack and peel from the molybdenum. This cracking was eliminated by initiating deposition at a temperature (50°C) which produced bright chromium, then reducing the temperature after the samples had been plated for a few minutes.

After chromium plating, the samples were etched in 1:1 hydrochloric acid until the surface appeared gray, given a nickel strike (20-60 amp/dm² for 1-3 min) in an all-chloride strike bath, and then plated with nickel from an all-chloride or a Watts nickel bath. The samples were not rinsed between the strike and plating operation. This procedure gave very good adhesion, as was indicated by bending a specimen until it fractured. The break was nearly always within the molybdenum and not between the electrodeposited layers.

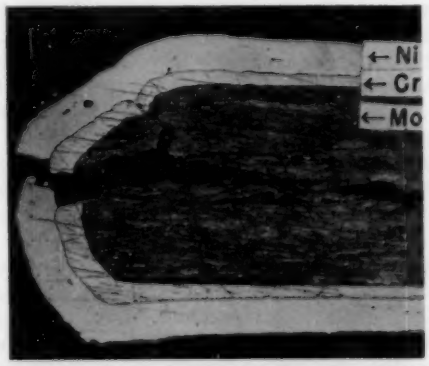

Fig. 2. Fracture of coating when heated to 900°C caused by discontinuities in the molybdenum sheet. Magnification 50X before reduction for publication.

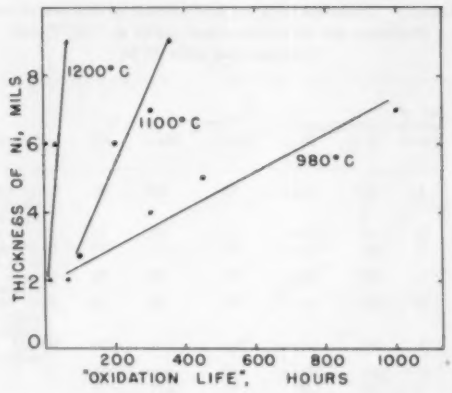

Fig. 3. Effect of temperature and nickel thickness on "oxidation life" of molybdenum plated with chromium and nickel.

Inspection methods.—The time to failure under oxidizing conditions is referred to hereafter as "oxidation life." It is the time the sample remains intact from the moment it is placed in the furnace, at temperature, to the first moment that molybdic oxide smoke is detected, or green nickel molybdate is observed. The early studies of the time to failure showed an appreciable amount of scattering. This led to the belief that there were flaws in the coating and a good inspection method prior to oxidation was needed.

Electrodeposited radioactive-chromium (11) was used as a possible method of detecting voids or inclusions in the nickel deposit. The chromium deposits were made from a bath that contained chromium 51 in concentrations of about 0.06 millicurie per milliliter. This method worked well and showed pores and voids in the nickel deposits when the deposits were less than 0.001 in. thick. However, with nickel thicknesses of 0.007 in., even visible pits did not produce sufficient contrast for the image to be seen.

The only satisfactory method of inspection found was to heat the plated panels in a helium or hydrogen atmosphere to 900°C, then carefully inspect them for cracks or blisters in the coating. A photomicrograph of a fracture caused by faulty molybdenum sheet is shown in Fig. 2.

Results and Discussion

Effect of Coating Thickness and Temperature on Oxidation Life

Figure 3 shows the relation between the thickness of nickel coating and the oxidation life of specimens tested at three different temperatures. The molybdenum was plated with 25μ (1 mil) of chromium prior to electrodepositing nickel. The samples tested at 1200°C oxidized very rapidly and even specimens coated with 225μ (9 mils) of nickel failed in less than 100 hr. Thus, it appeared that 1200°C was an excessive temperature for the study of these coatings.

Table I. "Oxidation lives" of molybdenum panels plated with chromium and chromium-nickel tested at 1100°C and thermocycled every 24 hr

Exp. No.	No. of panels tested	Thickness Cr μ	Thickness Ni μ	Time to failure, hr Min	Time to failure, hr Max	Time to failure, hr Av	Comments
1	4	60*	None	20	20	20	Low temperature chromium
2	2	60	None	20	40	30	—
3	3	60	None	90	240	170	Preheated 200 hr at 1100°C
4	3	100	None	20	80	45	Bright chromium
5	3	120	None	20	70	55	Low temperature chromium
6	3	180	None	140	160	150	Bright chromium
7	10	220	None	40	600	330	—
8	3	25	60	40	240	130	—
9	6	25	120	170	350	250	—
10	37	25	170	120	640	360	—
11	9	25	200	160	700	350	—
12	3	25	220	300	360	340	—
13	4	100	100	160	160	160	—
14	4	100	170	400	920	780	—
15	4	220	170	540	>800	—	Test discontinued after 800 hr
16	3	25	150	40	120	110	Preheated 250 hr
17	3	25	150	40	90	70	Preheated 500 hr

* Unless otherwise noted, all chromium deposits were prepared at 85°C, 100-120 amp/dm².

A temperature of 1100°C was chosen as a more practical condition for use in testing these coatings and was generally used in this investigation.

The oxidation lives of chromium-plated molybdenum, oxidized at 1100°C, were not reproducible. Some samples failed in less than 24 hr while others lasted several hundred hours. Table I shows the results for a series of panels plated with both chromium and nickel.

Generally, deposits 50μ (2 mils) or less in thickness failed in 20 hr or less, while deposits that were 220μ (9 mils) thick had widely different oxidation lives. Those samples that lasted over 50 hr usually had lives of several hundred hours. A chromium-molybdenum alloy forms at the interface and it may be that this alloy is a good oxidation barrier. To check this idea, a group of samples were chromium plated, and some of these were heated in an inert atmosphere at 1100°C for 200 hr before oxidation (experiments 2 and 3 of Table I). The controls had an average life of 30 hr while the preheated panels had an average life of 170 hr. This indicated the importance of forming the chromium-molybdenum diffusion alloy prior to oxidation.

Although chromium-plated molybdenum has desirable properties for the prevention of oxidation, if preheated prior to oxidation, one undesirable characteristic was noticed; after 2 or 3 thermocycles the chromic oxide usually scaled off in large flakes and exposed a bright chromium surface to further rapid oxidation.

The effect of the thickness of the composite chromium-nickel coating on the oxidation life of molybdenum panels is also shown in Table I.

Formation of a chromium-nickel alloy by heating the samples prior to oxidation had an adverse effect on the oxidation life (experiments 16 and 17, Table I). The type of chromium used to coat the molybdenum did not have a marked effect on the oxidation life of the panels (experiments 1, 2, 4, and 5, Table I). The low-contraction type of chromium was generally used because of its superior adhesion and covering power.

Table II. Results of oxidation tests of molybdenum panels plated with 1 mil of Cr and 7 mils of Ni

No. of samples tested	Type Ni	Temp, °C	Oxidation life Min hr	Oxidation life Max hr	Oxidation life Av hr	Comment
33	Cl	1100	70	360	150	
17	W	1100	210	760	320	
34	Cl	980	160	>1200	—	3 unfailed after 1200 hr
16	W	980	740	>1200	—	13 unfailed after 1200 hr

Cl—Nickel deposited from an all-chloride bath.
W—Nickel deposited from a Watts type of bath.

Effect of Plating Conditions on Oxidation Life

A large group of samples were prepared from molybdenum sheet 750μ (30 mils) thick. These samples, 2 x 5 cm in size, were plated with approximately 25μ (1 mil) of chromium and 175μ (7 mils) of nickel. After plating, the samples were oxidized at 980° or 1100°C in a laboratory furnace through which a slow stream of air was passed to remove the molybdic oxide that escaped from the samples which failed. The samples were thermocycled by removing them from the furnace and allowing them to cool to room temperature once every 24 hr.

Table II shows the results for 100 samples that were oxidized. The deposits from the Watts and chloride bath are shown separately in the table for the purpose of comparison. They were actually oxidized in random sequence to eliminate any differences arising from uncontrollable factors.

Panels plated under conditions that were known to give highly stressed deposits were the first to fail. Since the stress in the deposit is relieved by the heating used for inspection, it is not likely that the stress as such is a factor. However, the factors that cause high stress may also cause inclusions or other weaknesses in the deposit which could account for the early failures of these deposits. Weight gains due to oxidation were obtained for nickel electrodeposited from both the Watts and all-chloride-type baths. The results showed only small differences in oxidation rates and could not account for the differences in oxidation life that are shown in Table II.

Early failures may be due to "oxidation pathways" as illustrated in Fig. 4. Although only a small portion of the nickel deposit had been oxidized, the sample was almost ready to fail. Figure 5 is a more advanced case where the oxygen has actually reacted with the molybdenum leaving a shell of nickel around the void. Small holes of this type are usually filled with nickel molybdate.

Since molybdic oxide reacts with both nickel and nickel oxide to form nickel molybdate, the samples usually remain intact while in the furnace. However, when cooled, the nickel molybdate undergoes a transformation which causes violent spalling, thus rupturing the nickel oxide and laying open a hole where the molybdate had formed.

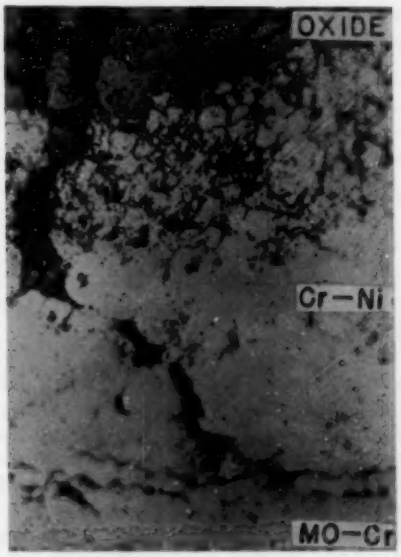

Fig. 4. Oxidation pathway through chromium-nickel coating. Magnification 500X before reduction for publication.

Typical failures are shown in Fig. 1B and 1C. Sometimes these failures could be detected in their early stages by the appearance of a small greenish spot on the outside of the black, adherent, vitreous nickel-oxide envelop. Occasionally, the nickel oxide cracked and flaked away from the sample and showed greenish areas beneath the scale.

Diffusion Studies

There was a possibility that the molybdenum diffusing out through these coatings would form a nickel-molybdenum alloy which would cause spalling when oxidized and thermocycled. To obtain a semi-quantitative measure of diffusion, two molybdenum bars, about ½ in. in diameter and 2 in. in length, were turned in a lathe on true centers. These bars were then plated with 25-50μ (1-2 mils) of chromium and 250-300μ (10-12 mils) of nickel, taking care to obtain uniform deposits. After plating, they were heated in hydrogen at 1100°C for 100 hr to permit diffusion of the metals, then returned to the lathe and a portion of the coating of each bar was turned off. The diameters of the bars were checked

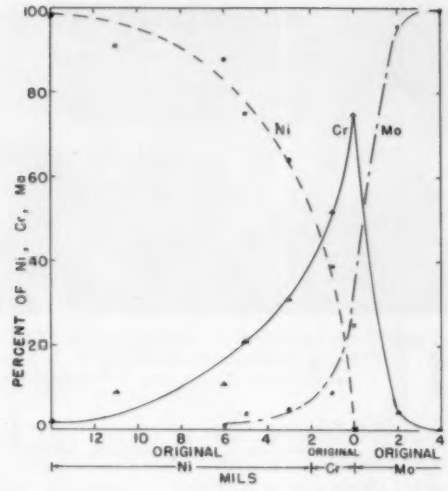

Fig. 6. Analysis of diffusion bar after heating 100 hr at 1100°C.

after each cut to insure that the turnings were coming from parallel layers. These lathe cuts were from 25 to 50μ (1-2 mils) per cut and were kept separate from each other for chemical analysis. Figure 6 shows the analysis of the coatings after 100 hr of diffusion, and Fig. 7 shows a photomicrograph of the bar.

The remaining portion of one of these bars was again heated for a total of 600 hr at 1100°C. It was then machined as previously described, and a chemical analysis for all three components was made of these turnings. The results of the analysis are shown in Fig. 8.

The chromium was distributed throughout the region which originally consisted of two layers, one of nickel and one of chromium. Figure 8 also shows some diffusion into the molybdenum, but there was a sizable amount of molybdenum that diffused outward into the chromium-nickel alloy. X-ray analysis showed the existence of a nickel-molybdenum intermetallic compound, NiMo.

A photomicrograph of the second bar after heating for 600 hr is shown in Fig. 9. Apparently, the diffusion of the molybdenum into the chromium-nickel layer did not change its structure appreciably at

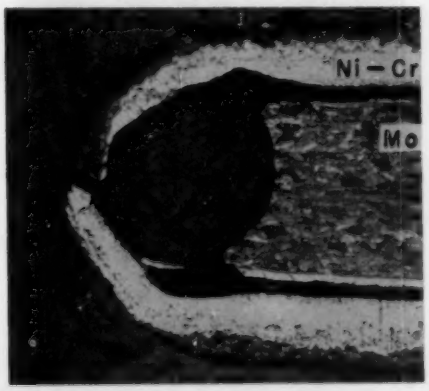

Fig. 5. Oxidation corrosion at edge of panel. Magnification 50X before reduction for publication.

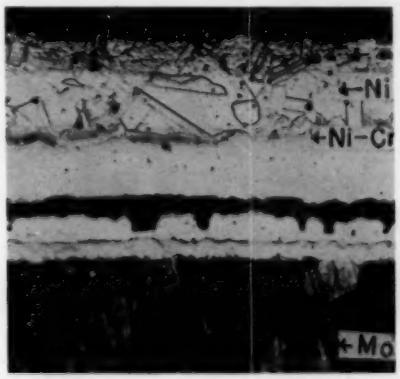

Fig. 7. Diffusion bar after heating 100 hr at 1100°C. Magnification 100X before reduction for publication.

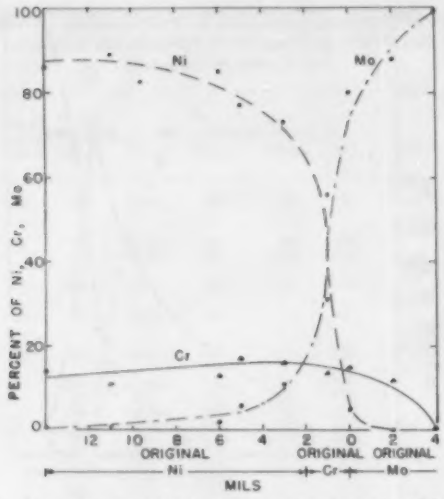

Fig. 8. Analysis of diffusion bar after heating 600 hr at 1100°C.

these concentrations. The chromium-molybdenum alloy is seen easily.

Since a wrought nichrome type of alloy is very resistant to oxidation, it was thought the formation of these alloys by heating, in an inert atmosphere, prior to oxidation would improve the protective value of the coating. To test this idea, a series of molybdenum panels were plated with 25μ (1 mil) of chromium and 175μ (7 mils) of nickel. Some of these were saved for control panels in the "as plated" condition; the others were heated for 250 and 500 hr at 1100°C in hydrogen. The results are included in Table I. Comparison of Exp. 16 and 17 with Exp. 9 and 10 shows that the formation by diffusion of these nickel-chromium-molybdenum alloys was detrimental to the life of the samples. This differs from the conclusions reached by Safranek and Schaer (12) who worked under somewhat different conditions. A rather loose oxide scale formed during oxidation and apparently permitted the oxidation to progress at a more rapid rate than would be expected from a parabolic law.

Effect of Mechanical Working

Variations in the oxidation life observed for a group of specimens indicated that some flaws in the deposit allowed a direct access of the oxygen to the molybdenum and thus caused the early failures. It was thought that mechanical working of the deposit might improve it by causing some flow of the metal with a resultant closing of pores.

Table III. Oxidation life of mechanically worked samples

Type of work performed on sample	Av life hr	Av life of unworked control hr
Shot peened	262	275
Heated to 1100°C then shot peened	72	72
Ball milled, 800°C in H_2 atm	230	320

One group of plated panels was shot peened[2] using several different nozzle pressures and shot sizes. Another group of plated panels was ball milled in a 4-in. diameter steel ball mill rotated at 20 rpm and operated at 800°C in an atmosphere of hydrogen. The samples were hot worked in this way for 3 hr using ½ in. ceramic balls. Neither the peening nor the ball milling caused any significant increases in life (Table III). This showed that mechanical working of this type (ball milling and shot peening) did not affect the causes of oxidation failure.

Causes of Failure

Metallographic examination and x-ray analysis of a series of specimens subjected to different periods of oxidation in air at 1100°C showed some interesting phenomena. Oxidation for 1 hr caused very little change in the samples except that the electrodeposited nickel and the molybdenum had recrystallized and some segregation of impurities had taken place at the grain boundaries of the nickel. By the end of 7 hr the nickel had started to show oxidation at the grain boundaries and a void had developed at the edge of the sample (Fig. 10). Continued oxidation and thermal cycling for from 50 to 150 hr caused a line of oxide inclusions to form such as that shown in Fig. 11. The time required for these oxides to develop was different for each sample. With nickel coatings 175μ (7 mils) thick, the inclusions could be seen as isolated spots after 50 hr and

[2] These samples were shot peened at the plant of the Pangborn Corporation, Hagerstown, Md.

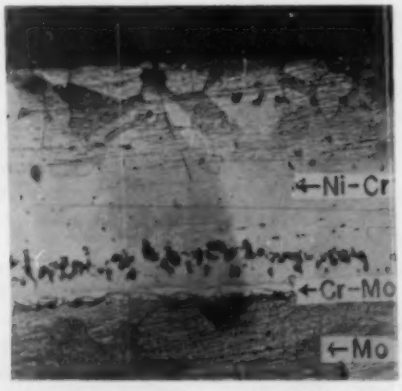

Fig. 9. Diffusion bar, after heating 600 hr at 1100°C. Magnification 100X before reduction for publication.

Fig. 10. Chromium-nickel-plated molybdenum panel after 7 hr of oxidation. Magnification 100X before reduction for publication.

Fig. 11. Subsurface oxide shown as isolated areas after 100 hr of oxidation at 1100°C. Magnification 500X before reduction for publication.

had usually grown into a solid band of subsurface oxide after 100 to 150 hr of oxidation.

To study the cause of these three formations, i.e., subsurface oxide, grain-boundary oxidation, and edge separations, electroformed nickel sheet instead of molybdenum was plated with chromium and nickel and then oxidized and sectioned for examination. The specimens showed the same three formations that were noted with the molybdenum samples (Fig. 12). Thus, the molybdenum was not involved in any of these processes.

In other experiments, electroformed nickel sheets of two thicknesses, 150μ (6 mils) and 250μ (10 mils), were plated with 50μ (2 mils) of chromium and 150μ (6 mils) of nickel on only one side. These samples (Fig. 13B and 14B) show a series of inclusions in the area of the original chromium deposit. Similar inclusions noticed in the diffusion bar studies are shown in Fig. 7 and 9. Figure 13B shows the formation of the subsurface oxide on both sides of the original chromium layer. In the other case, Fig. 14B and 14C, the subsurface oxide is visible on one side only. The side consisting of the 20-mil thick nickel shows only isolated spots of oxide which increased in size and number with increased oxidation time.

The subsurface oxide was not detected in samples that were heated in hydrogen or helium. These

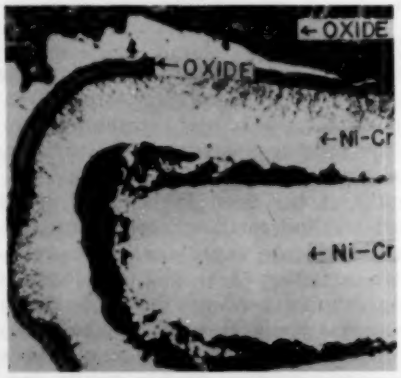

Fig. 12. Effects of 300 hr of oxidation on nickel-chromium-nickel sample.

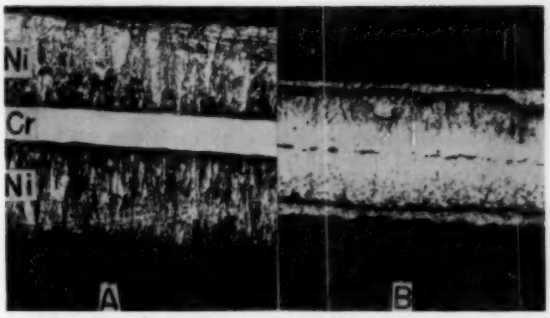

Fig. 13. Electrodeposited nickel-chromium nickel. A, as deposited; B, after 100 hr of oxidation at 1100°C. Magnification 100X before reduction for publication.

oxides were associated with atmospheric oxidation and were not a result of inclusion within the nickel deposit. Apparently, this subsurface oxide layer was caused by oxidation of the chromium-nickel alloy formed by diffusion, the oxygen either coming from dissolved oxygen in the nickel or along grain boundaries. According to Zima (13) chromium-nickel alloys that contain less than 10% chromium oxidize more rapidly than either pure nickel or alloys with over 10% chromium. The subsurface oxide layer formed through much thicker layers of nickel if it was over a curved surface. Grain boundary oxidation was also more severe at curved edges. The fact that the subsurface oxide forms at the chromium diffusion front was also demonstrated by the use of an etching solution for nickel. It etched the structure down to the subsurface oxide but not below, thus showing the alloy to be low in chromium above the subsurface oxide layer and rich in chromium below this layer (Fig. 11).

Comparisons of Actual and Theoretical Oxidation Life

It was of interest to compare the actual life of the plated panel with the oxidation rates of nickel given in the literature (14-16).

Table IV shows the oxidation rates of various types of nickel, reported in the literature, and those obtained in this laboratory. The maximum oxidation

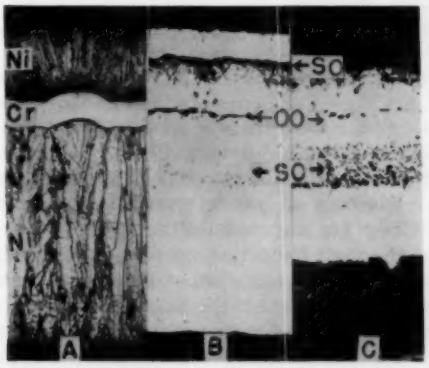

Fig. 14. Electrodeposited nickel-chromium-nickel. A, as deposited; B, after 70 hr of oxidation at 1100°C; C, after 300 hr of oxidation at 1100°C. In Band C, the subsurface oxide is shown as "SO" while the occluded oxide is marked "OO". Magnification 100X before reduction for publication.

Table IV. Oxidation rate constants of nickel (K_p)

Kind of Ni	Temp of oxidation, °C	K_p $g^2/cm^4/sec$
1. All-chloride bath as plated	1100	8.9×10^{-10}
2. As 1 but cold rolled 10% reduced	1100	20×10^{-10}
3. As 1 but cold rolled 50% reduced	1100	8.1×10^{-10}
4. Wrought rod	1100	24×10^{-10}
5. As plated Watts cobalt-free	1100	7.6×10^{-10}
6. Carbonyl (14)	1100	2.2×10^{-10}
7. Foil (15)	1100	0.17×10^{-10}
8. Commercial (16)	1100	1.6×10^{-10}

life at 1100°C of molybdenum panels coated with 25μ (1 mil) chromium and 175μ (7 mils) nickel was about 600 hr. This is reasonably close to the value of 560 hr calculated from the data for electrodeposited nickel (No. 1, 2, 3, and 5, Table IV). By using oxidation data reported in the literature (No. 6, 7, and 8, Table IV) an expected life of 2200 to 45,000 hr was obtained. These literature values were obtained from relatively short oxidation times, while that obtained in this work was for 100 to 200 hr of oxidation.

Acknowledgments

The authors express their appreciation to the Navy Department, Bureau of Aeronautics, for financial support of the project and for permission to publish the results.

Manuscript received Nov. 15, 1957.

Any discussion of this paper will appear in a Discussion Section to be published in the June 1959 JOURNAL.

REFERENCES

1. J. W. Spretnak and R. Speiser, ONR Contract N6onr 22582, NR 039-005 Report 13, Project 467, Ohio State University.
2. H. D. Kessler and M. Hansen, *Trans. Am. Soc. Metals*, **42**, 1008 (1950).
3. W. L. Bruckhart and R. I. Jaffee, *ibid.*, **44**, 176 (1952).
4. A. Korbelak, *Tech. Proc. Am. Electroplaters' Soc.*, **40**, 90 (1953).
5. S. S. Brenner, *Plating*, **43**, 1143 (1956).
6. L. E. Vaaler, C. A. Snavely, and C. L. Faust, U.S. Atomic Energy Report BMI 813, April 1, 1953.
7. "Metals Handbook," p. 1140, Am. Soc. for Metals, Cleveland, Ohio (1948).
8. M. G. Whitfield, U. S. Pat. 2,682,101, June 29, 1956.
9. R. J. Runck, *This Journal*, **104**, 74 (1957).
10. A. Brenner, P. Burkhead, and C. J. Jennings, *J. Research Natl. Bur. Standards*, **40**, 31 (1948).
11. R. H. Wolff, M. A. Henderson, and S. L. Eisler, *Plating*, **42**, 537 (1955).
12. W. H. Safranek and G. R. Schaer, *Proc. Am. Electroplaters' Soc.*, **43**, 105 (1956).
13. G. E. Zima, Contract N6onr 24430, Proj. NR 031-355 7th tech report, Calif. Inst. Tech. April 1956, ASTIA No. 92520.
14. S. F. Frederick and I. Cornet, *This Journal*, **102**, 285 (1955).
15. W. J. Moore and J. K. Lee, *Trans. Faraday Soc.*, **48**, 916 (1956).
16. A. Preece and G. Lucas, *J. Inst. Metals (London)*, **20**, 219 (1952).

Temperature Dependence of Fluorescence of Tin-Activated Orthophosphates

Richard W. Mooney

Chemical and Metallurgical Division, Sylvania Electric Products Inc., Towanda, Pennsylvania

ABSTRACT

Apparatus for measuring the temperature dependence of fluorescence is described. The variation of fluorescent intensity with temperature as a function of tin-activator concentration is given for the systems: strontium-zinc orthophosphate and strontium-calcium orthophosphate. In both cases, the quenching temperature is independent of activator concentration. The results are interpreted in terms of Johnson and Williams' theory of fluorescent quenching.

With the increasing use of phosphors in high-pressure mercury vapor lamps, it has become necessary to increase our knowledge of the properties of these phosphors at the elevated temperatures to which they are exposed during normal operation. One of the most important properties of such phosphors is the temperature dependence of fluorescence or the manner in which the fluorescent efficiency of the phosphor varies with temperature. This property has been measured for many phosphor systems that respond to the wave lengths present in the high-pressure mercury vapor arc and, in at least two cases, the variation of temperature dependence of fluorescence with activator concentration has been studied in some detail (1, 2). In both cases, the higher activator concentrations caused a decrease in the quenching temperature, i.e., the temperature at which the relative fluorescent efficiency begins to decrease.

Recently, it has been shown that certain tin-activated alkaline earth orthophosphate phosphors fluoresce efficiently under high-pressure mercury vapor arc excitation (3, 4), and therefore a study of the temperature dependence of fluorescence of these phosphors was undertaken. The object of the present study was to develop a method of measurement which would give reproducible results and to use this method to determine the efficiencies of these

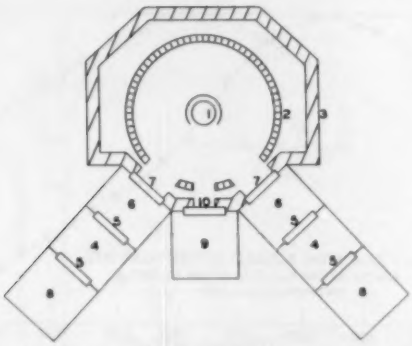

Fig. 1. Schematic diagram of apparatus for measuring temperature dependence of fluorescence.

phosphors at high temperatures. The results have been interpreted in terms of the Johnson and Williams theory of fluorescent quenching (5).

Apparatus and Method of Measurement

To measure the temperature dependence of fluorescence, one must be able to heat the phosphor at a controlled rate while measuring its light emission. The obvious problems in obtaining meaningful measurements are (*a*) keeping the rate of heating constant, (*b*) excluding all other light from the apparatus, and (*c*) maintaining the intensity of ultraviolet irradiation constant.

A schematic diagram of the apparatus for making these measurements is shown in Fig. 1. The phosphor is held in a small quartz cylinder, 1, located in the center of an oven, 2. Excessive heat loss is prevented by insulating the entire heating assembly consisting of the oven and associated strip heaters with magnesia blocks, 3. Ultraviolet excitation is furnished by Sylvania G4T4 lamps (254 mμ) or other suitable u.v. lamps located as shown, 4. The excitation is filtered by Corning 9863 glass filters, 5, to remove visible light. The lamps are separated from the oven by an insulating chamber, 6, to lower the amount of heat radiation reaching them. A Vycor filter, 7, at the front of this chamber adjacent to the oven also helps to cut down heat transfer. The output of the u.v. lamps is monitored by 1P28 photomultipliers, 8, while the fluorescence of the phosphor sample is picked up by a 1P21 photomultiplier, 9, located as shown. Colored filters, 10, may be inserted between the sample and the 1P21 photomultiplier.

With the phosphor sample in place and all equipment warmed up, the current through the G4T4 tubes is adjusted to slightly above the minimum operating value for each lamp. Successive readings of each of the three photomultiplier tubes are then made on a photometer (Photovolt Model 520-M). The readings of the 1P28 monitor tubes are set approximately equal and the fluorescence reading is adjusted to give a mid-scale reading on the photometer. The current through the heaters is gradually increased to maintain a rate of heating of approximately 2°C/min. Periodic temperature readings are taken on a L&N potentiometer with an iron-constantan thermocouple imbedded in the phosphor sample. The u.v. outputs of the G4T4's are monitored by the 1P28's and maintained at their room temperature values by adjustment of lamp currents. Readings of temperature and relative fluorescence of the phosphor sample are recorded.

When a dependent variable such as fluorescent efficiency is measured while an independent variable such as temperature is being varied continually, the correctness of labeling the results as true equilibrium data naturally arises. However, for true equilibrium data it would be necessary to use an infinitely slow rate of heating or to make point by point measurements. A compromise is normally arrived at, and in this case the relatively slow heating rate of 2°C/min was chosen. A check on the heating rate was conducted by following the fluorescent efficiency on both a heating and a cooling curve on several different phosphors. The greatest discrepancy was found at the highest temperatures where, when the heat was removed from the sample, the phosphor cooled very rapidly. In this region the relative efficiency varied from heating to cooling curve by as much as 5 to 7%. The difference in the measured values decreased with decreasing temperature, becoming approximately zero at room temperature.

Most of the measurements reported herein were made under 254 mμ excitation obtained from germicidal lamps due to the ease of operation of these lamps in the equipment. However, in the application of these phosphors, the exciting source is the high pressure mercury vapor arc with strong u.v. line emission at 313 and 365 mμ. Therefore, some measurements of temperature dependence of fluorescence were carried out using the radiation from a high-pressure mercury vapor arc lamp as the exciting medium. The data so obtained were in substantial agreement with those obtained under 254 mμ radiation and reported herein.

Relative efficiency data at room temperature were obtained on plaque testers of the type described by Butler and Mooney (6).

Experimental Results

In order to check the results obtained with this instrument, the temperature dependence of fluorescence of calcium halophosphate and magnesium tungstate was determined. The data so obtained were in agreement with previous measurements on the same phosphors made by Jerome (7).

A survey of the high temperature fluorescent properties of known phosphor systems was then conducted during which it was found that tin-activated calcium orthophosphate phosphors modified by strontium or barium (8) maintain or improve their room temperature efficiencies up to temperatures of about 270°C (543°K). With the calcium strontium orthophosphate system, these measurements were made with the phosphor in an atmosphere of helium, water vapor, air, and in vacuum, with the same result in all cases. Unfortunately, these tin-activated calcium orthophosphate phosphors do not respond to the wave lengths present in the high-pressure mercury vapor arc. However, an investigation of other tin-activated orthophosphates by Thomas and Butler (3) uncovered several sys-

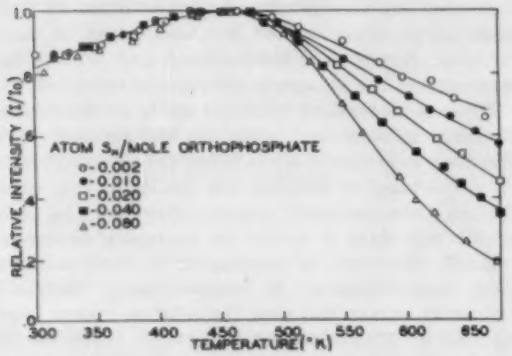

Fig. 2. Variation of fluorescent intensity with temperature for tin-activated strontium-zinc orthophosphate. Excitation $\lambda = 254$ mμ.

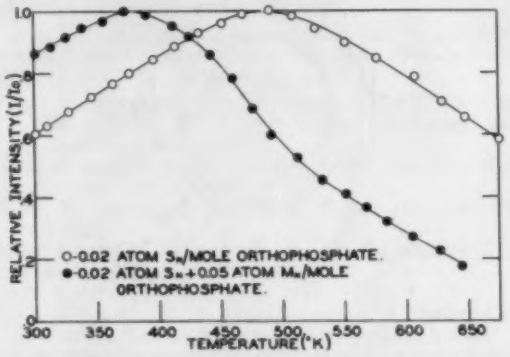

Fig. 4. Effect of Mn on the variation of fluorescent intensity with temperature for tin-activated strontium-calcium orthophosphate. Excitation $\lambda = 254$ mμ.

tems which were highly efficient under high-pressure mercury vapor arc excitation. The temperature dependence of fluorescence of some of these systems was investigated in detail, especially as regards the manner in which this property varies with activator concentration. Results on two of the systems studied are reported below.

Tin-activated strontium-zinc orthophosphate.—This phosphor has the approximate composition $Sr_{2.98}Zn_{6.98}(PO_4)_2$. It has been shown that the spectral energy distribution of the emission is dependent upon the wave length of excitation (3, 4). Thus when exposed to 254 mμ, the phosphor has a main emission band at about 600 mμ and a weaker band at about 390 mμ. When excited by 313 mμ the weak emission band at 390 mμ disappears, and the phosphor emits solely in the orange-red with negligible emission below 500 mμ. Therefore, the phosphor emission color when excited by the wave lengths present in the high-pressure mercury vapor arc lamp is largely orange-red with a very small blue component from the 254 mμ line.

The temperature dependence of fluorescence under 254 mμ excitation was measured for phosphors having activator concentrations of 0.002, 0.005, 0.01, 0.02, 0.04, and 0.08 gram-atoms Sn per gram-mole of the orthophosphate as given above. With the exception of the data for the phosphor containing 0.005 gram-atom Sn, the results are shown graphically in Fig. 2. The data for 0.005 gram-atom Sn were omitted due to their close proximity to the 0.002 gram-atom Sn data. All measurements were made using a Corning 3-76 filter, which absorbs 90% or more of the wave lengths below 540 mμ, in position 10, Fig. 1. Therefore, only the temperature dependence of fluorescence of the main emission band at 600 mμ was measured. Some of the measurements were checked using a Corning 3-72 sharp-cut type of filter with a wave-length "cut" (37% transmittance) equal to 460 mμ with identical results. An inspection of Fig. 2 shows that up to a temperature of 460°K the experimental results are independent of activator concentration. Above this temperature, however, an increase in the activator concentration causes a decrease in the relative intensity of fluorescence. It should be noted that the temperature at which quenching begins is independent of activator concentration.

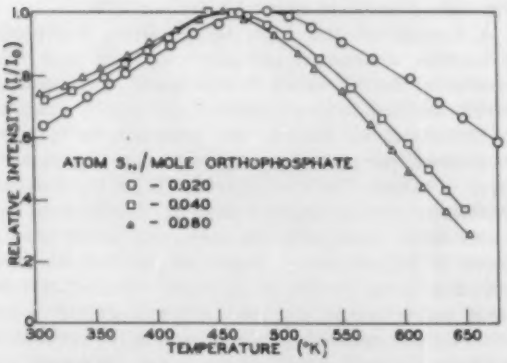

Fig. 3. Variation of fluorescent intensity with temperature for tin-activated strontium-calcium orthophosphate. Excitation $\lambda = 254$ mμ.

Tin-activated strontium-calcium orthophosphate.—This phosphor has the approximate composition $Sr_{2.98}Ca_{6.98}(PO_4)_2$. It has approximately the same response to 254 mμ and 313 mμ excitation as the tin-activated strontium-zinc orthophosphate phosphor described above. The variation of fluorescent intensity as a function of temperature was measured for phosphors having Sn concentrations of 0.02, 0.04, and 0.08 gram-atoms Sn per gram-mole of the orthophosphate as given above. The fluorescent emission was filtered by a Corning 3-77 filter which absorbs 90% or more of the wave lengths below 470 mμ. Results are shown graphically in Fig. 3. It is apparent that, although the relative intensity at 500°K and above falls off rapidly with increasing activator concentration, the temperature at which quenching begins is again independent of the Sn concentration.

The addition of Mn to this system as a secondary activator shifts the emission toward the red, and for phosphor applications in high-pressure mercury vapor lamps, an increase in red emission is very desirable. Unfortunately, however, the addition of manganese adversely affects the high temperature fluorescence as shown in Fig. 4 which compares the temperature dependence of fluorescence of a strontium calcium orthophosphate containing 0.02 gram-atom Sn per gram-mole of orthophosphate to one

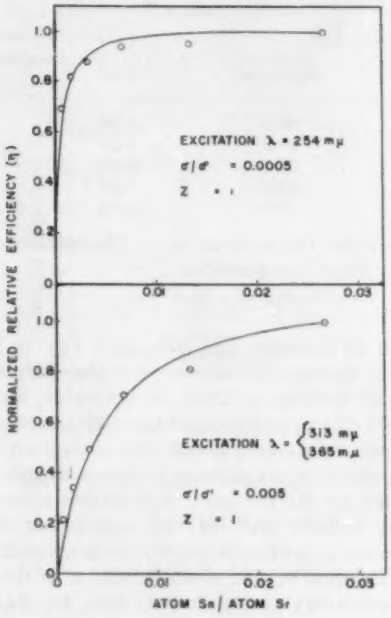

Fig. 5. Relative efficiency vs. activator concentration at 25°C (298°K).

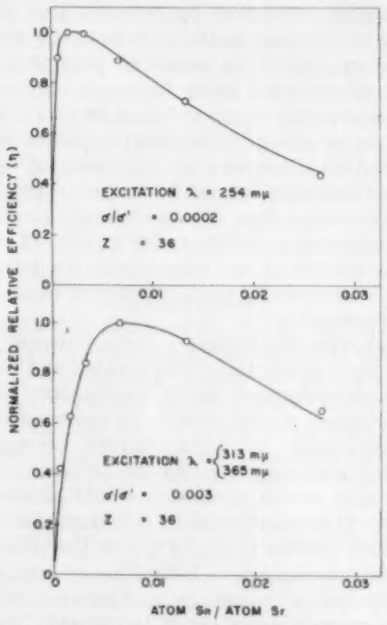

Fig. 6. Relative efficiency vs. activator concentration at 377°C (650°K).

containing 0.02 gram-atom Sn plus 0.05 gram-atom Mn per gram-mole of orthophosphate. The addition of manganese causes a marked lowering of the temperature at which quenching occurs, and therefore the red emission would not be improved at the operating temperatures of high-pressure mercury vapor lamps. The results shown in Fig. 4 were obtained using a Corning 3-72 filter (wave-length "cut" equal to 460 mμ) in position 10, Fig. 1.

Discussion

The efficiency of emission of a phosphor as a function of temperature will depend on the effectiveness with which the absorbed energy can be protected from loss by thermal dissipation. Any interaction of the atoms comprising the "luminescent center" with another "luminescent center" increases the probability of a nonradiative dissipation of energy and quenching of the emission becomes likely. Therefore, it would be expected that an increase in the concentration of "luminescent centers," i.e., activators, would increase the probability of quenching.

Johnson and Williams (5) have derived an expression for the efficiency as a function of activator concentration which has the form

$$\eta = \frac{c(1-c)^z}{c + (\sigma/\sigma')(1-c)} \qquad [1]$$

where c is the total mole fraction of activator and σ/σ' and z are adjustable parameters. The parameter σ/σ' is the ratio of the capture cross sections of nonactivators to the capture cross sections of luminescent activators, while the parameter z is defined as the number of lattice positions surrounding a given activator such that, if any one of these sites is occupied by another activator, luminescence is quenched.

By selecting appropriate values of σ/σ' and z, Eq. [1] may be fitted to the room temperature efficiency vs. activator concentration data for the $Sr_{2.42}Zn_{0.20}(PO_4)_2$ phosphor under 254 mμ and high-pressure mercury vapor arc excitation (*see* Fig. 5). In Fig. 5, and also in Fig. 6, the activator concentration is expressed as atom Sn per atom of Sr rather than as mole fraction in order to maintain the original definition of z in terms of lattice sites, in this case Sr sites, that could be occupied by Sn.

It is apparent from the experimental data that the efficiency as a function of Sn concentration varies with the type of excitation with the higher energy excitation (254 mμ) producing higher efficiencies at low activator concentrations. However, in both cases, the z value which gives the best fit is 1, in agreement with the prediction that z is independent of the type of excitation at a given temperature (5). The σ/σ' values which best fit the data are 0.0005 for 254 mμ excitation and 0.005 for high-pressure mercury vapor excitation.

Efficiency vs. activator concentration data may be calculated from the information given in Fig. 2 and 5 for any temperature up to about 675°K (398°C). The data plotted in Fig. 6 for a temperature of 377°C were arrived at in this manner. At this temperature the shift of peak efficiency toward lower activator concentrations with increasing energy of excitation is readily observable. Once again, the curves which gave the best fit to the data had the same z value, namely 36. The σ/σ' values are approximately the same as before, i.e., 0.0002 for 254 mμ excitation and 0.003 for high-pressure mercury vapor arc excitation. Thus in agreement with theory, temperature has a relatively negligible effect on the σ/σ' values for a given type of excitation. It is interesting that a slight trend toward lower σ/σ' values with increasing temperature is found in both cases.

The theory advanced by Johnson and Williams predicts an increase in the z value with increasing temperature, and it is apparent that this system behaves as expected going from a z value of 1 at room temperature to a z value of 36 at 377°C. The number of Sr atoms surrounding another Sr atom in the $Sr_3(PO_4)_2$ lattice may be calculated from the crystal structure work of Zachariasen (9). These values, corresponding to successively larger predicted values of z, are 6, 8, 14, 20, 32, 38, 50, etc. Exact agreement of the experimentally determined value of z with one of these calculated values would not be expected.

The experimental values of z are, however, qualitatively very interesting. The z value of 1 obtained at room temperature would imply that two Sn-activator atoms would have to be nearest neighbors at a separation of 3.97Å before concentration quenching were possible. At the activator concentrations used in this study this would be extremely unlikely. This conclusion is substantiated further by the data plotted in Fig. 2 where the relative intensity of fluorescence as a function of temperature is not affected by changes in activator concentration up to a temperature of about 460°K (187°C). Even at 377°C, the z value has only increased to 36. The calculated radius of a sphere containing 32 Sr atoms surrounding another is 6.8Å, while the radius of a sphere containing 38 Sr atoms is 7.4Å. However, the maximum activator concentration used, i.e., 0.080 atom Sn per mole of $Sr_{2.92}Zn_{0.08}(PO_4)_2$, corresponds to a Sn-Sn distance of 13.1Å assuming random distribution of activator atoms in a $Sr_3(PO_4)_2$ unit cell volume of 181.8Å^3 (9). A separation of 13.1Å corresponds to a z value between 170 and 182. Therefore, the experimental z value of 36 would still not give concentration quenching. It is evident, however, both from the efficiency data and the data on temperature dependence of fluorescence that concentration quenching is taking place especially at elevated temperatures. Therefore, the definition of the parameter z given by Johnson and Williams does not appear to be strictly applicable to this system.

It is interesting to compare the present results to those of Klasens (2), who measured the temperature dependence of fluorescence of $6MgO \cdot As_2O_5$ at various Mn activator contents. It would appear that two different processes are operating since Klasens' curves are shifted to lower temperatures with increasing Mn content, whereas, for the tin-activated phosphors, the quenching temperature seems to be independent of the activator concentration. The data are similar in that in both cases increasing activator concentrations cause the efficiency to drop at high temperatures. The falling portions of the temperature dependence curves at high temperatures were analyzed by Klasens in terms of the well-known quenchng formula

$$\eta = \frac{1}{1 + \frac{s}{A} e^{-E/kT}} = I/I_o \qquad [2]$$

giving values of E, the height of the energy barrier for the radiationless process for activator atoms separated by the finite distance r. The values of E so obtained fitted the equation

Table I

Sn	Av Sn-Sn distance (Å)	$Sr_{2.92}Zn_{0.08}(PO_4)_2$ E (eV)	ln (s/A)
0.002	45.0	0.36	5.9
0.010	26.3	0.37	6.2
0.020	20.9	0.41	7.3
0.040	16.6	0.46	8.5
0.080	13.1	0.58	11.6

$$E = E_o(1 - e^{-\alpha r}) \qquad [3]$$

also due to Johnson and Williams (5) if E_o, the height of the energy barrier for the radiationless process at infinite dilution of activator, were set equal to 1.45 e.v. and a equal to 0.075. Equation [3] is obtained by assuming that the activation energy for the radiationless process in the activator center is lowered by the presence of a second activator in the close vicinity and that the amount of this energy lowering is approximately proportional to the overlap integral for the wave functions of the interacting activators. It is obvious that Eq. [3] must give decreasing values of the energy barrier E for decreasing distance r between activator centers.

If, for purposes of comparison, the data for the strontium-zinc orthophosphate phosphors are analyzed by Eq. [2], values of E, and ln (s/A) may be determined. These values are tabulated in Table I for each of the activator concentrations in the strontium-zinc orthophosphate system. The use of Eq. [2] to analyze the temperature dependence data on strontium-zinc orthophosphate is rigorously inappropriate since it has been shown experimentally that concentration quenching is taking place. However, the analysis gives a direct comparison to Klasens' (2) data taken over the same range of concentration.

The average Sn-Sn distance was calculated as before, assuming random distribution of activator atoms. In order to check the fit of these parameters to the original data, the values of E and $\ln(s/A)$ for $Sr_{2.92}Zn_{0.08}(PO_4)_2$ were used to calculate values of I/I_o as a function of 1/T. The logarithm of the calculated value of I/I_o is plotted as a function of the reciprocal of the absolute temperature in Fig. 7, together with the experimental points. The fit of the curves to the data is quite good, especially at the higher temperatures.

However, although the experimental data on temperature dependence of fluorescence of $6MgO \cdot As_2O_5$:Mn and $Sr_{2.92}Zn_{0.08}(PO_4)_2$:Sn may both be equally well fitted to Eq. [2] over approximately the same range of activator concentrations, the meaning of the resulting values of E is open to question. In one case, E decreases with decreasing r whereas in the other, E increases with decreasing r. Therefore, the fit of the E values for Klasens' data to Eq. [3] is thought to be fortuitous since a corresponding analysis of the data for the tin-activated phosphors would give E values varying in exactly the opposite manner from that predicted by Eq. [3].

Summarizing, analysis of the efficiency data in terms of Eq. [1] yields values of z and σ/σ' which

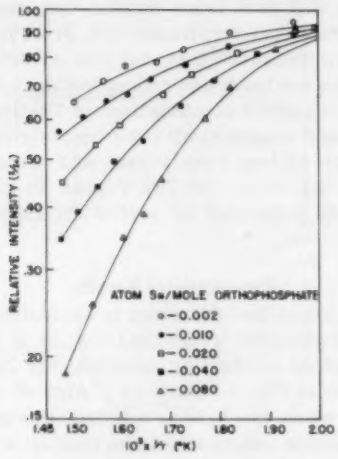

Fig. 7. The fit of the experimental data to the equation $I/I_0 = 1/\left(1 + \frac{se^{-E/kT}}{A}\right)$ using the values of the parameters E and $\ln \frac{s}{A}$ given in Table I for tin-activated strontium-zinc orthophosphate.

vary qualitatively in accordance with the predictions made by Johnson and Williams (5). Quantitatively, however, the derived values of z are not in accord with the experimental results since the z values are too small to explain the concentration quenching that is observed. The results are also compared to Klasens' data on $6MgO \cdot As_2O_5$ by the use of Eq. [2] for thermal quenching, although the use of this equation to interpret the data is not strictly appropriate since it has been shown that concentration quenching is taking place simultaneously. However, the comparison leads one to doubt the experimental verification of Eq. [3] claimed by Klasens in view of the widely differing trends of the E values. It is evident that further theoretical and experimental studies of concentration and thermal quenching of fluorescence are necessary in order to develop a consistent theory of fluorescent quenching for all phosphor systems.

Acknowledgment

The author is indebted to Dr. K. H. Butler for many helpful discussions in the course of this work and to the late Dr. E. F. Lowry for advice and encouragement. Thanks are also due to Dr. M. J. B. Thomas who supplied the phosphor samples.

Manuscript received Jan. 6, 1958. This paper was prepared for delivery before the Washington Meeting, May 12-16, 1957.

Any discussion of this paper will appear in a Discussion Section to be published in the June 1959 JOURNAL.

REFERENCES

1. G. R. Fonda, *J. Phys. Chem.*, **43**, 561 (1939).
2. H. A. Klasens, *Philips Res. Repts.*, **9**, 377 (1954).
3. M. J. B. Thomas and K. H. Butler, Paper presented at the ECS Washington Meeting, May 12-16, 1957.
4. M. J. B. Thomas, K. H. Butler, and J. M. Harris, *Illuminating Eng.*, **52**, 279 (1957).
5. P. D. Johnson and F. E. Williams, *J. Chem. Phys.*, **18**, 1477 (1950).
6. K. H. Butler and R. W. Mooney, *Sylvania Technologist*, **9**, 121 (1956).
7. C. W. Jerome, *This Journal*, **98**, 376 (1951).
8. K. H. Butler, *ibid.*, **100**, 250 (1953).
9. W. H. Zachariasen, *Acta Cryst.*, **1**, 263 (1948).

Electron Traps and the Electroluminescence Brightness and Brightness Waveform

Frederick F. Morehead, Jr.

Lamp Development Department, Lamp Division, General Electric Company, Nela Park, Cleveland, Ohio

ABSTRACT

This work describes an investigation of the effect of temperature, voltage, and rise time on the size and shape of the brightness waves of electroluminescence; sawtooth and square pulse voltage waveforms were used to excite copper-activated ZnS phosphors in a slightly conducting medium. A model is proposed which accounts for the major features of the experiments. Electrons which have been ionized from a region of high field are trapped in another part of the phosphor particle. A field opposite in polarity to that which produced the ionization serves to sweep the conduction electrons, which are at every instant in thermal equilibrium with the traps, back into the high field region where the electrons recombine, with radiative emission. The model is successfully applied to measurements of the average electroluminescence brightness for sinusoidal excitation of a binderless phosphor layer as a function of temperature, frequency, and voltage.

Several authors have already noted in the interpretation of their experiments a connection between electronic trapping levels in ZnS phosphors and the temperature and frequency dependence of electroluminescent brightness (1-4). Neumark (5) has shown that electrons released from traps during thermoluminescence greatly enhance the d-c electroluminescence of some ZnS single crystals. Thornton (6) accounts for the shape of brightness waves produced by sinusoidal excitation on the basis of field-controlled thermal release of electrons from traps.

Although there is disagreement in the details of the various theoretical treatments in the above references, the most general consensus is the following. Electrons which originate either from trapping or donor levels or from collision-ionized emission centers are swept by the field from a region of high field into a region of low field, where they are subsequently trapped. Light emission then depends on the release of the electrons from these traps in the bulk of the phosphor particle and their return to the region from which they were ionized where recombination with the ionized emission centers occurs. A change in temperature or frequency will change the number of electrons which return and recombine per half-cycle. It is then the rate of release of electrons from trapping levels in the bulk of the phosphor particle that accounts for the major details of the temperature and frequency dependence of the electroluminescent emission of ZnS:Cu phosphors at temperatures below thermal quenching.

Notable exceptions to this point of view are those published by Johnson, Piper, and Williams (2), and Zalm (4). A change in temperature is thought to affect the number of electrons which are thermally released during one half-cycle from the region in which the high, ionizing field is produced and hence alters the configuration of the field in that region.

It is the purpose of this paper to describe experimental results that support the former picture at least in a particular temperature range, and to supply from these results the important details of this process.

Experimental Technique

Glow curves and measurements of the temperature dependence of electroluminescence brightness and the brightness waveform were made in a vacuum-enclosed apparatus similar in structural details to that described by Johnson and Williams (7). For the electroluminescence measurements, a conducting glass plate held the phosphor layer against the heated copper block with an electrode separation of about 50μ. Electrical contact was made to the conducting glass plate through an insulated thimble in the copper block. Temperature measurements were made with a copper-constantan thermocouple in the copper block.

Measurements of the brightness waveform were performed on phosphors imbedded in a slightly conducting medium, tricresyl phosphate, so that the average field across the phosphor was approximately equal to and in phase with the average field applied to the cell (8). The conductivity of the tricresyl phosphate decreases with decreasing temperature, making the above approximation less valid at the lowest temperatures. One set of measurements of electroluminescence brightness as a function of temperature, frequency, and voltage was performed on a binderless layer of the phosphor with the same apparatus. A Corning filter No. 3389 was used in front of a 1P21 photomultiplier to change the response of the photomultiplier to be more nearly uniform to green and blue light.

The output of the photomultiplier tube was either displayed together with the exciting voltage on a Tektronix 532 dual trace oscilloscope, read with a Keithley electrometer, model 210, or in the case of glow curve measurements, fed into a L&N X-Y recorder. The sawtooth and pulsed voltages were generated with various combinations of Tektronix series 160 units and amplified by a d-c amplifier which has a rise time of less than 5 μsec and which can be driven to an output of 700 v peak to peak. Sine waves were generated by a Hewlett Packard wide range oscillator.

Experimental Results

When a repetitive d-c pulse is applied to a cell in which the phosphor (ZnS,ZnO:Cu,Cl) is imbedded in the slightly conducting medium, the light emission shown in Fig. 1 results (8). Almost no light is produced when the field is applied; the great bulk of the emission occurs when the field is removed. If another d-c pulse is added to the repetitive pattern in the opposite direction, as shown in Fig. 2, much greater light emission occurs, most of it when the field, positive or negative, is applied. The amount of light emitted when the field is removed is the same as that for the case of the single polarity pulsing, about 1/20 of the total for alternate polarity pulsing.

Note that this experiment differs from a similar one reported by Zalm (8) in which the brightness waveform and light output of a square-wave d-c field applied to a phosphor suspended in tricresyl phosphate are compared with that produced by a square-wave a-c field of the same peak to peak value and frequency. Thus the size of the ionizing field for the a-c case in Zalm's experiment is only half that for the d-c square wave. In our experiment the ionizing field is the same in both cases.

These observations suggest not only that recombination and light emission is delayed by one half-cycle following the ionization process (8) but also that most of the recombination occurs only when facilitated by a field opposite in sign to that field which produced the ionization. Obviously, a given voltage pulse will perform both of the two functions, ionizing and untrapping, but with respect to different active portions of phosphor particles which are nearer to the negative and positive electrodes, respectively.

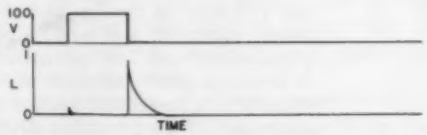

Fig. 1. Brightness waveform resulting from single polarity repetitive pulsing (ZnS,ZnO:Cu,Cl).

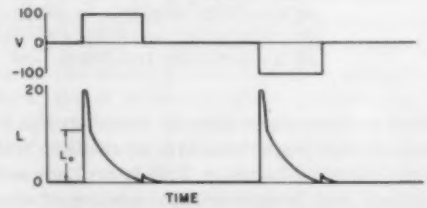

Fig. 2. Brightness waveform resulting from alternate polarity repetitive pulsing (ZnS,ZnO:Cu,Cl).

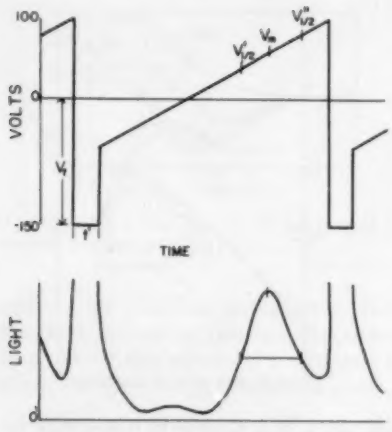

Fig. 3. Brightness waveform produced by the pulse and sawtooth voltage waveform (ZnS:Cu,Al).

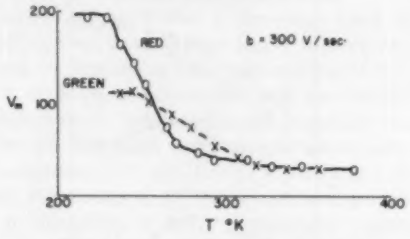

Fig. 4. The voltage of maximum light emission V_m as a function of temperature for two phosphors, ZnS:Cu,Al (green) and ZnS:Cu (red).

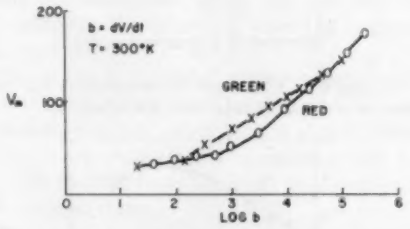

Fig. 5. The voltage of maximum light emission V_m as a function of $dV/dt = b$ at 300°K for two phosphors, ZnS:Cu,Al (green) and ZnS:Cu (red).

If the untrapping field rises linearly with time, as shown in Fig. 3, the light emission rises to a maximum at a particular value of the applied voltage and then falls as the supply of trapped electrons is depleted. The small light peak which occurs before the applied field has passed through zero corresponds to the secondary peak observed with sinusoidal excitation (9) and to the smaller peak produced by alternate polarity pulsing (Fig. 2). Changing the voltage V_f or the duration t' of the ionizing pulse (Fig. 3) alters the size of the subsequent light peak, but does not change its position (V_m).

The voltage V_m at which the light maximum occurs changes negligibly when the voltage waveform is moved up or down with respect to ground. V_m increases with decreasing temperature and with increasing values of $b = dV/dt$. Figure 4 shows the variation of V_m with T for two different phosphors, one a green-blue emitting ZnS:Cu, Al and the other a self-coactivated ZnS:Cu with orange-red emission (10, 11). Figure 5 shows the variation of V_m with b for the two phosphors at room temperature.

The shape of the brightness wave changes with T and with b but not the total light output (to 15%) within the range of these measurements so long as the filling pulse (Fig. 3) remains constant and the untrapping field rises to a voltage which is high enough to return all of the trapped electrons. Figure 6 shows three typical curves of instantaneous light intensity vs. voltage for three different temperatures at constant b for ZnS:Cu,Al. Figure 7 shows three similar plots for different values of b at room temperature for this phosphor. The ordinate in Fig. 7 is L/b so that equal areas under the three curves correspond to equal amounts of light, as they do in Fig. 6.

Figure 8 describes the change in shape of the brightness wave: the difference between the voltages at maximum and half-maximum $V_m - V'_{1/2}$ (Fig. 3) is linear with V_m up to 100 v for both phosphors regardless of whether the temperature or the value of b is held constant. Values of V_m above 100 v occur at low temperatures or very high values of b and hence are not so reliable experimentally.

The glow curve of the ZnS:Cu, Al phosphor consists of a single broad peak with a maximum at

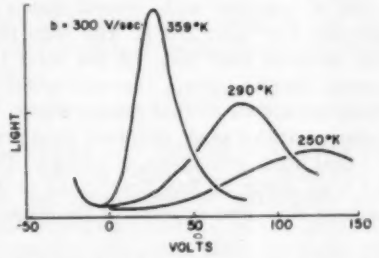

Fig. 6. Three brightness waveforms produced by sawtooth voltage at three different temperatures at a constant value of b (300 v/sec) (ZnS:Cu,Al).

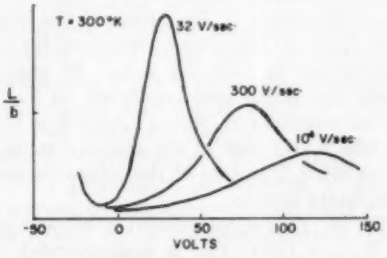

Fig. 7. Three brightness waveforms produced by sawtooth voltage for three different values of b at 300°K. Ordinate (L/b) has been chosen so that equal areas under the curves imply equal total light output (ZnS:Cu,Al).

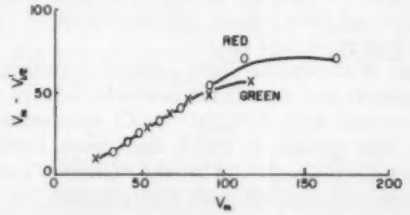

Fig. 8. The quarter width ($V_m - V'_{1/2}$) of the brightness wave produced by sawtooth voltage as a function of the voltage of maximum light emission (V_m). (See text.)

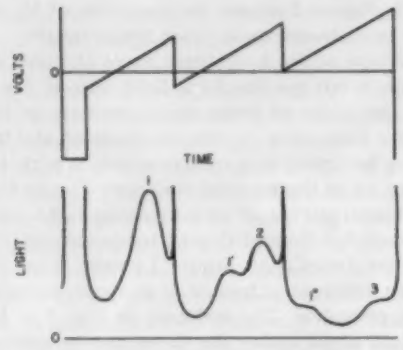

Fig. 9. Brightness waveform produced by pulse and multiple sawtooth voltage waveform, showing additional light peaks (ZnS,ZnO:Cu,Cl).

152°K. The phosphor, which was irradiated with 3650Å u.v. light at the temperature of liquid nitrogen, was heated to 136°K to empty the shallower traps, quenched with liquid nitrogen, and then the glow curve was rerun (12). Examination of the leading edge of the resulting glow peak showed an activation energy of 0.23 e.v. The glow curve of the self-coactivated ZnS:Cu shows a large, complex peak at 388°K together with several much smaller peaks between 140° and 250°K. The high temperature peak contains over 80% of the total thermoluminescence despite strong thermal quenching of the photoluminescence at that temperature. The activation energy of this peak, obtained by a procedure similar to that described above, is 0.52 e.v. The most important trap depth of ZnS,ZnO:Cu,Cl is 0.21 e.v. This phosphor was used in some of the experiments below.

Although the shape of the brightness waveform produced by alternate polarity pulsing (Fig. 2) is complicated by the effect of the fast rise time of the pulses, some measurements were made on a ZnS, ZnO:Cu,Cl phosphor of the value of the brightness intercept L_o and of the time $t_{1/2}$ required for the light emission to fall to half the value. In one experiment with the pulse pattern shown in Fig. 2, the value of the negative or "filling" pulse was held constant at 100 v and that of the positive pulse varied from 25 to 250 v. The data fit the following empirical equations quite closely:

$$L_o = V_+/20 \quad (L_o \text{ in convenient arbitrary units})$$

$$V_+ t_{1/2} = 1200 \quad (t_{1/2} \text{ in milliseconds})$$

In another experiment with the same pulse pattern, both pulses were set at 100 v and $t_{1/2}$ measured as a function of temperature from 280° to 330°K. When log $t_{1/2}$ was plotted against $1/T$, a good straight line was obtained with a slope corresponding to an activation energy of 0.23 e.v.

Figure 9 shows the light pattern resulting from the application of a multiple sawtooth voltage waveform to a cell with ZnS,ZnO:Cu,Cl with conducting binder. The voltage at which light peak 1 occurs is the same for peaks 1′ and 1″, the voltage V_m of peak 2 is larger and that for peak 3 larger still.

To measure the temperature dependence of electroluminescent brightness at different voltages and frequencies over as wide a temperature range as possible, a binderless layer of ZnS,ZnO:Cu,Cl phosphor was used. The results are summarized in Fig. 10. Figure 10a shows four brightness-temperature curves that illustrate the range of frequencies (5 cps to 50 kc) and voltages (150-700 v) which were employed and thus to point out the extremes in the variation of average brightness B with temperature which were encountered. Figure 10b shows the change in the temperature variation of brightness

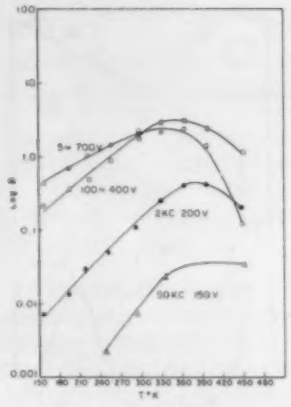

Fig. 10a. Log B as a function of temperature for several combinations of frequency and voltage (ZnS,ZnO:Cu,Cl).

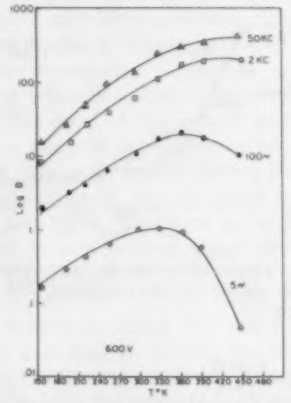

Fig. 10b. Log B as a function of temperature for different frequencies at a single voltage (ZnS,ZnO:Cu,Cl).

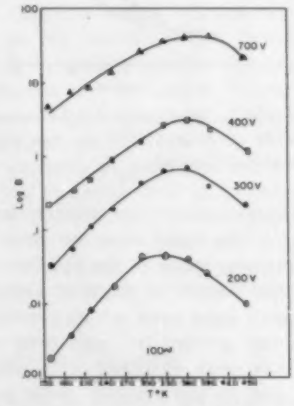

Fig. 10c. Log B as a function of temperature for different voltages at a single frequency (ZnS,ZnO:Cu,Cl).

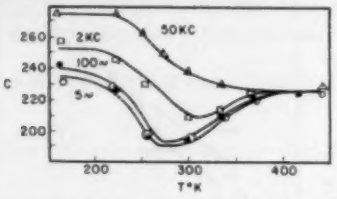

Fig. 11. Values of c (see text) as a function of temperature for several frequencies (ZnS,ZnO:Cu,Cl).

with frequency at constant voltage; Fig. 10c shows the change with voltage at constant frequency. Figure 11 is a plot of the values of c obtained at each temperature and frequency, where c is given by (4)

$$B = B_0 \exp\ (-c/\sqrt{V})$$

Discussion and Interpretation

As shown in Fig. 6 and 7, the total light emitted per half-cycle, for the voltage waveform diagrammed in Fig. 3, is approximately (15%) independent of both temperature and the value of b. This observation indicates quite strongly that the variation of B/f with both temperature and sinusoidal frequency f is not due to a frequency or temperature dependence of the excitation process but rather to the effect of these parameters in somehow limiting the number of electrons which can return from the bulk of the phosphor particles to the high field region where ionization occurs. To illustrate how this limitation can affect the average steady-state brightness, the following model is proposed. Assume and define:

1. There are n_e "mobile" electrons which emerge from and return to the high field region during each cycle in the phosphor particle at a steady state.

2. There are N_T electrons trapped in the bulk of the particle distant from the high field region which remain trapped there.

3. There are $N_+ = N_T + n_e$ ionized recombination centers in the high field region.

4. αn_e electrons recombine with ionized emission centers and this number of photons is emitted. $\alpha = N_+ X$, where X is proportional to the capture cross section of the ionized recombination centers.

5. βn_e electrons fill empty shallow traps or donor sites in the high field region. Field ionization of these electrons produces the exhaustion barrier which constitutes the high field region (4).

6. γn_e electrons fill empty deep traps or donor sites in the high field region (13).

7. At a steady-state condition as many recombination centers are ionized by electrons released from deep donors or traps and accelerated by the field as recombined during the previous half-cycle.

8. Of the $N \equiv N_T + n_e$ electrons in the bulk of the phosphor particle prior to the return step, only a fraction $\Psi = \Psi\ (T,f,V) = n_e/(n_e + N_T)$ have sufficient time and thermal activation to return.

9. There are many more shallow than deep donor sites or traps in the high field region, and their relative concentration is constant.

We then have the following:

$$\alpha + \beta + \gamma = 1 \qquad [1]$$

From Assumption 7, [cf. Ref. (4)]

$$\alpha n_e = \gamma n_e \exp\ (-c'/\sqrt{V}) \equiv \gamma n_e F \qquad [2]$$

From Assumption 9

$$\beta/\gamma = C\ \text{(const.)} >> 1 \qquad [3]$$

From Eqs. [1], [2], and [3]

$$\alpha = \frac{1}{1 + \dfrac{C+1}{F}} = \frac{F}{F + C + 1} \sim \frac{F}{C} \qquad [4]$$

From Assumptions 8, 3, and 4

$$\alpha = (X/\psi)\ n_e \qquad [5]$$

From Eqs. [5] and [4] we have for the equilibrium number of mobile electrons

$$n_e = (\psi/X)\ (F/C) \qquad [6]$$

Since the light emitted per half-cycle B/f is proportional to n_e, it follows that

$$B/f \propto (\psi/X)\ (F/C)^2 \qquad [7]$$

or

$$B/f \propto (X/\psi)\ n_e^2 \text{ (Assumptions 3, 4, and 8)} \qquad [8]$$

Equation [7] shows that light output per cycle B/f is proportional both to the usual ionization probability factor

$$F^2 = \exp\ (-2c'/\sqrt{V}) = \exp\ (-c/\sqrt{V})$$

and to a factor ψ, the fraction of trapped electrons returning from the bulk. Thus a reasonable picture based on the assumption of incomplete return of electrons trapped in the bulk of the phosphor particle is possible, consistent with the basic principle that when a steady state is reached as many electrons must return to the recombination or high field region as left that region during the previous half-cycle. It is interesting to note that this particular model also shows B/f to be proportional to n_e^2 (Eq. [8]) provided ψ is a weak function of the operational parameters under consideration, such as voltage, in agreement with the conclusions of Lehman (15) from loss measurements.

The nature of the function $\psi = \psi\ (T,f,V)$ is then an important question to be resolved, in particular the role played by the time-varying field in facilitating the return of the trapped electrons. Thornton (6) assigns to the field the function of lowering the effective trap depth E_0 by an amount $\mathcal{E}aV/l$, where a is the average trap separation, V the applied voltage, $\mathcal{E}$ the electronic charge, and l the cell thickness. The rate of recombination is assumed to be proportional to the rate of field-controlled thermal release of the trapped electrons. The instantaneous light output L is then given by[1] (6)

$$L \propto -\frac{dn}{dt} = sne \exp\left(-\frac{E - \mathcal{E}aV/l}{kT}\right) \qquad [9]$$

[1] Actually we have $L \propto \alpha n_e(t) = XN_+ n_e(t)$, and $-dn/dt \propto n_e(t)$, where $2n_e = \int_0^{1/f} n_e(t)\,dt$

Since we have assumed that only a small fraction of the returning n_e electrons recombine with the N_+ ionized activators, N_+ is a weak function of time so that $L \propto -dn/dt$.

Here n is the number of trapped electrons and s is a frequency factor or, more simply, a porportionality constant. Substituting $V = bt$, integrating, and setting $dL/dt = 0$ we have

$$V_m = \frac{E_o}{(\delta a/l)} - \frac{kT}{(\delta a/l)} \ln \frac{skt}{(\delta a/l)b} \qquad [10]$$

$$V_m - V'_{1/2} = 1.46 \frac{kT}{(\delta a/l)} \qquad [11]$$

where V_m and $V'_{1/2}$ are defined as shown in Fig. 3. Application of Eq. [10] to the experimental results shown in Fig. 4 and 5 for the ZnS:Cu,Al gives $E_o = 0.53$ e.v. and $a = 400$Å, corresponding to a trap concentration of 2×10^{16} cm^{-3}; the glow curve of this phosphor shows no traps of this depth. The most important glow peak corresponds to a trap depth of 0.23 e.v. Equation [11] requires $V_m - V'_{1/2}$ to be independent of b and to increase with temperature, contradicting the facts as shown in Fig. 6, 7, and 8, which show that $V_m - V'_{1/2}$ *decreases* with temperature and *increases* with b.

The other possible function of the field is that of simply sweeping thermally untrapped electrons back into the recombination region. This role has been used by Alfrey and Taylor (1) and by Zalm (8); the latter employed this model to construct a simple theory of the shift in phase of the brightness waves with respect to that of the exciting voltage as a function of frequency and voltage. We add to Zalm's expression, viz., $L \propto -dn/dt = nAV$, a thermal activation factor giving instantaneous light emission L

$$L \propto -dn/dt = nAV \exp(-E_o/kT) \qquad [12]$$

where V is the applied voltage and A is a proportionality constant which contains a mobility factor. The factor $n \exp(-E_o/kT)$ represents the number of electrons in the conduction band which are at any instant in thermal equilibrium with the trapped electrons n. We assume that the time constant for establishing this equilibrium is very short compared to $1/f$, at least for ordinary frequencies. For $V = bt$ we have

$$V_m = \sqrt{b/A} \exp(E_o/2kT) \qquad [13]$$

$$V_m - V'_{1/2} = 0.69\, V_m \qquad [14]$$

Experimentally we find that if we replot the data from which Fig. 4 was drawn for ZnS:Cu, Al in the form of log V_m vs. $1/T$, as required by Eq. [13] (Fig. 12) a straight line is obtained between 260° and 340°K, the slope of which yields from Eq. [13] a value of $E_o = 0.2$ e.v., in good agreement with the glow curve data for this phosphor. Similar treatment of the ZnS:Cu data gives $E_o = 0.4$ e.v., (240°-290°K) while the value obtained from the analysis of the glow curve described above is 0.52 e.v. Below the temperature range over which these activation energies apply, traps are probably ionized more often by collision with conduction electrons than thermally, hence V_m does not increase with further decrease in temperature. Note that the maximum value of V_m is 190 volts for ZnS:Cu and 107 for ZnS:Cu,Al; these values have roughly the same ratio

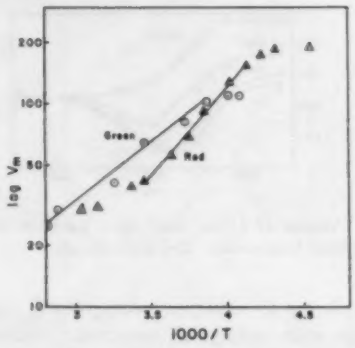

Fig. 12. Log V_m vs. 1000/T for ZnS:Cu, Al (green) and ZnS:Cu (red), from the same data as Fig. 4.

as the important trap depths, in agreement with the above hypothesis. Above this temperature range for this particular value of b (300 v/second) the rate-determining step leading to light emission is probably recombination in the barrier region rather than the supply of electrons to that region. Thus V_m decreases much more slowly with further increase in temperature.

A plot of log V_m vs. log b is linear for both phosphors, but with a slope of 0.3 rather than 0.5 as predicted by Eq. [13]. We can explain this discrepancy if we assume that the mobility of the electrons (contained in the constant A in Eq. [13]) is proportional to $b^{0.4}$, that is, that retrapping is diminished by evacuating the electrons faster. A similar assumption can bring the values of E_o obtained from the theory of field-controlled thermal release into reasonable agreement with experiment (16). However, this theory still does not predict correctly the dependence of $V_m - V'_{1/2}$ on T and b. The second model does predict correctly a linear relation between $V_m - V'_{1/2}$ and V_m (Eq. [14]); the experimental relation is (Fig. 8) $V_m - V'_{1/2} = 0.55\, V_m$, for both phosphors; the observed constant of proportionality differs from the predicted by only 20%.

For the case in which $V = V_o$, a constant value, which is applicable to the alternate pulsing experiments described above, we have for the proposed model of thermal release followed by field assisted return, (Eq. [12])

$$L \propto -dn/dt = n_o A' V_o \exp(-A' V_o t) \qquad [15]$$

where $A' = A \exp(-E_o/kT)$. Experimentally (ZnS:Cu,Cl), we found L_o (Fig. 2) and $t_{1/2}$ to be linear with V_o and that the temperature dependence of $t_{1/2}$ corresponded, as predicted by this model, to an activation energy of 0.23 e.v.

Having thus established a reasonable model for the return of electrons from the bulk, we can proceed to calculate a value of ψ (Eq. [7]) based on this model. The model has been checked against experiments in which electron injection from the conducting medium is possible (8), while Eq. [7] and [8] have been developed from assumptions which are strictly true only for insulated phosphor particles (Eq. [1]). However, it seems unlikely that "injection" significantly alters the nature of ψ.

With sinusoidal excitation the substitution $V = V_0 \sin 2\pi ft$ is made in Eq. [12]; integration yields (3)

$$L \propto n_0 V_0 A' \sin 2\pi ft \exp \mu \ (\sin^2 \pi ft) \qquad [16]$$

where

$$\mu = \frac{A'V_0}{\pi f} = \frac{AV_0}{\pi f} \exp \ (-E_0/kT)$$

also[2]

[2] n_0 is the total number of electrons trapped in the phosphor bulk at $V = 0$.

$$\frac{B}{f} = \int_0^{1/f} L dt \propto 2n_0 \ (1 - e^{-\psi}) = 2n_0$$

Therefore this model requires that the value of the factor ψ in Eq. [7], the fraction of the electrons trapped in the particle bulk which are returned each half-cycle, be proportional to $(1 - e^{-\psi})$. Note that at lower frequencies, high voltages, and high temperatures the value of ψ approaches unity, so that the over-all voltage dependence is exp $(-2c'/\sqrt{V}) =$ exp $(-c/\sqrt{V})$; at higher frequencies, lower voltages, and lower temperatures, ψ approaches μ, so that the voltage dependence of brightness is V exp $(-c/\sqrt{V})$. This latter dependence gives a higher absolute value to the slope of a plot of ln B vs. $1/\sqrt{V}$ which is approximately equal to $c + 2\sqrt{V}$.

For a binderless layer or for phosphor plus insulating binder, the supply of available electrons, $N_T + n_0$, can be regarded as independent of frequency since this supply is limited to sources within the particles themselves, which is, of course, not the case with conducting binder (4, 8). The excitation probability $F = \exp \ (-c'/\sqrt{V})$ is probably nearly independent of frequency for ordinary frequencies. The data in Fig. 11 indicate that the minimum value of $c = 2c'$ (*see* Eq. [2], [9]) obtained at each frequency, hence the closest to the actual value of $2c'$ is very nearly the same only at 5 and 100 cps, where $c = 195$; at 2 kc, $c = 210$, and at 50 kc, $c = 230$. Evidently the high-field region requires a small but finite build-up time. The difference between the highest and lowest values of c indicated in Fig. 11 is 44 units for 5 cps, 50 for 100 cps, 45 for 2 kc, and 50 for 50 kc. For $\overline{V} = 500$ volts, the predicted difference, $2\sqrt{\overline{V}}$, is 45 units, probably within experimental error of observed values. The maximum difference in c shown in Fig. 11 is 80 units, so that we must assume that c' increases somewhat with frequency.

The increase in c (Fig. 11) with T after passing a minimum at moderate frequencies probably arises from the increased diffusion of holes from the barrier, decreasing the barrier field at a given voltage (4). To show that the function $\psi = 1 - e^{-\psi}$ correctly predicts the temperature dependence of the electroluminescent brightness B, we multiply the data from which Fig. 10 was taken by the factor

$$\frac{e^{c(f)/\sqrt{V}}}{f}$$

Four such sets of normalized data are shown in Fig. 13. The solid lines correspond to the function

$$B = 700 \ (1 - e^{-\psi})$$
$$\mu = 50 \ (V/f^{0.6}) \exp \ (-E_0/kT)$$
$$E_0 = 0.2 \text{ e.v.}$$

Note that the frequency appears in the fitted equations to the 0.6 power. We have assumed here that the mobility constant A in Eq. [18] is proportional to f^{-1} just as it was necessary to assume that this same constant A (Eq. [14], [15]) is a function of $b = dV/dt$, that is, $A = A_0 b^{0.6}$.

The divergence of the experimental points toward higher brightnesses at the lower temperatures may indicate the onset with decreasing temperature of another thermally sensitive mechanism such as that proposed by Johnson, Piper, and Williams (2) or Zalm (4), which in this case overcomes somewhat the effect of the rapid decrease of the ψ function and in some cases leads to a minimum in the brightness-temperature curve at low temperatures. A second possible explanation is that the emptying of very shallow traps (~0.05 e.v.) contributes appreciably to the electroluminescence at temperatures too low to empty the 0.2-0.5 e.v. traps. Evidence for the existence of such traps has been given by Haake (3).

Summary and Conclusions

Measurements of both (*a*) the size and shape of electroluminescence brightness waves for simple voltage waveforms at different temperatures and voltage rise times, and (*b*) average brightness as a function of temperature, voltage, and frequency for sinusoidal excitation lead to the following conclusions: In agreement with most workers in the field (1, 3, 6), we find that the major effect of temperature on electroluminescence, apart from thermal quenching, is in the transfer of electrons from traps in the low field region in the phosphor particle bulk to ionized emission centers in the high field region. An increase in temperature increases the concentration of conduction electrons in thermal equilibrium with the traps in the low field region, which may then be swept by the applied field into the high field region. The applied field does not appear to lower the trap depths significantly; retrapping before recombination is probably an important factor. Although a single trapping level suffices to explain the major experimental details, Fig. 9 indicates that additional deeper levels are also involved.

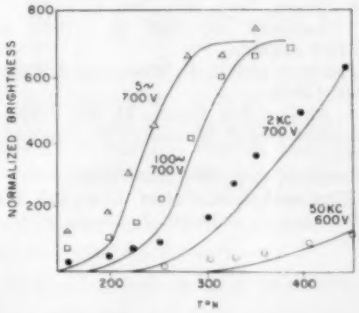

Fig. 13. Normalized brightness (see text) as a function of temperature for several frequencies (ZnS, ZnO:Cu, Cl). Plotted points are experimental; solid lines, theoretical.

Finally, a summary of the over-all trend in temperature dependence of electroluminescence in ZnS:Cu materials can be proposed. At very low temperatures the return of electrons from the phosphor bulk to the barrier is sustained by impact rather than thermal detrapping, so that finite light emission is maintained. Further, if in the barrier some of the electrons in the deeper "shallow" traps are held until the barrier field is at its maximum,[a] then their contribution to the brightness will diminish with increasing temperature so that a minimum in the brightness-temperature relation results, as found by Johnson, Piper, and Williams (2). At low to moderate temperatures the barrier field is relatively unaffected by thermal effects and brightness increases with temperature because of the increased number of electrons that can return to the barrier from the bulk in one half-cycle. This increased return current arises from increased thermal detrapping in the bulk (1). Finally at high temperatures positive holes escaping from ionized activators diffuse from the barrier, decreasing the barrier field (4) or simply become localized at killer centers (3), producing a maximum in the brightness-temperature curve.

[a] This amounts to a lower value of C, the ratio of shallow to deep donors, at these very low temperatures, so that if F is not too much lower (because of the very slightly diminished space charge developed in the barrier), then a higher brightness results than at some slightly higher temperature; viz., Eq. [7],

$$B/f \propto \frac{\psi}{X}\left(\frac{F}{C}\right)^2$$

ψ remains constant in this very low temperature range from impact detrapping. At higher temperatures the small increase in F associated with complete exhaustion of the barrier (3) (more effective acceleration of fewer electrons) may cooperate with increased thermal detrapping in the bulk again to increase the brightness.

Acknowledgment

The writer wishes to thank the following persons for much helpful discussion: Dr. M. Aven, Dr. R. M. Potter, Dr. J. S. Saby, Dr. M. A. Weinstein, and, in particular, Dr. F. E. Williams.

Manuscript received March 13, 1958. This paper was prepared for delivery before the Washington Meeting, May 12-16, 1957.

Any discussion of this paper will appear in a Discussion Section to be published in the June 1959 JOURNAL.

REFERENCES

1. G. F. Alfrey and J. B. Taylor, *Proc. Phys. Soc.*, **B68**, 775 (1956).
2. P. D. Johnson, W. W. Piper, and F. E. Williams, *This Journal*, **103**, 221 (1956).
3. C. H. Haake, *ibid.*, **104**, 291 (1957); *J. Opt. Soc. Amer.*, **47**, 881 (1957).
4. P. Zalm, *Philips Res. Repts.*, **11**, 417 (1956).
5. G. F. Neumark, *Phys. Rev.*, **103**, 41 (1956)
6. W. A. Thornton, *ibid.*, **102**, 38 (1956); *ibid.*, **103**, 1585 (L) (1956).
7. P. D. Johnson and F. E. Williams, *J. Chem. Phys.*, **21**, 126 (1953).
8. P. Zalm, *Philips Res. Repts.*, **11**, 353 (1956).
9. S. Nudelman and F. Matossi, *This Journal*, **101**, 546 (1954).
10. H. C. Froelich, *ibid.*, **100**, 280 (1953).
11. M. A. Aven and R. M. Potter, *ibid.*, **105**, 134 (1958).
12. J. J. Hill and P. Schwed, *J. Chem. Phys.*, **23**, 652 (1955).
13. W. W. Piper and F. E. Williams, *Phys. Rev.*, **87**, 151 (1952); *Brit. J. Appl. Phys.*, **54**, 539 (1955).
14. P. Zalm, G. Diemer, and H. A. Klasens, *Philips Res. Repts.*, **10**, 205 (1955).
15. W. Lehmann, *This Journal*, **103**, 24 (1956); *Optik*, **14**, 319 (1957).
16. F. F. Morehead, Jr., Enlarged Abstracts, Electronics Div., The Electrochemical Society, Washington Meeting, p. 2 (1957) (not published).

SYMBOLS

α	The relative probability of the capture of returning electrons by ionized activators in the high field region.
β	The relative probability of the capture of returning electrons by shallow traps in the high field region.
γ	The relative probability of the capture of returning electrons by deep traps in the high field region.
$\mathcal{E}$	The electronic charge.
μ	$AV_s \exp(-E_s/kT)/\pi f$
ψ	The fraction of electrons trapped in the bulk which return to the high field region.
A	The proportionality constant in Eq. [12], a function of electron mobility.
A'	$A \exp(-E_s/kT)$
a	The average separation of electron traps.
B	The average brightness.
b	dV/dt for sawtooth excitation.
C	β/γ
c	An empirical constant in the relation $B = B_s \exp(-c/\sqrt{V})$
c'	A constant in the expression of ionization probability $\exp(-c'/\sqrt{V})$ in Eq. [2]; $c = 2c'$
E_s	The trap depth.
F	$\exp(-c'/\sqrt{V})$
f	Frequency in cycles per second.
L	Instantaneous light emission.
L_s	Instantaneous light emission at the beginning of a square pulse (Fig. 2).
l	Cell thickness.
N_s	The number of ionized activator centers in the high field region.
N_T	The number of electrons trapped in the bulk of the phosphor which remain trapped throughout the voltage cycle.
n	The number of electrons trapped in the phosphor bulk at a given instant.
n_s	The number of electrons that go back and forth between the phosphor bulk and the high field region.
t'	The duration of the filling pulse (Fig. 3).
$t_{1/2}$	The time required for L to decay to $L_s/2$ for square pulses (Fig. 2).
$\bar{V}$	An "average" voltage for a given voltage range.
V_m	The voltage at which L is maximum for sawtooth excitation (Fig. 3).
$V'_{1/2}$	The voltages at which L is half of maximum for
$V''_{1/2}$	sawtooth excitation (Fig. 3).
X	A constant proportional to the capture cross section of the ionized activators.

Selective Electrolytic Etching of Germanium and Silicon Junction Transistor Structures

I. A. Lesk and R. E. Gonzalez

Electronic Components Division, General Electric Company, Syracuse, New York

ABSTRACT

The electrolytic dissolution of germanium and silicon has been applied to the selective etching of n-p-n and p-n-p junction transistor structures. By employing the electrical properties of p-n junctions internal to the pellet as well as the electrolytic behavior of the n- and p-type germanium or silicon, part of the emitter or collector (or both) of a transistor pellet may be etched away, leaving the rest of the pellet intact. The resulting exposure of part of the base region may be used to locate the base region and facilitate attachment of the transistor base lead.

Germanium and silicon junction transistor structures are in common use at the present time for making both high-frequency and high-power transistors. Methods for producing the n-p-n or p-n-p germanium or silicon bar include the double doped (1), rate grown (2), meltback (3-5), grown-diffused (6), surface diffused (7, 8), and diffused meltback (9, 10) processes. In order to fabricate a transistor from the bar, attachment of a base lead presents a problem common to each of the processes. For most transistors, the base region is so thin (generally 0.0001 in. to 0.0005 in.) that no practical method exists for attaching a lead to the side of it without spilling over onto emitter or collector regions, or both. Even if a contact could be made to the side of the base region only, it would generally be mechanically weak due to the small area of contact involved.

It is desirable to be able to expose part of the large dimension of the base region in a junction transistor structure. This may be used to identify the base, and permit making a base contact of convenient area (and slight penetration), minimizing or eliminating entirely overlap onto emitter and collector regions. This paper describes an electrolytic etching technique that removes germanium or silicon of one conductivity type without attacking the adjoining region of opposite conductivity type. When this etch is used to reduce the size of the emitter (or collector) of a transistor bar without etching the base, the desired geometry results. Electrolytic etching experiments were carried out on meltback [germanium n-p-n (3, 4) and silicon p-n-p (5)] and diffused meltback [germanium p-n-p (10) and silicon n-p-n (9, 10)] pellets. These particular pellet combinations were chosen because of the ease with which the structures could be made. Results should be applicable, however, to transistor bars made by any of the processes mentioned.

Etching Characteristics of Germanium and Silicon and Experimental Techniques

The following characteristics of the electrolytic dissolution of germanium (11) or silicon apply to the selective anodic etching of p-n junction structures.

1. Hole current at the surface is required to remove material.

2. P-n junctions internal to the structure to be etched may have potentials impressed across them due to the driving voltage. Reverse biased junctions block the current flow, and forward biased junctions inject minority carriers according to well-established principles.

3. A p-type layer forms on the surface of germanium or silicon in many electrolytes.

4. When high voltages are applied to n-type material, the surface p-n junction will avalanche, supplying at the surface large numbers of holes which can remove material.

5. Holes may be injected into n-type material by a forward biased p-n junction (item 2 above), or by the application of light.

The electrolyte used must not attack germanium (or silicon), or chemical etching will proceed simultaneously with electrolytic etching. Also, a high conductivity electrolyte appears to give the best preferential attack. Hydrofluoric-acetic acid mixtures worked best of all the electrolytes tried. Glacial acetic acid and 49% hydrofluoric acid were used. The ratio of acids was not critical, so a 1:1 mixture was used for convenience.

In the electrolytic etching circuit, contact to the germanium or silicon bar may be made most conveniently by means of an alloy or solder region. However, simply holding the pellet in a pair of tweezers generally gives satisfactory results. About 50 cc of electrolyte were used.

All etching was done in a dimly lit area to minimize effects of light injection of carriers. No agitation was used, but the violent bubbling at high current densities stirred the electrolyte well and minimized heating at the interface. The etching proceeded continuously, with no passivation phenomena at high current density.

Etching of Uniform Resistivity Pellets

To illustrate the different electrolytic etching rates of n- and p-type semiconductors, uniform re-

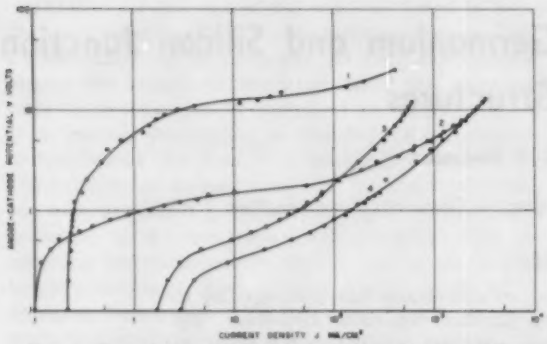

Fig. 1. Electrolytic etching of germanium. Curve 1, 4Ω-cm n-type; curve 2, 0.03Ω-cm n-type; curve 3, 12Ω-cm p-type; curve 4, 0.03Ω-cm p-type.

sistivity pellets of both types were used. Current density vs. applied (anode to cathode) voltage curves for low and high resistivity samples are shown in Fig. 1. The voltages measured in this way give no accurate information about the potential across the semiconductor-electrolyte boundary, which must be measured in order to correlate quantitatively with theory. However, all the essential features are illustrated well enough for application to p-n junction structure etching. Curve 1, for 4Ω-cm n-type Ge, shows the low current saturation and high voltage avalanche breakdown of the p-n junction formed on the surface. Curve 2, for 0.03Ω-cm n-type Ge, shows a smaller saturation current and lower voltage breakdown, as is expected for a (surface) p-n junction on a lower resistivity base. Curve 3, for 12Ω-cm p-type Ge, shows that relatively high currents may be drawn at low voltages due to the plentiful supply of holes and ineffective p-p^+ barrier at the surface. Curve 4, for 0.03Ω-cm p-type Ge, is much the same as curve 3, but more highly conducting due to the larger hole concentration. At high current levels, all currents are becoming limited by the bulk resistance of the pellet. Appreciable current fluctuation with time contributed to the scatter of points. At higher current levels, measurements had to be taken very quickly, because the bars were etching rapidly and hence the current changing continuously. At these levels, a loud crackling noise accompanied the rapid etching.

The results of various etching rates can be seen in Fig. 2. In each pair of pellets, the one on the left is 0.03Ω-cm n-type, the one on the right 0.03Ω-cm p-type. The pair at upper left were etched at 2 v for 15 min. The n-type pellet, drawing little current, is etched very slightly, whereas the p-type sample is severely attacked. The pair at the upper right were etched at 5 v for 4 min. In this case, the n-type sample is now being etched, but not as fast as the p-type bar. At lower left, 10 v for 3 min, and at lower right, 15 v for 1.5 min give almost equal etching rates for the n-type and p-type germanium. Irregularities in the shapes of the etched surfaces come from small voltage drops down the bars and from fluctuations in the position of the liquid surface due to severe bubbling at high current densities.

Electrolytic etching curves for silicon could not be obtained because of the excessive fluctuations

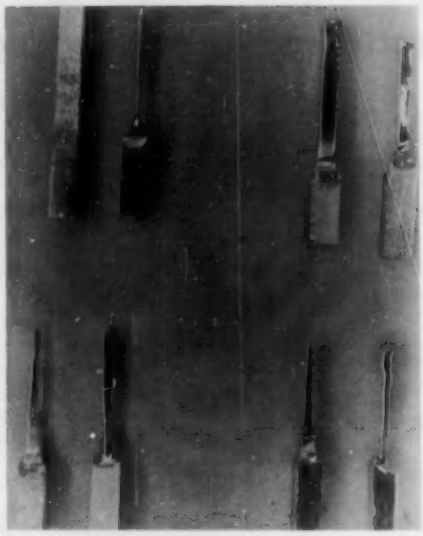

Fig. 2. Electrolytic etching of uniform resistivity pellets. For each pair, left pellet = 0.03Ω-cm n-type, right pellet = 0.03Ω-cm p-type. Unetched section of each pellet is on the bottom. Upper left, 2 v for 15 min; upper right, 5 v for 4 min; lower left, 10 v for 3 min; lower right, 15 v for 1.5 min.

with time of the current at a given voltage. However, since silicon junction structures etch in a manner much the same as those of germanium, the curves for uniform resistivity rods should be similar.

Etching of Transistor Structures

The same techniques may be applied to the selective etching of junction transistor structures. Results are illustrated in the photographs that follow. As an aid to visualizing the contours of the etched regions, a sketch of each case is drawn in Fig. 3. The shape of a meltback or diffused-meltback bar is shown in Fig. 3-1. The unmelted end of the pellet (top) serves as the emitter, and the meltback section (bottom) as the collector. The thin central region is the base, which is generally curved to an extent controlled by the isothermal contours during the melting cycle. The emitter, collector, or both in some cases may be etched to varying degrees, as

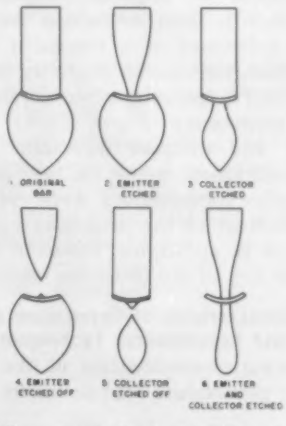

Fig. 3. Outlines of selectively etched transistor pellets

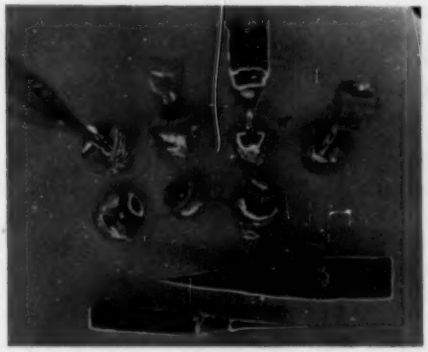

Fig. 4. Germanium n-p-n pellets. Top, emitter etched; center and bottom, emitter etched off.

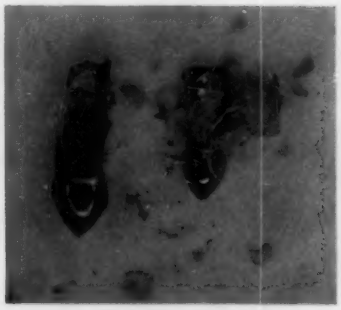

Fig. 6. Silicon n-p-n pellets. Left, immediately after electrolytic etching. Right, emitter pressed after etching to reveal flaky material, under which lies selectively etched pellet as in Fig. 5, top.

indicated in Fig. 3. Contact to the region to be etched was made by a small alloy dot using gold containing antimony for the n-type or gallium for the p-type region. The region to be etched was made the anode. Except where specifically mentioned, base widths are <0.0015 in. for the silicon p-n-p meltback bars, <0.0005 in. for all the other structures. All bars were approximately 0.030 in. square, 0.125 in. to 0.250 in. long. About 0.050 in. was melted in each case.

In order to ascertain that the base region is not attacked, the following commonly used methods of junction location were employed. (*a*) An ac voltage was applied from emitter to collector while the bar was held in a suspension of fine barium titanate particles in benzene. The titanate deposited lightly on the p-type regions and heavily on the p-n junctions. (*b*) A fine thermoelectric probe was moved over the bar surfaces. Direction of the emf determined the conductivity type. (*c*) Metallographic cross sectioning and polishing followed by a slight etch (HNO_3:HF = 4:1) showed up the junctions. Since the base regions were so thin, chipping of the edges limited the applicability of this method. (*d*) Completed transistors were made with base contacts alloyed to the base "shelf" only.

When measured by any of the above techniques, properly controlled electrolytic etching appeared to stop precisely at the base-emitter or base-collector junction.

Figures 4 through 6 deal with germanium and silicon n-p-n bars. The surface-induced p-n junction barrier between the (low resistivity) emitter and the electrolyte breaks down at low voltages and appreciable current flows through the emitter surface, etching it away. The emitter-base p-n junction is in the blocking direction, however, and keeps current from flowing into the base region. Hence the base is not attacked.

Figure 4 shows a group of germanium n-p-n bars. The top four have emitter regions etched (outline 4-2). The three pellets in the middle have emitters etched off (outline 4-4). A small spike of the emitter remains in the center of the base. Two of the separated emitter regions are shown at the bottom. These bars were etched at 20 v anode to cathode for about 30 sec. In Figs. 4, 5, 7, and 8 bars were given a slight chemical etch after electrolytic etching to produce shiny surfaces so that selectively attacked regions would show up better in the photomicrographs.

Figure 5 shows a group of silicon n-p-n pellets. Etching voltages and times are the same as for the germanium n-p-n bars (Fig. 4). The three pellets at the top have partially etched emitters (outline 4-2), while those in the center have emitters etched off (outline 4-4). At the bottom are two of the separated emitters.

A peculiar surface condition resulted only in the case of silicon n-p-n pellets. Visually, the pellets appeared to be unattacked by the electrolytic etch. They retained their shape and metallic appearance. However, slight mechanical pressure to the etched part of the emitter region revealed a flaky material that peeled off easily, exposing the selectively at-

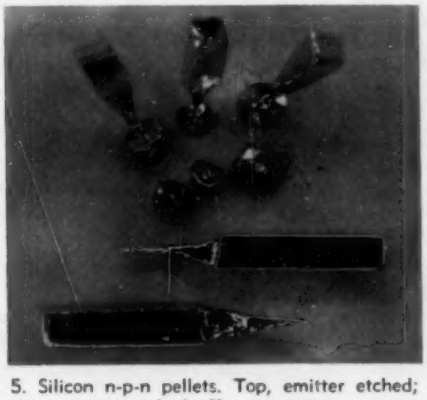

Fig. 5. Silicon n-p-n pellets. Top, emitter etched; center and bottom, emitter etched off.

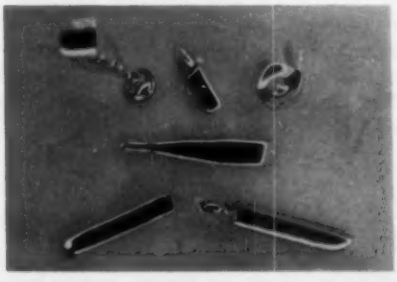

Fig. 7. Germanium p-n-p pellets. Top left, emitter etched; top right, emitter etched off; center, nonselective attack at higher voltages; bottom right, collector etched; bottom left, collector etched off.

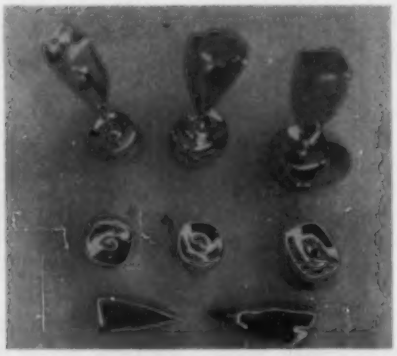

Fig. 8. Silicon p-n-p pellets. Top, emitter etched; center and bottom, emitter etched off.

Fig. 9. Silicon p-n-p pellets with ~0.003 in. bases. Emitter and collector etched.

tacked structure below. Figure 6 shows this effect. The bar on the left appears to be unetched, but the "emitter" surface is easily ruptured, as shown in the bar on the right. Underneath is a structure as shown in Fig. 5 (top). Identification of the flaky material has not been attempted. It is possibly an oxide of silicon. It does not interfere with the selective etching, but gives a wrinkled appearance to the etched part of the emitter region, Fig. 5 bottom.

Figures 7 through 9 deal with germanium and silicon p-n-p bars. To attack preferentially the emitter of such a structure, etching must be done at a voltage low enough so that the level of injected holes into the base by the (forward biased) emitter p-n junction is not large, and the surface p-n junction of the exposed part of the base does not avalanche. If the voltage is too low, etching is very slow. The collector may be attacked selectively by making it the anode instead of the emitter. In such a case, etching can be carried out at much higher current densities because the low injection efficiency of the collector p-n junction does not produce high hole densities in the base region.

A group of germanium p-n-p pellets is shown in Fig. 7. The bar at upper left has the emitter etched (outline 4-2). The bar at upper left was etched with 2 v anode to cathode for several minutes. Longer etching at the same potential results in a separation of the emitter, as shown in Fig. 7, upper right (outline 4-4). In the middle of Fig. 7 is shown a pellet etched in the same way but at a potential of 20 v. Selective attack no longer occurs because of larger injected densities of holes into the base. The collector is on the left. At the lower right in Fig. 7 is shown a p-n-p germanium bar with the collector etched (outline 4-3). Etching in this case was done at 20 v for approximately 1 min. At lower left in Fig. 7 is a pellet with the collector etched off (outline 4-5), which took 20 v for several minutes. The remaining tip of the collector region may be seen at the right end of the pellet.

Figure 8 illustrates selective etching of silicon p-n-p bars. The three top bars have emitters attacked (outline 4-2). They were etched at 20 v for about half a minute. The base and collector are not attacked, as they were for germanium p-n-p pellets at such a high voltage. This is probably due to the low minority carrier lifetime in silicon cooled so fast from its melting point, which results in a lower concentration of holes injected into the base than for the (emitter etched) germanium p-n-p bars. The two center rows show pellets with separated emitters, etched at 20 v for about a minute. Two silicon p-n-p bars with both emitter and collector etched down (outline 4-6) are shown in Fig. 9. Base widths in this case are about 0.003 in. so as to show up in the photograph. Emitter and collector were etched separately. The small dot on the bottom (emitter) of the pellet at left is the gold-gallium alloy contact. The white film on the exposed base of the pellet on the right is deposited during the electrolytic attack. It was easily cleaned off with a slight acid etch (HNO_3:HF=4:1).

Acknowledgment

The photomicrographs were taken by O. G. White and D. B. Blackwood.

Manuscript received Jan. 10, 1958. This paper was prepared for delivery before the San Francisco Meeting, April 29-May 3, 1956.

Any discussion of this paper will appear in a Discussion Section to be published in the June 1959 JOURNAL.

REFERENCES

1. G. K. Teal, M. Sparks, and E. Buehler, *Proc. I.R.E.*, **40**, 906 (1952).
2. R. N. Hall, *J. Phys. Chem.*, **57**, 836 (1953).
3. R. N. Hall, 1955 IRE-AIEE Semiconductor Device Research Conference. June 20, 1955.
4. J. I. Pankove, 1955 IRE-AIEE Semiconductor Device Research Conference. June 21, 1955. Published Transistors I, R.C.A. Laboratories, March 1956, p. 82.
5. I. A. Lesk, AIME Semiconductor Symposium, Feb. 25, 1957.
6. H. Statz, W. Leverton, J. Spanos, 1955 IRE-AIEE Semiconductor Device Research Conference. June 20, 1955; B. Cornelison and W. A. Adcock, 1957 I.R.E. Wescon Conv. Rec. Part 3 p. 22.
7. M. Tanenbaum and D. E. Thomas, *Bell System Tech. J.*, **35**, 1 (1956).
8. C. A. Lee, *ibid.*, **35**, 23 (1956).
9. K. Lehovec and A. Levitas, 1956 AIEE-IRE Semiconductor Devices Research Conference, June 27, 1956. Also, *J. Appl. Phy.*, **28**, 106 (1957).
10. I. A. Lesk, 1956 AIEE-IRE Semiconductor Devices Research Conference, June 27, 1956. Also, I.R.E.-P.G.E.D. Conference, Nov. 1, 1957. To be published I.R.E. Transactions on Electron Devices.
11. A. Uhlir, Jr., *Bell System Tech. J.*, **35**, 333 (1956).

Preparation and Identification of the Thorium Germanides

A. G. Tharp

Department of Chemistry, Purdue University, Lafayette, Indiana

and

Alan W. Searcy and Hans Nowotny

Ceramics Laboratories, Division of Mineral Technology, University of California, Berkeley, California

ABSTRACT

X-ray diffraction studies indicate the existence of at least six thorium germanide phases. The phase of highest germanium content is $ThGe_{2.0\pm0.2}$, tentatively identified as cubic or pseudo cubic with $a_o = 11.72$Å, α-$ThGe_2$, isostructural with α-$ThSi_2$ and α-USi_2, is tetragonal, space group $D^{19}_{4h} - I4/amd$, $a_o = 4.106 \pm 0.003$Å, $c_o = 14.193 \pm 0.005$Å. A phase of composition $ThGe_{1.0\pm0.2}$ (β-$ThGe_2$) has a distorted AlB_2 structure. ThGe is cubic, space group $O^5_h - Fm3m$ (NaCl Type), with $a_o = 6.033 \pm 0.001$Å. Th_3Ge_2 is primitive tetragonal, space group $D^5_{4h} - P4/mbm$, with $a_o = 7.971 \pm 0.004$Å and $c_o = 4.170 \pm 0.003$Å. A phase of composition $ThGe_{0.3\pm0.1}$ gives a complex diffraction pattern. Reactivities with a few common chemical reagents are reported for α-$ThGe_2$, $ThGe_{1.0}$ and $ThGe_2$.

Preparation and structure investigations for a number of silicides and for three germanides of actinon elements have been reported. Brauer and Mitius (1) prepared $ThSi_2$ and reported its structure. The preparations and structure determinations for $ThSi_{1.5}$ ("β-$ThSi_2$"), ThSi, and Th_3Si_2 were carried out by Jacobson, Freeman, Tharp, and Searcy (2). The thorium silicide phases are isostructural with the corresponding uranium silicides whose structures were earlier identified by Zachariasen (3). Zachariasen also found α-$PuSi_2$ and α-$NpSi_2$ to have the α-$ThSi_2$ structure (3). These uranium silicides as well as U_3Si and USi_3 had been first prepared by Kaufmann, Cullity, and Bitsianes (4). The structures of U_3Si (3) and of USi_3 (5, 6) and an isomorphous uranium germanide (6) have also been worked out. Runnals and Boucher (7) have prepared $PuSi_{1.5}$ ("β-$PuSi_2$") and have found it to be identical in structure to $USi_{1.5}$ ("β-USi_2").

The present research reports the first investigation of the thorium germanides.

Experimental

The thorium metal used in these experiments was obtained from the Fairmont Chemical Company as 200 mesh powder. Spectroscopic analysis showed trace amounts of iron and manganese and smaller amounts of a few other heavy metals. Spectroscopically pure germanium was obtained from the Eagle-Picher Company. Germanium oxide was removed by volatilization. From behavior of the thorium on ignition and toward compound formation, 20 to 30 mole % was estimated to be present as inert oxide. All stated compositions were calculated on the assumption that only 80% of the material added as thorium actually was available for reaction.

Preparations were made by direct synthesis from the powdered elements in graphite, alumina, or tungsten crucibles at 1000°-1500°C. Some samples were reground and reheated to insure obtaining equilibrium, and weight losses were assumed to be due to the vaporization of germanium. Cooling rates of different samples varied from 10°C/min to 300°C/min.

X-ray analyses were made with 114.59 mm powder diffraction cameras. Filtered copper K_α radiation was used for all but two preparations. Experimental procedures were similar to those described previously (8).

Identification and Structure of the Phases

Preparations with a Ge:Th ratio near 3.0 (allowing for the thorium oxide present) when heated in the temperature range of these experiments gave strong diffraction patterns of a thorium germanide phase, a faint pattern of germanium, and a medium-strong pattern of ThO_2. Attempts to index the germanide pattern on the basis of known structures were unsuccessful. All spacings were consistent with a cubic unit cell for which $a_o = 11.72$Å, but this large cell may not be the true crystallographic unit; further investigation is contemplated. Indexing of the first 20 spacings is shown in Table I. Although the phase is almost certainly $ThGe_2$, its composition will be designated as $ThGe_{2.0\pm0.4}$ because the exact oxide content of the thorium is unknown.

Samples near composition $ThGe_{2.5}$ showed a strong pattern of a new phase and the strongest lines of $ThGe_{2.0}$. Spacings of this new phase were compared with those of the α-$ThSi_2$ type compounds and were found to be almost identical. The $\sin^2\theta$ values were indexed on the basis of a tetragonal unit cell with $a_o = 4.106 \pm 0.003$Å and $c_o = 14.193 \pm 0.005$Å. Calculated intensities, as shown in Table II, are in good agreement with the observed intensities. The structure has group $D^{19}_{4h} - I4/amd$ symmetry.

Table I. Crystallographic data for $ThGe_{2.02\pm0.4}$

hkl	$\sin^2\theta_{obs.}$	$\sin^2\theta_{calc.}$	$I^*_{obs.}$
110	0.0086	0.0086	w
220	0.0344	0.0344	m
221	0.0388	0.0388	m
320‡	0.0558	0.0560	s
400	0.0689	0.0689	m
410	0.0732	0.0732	w
411, 330	0.0772	0.0776	w
421	0.0905	0.0905	vs
510	0.1119	0.1121	w⁻
520	0.1252	0.1250	w⁻
440	0.1378	0.1380	w⁺
522, 441	0.1422	0.1422	w⁺
620	0.1720	0.1724	w
621	0.1763	0.1768	w
541	0.1814	0.1810	w
630	0.1944	0.1940	w⁻
710, 550	0.2156	0.2157	m
640	0.2236	0.2241	w
641	0.2283	0.2282	w
730	0.2496	0.2500	w⁻

Plus many additional lines.

* w = weak, m = medium, s = strong, vs = very strong.
‡ Coincides with a germanium reflection.

There are four molecules of α-$ThGe_2$ per unit cell with four thorium atoms located in 0,0,0; ½,½,¼; ½,½,½; ½,0,¾; and eight germanium atoms in $0,0,z$; $0,0,-z$; $0,½,(¼+z)$; $0,½,(¼-z)$; $½,½,(½+z)$; $½,½,(½-z)$; $½,0,(¾+z)$; $½,0,(¾-z)$. The value of z is approximately 0.42. The c/a ratio is 3.456, and the calculated density at room temperature is 10.47 g-cm^{-3}.

Samples near composition $ThGe_{1.6}$ gave the diffraction pattern of an entirely new phase. Comparison of this germanide pattern with that for $ThSi_{1.8}$ (defect AlB_2 structure) showed a striking similarity between the two. However, there are more reflections shown by the germanide phase than by the silicide phase. In addition, some germanide reflections are diffuse with sharp lines showing on either side of the diffuse lines. The $\sin^2\theta$ values for the germanide phase index moderately well for a hexagonal unit cell similar to that for $ThSi_{1.8}$. Intensities calculated assuming that $ThGe_{1.6}$, like $ThSi_{1.8}$, belongs to the D^1_{6h} structure are compared with observed intensities in Table III.

Table II. Crystallographic data for α-$ThGe_2$

hkl	$\sin^2\theta_{obs.}$	$\sin^2\theta_{calc.}$	$I_{obs.}$	$I_{calc.}$
101	0.0387	0.0382	w⁺	139.2
004	0.0480	0.0474	m	41.7
103	0.0622	0.0619	s⁻	49.3
112	0.0825	0.0823	s⁺	295.0
105	0.1098	0.1092	s	125.6
200	0.1412	0.1410	m⁺	26.0
116	0.1782	0.1770	w⁻	
211	0.1801	0.1791	s⁻	4.9
107		0.1803		50.3
204	0.1887	0.1884	w⁺	25.9
008		0.1894		4.4
213	0.2027	0.2028	m⁻	39.3
215	0.2501	0.2502	s⁻	68.0
109	0.2749	0.2750	w⁺	14.9
220	0.2807	0.2819	m⁻	31.4
301	0.3207	0.3201	s⁻	4.2
217		0.3212		47.8
224	0.3288	0.3292	w⁺	10.8
208		0.3304		7.4
303	absent	0.3437		
1-1-10	0.3639	0.3655	s diffuse	22.4
312		0.3642		55.4
305	absent	0.3912		
1-0-11	absent	0.3934		
219	0.4146	0.4151	w	16.3
0-0-12	0.4240	0.4248	w⁻	7.8

Table III. Crystallographic data for $ThGe_{1.6}$

hkl	$\sin^2\theta_{obs.}$	$\sin^2\theta_{calc.}$	$I^*_{obs.}$	$I_{calc.}$
001	0.0341	0.0338	w⁻	78
100	0.0489	0.0486	m	646
101	0.0822	0.0824	vs	2605
002	0.1344	0.1346	w	330
110	0.1461	0.1459	m⁺	884
111	0.1796	0.1797	w	72
102	0.1830	0.1832	m	228
200	0.1960	0.1946	w	104
201	0.2267	0.2284	m⁺	564
112	0.2796	0.2805	s⁻	604
003	0.3033	0.3028	w⁻	6
202	0.3259	0.3304	w⁻	90
210	0.3406	0.3405	w⁻	86
103	0.3503	0.3517	m⁻	275
211	0.3734	0.3743	m	494
300	0.4400	0.4378	w⁺	150
113	absent	0.4478		19
301	0.4734	0.4716	w	18
212		0.4751		106
203	0.4934	0.4974	w	167

Plus several additional lines.

* w = weak, m = medium, s = strong, vs = very strong.

The pseudo-hexagonal unit cell contains one molecule of $ThGe_2$ with one thorium atom in 0,0,0 and two germanium atoms in 1/2,2/3,1/2 and 2/3,1/3,1/2. The calculated density at room temperature is 10.51 g-cm^{-3}.

Our data seem best explained by the assumption of a slight distortion of the ideal hexagonal cell in addition to the vacancies in the ideal MX_2 lattice like those noted for $USi_{1.8}$, $PuSi_{1.8}$, and $ThSi_{1.8}$ (2, 7). Assumption of an orthorhombic distortion does not appear to yield the proper calculated spacings. An attempt will be made to index the structure as a monoclinic or triclinic distortion of the hexagonal cell.

Preparations in the $ThGe_{1.33\pm0.3}$ composition range give a diffraction pattern of $ThGe_{1.6}$ and a stronger pattern of a new phase. After being recrushed and reheated at 1500°C for about 2 hr, a sample of composition $ThGe_{1.3}$ gave a diffraction pattern essentially free of $ThGe_{1.6}$. The $\sin^2\theta$ values for this new phase were indexed on the basis of a cubic unit cell. The hkl values are either all even or all odd, suggesting a sodium chloride type lattice. Relative intensities were calculated on the assumption that the symmetry was that of space group O^5_h-Fm3m (NaCl type) with four thorium atoms in 0,0,0,; ½,½,0; ½,0,½; 0,½,½; and four germanium atoms in ½,½,½; ½,0,0,; 0,½,0; 0,0,½. Calculated intensities are in excellent agreement with observed intensities. Table IV is a tabulation of these data. The good fit to the sodium chloride lattice leads one to conclude the phase to be ThGe.

Table IV. Crystallographic data for ThGe

hkl	$\sin^2\theta_{obs.}$	$\sin^2\theta_{calc.}$	$I^a_{obs.}$	$I_{calc.}$
111	0.0492	0.0488	s	137
200	0.0654	0.0651	vs	290
220	0.1307	0.1302	vs	216
311	0.1797	0.1791	s⁻	75
222	0.2697	0.2605	m⁺	36
331	0.3094	0.3093	m⁻	28
420	0.3260	0.3256	s	97
422	0.3910	0.3907	s⁻	74
511	0.4402	0.4396	w	18
333				6
440	0.5199	0.5210	w⁺	26
531	0.5695	0.5698	w⁺	28
600	0.5856	0.5861	m⁺	11
442				46
620	0.6533	0.6533	m	45
533	0.6995	0.6987	w⁻	14
622‡	0.7154	0.7151	m	47
444	0.7800	0.7801	w⁻	17
711	0.8290	0.8289	w⁺	18
551				18
641	0.8451	0.8451	m⁺	61
642	0.9103	0.9101	s	160
731	0.9592	0.9589	m diffuse	76
553				38

[a] w = weak, m = medium, s = strong, vs = very strong.
‡ Remainder of reflections are for CuKα_1 radiation.

The lattice parameter for ThGe was calculated using the sharp reflections in the back reflection region. Calculation from three different diffraction patterns gives the value $a_o = 6.044 \pm 0.001$Å. The calculated density at room temperature is 9.17 g-cm^{-3}.

Samples near composition $ThGe_{0.8}$ gave diffraction patterns showing a weak ThGe phase and a higher thorium phase. This phase was never prepared in the pure state and apparently did not crystallize well. It may be thermodynamically stable over only part of the temperature range studied. The low angle reflection region of the diffraction patterns of the new phase is very similar to that for U_3Si_2. The $\sin^2\theta$ values could be fitted to a unit cell with tetragonal symmetry. Intensities were calculated by use of the assumption that the compound is isostructural with U_3Si_2 and that the atoms are located in positions corresponding to those in the silicide. Table V contains the observed and calculated data. Since agreement is good, these data confirm the formula Th_3Ge_2. The structure is primitive tetragonal with space group D^5_{4h}-P4/mbm symmetry. There are two molecules per unit cell with the thorium atoms located as follows: $2Th_I$ in 0,0,0,; ½,½,0; $4Th_{II}$ in $x,½+x,½$; $-x,½-x,½$; $½+x,-x,½$; $½-x,x,½$; with x approximately equal to 0.18. The four germanium atoms are located in $x,½+x,0$; $-x,½-x,0$; $½+x,-x,0$; $½-x,x,0$; with x approximately equal to 0.39. The lattice parameters are $a_o = 7.971 \pm 0.004$Å and $c_o = 4.170 \pm 0.003$Å. The c/a ratio is 0.523, and the calculated density at room temperature is 10.55 g-cm^{-3}.

Table V. Crystallographic data for Th_3Ge_2

hkl	$\sin^2\theta_{obs.}$	$\sin^2\theta_{calc.}$	$I_{obs.}$	$I_{calc.}$
110	0.0180	0.0187	w⁻	7.0
001	absent	0.0342		3.1
200	absent	0.0374		1.4
210	0.0464	0.0467	m	78.8
111	0.0527	0.0529	m	67.0
201	0.0706	0.0716	vs	286.1
220	0.0749	0.0748	m⁻	79.6
211	0.0808	0.0809	vs	266.9
310	0.0933	0.0935	s	143.8
221	absent	0.1089		0.9
320	0.1216	0.1215	w	20.7
311	0.1277	0.1277	w⁻	7.9
002	0.1365	0.1368	m	57.4
400*	0.1506	0.1497	m	0.7
112	absent	0.1555		1.3
321	absent	0.1557		0.5
410	0.1589	0.1589	m	58.2
330	0.1680	0.1683	w⁻	7.4
202	absent	0.1742		0.5
212	0.1834	0.1835	w	25.5
401		0.1839		7.0
420	0.1872	0.1870	w⁻	14.8
411	0.1934	0.1931	m	63.1
331	0.2021	0.2025	m	78.0
222	0.2106	0.2116	w	34.8

* This reflection corresponds to a ThO_2 reflection.

Table VI. Nearest neighbors and interatomic distances

Compound	Nearest Neighbors	
α-$ThGe_2$	Thorium—	12 Ge at 3.14Å
	Germanium—	6 Th at 3.14Å
		3 Ge at 2.37Å
β-$ThGe_2$	Thorium—	12 Ge at 3.15Å
		6 Th at 4.04Å
		2 Th at 4.22Å
	Germanium—	6 Th at 3.15Å
		3 Ge at 2.34Å
ThGe	Thorium—	6 Ge at 3.022Å
		12 Th at 4.274Å
	Germanium—	6 Th at 3.022Å
		12 Ge at 4.274Å
Th_3Ge_2	Thorium I—	4 Ge at 3.23Å
		8 Th at 3.66Å
	Thorium II—	6 Ge at 3.16Å
		4 Th at 3.66Å
	Germanium—	1 Ge at 2.48Å
		2 Th at 3.23Å
		6 Th at 3.16Å

Samples of higher thorium content give a diffraction pattern for thorium, thorium dioxide, and a new phase of complicated structure. Attempts to index the spacings for the new phase were unsuccessful. Because of the ThO_2 contaminant it is not possible to assign to the phase an accurate composition. On the basis of the composition of samples which gave the best patterns of the known compounds, the compound is believed to be $ThGe_{0.810.1}$. This compound is the only one found whose structure is apparently different from that of a corresponding uranium silicide.

Nearest Neighbor Distances and Coordination Numbers

As can be seen from Table VI, the calculated interatomic distances are compatible with the structures determined for the different compounds. The same coordination numbers are found in α-$ThGe_2$ and $ThGe_{1.0}$ for the theoretical MX_2 structures with the interatomic distances being only slightly different. This observation is interesting because the

arrangement of atoms is quite different. In α-$ThGe_2$ the thorium atoms are contained in a three dimensional network of germanium atoms, and in β-$ThGe_2$ the thorium atoms are between a two dimensional, graphite-like layer of germanium atoms. In ThGe there is only thorium to germanium bonding. In the Th_5Ge_3 structure the thorium I is not equivalent to the thorium II atoms. There is thorium to thorium bonding and the germanium atoms are joined in pairs at approximately their single bond distance. The general structure is one of a layer of thorium atoms contained between layers which contain both thorium and germanium atoms.

It is interesting to note that by removing half of the germanium atoms from β-$ThGe_2$ in an alternate manner, and by shifting the atom positions only slightly, the ThGe structure is obtained. The 111 plane of β-$ThGe_2$ contains an almost identical arrangement of atoms to that found in ThGe.

Reactivity with Common Reagents

The reactivity at room temperature was observed for the $ThGe_{2.0\pm0.4}$, α-$ThGe_2$, and $ThGe_{1.0\pm0.2}$ phases. The other compounds were not tested for reactivity because they were not available as pure phases.

Reactions of the three compounds tested with 5% HCl, concentrated HF, aqua regia, and 10% NaOH were vigorous. Reaction with 30% H_2O_2, 3M H_2SO_4, 18M H_2SO_4, 6M HNO_3, and concentrated HNO_3 proceeded rather slowly. No reaction was observed to take place with 85% H_3PO_4 or 0.1N $KMnO_4$. It is possible that some of the reactivities were affected by the presence of ThO_2 in the samples.

Acknowledgment

This work was supported by the Office of Naval Research.

Manuscript received June 17, 1957. This paper was prepared for delivery before the Chicago Meeting, May 2-6, 1954.

Any discussion of this paper will appear in a Discussion Section to be published in the June 1959 JOURNAL.

REFERENCES

1. G. Brauer and A. Mitius, *Z. anorg. Chem.*, **249**, 325 (1942).
2. E. L. Jacobson, R. D. Freeman, A. G. Tharp, and A. W. Searcy, *J. Am. Chem. Soc.*, **78**, 4850 (1956).
3. W. H. Zachariasen, *Acta. Cryst.*, **2**, 94 (1949).
4. A. Kaufmann, B. Cullity, and G. Bitsianes, *J. Metals* **9**, *AIME Trans.* **209**, 23 (1957).
5. B. R. T. Frost and J. T. Maskrey, *J. Inst. Metals*, **8**, 177 (1953).
6. A. Iandelli and R. Ferro, *Ann. Chim. Applicata, Roma*, **42**, 598 (1952).
7. O. J. Runnalls and R. R. Boucher, *Acta Cryst.*, **8**, 592 (1955).
8. A. W. Searcy and R. A. McNees, Jr., *J. Am. Chem. Soc.* **75**, 1578 (1953).

The Mobilities of the Ions in Fused KNO_3-$AgNO_3$ Mixtures

F. R. Duke and Boone Owens

Institute for Atomic Research and Department of Chemistry, Iowa State College, Ames, Iowa

ABSTRACT

The mobilities of the three ions in fused KNO_3-$AgNO_3$ mixtures have been determined as a function of composition. The mobility of the nitrate ion is insensitive to composition changes; the cations, however, tend toward the mobility of the main constituent cation at each end of the composition scale. Temperature variation has no significant effect on the transport numbers of these ions.

The mobilities of the ions in a $NaNO_3$-$AgNO_3$ mixture have been determined (1). This mixture was ideal in the sense that the ion mobilities are independent of composition. However, since Na^+ and Ag^+ in the pure nitrates have essentially the same mobilities, it was considered advisable to repeat the work using a pair of cations having significantly different mobilities. Thus, a mixture of $AgNO_3$ and KNO_3 was chosen for study.

Experimental

C. P. Reagent Grade salts and pure silver wire were used in the study. The apparatus and techniques used were duplicates of those used in the $AgNO_3$-$NaNO_3$ work (1).

Results and Discussion

The values for the mobility of the two cations relative to the anion are expressed in terms of ϕ (2), where $\phi = 1 - t_{Ag^+} - N_1^\circ t_-$, where N_1° is the original mole fraction of $AgNO_3$ and t_- is the transport number of NO_3^-. If t_- is taken as zero, then $\phi = t_{K^+}$. A plot of ϕ vs. N_1 is shown in Fig. 1. It can be seen that there is some deviation from linearity, the K^+ being less mobile than the Ag^+.

The results of the volume change across a membrane during electrolysis of mixtures of $AgNO_3$ and KNO_3 serve to fix all three of the transport numbers when combined with the ϕ data.

Table I. Volume change of cathode per equivalent, ϕ, and t_- data for various mixtures of KNO_3-$AgNO_3$

Mole fraction $AgNO_3$	ϕ	V_c/Z (cm³/Eq.)	t_{Ag^+}	t_{K^+}
1.00	—	−1.5±2.6	0.72±.06	0.0
0.75	0.21±.01	−0.5±0.6	0.56±.03	0.15±.03
0.50	0.41±.01	−1.2±2.0	0.43±.04	0.25±.04
0.25	0.70±.01	−2.9±0.5	0.20±.03	0.40±.03
0.00	—	−0.9±1.3	0.0	0.60±.03

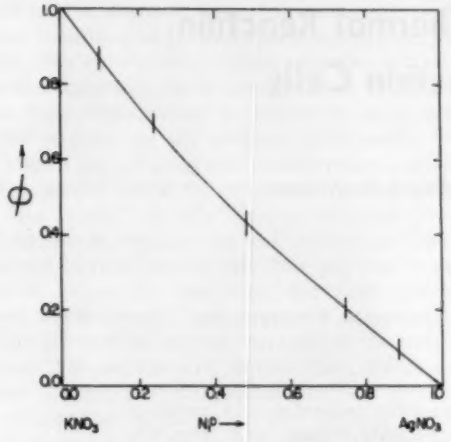

Fig. 1. ϕ vs. composition in the system $AgNO_3$-KNO_3

$$\frac{\Delta V_c}{Z} = \overline{V}_{Ag} + (t_{Ag^+} - 1)\overline{V}_{AgNO_3} + t_{K^+}\overline{V}_{KNO_3}$$

where V_c is the volume change of the catholyte, Z is the current, and the $\overline{V}$'s are the molar volumes of the species indicated. Molar volumes in this system are very nearly identical with partial molal volumes (3). In the pure salts, both transport numbers may be calculated from the volume-change equation (4). Table I shows values of $(\Delta V_c)/Z$ for the pure salts and salt mixtures.

The transport numbers calculated from the ϕ and ΔV_c equations are listed in Table I.

The ionic equivalent conductances, λ_i, are calculated from the total equivalent conductivities and the transport numbers using the equation $\lambda_i = \lambda t_i / N_i$, where λ is the total equivalent conductance, t_i the transport number, and N_i the equivalent fraction. The total equivalent conductivity of the mixture was calculated from the density data of Bloom and Rhodes (3) and from specific conductivity data obtained in this laboratory (5). These data are listed in Table II.

Table II. Ionic equivalent conductivities in the system $AgNO_3$-KNO_3 at 350°C

Mole fraction $AgNO_3$	λ	λ_{Ag^+}	λ_{K^+}	$\lambda_{NO_3^-}$
0.00	36.4	—	21.7±1.1	14.7±1.1
0.25	40.7	32.6±4.9	21.7±1.6	16.3±1.0
0.50	45.6	39.2±3.6	22.8±3.7	14.6±1.8
0.75	50.3	37.6±2.0	30.2±6.0	14.6±1.0
1.00	54.8	39.7±3.5	—	15.6±3.3

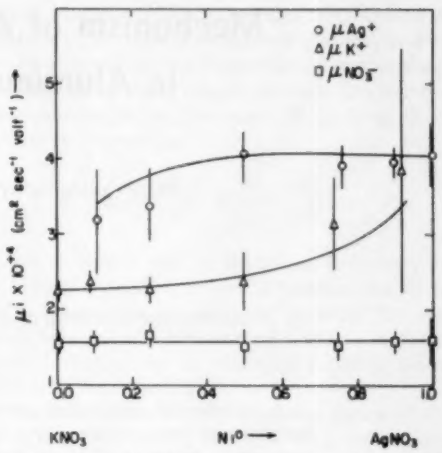

Fig. 2. Ionic mobilities in the system $AgNO_3$-KNO_3 at 350°C.

The mobilities, μ_i, are calculated using the equation $\mu_i = (\lambda_i)/96500$ and are plotted as functions of composition in Fig. 2.

The precision in the determination of mobilities becomes poor at high dilution of the ions because they carry so little of the total current. However, the mobility curves for the cations suggest that, at high dilution, the mobility of the minor constituent approaches that of the major constituent; this, in turn, suggests that some sort of chain mechanism involving more than one ion of the same kind is responsible for the normal mobility in the pure salts.

Manuscript received March 24, 1958. Contribution No. 605. Work was performed in the Ames Laboratory of the U. S. Atomic Energy Commission.

Any discussion of this paper will appear in a Discussion Section to be published in the June 1959 JOURNAL.

REFERENCES

1. F. R. Duke, R. W. Laity, and B. Owens, *This Journal*, **104**, 299 (1957).
2. P. M. Aziz and F. E. W. Wetmore, *Can. J. Chem.*, **30**, 779 (1952).
3. H. Bloom and D. C. Rhodes, *J. Phys. Chem.*, **60**, 791 (1956).
4. F. R. Duke and B. Owens, *This Journal*, To be published.
5. F. R. Duke and R. A. Fleming, *ibid.*

Mechanism of Anode Thermal Reaction in Aluminum Reduction Cells

Harry Stern

State College of Washington, Pullman, Washington

and

G. T. Holmes

Aluminum Company of America, New Kensington, Pennsylvania

ABSTRACT

A number of aluminum production potlines were subjected to a series of counter-emf tests wherein the decay of the reversible voltage with time was measured. Analysis of these data indicate that the reversible voltage during electrolysis is associated with an intermediate compound C*O on the anode surface which decomposes chemically to CO_2 by a reaction of approximately second order. At a current density of 0.95 amp/cm² and a temperature of 971°C, the reversible voltage is 1.45 v. The free energy of formation of C*O at 971°C from C and O_2 at 25°C is —67,150 cal/g mole.

The over all chemical reaction for the reduction of alumina as carried out normally in electrolytic cells by the Hall process is

$$2Al_2O_3 + 3C \rightarrow 4Al + 3CO_2 \qquad [1]$$

as judged from the initial reactants and final products. Experimental evidence is presented here to support the view that carbon dioxide is formed by a thermal reaction between the carbon anode and oxygen adsorbed on the carbon surface and that the actual electrochemical reaction should be written

$$2Al_2O_3 + 6C \rightarrow 4Al + 6C^*O \qquad [2]$$

where the symbol C*O represents oxygen adsorbed on the carbon surface. Specifically, it will be shown that the reversible decomposition voltage of the cell depends primarily on the concentration of adsorbed oxygen on the anode surface and not on the concentration of CO_2 nor on concentration gradients within the electrolyte. It is postulated that reaction [2] is followed by

$$6C^*O \rightarrow 3CO_2 + 3C \qquad [3]$$

to give the over-all reaction [1] and it will be shown that reaction [3] is a thermal reaction proceeding at a rate corresponding to approximately a second order reaction.

Experimental

The experimental measurements consisted entirely of a number of counter-emf tests performed on a series of production potlines. In a counter-emf test, a line of normally operating cells is suddenly disconnected from its operating electrical power source, and the open-circuit voltage generated by the resulting line of voltaic cells is measured as a function of time. The result is a recorded curve of the potline counter-emf on open circuit as it decays with time. The number of volts per pot is determined by dividing the potline counter-emf by the number of pots (cells) in the line.

The tests were performed at the Wenatchee, Washington, plant of the Aluminum Company of America. Tests were performed only on potlines that showed no anode effect for a considerable period before the test, and in which all of the cells were apparently operating normally. Of course it is probable that conditions varied somewhat from cell to cell. By taking a potline voltage and dividing by the number of cells in the line, an average cell voltage is obtained.

Fig. 1 is a diagram of the electrical connections used. Before the potline is tripped (disconnected from its power source), the d-c source shown is adjusted to the approximate value of the counter-emf of the potline which is about 200 v. This puts the pointer on the voltmeter at about the desired reading and greatly reduces overswing and "hunting." When the potline is tripped, the "b" contacts on the cathode breaker close. The coil of C_1 is energized by the "b" contact closing. C_1 closes and energizes the coil of C_2. When C_2 operates, the d-c

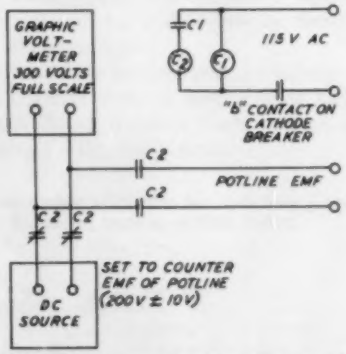

Fig. 1. Electrical connections for counter-emf tests

source is disconnected from the voltmeter and the potline counter-emf is simultaneously applied to the meter. The $C_1 - C_2$ relay chain provides a time delay which prevents the voltmeter from being placed across the potline during the inductive surge following the tripping of the potline. This surge, which was shown by oscillograph measurements to reach 1500 v, would cause the pointer to swing off scale and then "hunt." In this manner only the first few milliseconds of reading are lost, but the potline emf could not be read during this time anyway since the surge is caused by the high d-c field collapsing around the bus bars.

Time is taken as zero at the instant the potline is tripped. The counter-emf at time zero, which corresponds to the reversible decomposition voltage of the cells at the operating current density and temperature, could not be read directly for the reasons given above. Values for the reversible decomposition voltage were obtained by extrapolation of the voltage decay curves back to zero time using an analytical procedure as will be shown.

Data from these tests are given in Table I. In Table I, the time in minutes could be determined readily from the meter chart to 0.001 min and the voltage per pot to 0.01 v. An estimate of the next decimal place is given for each reading, although the correlation does not depend on this estimate. The response time of the meter was very small and would not affect the reading in view of the gradual drop of the voltage, except possibly during the first few seconds.

Theoretical Analysis

The voltaic cells generate a voltage which corresponds to the reverse of the postulated reaction [2], that is

$$2Al + 3C^*O \rightarrow Al_2O_3 + 3C \qquad [4]$$

The open-circuit (reversible) voltage generated by reaction [4] is given by the equation

$$E = E_\circ + \frac{RT}{nF} \ln \frac{a^2_{Al}\, a^3_{C^*O}}{a_{Al_2O_3}\, a^3_C} \qquad [5]$$

where E is the voltage of the cell, $E_\circ$ is the voltage that would be generated if all reactants and products of reaction [4] were in their standard states (arbitrarily chosen), and the a values are the activities of the reactants and products based on these standard states. R equals 8.313 joules/g mole °K; T equals °K; F equals 96,500 coulombs/g equiv; n equals 6 g equiv/g mole Al_2O_3; and ln equals log to the base e.

Since neither the aluminum nor the carbon are in solution phase, their activities are 1 and equation [5] becomes

$$E = E_\circ + \frac{RT}{nF} \ln \frac{a^3_{C^*O}}{a_{Al_2O_3}} \qquad [6]$$

Since the selection of standard states is arbitrary, let us select the conditions at time O, that is, when the electrical circuit is broken, as the standard states. Then let

$$a_{C^*O} = \frac{p}{p_\circ} \text{ and } a_{Al_2O_3} = \frac{c}{c_\circ}$$

where $p_\circ$ and $c_\circ$ are the fugacities of C^*O and Al_2O_3, respectively, at time O (standard states), and p and c are the corresponding fugacities at any subsequent time t when the open circuit voltage has decayed to E after starting with a value of $E_\circ$ at time O. Then equation [6] becomes

$$E = E_\circ + \frac{3RT}{nF} \ln \frac{p}{p_\circ} - \frac{RT}{nF} \ln \frac{c}{c_\circ} \qquad [7]$$

If now p and c can be found as functions of the time t, then equation [7] will express the decay of E with t and can be checked against the experimental data of the counter-emf tests. Before this is done, however, let us examine possible means of simplifying equation [7].

If we assume tentatively that the decay of E with time is due *entirely* to the rise in c caused by the equalization of the Al_2O_3 concentration gradient near the electrodes, then the p term can be eliminated and Eq. [7] becomes

$$E = E_\circ - \frac{RT}{nF} \ln \frac{c}{c_\circ} \qquad [8]$$

On the other hand, if we assume tentatively that the decay of E is due *entirely* to the fall in p caused by reaction [3], then the c term can be eliminated and equation [7] becomes

$$E = E_\circ + \frac{3RT}{nF} \ln \frac{p}{p_\circ} \qquad [9]$$

To test the validity of either of these assumptions, Eqs. [8] and [9] will be tested against the experimental data. If neither [8] nor [9] fits the data, then we may conclude that both effects are important and will be forced to use the more complex Eq. [7].

Test of Diffusion Hypothesis

Let us test Eq. [8] first. For the relation between c and t, assume that the change of c with time is due to the equalization of the Al_2O_3 concentration gradient formed near the electrodes during electrolysis. This equalization takes place by diffusion and convection after the electric current is shut off. The rate of equalization may be written in the form

$$\frac{dc}{dt} = K(c_b - c) \qquad [10]$$

where K is the mass transfer coefficient and will depend on the degree of turbulence as well as on the diffusivity of the bath at the electrode surface, c_b is the fugacity of the Al_2O_3 in the bulk of the bath, and c is the fugacity of the Al_2O_3 at the electrode surface. If we assume that K is a constant (a rough approximation especially near time O) we may write

$$\int_{c_\circ}^{c} \frac{dc}{c_b - c} = K \int_o^t dt \qquad [11]$$

where $c_\circ$ is the fugacity at the electrode surface at time O and c is the fugacity of the electrode surface at any subsequent time t. Integrating and rearranging Eq. [11] gives

$$c = \frac{c_b(e^{Kt} - 1)}{e^{Kt}} + c_\circ \qquad [12]$$

Table I. Decay of voltage with time for five counter-emf tests

Test No. 1 Prebake anode Current density 0.93 amp/cm² (before time O) Temperature, 971°C		Test No. 2 Prebake anode Current density 0.90 amp/cm² (before time O) Temperature, 973°C		Test No. 3 Prebake anode Current density 1.22 amp/cm² (before time O) Temperature, 976°C		Test No. 4 Prebake anode Current density 0.93 amp/cm² (before time O) Temperature, 967°C		Test No. 5 Soderberg anode Current density 0.79 amp/cm² (before time O) Temperature, 968°C	
t Min	E Volts/pot	t Min	E Volts/pot	t Min	E Volts/pot	t Min	E Volts/pot	t Min	E Volts/pot
0.0333	1.324	0.0130	1.437	0.0167	1.412	0.0319	1.305	0.0833	1.355
0.0639	1.296	0.0269	1.407	0.0833	1.303	0.0667	1.277	0.1667	1.331
0.1194	1.268	0.0425	1.380	0.1667	1.269	0.1194	1.248	0.2500	1.318
0.2152	1.239	0.0694	1.352	0.2500	1.244	0.1931	1.220	0.3300	1.289
0.3055	1.211	0.1237	1.324	0.3333	1.227	0.2569	1.191	0.4167	1.273
0.4444	1.183	0.2222	1.296	0.4167	1.202	0.2972	1.163	0.5000	1.248
0.7361	1.155	0.4053	1.268	0.5000	1.185	0.3417	1.135	0.5833	1.231
1.0693	1.126	0.7109	1.239	0.5833	1.168	0.4222	1.106	0.7500	1.223
1.764	1.098	1.4526	1.211	0.6667	1.151	0.8472	1.078	1.000	1.227
2.564	1.070	1.9387	1.183	0.7500	1.143	1.019	1.050	1.250	1.219
4.028	1.042	3.161	1.155	1.1667	1.118	1.669	1.021	1.500	1.204
6.030	1.014	4.792	1.127	1.6667	1.092	2.375	0.993	1.833	1.196
8.717	0.986			2.5000	1.067	3.643	0.965	2.500	1.192
				3.5000	1.042	5.287	0.936	3.000	1.174
				5.0000	1.017	7.249	0.908	4.000	1.162
				7.0000	0.994	9.639	0.876	6.000	1.141
				10.0000	0.967	11.47	0.862	7.000	1.134
				13.5000	0.943			9.000	1.123
								12.000	1.111
								19.000	1.095

Substituting for c from Eq. [12] into Eq. [8] gives

$$E = E_o - \frac{RT}{n\mathcal{F}} \ln\left[\frac{c_b}{c_o}\left(\frac{e^{Kt}-1}{e^{Kt}}\right)+1\right] \quad [13]$$

This is the equation to be tested against the data. The data indicate that in 10 minutes' time the voltage decays by about 0.4 v. That is, $E_o - E = 0.4$ when $t = 10$. Using these values in Eq. [13],

$$E_o - E = \frac{2.303\,RT}{nF} \log\left[\frac{c_b}{c_o}\left(\frac{e^{10K}-1}{e^{10K}}\right)+1\right] = 0.4 \quad [14]$$

The average temperature of these tests was 1244°K, so that

$$\frac{2.303\,RT}{nF} = \frac{2.303 \times 8.313 \times 1244}{6 \times 96{,}500} = 0.0411 \text{ v}$$

Then, from Eq. [14]

$$\log\left[\frac{c_b}{c_o}\left(\frac{e^{10K}-1}{e^{10K}}\right)+1\right] = \frac{0.4}{0.0411} \cong 10$$

If K is greater than or equal to 1, $\frac{e^{10K}-1}{e^{10K}}$ is very close to 1, $\log\left[\frac{c_b}{c_o}+1\right] = 10$, and $\frac{c_b}{c_o} = 10^{10}$. If K is less than 1, $\frac{c_b}{c_o}$ must be even larger than 10^{10}.

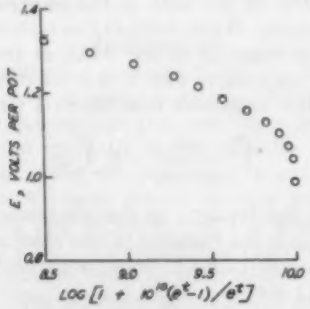

Fig. 2. Nonlinear plot showing that Eq. [15], representing diffusion, is not valid.

Thus we see that, for Eq. [13] to fit the data, it is necessary for the activity of the Al_2O_3 in the bulk of the bath to be at least 10 billion times the activity of the Al_2O_3 at the electrode surface during electrolysis (before and at time O). This does not seem likely. However, since we do not know the activity at the electrode surface, we may admit that this is possible at high current densities. Using 10^{10} for $\frac{c_b}{c_o}$ in Eq. [13] and tentatively letting $K = 1$,

$$E = E_o - 0.0411 \log\left[\frac{e^t-1}{e^t} \times 10^{10} + 1\right] \quad [15]$$

If Eq. [15] fits the data, a plot of E vs. $\log\left[\frac{e^t-1}{e^t} \times 10^{10} + 1\right]$ would give a straight line. The data of counter-emf test No. 1, Table I, are plotted in this way in Fig. 2 where it can be seen that the points definitely do not fall along a straight line and Eq. [15] does not represent the experimental data.

In Eq. [15], K was arbitrarily set equal to 1. Let us examine the effect of taking other values of K. Values of K greater than 1 yield curves that are even farther removed from a straight line than that shown in Fig. 2. Values of K less than 1 yield curves that are straighter than that shown in Fig. 2. In fact, when K is any value between 0 and 0.01, Eq. [13] can be made to represent the data. However, such representation must be regarded as trivial, for, when K is between 0 and 0.01, the function $\frac{e^{Kt}-1}{e^{Kt}}$

has essentially the same values as Kt for the range of t values in the tests and therefore does not represent the assumptions which led to Eq. [13]. Furthermore, the slopes of the straight lines obtained when Eq. [13] is used on the experimental tests with $K = 0.01$ are found to vary from -0.1 to -0.2. But Eq. [13] calls for a constant slope of -0.0411 at 1244°K. Thus Eq. [13] cannot account for either the magnitude or the variation of these slopes.

Thus it is seen that Eq. [13], and therefore Eq. [8], does not represent the data, and it can therefore be concluded that equalization of concentration gradients is not an important cause of voltage decay with time during counter-emf tests although it may have some effect.

Test of Chemical Reaction Hypothesis

Now let us test Eq. [9] for which the assumption was made that the only important cause of counter-emf decay is the depletion of oxygen atoms on the surface of the carbon anode caused by chemical reaction [3]. For the relation between p and t, we may write as the rate equation for reaction [3]

$$-\frac{dp}{dt} = kp^r \qquad [16]$$

where k is the reaction rate constant and r is the order of the reaction.

Reaction [3] may be written

$$2C^*O \rightarrow CO_2 + C$$

This reaction may be visualized as taking place by the mechanism of 2 adsorbed oxygen atoms combining directly with one carbon atom to form carbon dioxide and thus leave a freshly exposed carbon atom on the anode surface to adsorb another oxygen atom from the fused salt bath. The molecularity of the reaction is thus 2, and if the reaction occurs by the simple mechanism outlined then the order of the reaction is also 2 (1). The order of the reaction r can be determined experimentally and, if it turns out to be 2, we may consider this to be a confirming piece of evidence for our postulates.

Using limits of p_o at time O and p at time t, Eq. [16] becomes

$$\int_{p_o}^{p} \frac{dp}{p^r} = -k\int_0^t dt$$

Integrating and solving for p gives

$$p = \left[\, p_o^{1-r} + k(r-1)t \,\right]^{1/1-r} \qquad [17]$$

Substituting for p from Eq. [17] into Eq. [9] and rearranging gives

$$E = E_o - \frac{3RT}{nF}\ln p_o + \frac{3RT}{nF(1-r)}\ln[k(r-1)] + \frac{3RT}{nF(1-r)}\ln\left(\frac{p_o^{1-r}}{k(r-1)} + t\right) \qquad [18]$$

Equation [18] can be written in the form

$$E = S + W\log(t+U) \qquad [19]$$

where the constants S, W, and U have values as follows:

$$S = E_o - \frac{3RT}{nF}\ln p_o + \frac{3RT}{nF(1-r)}\ln[k(r-1)] \qquad [20]$$

$$W = \frac{(2.303)\,3RT}{nF(1-r)} \qquad [21]$$

$$U = \frac{p_o^{1-r}}{k(r-1)} \qquad [22]$$

If Eq. [19] fits the data, a plot of E vs. log $(t + U)$ should give a straight line. The data of five counter-emf tests, given in Table I, are plotted this way in Fig. 3 to 7. As can be seen, the points do in fact fall along straight lines. Furthermore, Eq. [19] accounts for the variation and magnitude of the slopes of these lines. The slope W varies from test to test because of variation in r, the kinetic order of reaction [3]. For the five tests, r is found from Eq. [21] to have values ranging from 1.64 to 2.11. Thus reaction [3] is found to be approximately a second

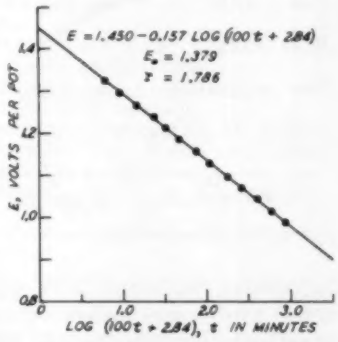

Fig. 3. Counter-emf test No. 1

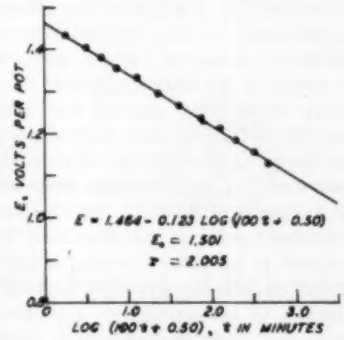

Fig. 4. Counter-emf test No. 2

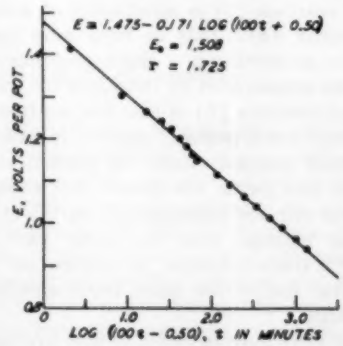

Fig. 5. Counter-emf test No. 3

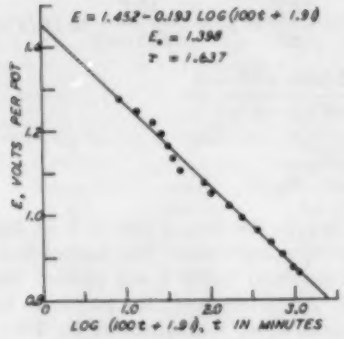

Fig. 6. Counter-emf test No. 4

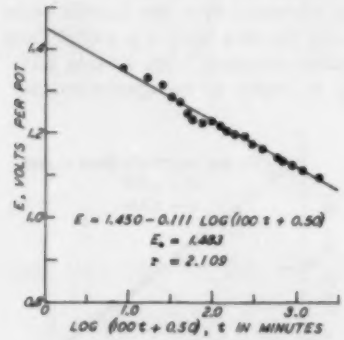

Fig. 7. Counter-emf test No. 5

order kinetic reaction, the variation in order possibly being caused by different surface characteristics of the anode carbons. The magnitude of τ thus confirms the assumptions made in deriving Eq. [19].

The validity of Eq. [19], and therefore Eq. [9], is thus substantiated. It may therefore be concluded that the thermal reaction of oxygen atoms with carbon at the anode is the only important cause of the voltage decay with time during the counter-emf tests. From this it follows that during normal electrolysis the depolarization must be due almost entirely to reaction [3] and depends only slightly on the rate of diffusion of Al_2O_3 to the electrodes. The long time constant polarization discussed by Haupin (3) is thus seen to be caused predominantly by the kinetics of the carbon-oxygen reaction rather than by equalization of concentration gradients in the electrolyte.

The fact that, in general, τ is not exactly 2, indicates that reaction [3] is kinetically of a somewhat complex order (4). This in turn may mean that the reaction proceeds via a chain reaction and may therefore be accelerated or inhibited by trace catalysts. Since reaction [3] is also the controlling step in the normal combustion of carbon (5) the following possibility suggests itself. A carbon anode can be made in two parts, the lower part containing a trace accelerator for reaction [3] to lower the decomposition voltage, and the upper part or stub containing a trace inhibitor to reduce air burning. A systematic search for such trace catalysts may prove fruitful.

Equation [19] may be used to find precise values for the decomposition voltage. The voltage at O time, E_o, is virtually impossible to obtain by direct experimental observation. It can be obtained, however, by extrapolation of the data to O time. This is best done by setting $t = 0$ in Eq. [19] and solving for E which then becomes E_o, the decomposition voltage of the cell reaction. The constants for Eq. [19] together with values for E_o and τ are given in Fig. 3 to 7. The range of E_o is 1.38 to 1.51 v.

Individual values of k and p_o in Eq. [18] cannot be obtained from the empirical constants because there are only 3 empirical constants, S, W, and U to determine 4 unknowns, E_o, τ, k, and p_o. It may be possible to find k and p_o by running a series of counter-emf tests over a range of temperatures and using the Arrhenius equation

$$k = Ae^{-B/T} \qquad [23]$$

together with Eq. [20] and [22] and their first derivatives with respect to temperature.

It may be argued that Eq. [18] could apply to any thermal reaction such as

$$CO_2 + C \rightarrow 2CO$$

But, if this were the case, the voltage would start at 1.2 v which is the voltage corresponding to the electrochemical reaction

$$2Al_2O_3 + 3C \rightarrow 3CO_2 + 4Al$$

and decay to 1.1 v which is the voltage corresponding to the reaction

$$Al_2O_3 + 3C \rightarrow 3CO + 2Al$$

The fact is that the voltage starts at 1.4 to 1.5 v and decays steadily and indefinitely to values well below 1.1 with no sign of leveling off. This is best explained by assuming the indefinite depletion of oxygen atoms at the carbon surface, with the CO_2 product having no effect on the voltage.

The results of this analysis are in line with the reports of recent investigators. Pearson and Waddington (6) have shown that the primary anode gas evolved is CO_2 and that CO is formed as a secondary product by reduction of CO_2 either by the anode carbon or by metal fog. Schadinger (7) has shown that CO is not affected by contact with metal fog so that the drop in voltage below 1.1 cannot be explained on the basis of reduction of CO by metal fog. Grjotheim (8), using a platinum anode, found that no measurable overvoltage occurs for the discharge of aluminum on an aluminum cathode so that the disregard of cathode polarization in the above analysis is justified. A number of investigators (9-11) have used the hypothesis of the formation of intermediate carbon oxides on the anode surface to explain results that are related to those presented here.

*Free Energy of Formation of the Compound C*O*

If we assume that the compound C*O exists on the surface of the anode during electrolysis and that reaction [2] represents the electrochemical reaction, then the results of these counter-emf tests permit the calculation of an approximate value for the free energy of formation of C*O which may be compared with that for CO and CO_2. This calculation is performed as follows:

The average value of the reversible voltage E_o obtained from these tests is 1.45 v and therefore the voltage associated with the electrochemical reaction

$$Al_2O_3 + 3C \rightarrow 2Al + 3C^*O$$

is −1.45 v at 971°C with the Al in the pure molten state, the carbon in the pure solid state, the Al_2O_3 dissolved in cryolite to give a 5% solution by weight, and the compound C*O attached to the carbon anode surface. The free energy change for the reaction as written above is then

$$\Delta G_r = -n\,FE = \frac{6 \times 96{,}500 \times 1.45}{4.185} = +200{,}609 \text{ cal}$$

The free energy of formation ΔG_f of each of the compounds in their above designated states as formed from their elements at 25°C was calculated from published data (12, 13) to give

for Al (molten at 971°C) $\Delta G_f = -12{,}610$ cal/g mole

for Al_2O_3 (in 5% solution cryolite at 971°C) $\Delta G_f = -414{,}668$ cal/g mole

for C (solid at 971°C) $\Delta G_f = -4{,}202$ cal/g mole

The free energy of formation of C*O at 971°C from its elements at 25°C is then calculated from the relation

$$\Delta G_r = -\Delta G_{Al_2O_3} - 3\,\Delta G_C + 2\,\Delta G_{Al} + 3\,\Delta G_{C^*O}$$

or

$$\Delta G_{C^*O} = 1/3\,(\Delta G_{Al_2O_3} + 3\,\Delta G_C - 2\,\Delta G_{Al} + \Delta G_r)$$
$$= 1/3\,(-414{,}668 - 12{,}606 + 25{,}220 + 200{,}609)$$
$$= 1/3\,(-201{,}445) = -67{,}148 \text{ cal/g mole}$$

It is interesting to compare this value with the corresponding values for CO and CO_2. The free energies of formation of CO and CO_2 in gaseous state at 971°C as formed from the elements at 25°C are listed below:

CO_2 $\Delta G_f = -151{,}500$ cal/g mole CO_2

CO $\Delta G_f = -\ 76{,}570$ cal/g mole CO

C*O $\Delta G_f = -\ 67{,}150$ cal/g mole C*O

Thus it appears that the compound C*O is thermodynamically less stable than either CO or CO_2, and its formation during electrolysis must be postulated to account for the observed reversible voltage and its decay with time on open circuit.

Manuscript received Aug. 13, 1957.

Any discussion of this paper will appear in a Discussion Section to be published in the June 1959 JOURNAL.

REFERENCES

1. O. A. Hougen and K. M. Watson, "Chemical Process Principles," Vol. 3, p. 807, John Wiley & Sons, New York (1947).
2. D. S. Davis, "Empirical Equation and Nomography," 1st ed. p. 5, Type 5, McGraw-Hill Book Co., New York (1943).
3. W. E. Haupin, *This Journal*, **103**, 174 (1956).
4. O. A. Hougen and K. M. Watson, *ibid.*, **103**, 819 (1956).
5. S. I. Rempel and L. P. Khodak, *Doklady Akad. Nauk SSSR*, **75**, 833 (1950).
6. T. G. Pearson and J. Waddington, *Disc. Faraday Soc.* **1**, 314 (1947).
7. R. Schadinger, *Alluminio*, **22**, 691 (1953).
8. K. Grjotheim, *Kgl. Norske Videnskab. Selskabs, Skrifter 2*, **5**, 1 (1957).
9. S. I. Rempel and L. P. Khodak, *Zhur. Priklad. Khim.*, **26**, 931 (1953).
10. V. P. Mashovets and A. A. Revazyan, *ibid.*, **30**, 1006 (1957).
11. A. Vajna, *Bull. soc. franc. elec.*, **2**, 85 (1952).
12. J. H. Perry, "Chemical Engineers' Handbook," McGraw Hill Book Co., New York (1950).
13. "Selected Values of Chemical Thermodynamic Properties," *Natl. Bur. Standards Circ.* 500 (1952).

Technical Notes

The Effect of Gamma Irradiation on the Potential Behavior of Platinum and Stainless Steel Electrodes

Walter E. Clark

Chemistry Division, Oak Ridge National Laboratory, Oak Ridge, Tennessee

The recent studies by Cartledge (1, 2) of the potential behavior of stainless steel in 0.1*N* H_2SO_4 have presented interpretations of almost every part of the potential-time plots in terms of reactions taking place at the electrode surface. The purpose of the present work is to determine the effect of gamma irradiation on the potential of stainless steel under the same conditions as those employed by Cartledge.

The radiation source employed was a cylindrical cobalt-60 source of the type described by Ghormley and Hochanadel (3) with 1000 curie loading. The dose rate in the center of the cylinder amounted to 8.5×10^{17} ev/g H_2O/min The solution and the metal electrodes were contained in a glass cell of 20 ml capacity connected to an external silver-silver sulfate-0.1*M* H_2SO_4 reference electrode by means of a glass and Tygon bridge. The solution was stirred by means of a magnetic stirrer and a 300 rpm electric motor. Temperature of the solution was automatically controlled to ±1.5°C. Potentials were measured to ±2 mv by means of a vibrating reed electrometer and a Brown continuous recorder. All measurements were carried out in 0.1*N* H_2SO_4 solution at 85°C. These conditions were chosen because steady-state

potentials are reached with relative rapidity at this temperature (2) and because a considerable amount of experience has been acquired with various stainless steels in this system and under these conditions (4). The work reported was carried out on type 347 stainless steel. Exploratory comparative experiments were carried out on types 302, 304, 309, 310, 316, and 321. The general pattern of behavior was found to be the same in all cases.

The stainless steel electrodes consisted of cylinders 1 cm in length and 0.16 cm in diameter having a nominal area of 0.54 cm^2 sealed into Pyrex glass tubes. The electrode was abraded with 2/0 emery paper, rinsed, and stored in an oven at 110°C until use. A few samples were heated in air at 200°C before use, in order to build up an oxide film. Usually, however, it was felt desirable to use metal with a minimum amount of oxide film to avoid the complication of appreciable concentrations of iron in the solution during the early stages of the experiments.

In order to employ the platinum electrode as a monitor of the redox potential of the solution, it was necessary to investigate the effect of radiation on the potential of platinum. The only known study of this system was made by Veselovsky (5) and few details are given.

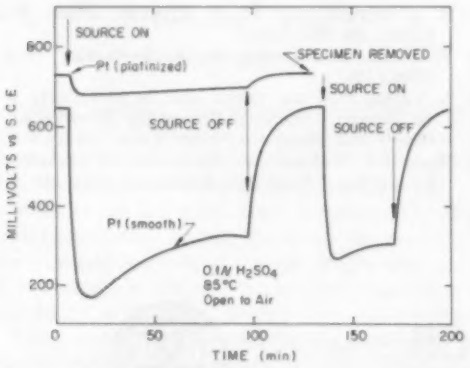

Fig. 1. Effect of gamma irradiation on the potential of smooth platinum and of platinized platinum electrodes in 0.1N H_2SO_4 open to air.

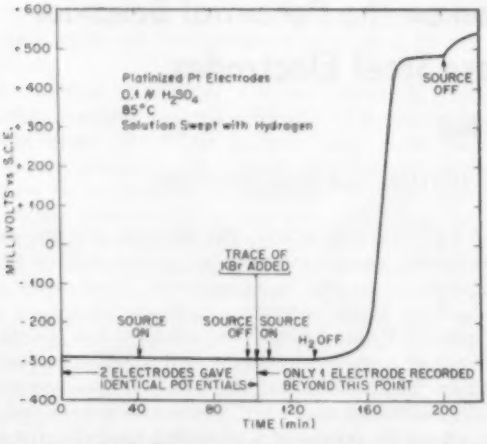

Fig. 2. Effect of gamma radiation on the potential of the hydrogen electrode in 0.1N H_2SO_4.

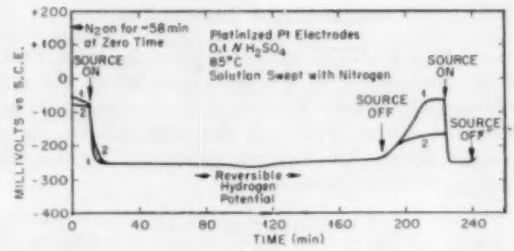

Fig. 3. Effect of gamma radiation on the potential of platinized platinum in deoxygenated 0.1N H_2SO_4.

Figures 1, 2, and 3 show the effect of gamma irradiation on platinum electrodes under atmospheres of air, hydrogen, and nitrogen, respectively. Although smooth platinum electrodes are much more sensitive to products of radiolysis than are platinized electrodes, the general behavior of both types is the same. Imposition of the source causes rapid debasement. Under an atmosphere of air this is followed by slow ennoblement which does not occur under hydrogen or nitrogen. Removal of the source results in rapid ennoblement. A second imposition of radiation causes a second rapid debasement. Under air the degree of this debasement appears to be somewhat a function of the time elapsed since the source was last removed, indicating a probable buildup in the solution of some oxidizing species having a finite lifetime. The addition of potassium bromide ($10^{-4}M$) to the solution as indicated in Fig. 2 produced no change in potential due to postulated changes in the reactions of the products of radiolysis. (6).

Figures 4 and 5 represent two types of behavior which were observed during exposure of type 347 stainless steel. In the first case (Fig. 4) the initial debasement was not sufficiently drastic to result in the evolution of hydrogen, and the behavior of the steel under irradiation was essentially that of an indicator electrode. In the second case (Fig. 5) even though the potential of the steel recovered from its initial debasement immediately following immersion, the imposition of irradiation caused it to drop to a value indicating active corrosion. In this particular case the steel eventually recovered its noble potential while still under irradiation. The fact that

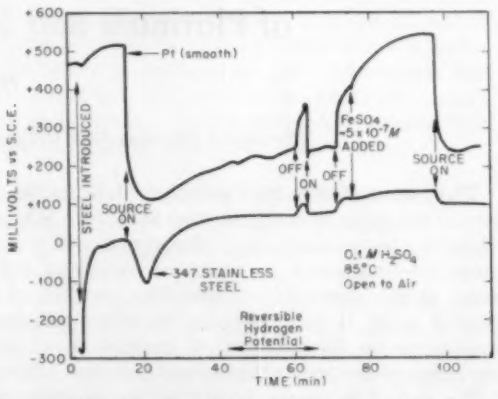

Fig. 4. Usual potential behavior of Type 347 stainless steel under gamma irradiation in 0.1N H_2SO_4.

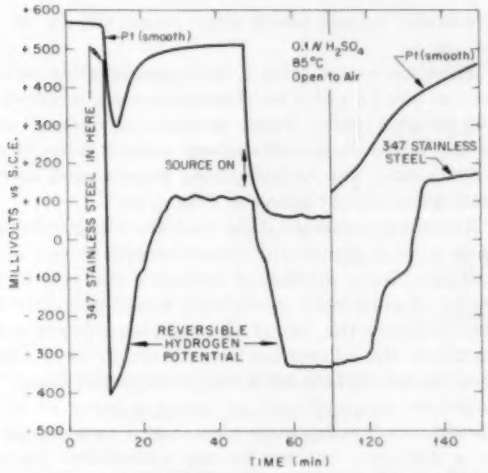

Fig. 5. Failure and subsequent recovery of Type 347 stainless steel under gamma irradiation in 0.1N H_2SO_4.

the potential of the smooth platinum electrode remains debased so long as the steel corrodes actively demonstrates the value of the platinum electrode as a qualitative monitor of the continuing production of Fe(II) in the solution even in the presence of the products of the radiolytic decomposition of water.

Hochanadel (7) lists the following reactions as being among those of importance in the radiolysis of water at 25°C:

$$H_2O \xrightarrow{\gamma} H_2O_2 + H_2 + H + OH \quad \text{(Net decomposition reaction)} \qquad [1]$$

$$H_2 + OH \rightarrow H_2O + H \qquad [2]$$

$$O_2 + H \rightarrow HO_2 \qquad [3]$$

$$HO_2 + HO_2 \rightarrow H_2O_2 + O_2 \qquad [4]$$

As peroxide builds up in solution:

$$H_2O_2 + H \rightarrow H_2O + OH \qquad [5]$$

$$H_2O_2 + OH \rightarrow HO_2 + H_2O \qquad [6]$$

At elevated temperatures hydrogen peroxide decomposes thermally, but even at 150°C peroxide was present at the end of irradiation.

The results reported here confirm the expected buildup of peroxide in the irradiated solution when open to air. Under hydrogen, reaction [2] will predominate, peroxide will be removed, and a platinized platinum electrode will assume the reversible hydrogen potential. Under nitrogen, both hydrogen and oxygen from radiolysis will tend to be removed and the potential will approach that of the hydrogen electrode, due to the great solubility of hydrogen in platinum and to the greater speed of the hydrogen reaction on platinum compared to the reactions involving oxidizing species.

The potential assumed by the stainless steel depends on the nature of the surface of the electrode as well as on the redox species in solution. When the steel is passivated, it tends to behave as an indicator electrode. The presence of radiolytic hydrogen causes rapid debasement of such an electrode. Since no film on stainless steel is completely protective, the "indicator electrode potential" will always be modified somewhat by the effect of a simultaneous corrosion reaction. The effect of the radiolytic oxidizing species will not be felt immediately since these species diffuse more slowly than hydrogen. If the protective film on the steel is destroyed or reduced before the effect of the oxidants is appreciable, active corrosion may continue indefinitely. At present quantitative methods for evaluating the balance between oxidizing and reducing reactions are not available for such systems.

Manuscript received Feb. 14, 1957. This work was done for the U. S. Atomic Energy Commission, under contract with the Union Carbide Nuclear Company.

Any discussion of this paper will appear in a Discussion Section to be published in the June 1959 JOURNAL.

REFERENCES

1. G. H. Cartledge, *Nature*, **177**, 1812 (1956).
2. G. H. Cartledge, *This Journal*, **104**, 420 (1957).
3. J. A. Ghormley and C. J. Hochanadel, *Rev. Sci. Instruments*, **22**, 473 (1951).
4. G. H. Cartledge, F. A. Posey, and Walter E. Clark, Unpublished work.
5. V. I. Veselovsky, A/Conf. Proc. International Conf. on Peaceful Uses of Atomic Energy, **7**, 521 (1956).
6. T. J. Sworski, *J. Am. Chem. Soc.*, **76**, 4687 (1954).
7. C. J. Hochanadel, Proc. International Conf. on Peaceful Uses of Atomic Energy, **7**, 599 (1956); cf. *ibid., J. Phys. Chem.*, **56**, 587 (1952).

The Use of Nickel-Aluminum Alloy Coatings for the Protection of Molybdenum from Oxidation

D. E. Couch, H. Shapiro, and A. Brenner

Electrodeposition Section, Division of Chemistry, National Bureau of Standards, Washington, D. C.

Recent reports (1, 2) have shown that wrought nickel-aluminum alloys are very resistant to oxidation. However, because of their hardness and brittle nature, they are difficult to fabricate.

The protective coatings described herein were prepared by plating the molybdenum with 25μ (1 mil) of chromium followed by 175μ (7 mils) of nickel. These samples were then plated with 50-75μ (2-3 mils) of aluminum.

Several methods of forming nickel-aluminum alloy coatings were studied and found unsatisfactory. Aluminum plating from the hydride bath (3) was

tried, but the adhesion to the nickel was poor and the deposits often blistered during the heating cycle at 600° to 700°C which was required to alloy the aluminum with the nickel.

Low temperature fused salt baths were also used, such as potassium bromide, aluminum bromide (4) and potassium chloride, sodium chloride, aluminum chloride (5). With these fused salt baths the limiting thickness of the aluminum deposit was about 12μ (0.5 mil) before treeing and rough deposits prevented further build up.

The most effective method of forming the nickel-aluminide layer was by electrodeposition from a fused cryolite bath operated at 1000°C.

With current densities of 50 amp/dm^2, aluminum deposited too rapidly for complete alloying. The excess aluminum ran to the bottom of the cathode and collected as a metal bead. At current densities of 10-20 amp/dm^2, the aluminum was deposited at sufficiently slow rates to allow complete alloying with the nickel. At 20 amp/dm^2, about 2.5 hr were required to deposit 65μ (2.5 mils) of aluminum.

Several molybdenum panels which had been previously plated with chromium and nickel were plated with aluminum from the various baths just described. The amount of aluminum deposited was determined by weight from which an average thickness was calculated. Panels with 12μ (0.5 mil) of aluminum or less oxidized at about the same rate as electrodeposited nickel, and they acquired the vitreous black nickel oxide coating typical of nickel oxidized in air at 1100°C. With aluminum thicknesses of between 12μ (0.5 mil) and 20μ (0.8 mil) the rate of oxidation during the first 24-48 hr was markedly reduced; the panels acquired a bluish coating which gradually turned black after about 100 hr of oxidation.

Samples coated with a thickness of alloy equivalent to 50μ (2 mils) of aluminum were oxidized for 400 hr at 1100°C. These samples developed white or tan oxide films and showed weight gains of only 0.005 g/cm^2. The nickel plated panels used as controls gave weight gains of 0.04 g/cm^2.

These experiments show that the aluminide layer gave a very significant improvement to the nickel coatings. Some method of reducing the rate of diffusion of aluminum into nickel would probably further improve the life of the samples since it would maintain the aluminum concentration at a higher level in the surface for a longer period of time. This might be accomplished by using a layer of nickel 75-125μ (3-5 mils) over some metal that would act as a diffusion barrier to the aluminum, possibly chromium. In this way the nickel aluminide composition could be controlled at the most oxidation resistant ratio and it would be possible to obtain the same oxidation life with much thinner coatings than are being used at the present time.

Manuscript received Dec. 9, 1957.

Any discussion of this paper will appear in a Discussion Section to be published in the June 1959 JOURNAL.

REFERENCES

1. W. A. Maxwell and E. M. Grala, Lewis Flight Propulsion Lab., Cleveland, Ohio, Tech. Note 3259.
2. J. H. Westbrook, *This Journal*, **103**, 54 (1956).
3. D. E. Couch and A. Brenner, *ibid.*, **99**, 234 (1952).
4. W. G. Lovell and N. E. Phillips, U. S. Pat. 2,373,320, April 1945.
5. W. H. Wade, G. O. Twellmeyer, and L. F. Yntema, *Trans. Electrochem. Soc.*, **78**, 77 (1940).

Correction

In the paper "The Effect of Temperature and Thickness on the Electrical Resistivity of Ceramic Coatings" by Wm. H. Fischer which appeared on pp. 201-203 in the April 1958 JOURNAL, Vol. 105, No. 4, the last column (H-147) in Table I should read:

	H-147
SiO_2	49.44
B_2O_3	4.84
Al_2O_3	0.54
Cr_2O_3	16.67
BaO	18.46
CaO	1.64
ZnO	2.08

	H-147 (cont'd)
BeO	—
Na_2O	1.24
K_2O	0.89
F_2	0.43
MnO	—
CoO	—
NiO	—
TiO_2	1.92
ZrO	1.16
MgO	0.09
P_2O_5	0.34
Co_2O_3	0.01
MnO_2	0.03
Ni_2O_3	0.03

Ottawa Program

THE ELECTROCHEMICAL SOCIETY

One Hundred and Fourteenth Meeting

September 28, 29, 30, Oct. 1, and 2, 1958

Sunday through Thursday

CONDENSED TECHNICAL PROGRAM

Monday, September 29, 1958

Battery (Abs. 1-12) 9:30 A.M.-12:00 M.; 2:00-5:00 P.M. (Convention Hall, Ground Floor)
Corrosion — Theoretical Electrochemistry — Battery (Abs. 29-39) 9:30 A.M.-12:00 M.; 2:00-5:00 P.M. (Drawing Room, Ground Floor)
Electronics—Semiconductors (Abs. 96-105) 9:30 A.M.-12:00 M.; 2:00-5:00 P.M. (Ballroom, Ground Floor)
Electrothermics and Metallurgy (Abs. 120-129) 9:30 A.M.-12:00 M.; 2:00-4:30 P.M. (Quebec Suite, First Floor)

Tuesday, September 30, 1958

Battery (Abs. 13-21) 9:00-11:55 A.M.; 2:00-5:00 P.M. (Convention Hall, Ground Floor)
Corrosion — Theoretical Electrochemistry — Battery (Abs. 40-51) 9:00 A.M.-12:00 M.; 2:00-5:00 P.M. (Drawing Room, Ground Floor)
Electronics—Semiconductors (Abs. 106-113A) 9:00-11:45 A.M.; 2:00-5:00 P.M. (Ballroom, Ground Floor)
Electrothermics and Metallurgy (Abs. 130-140) 9:00-11:45 A.M.; 2:00-4:40 P.M. (Quebec Suite, First Floor)

Wednesday, October 1, 1958

Battery (Abs. 22-28) 2:00-4:55 P.M. (Convention Hall, Ground Floor)
Corrosion — Theoretical Electrochemistry — Battery (Abs. 52-57) 9:00 A.M.-12:00 M (Drawing Room, Ground Floor)
Corrosion (Abs. 58-63) 2:00-5:05 P.M. (Drawing Room, Ground Floor)
Electrodeposition (Abs. 76-86) 9:00-11:30 A.M.; 2:00-5:00 P.M. (Convention Hall, Ground Floor)
Electronics—Semiconductors (Abs. 114-119) 9:00 A.M.-12:00 M. (Ballroom, Ground Floor)
Electrothermics and Metallurgy (Abs. 141-150) 9:00-11:30 A.M. (Quebec Suite, First Floor)

Thursday, October 2, 1958

Corrosion (Abs. 64-75A) 9:00-11:45 A.M.; 2:00-4:55 P.M. (Drawing Room, Ground Floor)
Electrodeposition (Abs. 87-95) 9:00-11:30 A.M.; 2:00-4:00 P.M. (Banquet Room, Ground Floor)

GENERAL INFORMATION

Convention Headquarters will be the Chateau Laurier Hotel, Ottawa.

Rates per day for rooms (with bath) are single room $9.00-10.50; bed-sitting room (single) $12.50; double-bed room $13.00-15.00; twin-bed room $13.50-15.00; suite-living room, bedroom, and bath $28.00-31.50 (limited number available).

Other hotels are only a few blocks away and their rates (with bath) are as follows:

Beacon Arms, 88 Albert St., double $11.50-13.50.

Lord Elgin, Laurier and Elgin Sts., single $8.00, double $10.50, twin-bed $11.00-12.00.

Other hotels at a still greater distance have rates (with bath) as follows:

Albion, Daly and Nicholas Sts., single $5.00-6.00, double $6.00-9.00.

Alexandra, Bank and Gilmour Sts., single $5.50-7.50, double $8.50-11.00.

Eastview, 200 Montreal Rd., single $5.50-6.50, double $7.50-9.00.

The nearest motel, the Parkway, 475 Rideau St., charges $11.00-14.00 per unit.

All reservations should be made through: The Chairman, Hotel Reservations Committee, The Electrochemical Society, Inc., c/o Mines Branch, 568 Booth St., Ottawa, Ont., Canada.

The Office of the Secretary will be the Terrace Room (Ground Floor).

Ladies' Headquarters will be in the Tudor Room (First Floor).

All technical sessions will be held on the Ground Floor and First Floor.

REGISTRATION

The registration desk will be in the south wing of the Lounge (Ground Floor). Following is the registration schedule:

Sunday, Sept. 28—3:00 to 9:00 P.M.
Monday, Sept. 29—8:00 A.M. to 6:00 P.M.
Tuesday, Sept. 30—8:30 A.M. to 5:00 P.M.
Wednesday, Oct. 1—8:30 A.M. to 4:00 P.M.
Thursday, Oct. 2—8:30 A.M. to 1:00 P.M.

Registration fees are:

Members	$ 7.00
Nonmembers	13.00*
Ladies	5.00
Students	2.00

*If a nonmember fills out an application blank and is subsequently elected to membership in the Society, the difference between the nonmember and member registration fee will be applied to his first year's dues.

INFORMATION ABOUT OTTAWA

Many places of interest await those planning to attend the Electrochemical Society convention in Canada's Capital City. Situated on the Ottawa River, the boundary between the provinces of Ontario and Quebec, the city has a population of approximately 230,000. Parliament Hill is but a few steps from the Chateau Laurier, the Headquarters Hotel for the convention. The Centre Block of the parliament buildings containing the House of Commons, the Senate Chamber, the Parliamentary Library, the Memorial Chamber, and the Peace Tower dominates the Hill and overlooks the river. This is flanked by the East and West Blocks which contain other government offices. The National War Memorial is situated in a plaza near the Chateau Laurier entrance. Rideau Hall, the residence of the Governor-General (the Queen's representative in Canada), is located about a mile east of Parliament Hill in a beautifully landscaped estate. The National Gallery, the National Museum, the Public Archives, and the Bytown Museum house many of Canada's cultural and historical records.

Two universities are located in the city, Ottawa University and Carleton University, both of which at present are undergoing rapid expansion. A new City Hall has just been erected near the juncture of the Rideau and Ottawa Rivers.

The beauty of the city can be seen best while motoring along the system of scenic Federal parkways. This system extends several miles into the beautiful Gatineau hills north of the city. Another driveway leads to the 1200-acre Dominion Experimental Farm in the western part of the city, with its extensive facilities

for agricultural research, lovely gardens, and an arboretum containing species of trees from many parts of the world. Pleasant boat trips can be taken through the Rideau Canal, built in the early part of the nineteenth century to provide a link between the Ottawa River and Lake Ontario. The Chateau Laurier overlooks the locks by which the canal is joined to the Ottawa River.

The history of Ottawa is intimately associated with the lumbering industry which flourished in the Ottawa River valley in the last century, and today two pulp and paper mills are located just across the river. The city was formerly known as Bytown, so named in honor of Colonel John By, the builder of the Rideau Canal. In 1854 the name was changed to Ottawa, and in 1858 Queen Victoria selected it as the Capital City. The people of Canada's two main cultural heritages, the British and the French, mingle freely in the city, and visitors will find both languages freely spoken.

Ottawa is the center of much of the scientific research done by the Canadian government, and tours have been arranged to laboratories of the National Research Council and the Department of Mines and Technical Surveys.

The weather at the end of September is usually pleasant, with temperatures in the range 50°-60°F.

SYMPOSIA AND ROUND TABLE

The Battery Division has scheduled symposia on Unconventional Battery Systems; Oxide Electrodes—Research Papers, Review of Battery Oxide Electrode Systems; and General Battery Papers.

The Corrosion—Theoretical Electrochemistry—Battery Divisions have scheduled a Joint Symposium on Films Formed in Contact with Liquids.

The Corrosion Division has scheduled three general sessions.

The Electrodeposition Division has scheduled symposia on Electrodeposition from Fused Salts; and Electrodeposition on Uncommon Metals.

The Electronics Division—Semiconductor Group has scheduled symposia on Thermoelectric Materials and Device Design; Structural Chemistry, Preparation, and Properties of Compound Semiconductors; Physics and Chemistry of Silicon and Germanium Crystals; PN Junctions in Silicon and Germanium Crystals; and Surface Treatments and Device Technology.

The Electrothermics and Metallurgy Division has scheduled symposia on Properties of Graphite; Arc Phenomena; Arc Applications; Oxidation; and Electric Smelting.

GENERAL FUNCTIONS

Symposia Chairmen Breakfasts

On **Monday, Tuesday, Wednesday,** and **Thursday,** Sept. 29, 30, Oct. 1, and 2, special breakfasts will be held for symposia chairmen. On the day on which he presides at a symposium, each chairman should be at the Office of the Secretary (Terrace Room, Ground Floor) *by 7:45 A.M.*

Monday Society Luncheon

The Electrochemical Society Luncheon will be held on Monday, Sept. 29, at 12:30 P.M. in the Ballroom, Ground Floor. Dr. G. C. Monture will be the speaker.

Monday Buffet Supper

On Monday evening, Sept. 29, an opportunity will be provided for the registrants to relax and become better acquainted with one another at an informal Buffet Supper at HMCS Carleton on the shore of beautiful Dow's Lake in the western part of the city. Cocktails will be served beforehand; light entertainment will follow the dinner. Buses will be provided to take people from the Chateau to the Lake. Definite information on time and place to meet will be available at the registration desk.

Tuesday Battery Division Award Luncheon

Dr. John J. Lander, of Delco-Remy Div. of General Motors Corp., will be the first recipient of the Research Award of the Battery Division of The Electrochemical Society in recognition of his distinguished work on the anodic corrosion of lead in sulfuric acid solutions. The presentation will be made at the Battery Division Luncheon on Tuesday, Sept. 30, in Salons B-D, Mezzanine.

Tuesday Acheson Medal Banquet

On Tuesday evening, Sept. 30, a reception and banquet will be held for the Acheson Medalist, Dr. W. J. Kroll. Cocktails will be served from 6:30 to 7:30 P.M. in the Lounge (Ground Floor), followed by dinner at 7:30 P.M. in the Ballroom. Dr. Kroll will deliver the Acheson Medal Address. Guests are invited to linger for a program of entertainment. (Dress is optional.)

PLANT TRIPS

Five inspection or plant trips have been arranged for the Ottawa Meeting, three on Thursday afternoon, Oct. 2, and two on Friday, Oct. 3. Please register for the trips early in the week. Each trip on Friday is limited to 40; applications to see the atomic reactors at the Chalk River Plant had to be filed by July 30.

Thursday, Oct. 2, 1958

Buses on Thursday will leave the Chateau at 1:30 and return at 4:00 P.M. The three trips on Thursday are:

(A) National Research Council: Divisions of Applied Chemistry, Building Research, Radio and Electrical Engineering, and Mechanical Engineering can be visited.

(B) Mines Branch, Department of Mines and Technical Surveys: Divisions of Mineral Dressing and Process Metallurgy, Fuels, Physical Metallurgy, and Industrial Minerals.

(C) Ottawa University: Departments of Chemical Engineering, and Chemistry.

Friday, Oct. 3, 1958

Two trips are planned for Friday to plants some distance from Ottawa:

(D) Atomic Energy of Canada, Chalk River, Ont., to see the atomic reactors. Applications for this trip had to be made by July 30 and are restricted to 40. Those making this trip should be in the Lobby of the Chateau Laurier by 8:00 A.M. to take the bus.

(E) Dominion Magnesium Ltd., Haley, Ont., to see the Pidgeon electrothermic process for producing magnesium metal. Those making this trip should be in the Lobby of the Chateau by 8:00 A.M. to take the bus.

LADIES' PROGRAM

A warm and friendly invitation is extended to all the ladies attending the convention to make the Tudor Room (First Floor) of the Chateau Laurier their headquarters during their visit to Ottawa. The Coffee Hour will be a daily event. It is a sincere hope that through this medium everyone will become acquainted. Members of the Ladies' Committee will be on hand to assist and acquaint you with the program which has been planned for your enjoyment.

It is further suggested that, because of the nature of the trips, a pair of walking shoes may prove to be a further incentive to the full enjoyment of Ottawa's Gatineau Park and surrounding country.

Weather-wise, temperatures in Ottawa at the end of September should be from 50° to 60°F.

Sunday, Sept. 28—Registration from 3:00 to 9:00 P.M.

Monday morning, Sept. 29—Coffee Hour and get-acquainted meeting in the Tudor Room from 9:30 to 10:30 A.M. The rest of the morning is left free. An information desk will be situated in the Tudor Room. The Ladies' Committee would appreciate the help of the visitors in making known to the members of the Committee their preferences and participation in the activities of the Ladies' Program. A limited number of guides will be available to escort small parties to places of interest such as shops, art galleries, museums, etc.

Monday noon, Sept. 29—The ladies are invited to attend the Society Luncheon at 12:30 P.M. in the Ballroom (Ground Floor). Tickets should be purchased in advance at the registration desk. *See* General Functions.

Monday afternoon, Sept. 29—The ladies are invited to attend a conducted tour of the Canadian Parliament Buildings. Information about the tour will be available when you register.

Monday evening, Sept. 29—The ladies are invited to attend a buffet supper at HMCS Carleton. *See* General Functions.

Tuesday morning and afternoon, Sept. 30—Coffee Hour from 9:00 to 10:00 A.M. in the Tudor Room. Buses leave at 10:00 A.M., Mackenzie Street entrance, Chateau Laurier, for a sight-seeing tour of the Gati-

neau Hills located on the Quebec side of the Ottawa River. Luncheon will be served at the Country Club Lodge. The excursion will be resumed at 2:30 P.M to complete the tour of the Ottawa district. This tour gives a profile of Canada's Capital City and surrounding district. Return to Chateau at approximately 4:30 P.M.

Tuesday evening, Sept. 30—The ladies are invited to attend the Acheson Medal Reception and Banquet starting at 6:30 P.M. in the Ballroom, Ground Floor. *See* General Functions.

Wednesday morning and afternoon, Oct. 1—Coffee Hour from 9:00 to 10:00 A.M. in the Tudor Room. Special arrangements have been made for the ladies to visit one of Canada's scenic and exclusive clubs, the Seigniory Club. This picturesque chalet is located on the Ottawa River about fifty miles due east of Ottawa and occupies land previously held by a French seigneur. This locale perpetuates the memory of old French Canada. Luncheon and afternoon tea will be served in the chalet. Buses will leave the Seigniory Club in time for arrival in Ottawa by 6:30 P.M.

Thursday morning, Oct. 2—Coffee Hour from 9:30 to 10:30 A.M. in the Tudor Room. The day is left free for individual plans. Arrangements can be made for those who wish to accompany their husbands on the tours of the National Research Council, Mines Branch, or Ottawa University.

LUNCHEONS AND BUSINESS MEETINGS OF DIVISIONS

Battery Division Luncheon and Business Meeting and Presentation of the Research Award of the Battery Division to Dr. John J. Lander, Tuesday, Sept. 30, at 12:15 P.M. in Salons B-D, Mezzanine.

Corrosion Division Luncheon and Business Meeting on Wednesday, Oct. 1, at 12:15 P.M. in the Banquet Room, Ground Floor.

Electrodeposition Division Luncheon and Business Meeting on Wednesday, Oct. 1, at 12:15 P.M. in Salons B-D, Mezzanine.

BOARD AND COMMITTEE MEETINGS

Sunday, Sept. 28, 2:00 P.M.—Meeting of the **Board of Directors** in the Tudor Room, First Floor.

Sunday, Sept. 28, 7:30 P.M.—Meeting of the **Investment Advisory Panel** in the Terrace Room, Ground Floor.

Monday, Sept. 29, 5:00 P.M.—Meeting of the **Membership Committee** in Salon A, Mezzanine.

Tuesday, Sept. 30, 5:00 P.M.—Meeting of the **Editorial Staff** of JOURNAL in the Terrace Room, Ground Floor.

Wednesday, Oct. 1, 5:00 P.M.—Meeting of the **Council of Local Sections** in Salon A, Mezzanine.

COST OF VARIOUS FUNCTIONS

(other than registrations)

Please buy tickets as early as possible.

Symposia Chairmen breakfasts	Standard menu prices
Monday Society Luncheon	$4.00
Division Luncheons	3.75
Monday Social Evening at HMCS Carleton	3.50
Tuesday Acheson Award Reception and Banquet	
Gentlemen	8.00
Ladies	5.00
Ladies' Functions	Largely complimentary

JOURNALS

Copies of the June, July, August, and September issues of the JOURNAL of The Electrochemical Society will be available at the registration desk. The price of a single copy of the JOURNAL is $1.25 to members and $1.75 to nonmembers.

EXTENDED ABSTRACTS

The Battery Division is making available an extended abstract booklet containing 1000-word abstracts of most of the papers presented at the Division's Ottawa symposia. Copies of the booklet will be on sale for $2.50 at the registration desk.

DISCUSSION

No recordings will be made of oral discussions. Those contributing to the discussion of a paper and desiring their remarks to be published will be supplied by the symposium chairman with a printed form on which any discussion may be written. These forms should be given to the Secretary-Treasurer of the Division or to the Managing Editor of the JOURNAL after the session; they can be mailed to the Managing Editor of the JOURNAL, 1860 Broadway, New York 23, N. Y. The discussion will then be referred to the author for reply. Publication of the discussion and the comments of the author depends on publication of the article in the JOURNAL.

Written discussion should be submitted within two months following publication of the article in the JOURNAL. A Discussion Section is published semiannually in the JOURNAL.

EMPLOYMENT POSTERS

Companies which desire to recruit employees at the Ottawa Meeting will have posters to this effect on a bulletin board near the registration desk.

NOTE

In the Index to Authors, the abstract number is used. Address of author(s) is included with the abstract.

SPRING MEETING
at the
Sheraton Hotel
PHILADELPHIA, PA.
May 3, 4, 5, 6, and 7, 1959

Sessions probably will be scheduled on

Electric Insulation
Electronics (including **Luminescence** and **Semiconductors**)
Electrothermics and Metallurgy
Industrial Electrolytics
Theoretical Electrochemistry

Abstracts for the Spring Meeting (*not exceeding 75 words in length*) must reach Society Headquarters, 1860 Broadway, New York 23, N. Y., *not later than January 2, 1959* in order to be included in the program.

Indicate on abstract for which Division's symposium the paper is to be scheduled, and underline the name of the author who will present the paper.

MEETING ROOM SCHEDULES

Meeting	Monday A.M.	Monday P.M.	Tuesday A.M.	Tuesday P.M.	Wednesday A.M.	Wednesday P.M.	Thursday A.M.	Thursday P.M.
Battery	A	A	A	A		A		
Corrosion—Theoretical Electrochemistry—Battery	B	B	B	B	B			
Corrosion						B	B	B
Electrodepo ion					A	E	E	E
Electronics—Semiconductors	C	C	C	C	C			
Electrothermics and Metallurgy	D	D	D	D	D	D		

A = Convention Hall (Ground Floor)
B = Drawing Room (Ground Floor)
C = Ballroom (Ground Floor)
D = Quebec Suite (First Floor)
E = Banquet Room (Ground Floor)

Technical Program

BATTERY

Monday, Sept. 29, 1958

Unconventional Battery Systems
with W. S. Herbert presiding
(CONVENTION HALL, Ground Floor)

9:30 A.M.—"Investigation of the Electrochemical Characteristics of Organic Compounds, III. Nitroalkanes" by R. Glicksman and C. K. Morehouse (Abstract No. 1)

9:55 A.M.—"Investigation of the Electrochemical Characteristics of Organic Compounds, IV. Quinone Compounds" by R. Glicksman and C. K. Morehouse (Abstract No. 2)

10:20 A.M.—"Fused Salt Relatives of the Leclanché Cell: A Thermodynamic Appraisal" by R. E. Wood (Abstract No. 3)

10:45 A.M.—"Studies on Depolarizers for Fused Salt Cells" by S. M. Selis, E. S. McKee, L. G. Bockstie, Jr., and L. P. McGinnis. (Abstract No. 4)

11:10 A.M.—"Thermally Regenerative Ionic Hydride Galvanic Cell" by R E. Shearer and R. C. Werner (Abstract No. 5)

11:35 A.M.—"Iodine-Activated Solid Electrolyte Cell for Use at High Temperature" by J. L. Weininger (Abstract No. 6)

12:30 P.M.—The Electrochemical Society Luncheon in the Ballroom, Ground Floor

Battery (cont'd)
Monday, Sept. 29, 1958
Unconventional Battery Systems (cont'd)
with W. S. Herbert presiding
(CONVENTION HALL, Ground Floor)

2:00 P.M.—"The Silver-Silver Chloride-Chlorine Solid Electrolyte Cell" by D. M. Smyth (Abstract No. 7)

2:25 P.M.—"Zinc-Mercuric Dioxysulfate Dry Cell" by Samuel Ruben (Abstract No. 8)

Oxide Electrodes—Research Papers
with U. B. Thomas presiding
(CONVENTION HALL, Ground Floor)

3:00 P.M.—"Magnesium-Bismuth Oxide Dry Cells" by C. K. Morehouse and R. Glicksman (Abstract No. 9)

3:30 P.M.—"An Investigation of the Discharge Characteristics of High Oxidation State Compounds of the Groups VI-VIII Elements in an Alkaline Electrolyte" by C. K. Morehouse and R. Glicksman (Abstract No. 10)

4:00 P.M.—"The Anodic Oxidation of Cadmium" by P. E. Lake and E. J. Casey (Abstract No. 11)

4:30 P.M.—"Dependence of Rate of Oxidation and Reduction of Cd and Ag on Overpotential" by G. T. Croft (Abstract No. 12)

Battery (cont'd)
Tuesday, Sept. 30, 1958
Oxide Electrodes—Research Papers (cont'd)
with U. B. Thomas presiding
(CONVENTION HALL, Ground Floor)

9:00 A.M.—"Textures of Electrodeposited Lead Dioxide" by Y. Shibasaki (Abstract No. 13)

9:30 A.M.—"Oxygen Overvoltage and Electrode Potentials of α- and β-PbO_2" by P. Ruetschi, B. D. Cahan, and R. T. Angstadt (Abstract No. 14)

10:00 A.M.—"Ion Exchange Property of Manganese Dioxide" by Akiya Kozawa and Kumazo Sasaki (Abstract No. 15)

10:30 A.M.—"Cathodic Reduction of Manganese Dioxide in Alkaline Electrolyte" by N. C. Cahoon and M. P. Korver (Abstract No. 16)

Review of Battery Oxide Electrode Systems
with E. Willihnganz presiding
(CONVENTION HALL, Ground Floor)

11:10 A.M.—"Silver and Its Oxides" by T. P. Dirkse (Abstract No. 17)

12:15 P.M.—Battery Division Luncheon, Business Meeting, and Presentation of the Battery Division Research Award in Salons B, C, and D, Mezzanine

Battery (cont'd)
Tuesday, Sept. 30, 1958
Review of Battery Oxide Electrode Systems (cont'd)
with E. Willihnganz presiding
(CONVENTION HALL, Ground Floor)

2:00 P.M.—"The Oxides and Hydroxides of Nickel, Their Composition, Structure, and Electrochemical Properties—A Review" by U. B. Thomas (Abstract No. 18)

2:45 P.M.—"The Manganese Dioxide Electrode" by W. C. Vosburgh (Abstract No. 19)

3:30 P.M.—"The Electrochemistry of the Lead Anode in Aqueous Solutions" by Jeanne Burbank (Abstract No. 20)

4:15 P.M.—"Oxide Electrode Processes in Batteries" by E. Willihnganz (Abstract No. 21)

Battery (cont'd)
Wednesday, Oct. 1, 1958
General Battery Papers
with C. K. Morehouse presiding
(CONVENTION HALL, Ground Floor)

2:00 P.M.—"Corrosion of the Zinc Electrode in the Silver-Zinc-Alkali Cell" by T. P. Dirkse and Frank De Haan (Abstract No. 22)

2:25 P.M.—"Studies on Lead Sulfate Crystals" by E. J. Casey, K. N. Campney, and I. H. S. Henderson (Abstract No. 23)

2:50 P.M.—"Battery Pastes—Compositions and Characteristics" by J. F. Schaefer and H. R. Karas (Abstract No. 24)

3:15 P.M.—"A Reference Half-Cell for Laboratory and Industrial Applications" by N. C. Cahoon and J. P. Oliver (Abstract No. 25)

3:40 P.M.—"A New Separator for the Aluminum Dry Cell" by N. C. Cahoon and M. P. Korver (Abstract No. 26)

4:05 P.M.—"Morphological Characteristics of Nickel Powders for Use in Sintered Plate Nickel Cadmium Storage Batteries" by C. F. Cook, Jr., W. F. Nye, and F. W. Leonhard (Abstract No. 27)

4:30 P.M.—"Nickel Cadmium Batteries, Pocket-Type Construction" by A. B. Eilbeck (Abstract No. 28)

CORROSION—THEORETICAL ELECTROCHEMISTRY—BATTERY

Joint Symposium
Monday, Sept. 29, 1958
Films Formed in Contact with Liquids
with C. V. King presiding
(DRAWING ROOM, Ground Floor)

9:30 A.M.—"Some Observations on Films Formed on Steel in Contact with Aqueous Media" by M. C. Bloom and M. J. Strauss (Abstract No. 29)

10:00 A.M.—"The Cracking of Low-Carbon Steel during Heating with Aqueous Slurries of γ-FeOOH" by M. J. Strauss and M. C. Bloom (Abstract No. 30)

10:30 A.M.—"The Reaction between Iron and Water in the Absence of Oxygen" by V. J. Linnenbom (Abstract No. 31)

11:00 A.M.—"A Study of Corrosion Films on Zirconium and Its Alloys by Impedance Measurements" by J. N. Wanklyn and D. R. Silvester (Abstract No. 32)

11:30 A.M.—"Direction of Ionic Movement in the Anodic Oxidation of Aluminum" by J. E. Lewis and R. C. Plumb (Abstract No. 33)

12:30 P.M.—The Electrochemical Society Luncheon in the Ballroom, Ground Floor

Corrosion—Theoretical
Electrochemistry—Battery (cont'd)
Joint Symposium
Monday, Sept. 29, 1958
Films Formed in Contact with Liquids (cont'd)
with M. A. Streicher presiding
(DRAWING ROOM, Ground Floor)

2:00 P.M.—"A Radiochemical Method for Measuring the Surface Area of Aluminum Metal and Powders" by J. E. Lewis (Abstract No. 34)

2:30 P.M.—"Observations on the Anodic Oxidation of Aluminum" by R. C. Plumb (Abstract No. 35)

3:00 P.M.—"The Specific Surface Area of Aluminum as Determined with Continuously Variable Resolution from 20 to 1000Å by R. C. Plumb (Abstract No. 36)

3:30 P.M.—"A Study of the Structure of Anodic Oxide Films on Aluminum" by D. J. Stirland and R. W. Bicknell (Abstract No. 37)
4:00 P.M.—"Structure of Hydrous Oxides on Aluminum" by W. E. Tragert (Abstract No. 38)
4:30 P.M.—"Effect of Stripping of Anodized Coatings from Aluminum on Electrical Resistance" by Walter Beck, E. D. Zavaglia, and S. J. Ketcham (Abstract No. 39)

Corrosion—Theoretical Electrochemistry—Battery (cont'd)
Joint Symposium
Tuesday, Sept. 30, 1958
Films Formed in Contact with Liquids (cont'd)
with M. A. Streicher presiding
(DRAWING ROOM, Ground Floor)

9:00 A.M.—"The Aluminum Electrode, I. The Effect of the Oxide Film" by R. C. Plumb (Abstract No. 40)
9:30 A.M.—"The Aluminum Electrode, II. The Reactions Taking Place at the Electrolyte-Aluminum Interface" by R. C. Plumb (Abstract No. 41)
10:00 A.M.—"Films Formed by A-C Anodization of Aluminum in Sulfuric Acid Solutions" by W. H. Fischer and J. A. Consiglio (Abstract No. 42)
10:30 A.M.—"Anodic Behavior of Aluminum at Low Potentials" by J. V. Petrocelli (Abstract No. 43)
11:00 A.M.—"The Flade Potential of Iron Passivated by Various Inorganic Corrosion Inhibitors" by H. H. Uhlig and P. F. King (Abstract No. 44)
11:30 A.M.—"The Mechanism of Passivating-Type Inhibitors" by Milton Stern (Abstract No. 45)
12:15 P.M.—Battery Division Luncheon, Business Meeting, and Presentation of the Battery Division Research Award in Salons B, C, and D, Mezzanine

Corrosion—Theoretical Electrochemistry—Battery (cont'd)
Joint Symposium
Tuesday, Sept. 30, 1958
Films Formed in Contact with Liquids (cont'd)
with H. C. Gatos presiding
(DRAWING ROOM, Ground Floor)

2:00 P.M.—"Polarization at Hafnium Electrodes" by Norman Hackerman and Lewis Battist (Abstract No. 46)
2:30 P.M.—"The Oxygen-Evolution Reaction at Gold Anodes, I. Accuracy of Overpotential Measurements" by Sidney Barnartt (Abstract No. 47)
3:00 P.M.—"Strain Electrometry and Corrosion, V. Film Properties and Strain Potential" by J. C. Giddings, A. G. Funk, C. J. Christensen, and Henry Eyring (Abstract No. 48)
3:30 P.M.—"Kinetics of Ion Motion in Anodic Ta_2O_5 Films" by D. A. Vermilyea (Abstract No. 49)
4:00 P.M.—"Growth of Oxide Films on Copper Single Crystal Surfaces in Water" by Jerome Kruger (Abstract No. 50)
4:30 P.M.—"Formation of Calomel Films on Mercury Anodes" by D. C. Cornish, D. J. G. Ives, R. W. Pittman, and H. P. Dibbs (Abstract No. 51)

Corrosion—Theoretical Electrochemistry—Battery (cont'd)
Joint Symposium
Wednesday, Oct. 1, 1958
Films Formed in Contact with Liquids (cont'd)
with J. C. White presiding
(DRAWING ROOM, Ground Floor)

9:00 A.M.—"The Performance of Zinc, Magnesium, and Aluminum Primary Cell Anodes—A Review" by R. Glicksman (Abstract No. 52)
9:30 A.M.—"The Magnesium Anode in Aqueous Solutions, I. Steady-State Behavior" by J. L. Robinson, J. L. Nichols, and M. R. Bothwell (Abstract No. 53)
10:00 A.M.—"The Magnesium Anode in Aqueous Solutions, II. Transient Behavior" by P. F. King and J. L. Robinson (Abstract No. 54)
10:30 A.M.—"Potential-Time Changes at Anodically and Cathodically Polarized Magnesium" by G. R. Hoey and M. Cohen (Abstract No. 55)
11:00 A.M.—"A New Experimental Technique for the Study of Films Produced at Electrochemical Interfaces" by B. D. Cahan and P. Ruetschi (Abstract No. 56)
11:30 A.M.—"Anodic Films Formed on Lead in Aqueous Solutions" by Jeanne Burbank (Abstract No. 57)
12:15 P.M.—Corrosion Division Luncheon and Business Meeting in the Banquet Room, Ground Floor

CORROSION

Wednesday, Oct. 1, 1958
General Session
with C. V. King presiding
(DRAWING ROOM, Ground Floor)

2:00 P.M.—"Corrosion Studies and the Protection of Ferrous Metals Against Corrosion" by J. C. Hudson and J. F. Stanners (Abstract No. 58)
3:00 P.M.—"The Oxidation of Aluminum and Certain of Its Binary Alloys below 450°C" by M. J. Dignam (Abstract No. 59)
3:25 P.M.—"The Diffusion of Oxygen in Alpha and Beta Zircaloy 2 and Zircaloy 3 at High Temperatures" by M. W. Mallett, W. M. Albrecht, and P. R. Wilson (Abstract No. 60)
3:50 P.M.—"Oxidation Studies on the Iron-Chromium-Aluminum Heater Alloys" by E. A. Gulbransen and K. F. Andrew (Abstract No. 61)
4:15 P.M.—"Transitions from Parabolic to Linear Kinetics in Scaling of Metals" by E. W. Haycock (Abstract No. 62)
4:40 P.M.—"High-Temperature Sulfiding of Iron and Steel in Hydrogen Sulfide-Hydrogen Mixtures" by E. W. Haycock (Abstract No. 63)

Corrosion (cont'd)
Thursday, Oct. 2, 1958
General Session (cont'd)
with R. T. Foley presiding
(DRAWING ROOM, Ground Floor)

9:00 A.M.—"Corrosion Research at the National Research Council of Canada Laboratories" by Morris Cohen (Abstract No. 64)
9:40 A.M.—"Anodic Behavior of Copper in Phosphoric Acid" by F. H. Giles and J. H. Bartlett (Abstract No. 65)
10:05 A.M.—"Corrosion of Uranium and Uranium Alloys by Differential Aeration" by J. W. Ward and J. T. Waber (Abstract No. 66)
10:30 A.M.—"General and Intergranular Corrosion of Austenitic Stainless Steels in Solutions Used for Evaluation Tests" by M. A. Streicher (Abstract No. 67)
10:55 A.M.—"Corrosion of Metals in Boiling Acids when Contacted to Noble Metals" by W. R. Buck, III, and Henry Leidheiser, Jr. (Abstract No. 68)
11:20 A.M.—"Corrosion of Mild Steel in Alkaline Leaching and Grinding Solutions for Uranium Ore" by R. R. Rogers and I. I. Tingley (Abstract No. 69)

Corrosion (cont'd)
Thursday, Oct. 2, 1958
General Session (cont'd)
with R. T. Foley presiding
(DRAWING ROOM, Ground Floor)

2:00 P.M.—"Kinetics of Germanium Dissolution in the Presence of Electrolytes" by W. W. Harvey and H. C. Gatos (Abstract No. 70)
2:25 P.M.—"Kinetic Studies on Corrosion Systems, I. A Theory of Multi-Component Electrochemical Systems under Activation Control" by F. A. Posey (Abstract No. 71)
2:50 P.M.—"Kinetic Studies on Corrosion Systems, II. The Reduction of Cupric Ion on Passive Stainless Steel Electrodes" by F. A. Posey, G. H. Cartledge, and R. P. Yaffe (Abstract No. 72)
3:15 P.M.—"Galvanic Corrosion, II. Effect of pH and Dissolved Oxygen Concentration on the Aluminum-Steel Couple" by M. J. Pryor and D. S. Keir (Abstract No. 73)
3:40 P.M.—"Corrosion of Copper in Aqueous Media" by D. J. G. Ives and A. E. Rawson (Abstract No. 74)
4:05 PM.—"Tarnishing Reactions of Silver in Iodine Atmospheres" by D. M. Smyth and Marjorie Cutler (Abstract No. 75)
4:30 P.M.—"Oxidation of Titanium, Zirconium, and Hafnium" by G. R. Wallwork and A. E. Jenkins (Abstract No. 75A)

ELECTRODEPOSITION

Wednesday, Oct. 1, 1958
Electrodeposition from Fused Salts
with Sidney Barnartt presiding
(CONVENTION HALL, Ground Floor)

9:00 A.M.—"Deposition of Titanium, Zirconium, Hafnium, Chromium, Vanadium, and Molybdenum from

Fused Chloride Baths" by R. S. Dean, W. W. Gullett, and F. X. McCawley (Abstract No. 76)
9:30 A.M.—"The Electrolytic Preparation of Titanium from Fused Salts, II. Design of Laboratory Cells" by M. B. Alpert, J. A. Hamilton, F. J. Schultz, and W. F. Sullivan (Abstract No. 77)
10:00 A.M.—"Electromotive Series of Metals in Fused Salts" by S. N. Flengas and T. R. Ingraham (Abstract No. 78)
10:30 A.M.—"A Sodium-Ion-Conductive Porcelain Reference Electrode for Molten Salt Systems" by R. J. Labrie and V. A. Lamb (Abstract No. 79)
11:00 A.M.—"Nickel-Aluminum Alloys Formed by Electrodeposition" by Dwight Couch and Jean Connor (Abstract No. 80)
12:15 P.M.—Electrodeposition Division Luncheon and Business Meeting in Salons B, C, and D, Mezzanine

Electrodeposition (cont'd)
Wednesday, Oct. 1, 1958
with Abner Brenner presiding
(BANQUET ROOM, Ground Floor)

2:00 P.M.—"On the Growth and Properties of Electrolytic Whiskers" by P. B. Price, D. A. Vermilyea, and M. B. Webb (Abstract No. 81)
2:30 P.M.—"Electrodeposition Behavior of Trace Amounts of Copper" by R. C. DeGeiso and L. B. Rogers (Abstract No. 82)
3:00 P.M.—"The Electrolytic Pointing of Tungsten Whiskers" by P. F. Russo, R. B. Soper, and Pei Wang (Abstract No. 83)
3:30 P.M.—"A Radioisotopic Study of Leveling in Bright Nickel Electroplating Baths" by S. E. Beacom and B. J. Riley (Abstract No. 84)
4:00 P.M.—"Electrodeposition of Porous Nickel" by J. J. MacDonald, D. G. Gage, and E. C. Brown (Abstract No. 85)
4:30 P.M.—"Electroplating of Nickel from the Pyrophosphate Bath" by S. K. Panikkar and T. L. Rama Char (Abstract No. 86)

Electrodeposition (cont'd)
Thursday, Oct. 2, 1958
Electrodeposition on Uncommon Metals
with C. L. Faust presiding
(BANQUET ROOM, Ground Floor)

9:00 A.M.—"Electroplating on Group IVB-VIB Metals" by E. B. Saubestre (Abstract No. 87)
9:30 A.M.—"Novel Nickel Plating Process" by J. T. N. Atkinson (Abstract No. 88)
10:00 A.M.—"Electroplating Metal Contacts on Semiconductors" by D. R. Turner (Abstract No. 89)
10:30 A.M.—"Electrodeposition of Aluminum on Uranium" by J. G. Beach and C. L. Faust (Abstract No. 90)
11:00 A.M.—"Electroplating on Thorium" by J. G. Beach and G. R. Schaer (Abstract No. 91)

Electrodeposition (cont'd)
Thursday, Oct. 2, 1958
Electrodeposition on Uncommon Metals (cont'd)
with J. G. Beach presiding
(BANQUET ROOM, Ground Floor)

2:00 P.M.—"Immersion Plating on Zircaloy 2" by L. R. Kohan (Abstract No. 92)
2:30 P.M.—"Electrocladding of Zirconium with Platinum" by A. B. Tripler, J. G. Beach, and C. L. Faust (Abstract No. 93)
3:00 P.M.—"Chromium Plating on Titanium Alloys" by Charles Levy (Abstract No. 94)
3:30 P.M.—"Plated Coating on Titanium Gears" by W. J. Hyink (Abstract No. 95)

ELECTRONICS—SEMICONDUCTORS

Monday, Sept. 29, 1958

Thermoelectric Materials and Device Design
with E. Mooser presiding
(BALLROOM, Ground Floor)

9:30 A.M.—Keynote Address—"Design of Thermoelectric Materials for Power Generation and Refrigeration" by R. R. Heikes (Abstract No. 96)
10:20 A.M.—"Preparation and Thermoelectric Properties of Bi_2Te_3 and Alloys with Bi_2Se_3" by T. C. Harman, M. J. Logan, B. Paris, and E. H. Lougher (Abstract No. 97)
10:50 A.M.—"Thermoelectric Measurements at Low Temperatures" by E. Mooser, W. B. Pearson, and I. M. Templeton (Abstract No. 98)
11:15 A.M.—"The Use of Controlled Solidification in Equilibrium Diagram Studies" by W. A. Tiller (Abstract No. 99)
11:40 A.M.—Recent News Papers. Short abstracts of these papers will be available at the meeting
12:30 P.M.—The Electrochemical Society Luncheon in the Ballroom, Ground Floor

Electronics—Semiconductors (cont'd)
Monday, Sept. 29, 1958
Structural Chemistry, Preparation, and Properties of Compound Semiconductors
with R. K. Willardson presiding
(BALLROOM, Ground Floor)

2:00 P.M.—Review Paper—"Crystal Chemistry and Physical Properties of Semiconductors" by E. Mooser (Abstract No. 100)
2:50 P.M.—"Inorganic Compounds for Semiconductor Devices" by A. J. Cornish (Abstract No. 101)
3:15 P.M.—"Silicon Carbide Crystal Formation" by A. H. Smith (Abstract No. 102)
3:35 P.M.—"Oxidation of Indium Antimonide" by A. J. Rosenberg, M. C. Levine, and C. S. Martel, Jr. (Abstract No. 103)
3:55 P.M.—"Purification of Semiconductor Materials by Chemical Methods" by J. A. Kafalas and P. H. Robinson (Abstract No. 104)
4:15 P.M.—"Stability of the Zinc Blende Structure of III-V Compounds" by Carol Kolm (Abstract No. 105)
4:35 P.M.—Recent News Papers. Short abstracts of these papers will be available at the meeting.

Electronics—Semiconductors (cont'd)
Tuesday, Sept. 30, 1958
Physics and Chemistry of Silicon and Germanium Crystals
with R. N. Hall presiding
(BALLROOM, Ground Floor)

9:00 A.M.—"The Use of Bismuth as a Donor Type Impurity in Germanium Single Crystals" by George Mortimer (Abstract No. 106)
9:25 A.M.—"Simple Method of Determining Crystal Perfection" by H. K. Herglotz (Abstract No. 107)
9:50 A.M.—"Vapor Deposition of Single-Crystal Ge by the Decomposition of GeI_2" by R. C. Sirrine (Abstract No. 108)
10:15 A.M.—"Analog Computation of Silicon Crystal Profiles with Three Active Impurities" by K. M. Kolb (Abstract No. 109)
10:40 A.M.—"Imperfections in Silicon" by H. L. Taylor (Abstract No. 109A)
11:00 A.M.—Recent News Papers. Short abstracts of these papers will be available at the meeting

Electronics—Semiconductors (cont'd)
Tuesday, Sept. 30, 1958
PN Junctions in Silicon and Germanium Crystals
with F. M. Smits presiding
(BALLROOM, Ground Floor)

2:00 P.M.—"Effects on Concentration Profiles of Variable Diffusion Coefficient and Surface Concentration" by Worden Waring (Abstract No. 110)
2:25 P.M.—"Evaluation and Control of Surface Concentration in Diffused Germanium Systems" by H. S. Veloric and W. Greig (Abstract No. 111)
2:50 P.M.—"Conversion Control during the Diffusion of Impurities into N-Type Germanium" by F. Barson, M. J. Dyett, C. Karan, and W. E. Mutter (Abstract No. 112)
3:15 P.M.—"Germanium Diffused Minicrystals and Their Use in Transistors" by I. A. Lesk and R. E. Coffman (Abstract No. 113)
3:40 P.M.—"Area Control in Diffused Silicon Devices through Variations in Diffusant Surface Concentrations" by L. D. Armstrong (Abstract No. 113A)
4:05 P.M.—Recent News Papers. Short abstracts of these papers will be available at the meeting.

Electronics—Semiconductors (cont'd)
Wednesday, Oct. 1, 1958
Surface Treatments and Device Technology
with W. T. Eriksen presiding
(BALLROOM, Ground Floor)

9:00 A.M.—"Chemical Etching of Silicon, II. The System HF, HNO_3, H_2O, $HC_2H_3O_2$" by H. Robbins and B. Schwartz (Abstract No. 114)
9:25 A.M.—"Reactions of Silicon with Aqueous Solutions of HF and Various Oxidizing Agents" by W. T. Eriksen and A. E. Baker (Abstract No. 115)
9:50 A.M.—"New Low-Melting Glasses Potentially Useful as Protective Coatings for Semiconductors" by S. S. Flaschen and A. D. Pearson (Abstract No. 116)

10:15 A.M.—"Selective Deposition of Metals on n- and p-Type Silicon by Electrochemical Displacement" by D. R. Turner (Abstract No. 117)
10:40 A.M.—"Germanium Electrode Behavior" by W. W. Harvey (Abstract No. 118)
11:05 A.M.—"An Analysis of Diode Characteristics with Application of Inversion Layer Theory to Forward Bias Conditions" by C. D. Root (Abstract No. 119)
11:30 A.M.—Recent News Papers. Short abstracts of these papers will be available at the meeting

ELECTROTHERMICS AND METALLURGY

Monday, Sept. 29, 1958
Properties of Graphite
with L. H. Juel presiding
(QUEBEC SUITE, First Floor)

9:30 A.M.—"High-Temperature Mechanical Properties of Two Commercial Graphites" by L. Green, Jr., M. L. Stehsel, and C. E. Waller (Abstract No. 120)
10:00 A.M.—"Some Physical Properties of a Commercial Graphite from Ambient Temperature to 2500°C" by P. N. Wagner, A. R. Driesner, E. A. Kmetko, and D. P. MacMillan (Abstract No. 121)
10:30 A.M.—"High-Temperature Short-Time Creep of Graphite" by H. E. Martens, L. D. Jaffe, and D. D. Button (Abstract No. 122)
11:00 A.M.—"Measurement of Creep in Graphite at 2500°-3000°C" by H. C. Stieber and R. C. Stroup (Abstract No. 123)
11:30 A.M.—"A Comparison of Physical, Electrical, and Thermal Properties of Graphite with Some Common Reference Materials" by G. B. Engle and L. M. Liggett (Abstract No. 124)
12:30 P.M.—The Electrochemical Society Luncheon in the Ballroom, Ground Floor

Electrothermics and Metallurgy (cont'd)
Monday, Sept. 29, 1958
Properties of Graphite (cont'd)
with R. P. Stambaugh presiding
(QUEBEC SUITE, First Floor)

2:00 P.M.—"Photomicrographic Examination of Cokes and Formed Carbon Bodies" by E. C. Thomas (Abstract No. 125)
2:30 P.M.—"Some Characteristics of Low Permeability Graphite" by R. L. Robinson and R. L. Mansfield (Abstract No. 126)
3:00 P.M.—"Thermal Conductivity of Pre- and Post-irradiated Graphite as a Function of Temperature" by R. A. Meyer (Abstract No. 127)
3:30 P.M.—"Electrical Resistance of Graphite-Graphite Connectors" by E. C. Thomas and J. H. Whitwell (Abstract No. 128)
4:00 P.M.—"Typical Distributions of Graphite Properties" by N. C. Hodge (Abstract No. 129)

Electrothermics and Metallurgy (cont'd)
Tuesday, Sept. 30, 1958
Arc Phenomena
with Charles Sheer presiding
(QUEBEC SUITE, First Floor)

9:00 A.M.—"The Continuous Transfer of Energy to Materials from an Arc Discharge" by J. Holmgren, L. Mead, and C. Sheer (Abstract No. 130)
9:25 A.M.—"Pressures in and around a High-Current Metallic Arc" by F. W. Wood (Abstract No. 131)
9:50 A.M.—"Positional Instability Behavior of Low Pressure D-C Arcs" by E. W. Johnson and R. Itoh (Abstract No. 132)
10:30 A.M.—"Crater Resistance of Submerged Arc Smelting Furnaces Simulated by a Simple Model" by O. Chr. Böckman (Abstract No. 133)
10:55 A.M.—"Arc Behavior in Variable Pressure Systems" by R. P. Morgan and T. E. Butler (Abstract No. 134)
11:20 A.M.—"Heat Transfer Ratio of the Argon Plasma Jets" by C. S. Stokes, W. W. Knipe, and L. A. Strevg (Abstract No. 135)

Electrothermics and Metallurgy (cont'd)
Tuesday, Sept. 30, 1958
Arc Applications
with E. W. Johnson presiding
(QUEBEC SUITE, First Floor)

2:00 P.M.—"Some Applications of the Carbon Arc Image Furnace" by M. R. Null and W. W. Lozier (Abstract No. 136)
2:30 P.M.—"The Carbothermic Reduction of Magnesium Oxide in the High-Intensity Arc" by S. Korman, A. Diniak, and C. Sheer (Abstract No. 137)
3:00 P.M.—"Arc Decomposition of Rhodonite" by V. Harris, J. Holmgren, S. Korman, and C. Sheer (Abstract No. 138)
3:40 P.M.—"Arc Furnace Preparation of Refractory Compounds" by H. A. Johansen (Abstract No. 139)
4:10 P.M.—"Electron Beam Vacuum Welding—Development of Process" by W. L. Wyman and W. I. Steinkamp (Abstract No. 140)

Electrothermics and Metallurgy (cont'd)
Wednesday, Oct. 1, 1958
Oxidation
with W. Tragert presiding
(QUEBEC SUITE, First Floor)

9:00 A.M.—"Special Optical Techniques for the Direct Observation of Oxidation in Metals" by S. J. Majka (Abstract No. 141)
9:30 A.M.—"The Initial Suggestion of Oxidation and the Problems of Discontinuous Oxidation" by U. M. Martius (Abstract No. 142)
10:00 A.M.—"High-Temperature Oxidation of Aluminum in Water Vapor" by P. E. Blackburn and E. A. Gulbransen (Abstract No. 143)
10:30 A.M.—"Kinetics of the Oxidation of Platinum" by G. C. Fryburg and H. M. Murphy (Abstract No. 144)
11:00 A.M.—"Kinetics of the Uranium-Steam Reaction" by B. E. Hopkinson (Abstract No. 145)

Electrothermics and Metallurgy (cont'd)
Wednesday, Oct. 1, 1958
Oxidation; Electric Smelting
with A. C. Haskell, Jr., presiding
(QUEBEC SUITE, First Floor)

2:00 P.M.—"Selective Oxidation of Al from an Al-Fe Alloy" by R. E. Grace and A. U. Seybolt (Abstract No. 146)
2:30 P.M.—"Selective Oxidation of 3¼% Si-Fe" by A. U. Seybolt (Abstract No. 147)
3:00 P.M.—"Oxidation Studies on the Iron-Chromium-Aluminum Heater Alloys" by E. A. Gulbransen and K. F. Andrew (Abstract No. 148)
3:30 P.M.—"Experimental Electric Smelting of a Siliceous Iron Ore" by G. E. Viens, G. V. Sirianni, and R. R. Rogers (Abstract No. 149)
4:00 P.M.—"Iron and Phosphate Slag from Byproduct Ferrophosphorus" by J. M. Potts, W. C. Scott, Jr., J. U. Campbell, and J. A. Wilbanks (Abstract No. 150)

ABSTRACTS

In the Index to Authors the Abstract Number is the number listed in the right-hand column.

BATTERY

Abstract No. 1

Investigation of the Electrochemical Characteristics of Organic Compounds, III. Nitroalkanes

R. Glicksman and **C. K. Morehouse**, RCA Labs., Radio Corp. of America, Princeton, N. J.

A theory based on the electron density in the vicinity of a reducible nitro group which had been used to explain the effect of substituent groups and their position on the operating potential of aromatic nitro compounds has been extended to the nitroalkane compounds. The high theoretical ampere-minute capacity of the nitroalkane compounds, along with their high operating potentials, shows these compounds to have considerable promise for use as cathode materials in primary cells.

Abstract No. 2

Investigation of the Electrochemical Characteristics of Organic Compounds, IV. Quinone Compounds

R. Glicksman and **C. K. Morehouse**, RCA Labs., Radio Corp. of America, Princeton, N. J.

A study of the electrochemical characteristics of various quinone compounds shows that the cathode potential of these compounds during current flow is dependent on the type and position of substituent groups in the molecule, the *p*H of the electrolyte, and

the nature of the quinone itself. Experimental data are presented for dry cells containing 2,5-dichloro-p-quinone and p-quinonedioxime as cathodes coupled with a magnesium anode.

Abstract No. 3

Fused Salt Relatives of the Leclanché Cell: A Thermodynamic Appraisal

R. E. Wood, U. S. Dept. of Commerce, National Bureau of Standards, Washington 25, D. C.

Available thermodynamic data permit the prediction of many aspects of the behavior of fused salt cells. Such data are used here in a study of cells comprising a zinc negative electrode, a positive electrode which is MnO_2, Mn_2O_3, or $ZnMn_2O_4$, and an electrolyte which is fused zinc chloride containing various concentrations of manganous chloride. Chemical reactions and equilibria in these cells are considered, and the cell potentials are estimated for the temperature range 350° to 500°C.

Abstract No. 4

Studies on Depolarizers for Fused Cells

S. M. Selis, E. S. McKee, and **L. G. Bockstie, Jr.,** Catalyst Research Corp., Baltimore, Md., and **L. P. McGinnis,** Diamond Ordnance Fuze Labs., Washington, D. C.

Iron oxides and tungstic oxide have been studied as depolarizers in molten salt cells. The system was Mg or Ca/LiCl-KCl (1)/depolarizer, Ni. With α-Fe_2O_3, reaction products are of the type (Li_2O) (FeO). Factors affecting depolarization by iron oxide include crystalline form, SiO_2 and TiO_2 content, and porosity. Mixtures yield potentials over a 500-mv range. Activation and discharge times with WO_3-depolarized cells depend on macroscopic and microscopic area, particle shape, and degree of agglomeration.

Abstract No. 5

Thermally Regenerative Ionic Hydride Galvanic Cell

R. E. Shearer and **R. C. Werner,** MSA Research Corp., Callery, Pa.

A system has been developed which has produced electrical energy and which has easily regenerated the reactants by raising the temperature of the product. The cell is based on the electrochemical formation of ionic hydrides in a fused halide eutectic. Regeneration has been accomplished by heating the solution of hydride in the eutectic, driving off hydrogen, and floating the liquid metal reactant.

Abstract No. 6

Iodine-Activated Solid Electrolyte Cell for Use at High Temperature

J. L. Weininger, Research Lab., General Electric Co., P.O. Box 1088, Schenectady, N. Y.

Miniature cells, $Ta(I_2)/AgI/Ag$, have been studied at 150°-550°C. In this temperature range the cells have the following characteristics: complete conversion of the consumable silver anode into its electrical equivalent, open-cell voltage of 0.67 v, short-circuit currents up to 30 ma (current density 480 ma/cm^2), capacity of 10 ma-hr, power output up to 5 mw-hr/cell, definite activation temperatures obtained by selecting suitable depolarizers, and indefinitely long shelf life below those temperatures.

Abstract No. 7

The Silver-Silver Chloride-Chlorine Solid Electrolyte Cell

D. M. Smyth, Sprague Electric Co., North Adams, Mass.

A $Ag/AgCl/Cl_2$ cell has been developed in which the chlorine is furnished by the dissociation of potassium tetrachloroiodide, $KICl_4$. These solid electrolyte cells are extremely stable and compact and deliver current in the microampere range. The properties of this cell system are discussed in terms of the electrical properties of silver chloride and the dissociation chemistry of the polyhalide cathode.

Abstract No. 8

Zinc-Mercuric Dioxysulfate Dry Cell

Samuel Ruben, Ruben Labs., New Rochelle, N. Y.

A dry cell is described which provides some of the desirable characteristics of the mercuric alkaline cell while allowing the use of inexpensive conventional dry cell construction. The system is $Zn/ZnSO_4/HgSO_4 \cdot 2HO + C$ and has an over-all reaction of $3Zn + HgSO_4 \cdot 2HgO \rightarrow ZnSO_4 + 2ZnO + 3Hg$. A relatively flat discharge characteristic is obtained within the proper limits of current density. The cell capacity is directly referable to the $HgSO_4 \cdot 2HgO$ or $3HgO \cdot SO_3$.

Abstract No. 9

Magnesium-Bismuth Oxide Dry Cells

C. K. Morehouse and **R. Glicksman,** RCA Labs., Radio Corp. of America, Princeton, N. J.

Bismuth oxide, because of its high theoretical capacity, flat voltage-discharge curve, and low solubility in neutral solution, shows promise for use as a cathode material when coupled with a magnesium anode in an aqueous $MgBr_2$ electrolyte. Magnesium-bismuth oxide dry cells have a flat operating voltage between 0.90 and 1.05 v over a wide range of current drains and give greater watt-hour capacities per unit of weight and volume than the commercial Leclanché dry cell.

Abstract No. 10

An Investigation of the Discharge Characteristics of High Oxidation State Compounds of the Groups VI-VIII Elements in an Alkaline Electrolyte

C. K. Morehouse and **R. Glicksman,** RCA Labs., Radio Corp. of America, Princeton, N. J.

Experimental half-cell discharge data are given for a number of compounds of the Groups VI-VIII elements in strongly alkaline NaOH solution, along with comparisons between these data and their theoretical potentials. Among the compounds studied were those of the 0, +4, and +6 oxidation states of S, Se, and Te, the +5 and +7 states of the halogens, manganese in various oxidation states, and the oxides of the Group VIII metals.

Abstract No. 11

The Anodic Oxidation of Cadmium

P. E. Lake and **E. J. Casey,** Defence Research Chemical Labs., Defence Research Board, Ottawa, Ont., Canada.

Electrical properties of the anodic films formed on cadmium in caustic electrolytes have been examined by an analysis of voltage decay after current interruption. The effects of current density, time, temperature, and electrolyte composition have been studied. An interpretation of the results is suggested.

Abstract No. 12

Dependence of Rate of Oxidation and Reduction of Cd and Ag on Overpotential

G. T. Croft, Edison Lab., Thomas A. Edison Industries, McGraw-Edison Co., West Orange, N. J.

The rate of electrochemical oxidation and reduction of both cadmium and silver in potassium hydroxide electrolyte has been measured as a function of overpotential. The rate of oxidation of cadmium is maximum at overpotentials of 18.0 and approximately 40 mv. The rate of reduction is a monotonically increasing function of overpotential. The rate of oxidation of silver increases with overpotential, and the rate of reduction is maximum at an overpotential equal to 46.0 mv.

Abstract No. 13

Textures of Electrodeposited Lead Dioxide

Yasuichi Shibasaki, 30 Dai-machi, Kanagawa-ku, Yokohama, Japan (Present address: Chemistry Dept., Ohio State University, Columbus 10, Ohio)

Powder gathering, dull smooth, bright smooth, fibrous, columnar, rough, and porous textures, are obtained about electrodeposited lead dioxide. Relations

among the texture, conditions of the electrodeposition, and strengths of the lead dioxide are obtained from lots of experiments. The bright smooth lead dioxide is the strongest, and many conditions from which samples of this kind were obtained are shown.

Abstract No. 14

Oxygen Overvoltage and Electrode Potentials of α- and β-PbO_2

P. Ruetschi, B. D. Cahan, and **R. T. Angstadt,** Electric Storage Battery Co., P.O. Box 5723, Philadelphia 20, Pa.

Buildup and decay of oxygen overvoltage on α- and β-PbO_2 have been studied. Layers of the two PbO_2 modifications were electrodeposited on Pt wires, sealed at both ends into glass. Initial buildup of oxygen overvoltage at constant current is linear with time, and decay on open circuit is logarithmic with time. The results are explained on the basis of a generalized theory of overvoltage. Oxygen evolution proceeds under formation of activated complexes ("higher oxides") which are responsible for a large apparent electrical capacity. Electrode potentials of α- and β-PbO_2 have been measured as a function of pH and temperature.

Abstract No. 15

Ion Exchange Property of Manganese Dioxide

Akiya Kozawa (Present address: Dept. of Chemistry, Western Reserve University, Cleveland, Ohio) and **Kumazo Sasaki,** Dept. of Applied Chemistry, Faculty of Engineering, Nagoya University, Nagoya, Japan

When manganese dioxide is shaken with an electrolyte solution, the cation is adsorbed and hydrogen ion is released: an ion exchange reaction takes place on the surface of the manganese dioxide. A simple method based on zinc ion adsorption is proposed to measure the ion-exchange capacity of various manganese dioxides. The results have been compared to the surface area of those samples measured by the B.E.T. method based on nitrogen gas adsorption, and a fairly good relationship was found between them. The mechanism of the ion exchange is correlated with the structure of a surface complex.

Abstract No. 16

Cathodic Reduction of Manganese Dioxide in Alkaline Electrolyte

N. C. Cahoon, Edgewater Development Labs., and **M. P. Korver,** Research Labs., National Carbon Co., Division of Union Carbide Corp., Cleveland, Ohio

A study of the mechanism of the reduction of manganese dioxide in strongly alkaline electrolytes has shown that the rather complex process may be considered as occurring in three steps. The first is the simultaneous reduction to form $Mn(OH)_2$ and an intermediate oxide tentatively identified as Mn_2O_3; the second step is the electrochemical reduction of Mn_2O_7 to form both Mn_3O_4 and $Mn(OH)_2$; the final step is the electrochemical reduction of Mn_3O_4 to $Mn(OH)_2$. Both chemical and x-ray diffraction analyses of cathodes at various stages of reduction are presented.

Abstract No. 17

Silver and Its Oxides

T. P. Dirkse, Dept. of Chemistry, Calvin College, Grand Rapids 6, Mich.

A review has been prepared of the electrochemistry of the silver oxide electrode. The discussion covers the structure and electrochemistry of the oxides of silver and their behavior in batteries.

Abstract No. 18

The Oxides and Hydroxides of Nickel, Their Composition, Structure, and Electrochemical Properties—A Review

U. B. Thomas, Bell Telephone Labs., Inc., Murray Hill, N. J.

The literature on the structure, composition, and properties of nickel oxides and hydroxides has been reviewed with special emphasis on their relation to electrochemical processes. In addition to certain well-crystallized compounds, others of ill-defined structure and nonstoichiometric composition contain nickel in average oxidation states between two and four. Oxidation and reduction of these compounds does not take place in the solution but on or within the solid. According to a hypothesis proposed independently by Feitknecht and Wynne-Jones and their co-workers, the mobile species is the proton. On this basis, the operation of nickel oxide electrodes is described as involving the transport of electron holes and proton vacancies in a disordered nickelous hydroxide lattice.

Abstract No. 19

The Manganese Dioxide Electrode

W. C. Vosburgh, Dept. of Chemistry, Duke University, Durham, N. C.

Recent work on the structure and properties of MnO_2 and the discharge mechanism of the electrode are reviewed. Most poorly crystallized forms of artificial and natural MnO_2 can now be related to one or another of the well crystallized natural oxides. Interesting properties of MnO_2 recently investigated are semiconductivity, transformations on heating, surface area and exchange with radioactive Mn. Recent theories of the discharge mechanism assume a reaction in the solid phase and involve diffusion in the solid.

Abstract No. 20

The Electrochemistry of the Lead Anode in Aqueous Solutions

Jeanne Burbank, Naval Research Laboratory, Washington 25, D. C.

A review has been prepared of the electrochemistry of the lead oxide and lead dioxide electrodes. The discussion covers the conditions under which each of the oxides may be formed, the regions of thermodynamic stability, and the conditions under which they operate in a storage battery.

Abstract No. 21

Oxide Electrode Processes in Batteries

E. Willihnganz, C & D Batteries, Conshohocken, Pa.

A review is presented of the anodic processes in batteries. The limitations imposed by reaction kinetics on the application of equations which are valid under equilibrium conditions are discussed. Factors which may cause an electrode to operate at less than 100% efficiency are considered and applied to the various types of batteries.

Abstract No. 22

Corrosion of the Zinc Electrode in the Silver-Zinc-Alkali Cell

T. P. Dirkse and **Frank De Haan,** Dept. of Chemistry, Calvin College, Grand Rapids 6, Mich.

A study has been made of the factors that affect or bring about the corrosion of the zinc electrode in a silver-zinc-alkali cell. Cells containing 30% potassium hydroxide as electrolyte were used and kept at room temperature. Special attention was centered on open circuit or stand conditions. This corrosion is affected primarily by oxygen and by dissolved silver oxides.

Abstract No. 23

Studies on Lead Sulfate Crystals

E. J. Casey, K. N. Campney, and **I. H. S. Henderson,** Defence Research Chemical Labs., Defence Research Board, Ottawa, Ont., Canada

Studies on crystallization, measurements of zeta potential, and measurements of electrical conductivity are presented and discussed. The results throw some light on the effects of foreign ions on lead sulfate surfaces in sulfuric acid.

Abstract No. 24

Battery Pastes—Compositions and Characteristics

J. F. Schaefer and **H. R. Karas,** Globe-Union Inc., Milwaukee 1, Wis.

Four battery grade lead oxides, two leady, two non-leady, were examined. A method is outlined for con-

struction of a comprehensive mixing curve relating acid concentration, water concentration, cube weight, and consistency (penetration). Composition of the paste at various points on the mixing curve is discussed on the basis of x-ray powder diffraction patterns and microscopic examination of paste samples. Characteristics of the mixing curve are discussed on the basis of findings.

Abstract No. 25

A Reference Half-Cell for Laboratory and Industrial Applications

N. C. Cahoon and **J. P. Oliver,** Development Div., National Carbon Co., Div. of Union Carbide Corp., P.O. Box 6056, Cleveland 1, Ohio

A reference half-cell for both laboratory and industrial use is presented. This unit consists of a primary cell in which one of the electrodes serves as the reference element. In units utilizing Leclanché cells, the zinc electrode is the reference element, while the MnO_2 electrode serves as a secondary electrode against which the potential of the zinc electrode may be measured readily to give the cell voltage. As long as the cell voltage is within prescribed limits, the potential of the zinc electrode is maintained at or near its initial value. Design features enable the preparation of units with resistances as low as 10 ohms. The construction is sufficiently rugged to enable its broad application in industrial production and testing facilities where the use of conventional half-cells is precluded.

Abstract No. 26

A New Separator for the Aluminum Dry Cell

N. C. Cahoon, Edgewater Development Labs., and **M. P. Korver,** Research Labs., National Carbon Co., Division of Union Carbide Corp., Cleveland, Ohio

A new and improved separator medium for the aluminum dry cell is described. It provides an adhesive contact with the anode and a satisfactory electrolytic contact with the cathode. The method by which this separator is prepared involves a new technique which is described. The separator layer significantly improves the keeping quality and delayed service performance of the aluminum-manganese dioxide cell.

Abstract No. 27

Morphological Characteristics of Nickel Powders for Use in Sintered Plate Nickel Cadmium Storage Batteries

C. F. Cook, Jr., W. F. Nye, and **F. W. Leonhard,** U. S. Army Signal Research and Development Lab., Fort Monmouth, N. J.

The relationship of the morphological characteristics of nickel powders to plaque porosity, abrasion resistance, sintering, and impregnating characteristics is revealed by stereoelectron-microscopy, using a new replica technique. The powders studied include those prepared by thermal decomposition, electrolysis, and chemical precipitation. Unique among the nickel powders studied is carbonyl nickel, which exhibits a three-dimensional dendritic structure with well-developed crystal faces. It is this characteristic which appears to give the material unique sintering characteristics.

Abstract No. 28

Nickel Cadmium Batteries, Pocket-Type Construction

A. B. Eilbeck, Nife, Inc., 60 E. 42 St., New York 17, N. Y.

During a period of nearly fifty years, the pocket-type nickel cadmium batteries have given exceptionally fine service. However, there have been many misconceptions regarding the cycle life and the charge and discharge characteristics. Tests have been run on life cycles, deep discharges and reverse charges, a series or repeated high-rate discharges, and charges at low voltage, which show good results and excellent voltage characteristics.

CORROSION—THEORETICAL ELECTROCHEMISTRY—BATTERY

Abstract No. 29

Some Observations on Films Formed on Steel in Contact with Aqueous Media

M. C. Bloom and **M. J. Strauss,** U. S. Naval Research Lab., Washington 25, D. C

A survey is made of experimental data obtained from the reaction of iron and steel with aqueous media at room temperature and at 316°C. The reaction was followed by *pH* measurement of the solution and by microscopic, x-ray, and electron diffraction analysis of the corrosion product films. A study of the transformation properties of the oxide corrosion products involved and some data involving the use of hydrogen peroxide as an oxygen source are included.

Abstract No. 30

The Cracking of Low-Carbon Steel during Heating with Aqueous Slurries of γ-FeOOH

M. J. Strauss and **M. C. Bloom,** U. S. Naval Research Lab., Washington 25, D. C

γ-FeOOH is generated as a corrosion product film during corrosion of low-carbon steel in oxygen-containing aqueous solutions at room temperature. When aqueous slurries of γ-FeOOH are heated in sealed steel capsules at 316°C, cracks develop rapidly and penetrate the 0.020-in. capsule walls in a few hours. This phenomenon is critically examined and is apparently a form of stress corrosion cracking.

Abstract No. 31

The Reaction between Iron and Water in the Absence of Oxygen

V. J. Linnenbom, U. S. Naval Research Lab., Washington 25, D. C.

The reaction between pure iron and oxygen-free water has been investigated at 25°, 60°, and 300°C. At room temperature, the primary product of reaction appears to be $Fe(OH)_2$; no evidence was found to indicate the presence of Fe_3O_4. Formation of Fe_3O_4, however, occurs readily in the iron-water system at both 60° and 300°C. The possibility that this Fe_3O_4 is produced via formation and subsequent decomposition of $Fe(OH)_2$ is discussed; the conclusion is reached that the mechanism of formation of Fe_3O_4 from the reaction of iron and water cannot be definitely decided at this time.

Abstract No. 32

A Study of Corrosion Films on Zirconium and Its Alloys by Impedance Measurements

J. N. Wanklyn and **D. R. Silvester,** Atomic Energy Research Establishment, Harwell, Berkshire, England

The oxide films formed on zirconium and some of its alloys during corrosion in steam and water at 325°C have been studied by impedance measurements made by immersion in an electrolyte. A fall in the protective character of the film is accompanied by an increase of capacity, and measurements of the latter provide a useful method of comparing films. The behavior of the resistive part of the impedance, and the influence of frequency and electrolyte conductivity are complex, and only a partial interpretation can be given.

Abstract No. 33

Direction of Ionic Movement in the Anodic Oxidation of Aluminum

J. E. Lewis and **E. C. Plumb,** Alcoa Research Labs., New Kensington, Pa.

It is demonstrated, by a series of marker experiments in which layers of nonporous anodic oxide were tagged by incorporating radioactive material in them, that nonporous anodic oxide grows at, close to, the oxide-electrolyte interface; it is concluded that the aluminum

ion is the mobile species. Similar experiments with a porous oxide may also be interpreted in terms of formation of the oxide at the oxide-electrolyte interface, but in this case the interface is at the bottom of pores filled with electrolyte.

Abstract No. 34

A Radiochemical Method for Measuring the Surface Area of Aluminum Metal and Powders

J. E. Lewis, Alcoa Research Labs., New Kensington, Pa.

In chemically stripping the oxide film from aluminum with a phosphoric-chromic acid mixture, the solution reacts superficially with the metal forming a residual phosphoric-chromate film. Using a radioactive phosphoric acid component, one obtains the weight of film deposited. Relating the film weight to the geometric area of a metal specimen or the weight of a powdered specimen, one obtains the specific surface area with a resolution of 10-20Å.

Abstract No. 35

Observations on the Anodic Oxidation of Aluminum

R. C. Plumb, Research Group on the Physics and Chemistry of Solids, Cambridge University, Cambridge, England (Present Address; Alcoa Research Labs., New Kensington, Pa.)

The anodic conversion of aluminum to aluminum oxide is essentially quantitative in a buffered neutral electrolyte containing no halogen ions. Film thickness is proportional to the voltage gradient. The film contains a quantity of the anion from the electrolyte. The coulombic transfer during film formation is quantitatively accounted for by oxidation of aluminum to the trivalent state and liberation of oxygen gas.

Abstract No. 36

The Specific Surface Area of Aluminum as Determined with Continuously Variable Resolution from 20 to 1000Å

R. C. Plumb, Research Group on the Physics and Chemistry of Solids, Cambridge University, Cambridge, England (Present address: Alcoa Research Labs., New Kensington, Pa.)

A new technique for studying surface topography of metals that can be oxidized anodically is described. Coulometric measurements of the formation of films in steps as small as 20Å give a measure of the specific area with what may be described as variable resolution from 40 to 1000Å. Results are compared with work described earlier by a radiochemical technique which has a resolution of about 20Å and with optical measurements made at resolutions greater than 1000Å. The shape of a surface area vs. resolution curve gives information about the topography of the surface.

Abstract No. 37

A Study of the Structure of Anodic Oxide Films on Aluminum

D. J. Stirland and **R. W. Bicknell,** Caswell Research Laboratories, Towcester, Northants, England

The influence of the formation voltage on the structure of anodic aluminum oxide films has been studied by electron microscope and electron diffraction methods. It has been shown that low formation voltages (< 100 v) produce an amorphous oxide layer, whereas high formation voltages produce amorphous oxide together with some crystalline γ' -alumina. The location of this crystalline oxide within the anodic layer is discussed.

Abstract No. 38

Structure of Hydrous Oxides on Aluminum

W. E. Tragert, Research Lab., General Electric Co., Schenectady, N. Y.

The oxidation of aluminum in water or water vapor generally produces an oxide film which can be classified on the basis of the crystalline arrangement of the oxygen ions. Of the eleven crystallographically distinguishable aluminum oxides, four have been formed on metallic aluminum; of these, three exhibit cubic close packing and one exhibits hexagonal close packing of oxygen ions. It is shown that the relative proportions of aluminum and hydrogen ions in the oxide lattice comprise a significant parameter in evaluating the influences of temperature, pressure, and electric field on the crystal structure.

Abstract No. 39

Effect of Stripping of Anodized Coatings from Aluminum on Electrical Resistance

Waltr Beck, E. D. Zavaglia, and **S. J. Ketcham,** Aeronautical Materials Lab., Naval Air Material Center, Philadelphia 12, Pa.

Stripping of anodized coatings from aluminum by action of chromic-phosphoric or hydrofluoric-nitric acid mixtures was studied by surface resistance measurements, using a spring loaded probe electrode and Kelvin bridge circuit. The effect of stripping time on resistance was proved by statistical analysis to be significant. Based on the surface resistance, tentative calculations of distribution and area of pores in the coating were made and a mechanism of stripping action postulated which was supported by weight loss measurements, microscopic, and electron microscopic observations.

Abstract No. 40

The Aluminum Electrode, I. The Effect of the Oxide Film

R. C. Plumb, Alcoa Research Labs., New Kensington, Pa.

A technique has been developed for measuring the potential of initially oxide-free aluminum surfaces after different periods of oxidation. The potential decreases as a logarithmic function of time exposed to the atmosphere. The decrease appears to be in direct proportion to the thickness of the film. Oxide films form in solution as well as in gaseous atmospheres but at a much higher rate. The potential of the oxide-free surface may be obtained by extrapolating to zero time. The effects of the oxide films on tantalum and copper have also been observed.

Abstract No. 41

The Aluminum Electrode, II. The Reactions Taking Place at the Electrolyte-Aluminum Interface

R. C. Plumb, Alcoa Research Labs., New Kensington, Pa.

The technique described in the previous paper has been used to determine the potential of oxide-free aluminum surfaces with a variety of electrolytes over a wide pH range. The measured potentials may be related directly to the thermodynamic potentials by assuming that aluminum ions in the double layer dissociate water into hydroxyl ions and protons. The results indicate that the aluminum ion in solution has an anion atmosphere so that it is essentially a neutral entity. The observed potentials and their variation with pH agree quantitatively with the thermodynamic values.

Abstract No. 42

Films Formed by A-C Anodization of Aluminum in Sulfuric Acid Solutions

W. H. Fischer and **J. A. Consiglio,** General Electric Co., Schenectady, N. Y.

A pilot plant for the continuous strand annealing, cleaning, degreasing, and anodizing of aluminum wires has been constructed. The electrolyte is 40 wt % sulfuric acid. The effects of such process variables as annealing temperature, electrolyte temperature, residence time, and current density have been evaluated in relation to electrical and physical properties of the anodized coating. Progress to date indicates that an insulated electrical conductor suitable for operation at temperatures up to possibly as much as 400°C can be produced successfully.

Abstract No. 43

Anodic Behavior of Aluminum at Low Potentials

J. V. Petrocelli, Research Lab., The International Nickel Co., Inc., Bayonne, N. J.

Electrode potentials, differential capacity, and anodic polarization curves have been determined for aluminum in sulfuric acid solutions. It is shown that the anodic behavior in the region of low potentials (−1.0 v to + 3.0 v, S.C.E. scale) follows the relationship $i = A \exp(BF)$. Differential capacity measurements show that the capacitance is inversely proportional to the potential. The analysis of the experimental data indicates the existence of a very thin film on the aluminum in this low potential region.

Abstract No. 44

The Flade Potential of Iron Passivated by Various Inorganic Corrosion Inhibitors

H. H. Uhlig and **P. F. King,** Dept. of Metallurgy, Massachusetts Institute of Technology, Cambridge, Mass.

The characteristic potential obtained just before decay of passivity (Flade potential) was measured for iron passivated in various ways. The Flade potential is linear with pH, of slope 0.059 up to approximately pH 4.5. At higher pH values there is some divergence and the potentials reach a constant value for iron passivated anodically or by conc. HNO_3. The standard Flade potential (pH − 0) for various passivators is increasingly noble in the order: nitrite (−0.50v); chromate, ferrate, molybdate (−0.54 v); tungstate (−0.61 v); and anodic polarization or conc. HNO_3 (−0.64 v). Deviations from the average are small, indicating that the structure and composition of the passive film on iron is largely independent of the passivation process.

Abstract No. 45

The Mechanism of Passivating-Type Inhibitors

Milton Stern, Metals Research Labs., Electro Metallurgical Co., Division of Union Carbide Corp., Niagara Falls, N. Y.

A passivating-type inhibitor functions by producing local-action current which anodically polarizes a metal into the passive potential region. The major factors which determine whether a particular system will exhibit passivity are: (*a*) the reversible potential of the redox system created by the oxidizing inhibitor; (*b*) the electrochemical parameters for reduction of the inhibitor on the metal surface (exchange current, Tafel slope, and limiting diffusion current); and (*c*) the critical anodic current and Flade potential of the metal. The amount of inhibitor found associated with the surface is not necessarily related to adsorption. Data are presented for passivation of stainless steel and titanium. The mechanism is discussed in terms of various oxidizing agents including oxygen, chromate, molybdate, and pertechnetate.

Abstract No. 46

Polarization at Hafnium Electrodes

Norman Hackerman and **Lewis Battist,** Dept. of Chemistry, University of Texas, Austin, Texas

Measurements were made in the range of 10^{-1} to 10^{-4} $\mu a/cm^2$ in neutral NaCl and alkaline Na_2SO_4. In oxygen-saturated NaCl and Na_2SO_4 and in air-free Na_2SO_4 the Tafel slope for hydrogen evolution was 0.12, while in air-free NaCl it was 0.06. The hydrogen overpotential at 1 ma/cm^2 in the former was 0.83 v and in the latter 0.65 v. The metal blistered at higher current densities. In Na_2SO_4, the Tafel slope for oxygen evolution was 0.138 with overvoltage of 1.54 v at 1 $\mu a/cm^2$, but in air-free NaCl the metal pitted at and above 5 $\mu a/cm^2$ (anodic).

Abstract No. 47

The Oxygen-Evolution Reaction at Gold Anodes, I. Accuracy of Overpotential Measurements

Sidney Barnartt, Research Labs., Westinghouse Electric Corp., Pittsburgh 35, Pa.

The literature data on steady-state values of oxygen overpotential are highly discrepant. The factors affecting the accuracy of the measurements and a new cell design for improved accuracy with a Luggin-Haber capillary are described. Current distribution in the cell, limitations imposed by the current efficiency, and the *IR* drop included in the measurement, overpotential-time curves at constant current density, and the accuracy with which Tafel's equation is obeyed are presented.

Abstract No. 48

Strain Electrometry and Corrosion, V. Film Properties and Strain Potential

J. C. Giddings, A. G. Funk, C. J. Christensen, and **Henry Eyring,** Graduate School, 207 John R. Park Bldg., University of Utah, Salt Lake City, Utah

Measurements of the strain transients have been recorded here for several metal electrodes including copper, aluminum, zinc, nickel, silver, and iron. The magnitude of the transients as a function of the percentage strain are treated by an extension of previous theoretical results. It is found that the transients depend on the position of an electrode in the emf series and on the protective nature of the film as predicted by the theoretical considerations. In addition to the above, several experiments have been reported concerning the effect of corrosion inhibitors on strain transients. Some possible theoretical interpretations are made on these preliminary results.

Abstract No. 49

Kinetics of Ion Motion in Anodic Ta_2O_5 Films

D. A. Vermilyea, Research Lab., General Electric Co., Schenectady, N. Y.

When the electric field in a Ta_2O_5 film is suddenly changed, there is a sudden change of current followed by a slower change which occurs over a period of a few seconds under most conditions. An analysis of studies of these transients and of other experiments such as x-ray diffraction and dissolution behavior of the film has shown that changes in film structure accompany changes in the temperature and electric field within the film.

Abstract No. 50

Growth of Oxide Films on Copper Single Crystal Surfaces in Water*

Jerome Kruger, National Bureau of Standards, Washington 25, D.C.

Kinetic studies of the growth of oxide films formed on the surfaces of copper single crystals in contact with high-purity water containing oxygen at room temperature using the polarimetric technique of Winterbottom to determine film thickness are described. The influence of crystallographic orientation of the reacting surface, presence of CO_2, oxygen concentration, and stirring on rate of film growth were investigated.

* The work is supported in part by the Corrosion Research Council.

Abstract No. 51

Formation of Calomel Films on Mercury Anodes

D. C. Cornish, D. J. G. Ives, and **R. W. Pittman,** Dept. of Chemistry, Birkbeck College, University of London, England, and **H P. Dibbs,** Atomic Energy Authority of Canada, Ottawa, Ont., Canada

The anodization of mercury in aqueous HCl produces a complex sequence of changes at the metal-solution interface which have been studied by means of oscillographic potential/time records under galvanostatic conditions. Except at extremely low current densities, an abrupt transition between polarized and depolarized states occurs, marked by characteristic and reproducible potential changes associated with the formation, crystallization, and further growth of a calomel monolayer. At a later stage, two distinguishable kinds of passive state are attained successively, in which current continues to flow at elevated potentials, perhaps by alternative mechanisms.

Abstract No. 52

The Performance of Zinc, Magnesium, and Aluminum Primary Cell Anodes—A Review

R. Glicksman, RCA Labs., Radio Corp. of America, Princeton, N. J.

In this paper some of the factors involved in the operation of a primary cell anode are presented. The effect of such variables as alloy composition, inhibitors, pH, electrolyte composition, current density, and type of service, on the performance characteristics of zinc, magnesium, and aluminum anodes is discussed.

Abstract No. 53

The Magnesium Anode in Aqueous Solutions, I. Steady-State Behavior

J. L. Robinson, J. L. Nichols, and **M. R. Bothwell,** Dow Chemical Co., Midland, Mich.

The weight loss at the magnesium anode generally increases linearly with impressed current at a rate which is greater than that expected for Mg^{++} ion production as the sole anode process. Since this rate is occasionally too great to be accounted for by Mg^{+} production as the only other process, it is concluded that a current dependant corrosion process is necessary and indeed may be sufficient by itself to explain all of the facts.

Abstract No. 54

The Magnesium Anode in Aqueous Solutions, II. Transient Behavior

P. F. King and **J. L. Robinson,** Dow Chemical Co., Midland, Mich.

The magnesium anode exhibits a transient polarization (so-called "delayed action") on initiating drain. The results of some studies of this phenomenon are presented.

Abstract No. 55

Potential-Time Changes at Anodically and Cathodically Polarized Magnesium

G. R. Hoey and **M. Cohen,** National Research Council, Ottawa, Ont., Canada

A preliminary study of potential-time decay curves at anodically and cathodically polarized magnesium by the d-c current interrupter method is presented. Double layer capacity and resistance data for polarized magnesium in buffered aqueous solutions containing chloride, bromide, and iodide is discussed in terms of the structure of the electrical double layer.

Abstract No. 56

A New Experimental Technique for the Study of Films Produced at Electrochemical Interfaces

B. D. Cahan and **P. Ruetschi,** The Electric Storage Battery Co., Philadelphia, Pa.

Measurements of the initial electrical characteristics of electrolytically produced surface films are frequently complicated by the transient nature of the intermediate steps. In constant current anodizations, these transients can be investigated by the use of an interrupter and an oscilloscope camera. Instrumentation for this purpose is discussed, and an interrupter coupled to an oscilloscope controlled by the single electrode potentials produced, for use with a lead electrode system, is described.

Abstract No. 57

Anodic Films Formed on Lead in Aqueous Solutions

Jeanne Burbank, Naval Research Lab., Washington 25, D. C.

The films formed on lead in aqueous media have been identified by electron and x-ray diffraction, and examined by light and electron microscopy. The structural and chemical nature of the deposits is determined by the conditions of deposition. In the presence of air or oxygen, oxides containing both di- and tetravalent lead were formed, depending on the pH of the corrosive medium. At high impressed anodic potentials, deposits of PbO_2 were identified. Discharge of PbO_2 films on lead and its alloys in sulfuric acid solutions was observed by microscopy to result in variations in the physical nature of the lead sulfate deposited.

CORROSION

Abstract No. 58

Corrosion Studies and the Protection of Ferrous Metals Against Corrosion
An account of the work of the Corrosion Committee of the British Iron and Steel Research Association

J. C. Hudson and **J. F. Stanners,** British Iron and Steel Research Association, 140 Battersea Park Rd., London S.W. 11, England

The Corrosion Committee has been investigating corrosion problems relating to ferrous metals since 1928. Particular emphasis has been laid on long-term researches concerned with atmospheric corrosion and its prevention by means of metal coatings and paints. In the marine field, successful anticorrosive compositions for ships' bottoms have been developed. Considerable attention has also been devoted to the corrosion of buried iron and steel. In addition, various accelerated performance tests for protective coatings have been compared. Short-term investigations designed to overcome specific industrial problems have supplemented these researches. The paper concludes with an outline of the Committee's current research program.

Abstract No. 59

The Oxidation of Aluminum and Certain of Its Binary Alloys Below 450°C

M. J. Dignam, Aluminium Labs., Ltd., Kingston, Ont., Canada

The thicknesses of oxide films formed in dry oxygen were estimated from current-voltage curves obtained by anodically polarizing the samples with linearly increasing applied potential. Below 450°C the results are in agreement with the Cabrera-Mott theory for the growth of thin oxide films on metals. The effects of certain alloying additions, in particular copper and silicon, were also studied by comparing polarization curves and weight gain data obtained for the different alloys.

Abstract No. 60

The Diffusion of Oxygen in Alpha and Beta Zircaloy 2 and Zircaloy 3 at High Temperatures

M. W. Mallett, W. M. Albrecht, and **P. R. Wilson** (Present address: Dept. of Chemistry, University of Massachusetts, Amherst, Mass.), Battelle Memorial Institute, Columbus, Ohio

The diffusion rates of oxygen in alpha and beta Zircaloy 2 and Zircaloy 3 were determined in the range 1000°-1500°C. For Zircaloy 2, the variation of the diffusion coefficients (in cm^2/sec) with temperature are given by the equations

$$D\alpha = 0.196 \exp(-41{,}000 \pm 1500/RT)$$
$$D\beta = 0.0453 \exp(-28{,}200 \pm 2400/RT)$$

The diffusion rates of oxygen in alpha and beta Zircaloy 3 at 1100° and 1400°C are in close agreement with those for oxygen in Zircaloy 2. Diffusion coefficients are about 10 times greater than those for nitrogen in high-purity beta zirconium.

Abstract No. 61

Oxidation Studies on the Iron-Chromium-Aluminum Heater Alloys

E. A. Gulbransen and **K. F. Andrew,** Research Labs., Westinghouse Electric Corp., Pittsburgh 35, Pa.

Three iron-chromium-aluminum alloys were studied from 700° to 1100°C. A transformation occurs in the rate of oxidation and the crystal structure of the oxide film between 900° and 1050°C. The rate of oxidation remained constant while the α-Al_2O_3 content of

the oxide increased. Thermochemical, crystal structure, and kinetic studies indicate that the vapor pressure of iron and chromium are limiting the rate of reaction above 1050°C. Design principles are proposed for heat-resistant alloys.

Abstract No. 62

Transitions from Parabolic to Linear Kinetics in Scaling of Metals

E. W. Haycock, Shell Development Co., Emeryville, Calif.

A brief discussion is given of mechanisms associated with linear scaling kinetics. A general rate equation, derived on the basis of a model involving scale recrystallization, is applied to the oxidation of aluminum and hafnium. It is shown that a single equation satisfies the rate curves for these systems over ranges of temperature and scale thickness where two or three rate equations have been used previously.

Abstract No. 63

High-Temperature Sulfiding of Iron and Steel in Hydrogen Sulfide-Hydrogen Mixtures

E. W. Haycock, Shell Development Co., Emeryville, Calif.

Scaling rates of pure iron, carbon steel, and a series of chromium steels in hydrogen sulfide-hydrogen mixtures have been studied over a wide range of experimental conditions. A detailed mechanism of scaling is proposed and substantiated by studies of the chemical and physical properties of the scales formed on the various metals investigated. On the basis of this mechanism, a general rate equation is derived and used in the kinetic analysis of the experimental data.

Abstract No. 64

Corrosion Research at the National Research Council of Canada Laboratories

Morris Cohen, Div. of Applied Chemistry, National Research Council, Ottawa, Ont., Canada

A review of research done in this laboratory since World War II is presented. This includes work in the fields of inhibition and passivity, dry oxidation, and electrochemistry. The methods of measurement and some results are discussed.

Abstract No. 65

Anodic Behavior of Copper in Phosphoric Acid

F. H. Giles (Present address: Dept. of Physics, University of South Carolina, Columbia, S. C.) and **J. H. Bartlett,** Dept. of Physics, University of Illinois, Urbana, Ill.

The electrochemical characteristics of copper anodes in phosphoric acid solutions have been studied by observing the make and break transients. The floating potential is about — 0.16 v, and there are two higher characteristic potentials, one at 0.00 v and one at + 0.16 v, * approximately. A current-voltage plateau is observed, upon which the resistance is constant. Electropolishing is found to occur in two separate regions of voltage, one a little above the knee of the current-voltage curve, and one above 0.8 v.

* The reference electrode was a 0.1*N* calomel half-cell.

Abstract No. 66

Corrosion of Uranium and Uranium Alloys by Differential Aeration*

J. W. Ward and **J. T. Waber,** Los Alamos Scientific Lab., University of California, Los Alamos, N. Mex.

Differential aeration currents have been measured in 0.1 F $KClO_4$, KCl, KNO_3, and $KC_2H_3O_2$, using a recording vibrating reed electrometer. Concentration effects on local corrosion processes and film types are noted. Electrode potentials, as well as anodic and cathodic polarization values, were measured against 0.1 F calomel electrodes. Values for resistance polarization and stirring effects were included. Finally, the effects of several XO_4^{-n} type ions and buffering are discussed as a function of concentration.

* Work done under the auspices of the U.S.A.E.C.

Abstract No. 67

General and Intergranular Corrosion of Austenitic Stainless Steels in Solutions Used for Evaluation Tests

M. A. Streicher, Engineering Research Lab., Engineering Dept., E. I. du Pont de Nemours & Co., Inc., Wilmington, Del.

A study has been made of general and intergranular attack produced by nitric acid, ferric sulfate-sulfuric acid, and copper sulfate-sulfuric acid solutions. Special attention has been given to the electrochemical action of the cations encountered in these solutions, either as inhibitors of general corrosion or as corrosion products, which may accelerate or retard intergranular attack. Among the pertinent factors in the stainless steels, chromium carbides, sigma phase, and grain size have been investigated in their effect on intergranular attack.

Abstract No. 68

Corrosion of Metals in Boiling Acids when Contacted to Noble Metals

W. R. Buck, III, and **Henry Leidheiser, Jr.,** Virginia Institute for Scientific Research, Richmond, Va.

A study was made of the acceleration of the corrosion of 9 metals and the deceleration of the corrosion of titanium (in some cases) in boiling hydrochloric and sulfuric acids when contacted ot platinum, iridium, rhodium, palladium, ruthenium, osmium, silver, and gold. The relative effectiveness of these 8 noble metals in changing the corrosion rate varied greatly with the corroding metal. The significance of this observation was discussed.

Abstract No. 69

Corrosion of Mild Steel in Alkaline Leaching and Grinding Solutions for Uranium Ore

R. R. Rogers and **I. I. Tingley,** Mines Branch, Div. of Mineral Dressing and Process Metallurgy, Dept. of Mines and Technical Surveys, Ottawa, Ont., Canada.

The corrosion of comparatively mild steel in aqueous solutions containing sulfate, carbonate, bicarbonate, and (in some cases) chloride was investigated. Under certain conditions, pitting corrosion was obtained, the pits resembling those observed in severely corroded equipment in a uranium ore processing plant. The investigation included experiments demonstrating the effect of aeration and the presence of the uranium ore.

Abstract No. 70

Kinetics of Germanium Dissolution in the Presence of Electrolytes*

W. W. Harvey and **H. C. Gatos,** Lincoln Lab., Massachusetts Institute of Technology, Lexington,Mass.

The previous study of the reaction of germanium with water containing dissolved oxygen has been extended to solutions of nonoxidizing electrolytes. For a given salt the dissolution rate exhibits a pronounced maximum at a characteristic concentration. The role of dissolved oxygen in the occurrence of this maximum has been established, and a comparison is made between germanium and metal-aqueous electrolyte systems. The investigation includes effects of illumination and of variations in bulk electronic properties.

* The research reported in this document was supported jointly by the Army, Navy, and Air Force under contract with M.I.T.

Abstract No. 71

Kinetic Studies on Corrosion Systems, I. A Theory of Multi-Component Electrochemical Systems under Activation Control

F. A. Posey, Oak Ridge National Lab., Oak Ridge, Tenn.

The absolute rate theory of electrochemical reactions has been extended to the case of multi-component electrode systems under activation control. In partic-

ular, the application of the theory to the study and interpretation of corrosion systems is considered. Some previous theories of corrosion reactions in solution arise as special cases of the present treatment and their inadequacies and inconsistencies are noted. It is shown that d-c potentiostatic, galvanostatic, and polarization measurements yield valuable information on the rates, mechanisms, and independent simultaneity of the individual partial processes present in complex electrode systems.

Abstract No. 72

Kinetic Studies on Corrosion Systems, II. The Reduction of Cupric Ion on Passive Stainless Steel Electrodes

F. A. Posey, G. H. Cartledge, and **R. P. Yaffe** (Present address: Dept. of Chemistry, San Jose State College, San Jose, Calif.), Oak Ridge National Lab., Oak Ridge, Tenn.

The reduction of cupric ion on the surface of passive stainless steel electrodes in aerated, dilute sulfuric acid medium has been investigated using potentiostatic, galvanostatic, and tracer techniques. The independent simultaneity of the electrode reactions has been demonstrated. A mechanism is advanced for the reduction of cupric ion on the oxide surface. The absolute rate theory of electrochemical reactions for multi-component systems is shown to provide a quantitative interpretation of the data. Evidence is presented which argues against the existence of an important film potential in the passive oxide layer.

Abstract No. 73

Galvanic Corrosion, II. Effect of pH and Dissolved Oxygen Concentration on the Aluminum-Steel Couple

M. J. Pryor and **D. S. Keir,** Metallurgical Labs., Olin Mathieson Chemical Corp., New Haven, Conn.

The effect of pH, dissolved gas composition, and deaeration on the galvanic characteristics of the aluminum-steel couple was investigated. High-purity aluminum cathodically protects steel completely in chloride solutions within the pH range 0.2–14.0. The galvanic currents and weight losses of the aluminum anodes are at a minimum from pH 4.0 to 10.0, and are controlled by oxygen depolarization at the steel cathodes. The galvanic current fluctuates because the oxide film on the steel cathode is thickening with time in an erratic manner. At higher and lower pH the rate of galvanic corrosion is much greater, independent of oxygen concentration, and is extremely steady and reproducible.

Abstract No. 74

Corrosion of Copper in Aqueous Media

D. J. G. Ives, Dept. of Chemistry, Birkbeck College, University of London, England, and **A. E. Rawson,** The Colne Valley Water Co., Watford, Hertfordshire, England

Measurements have been made of the rates of formation of soluble and insoluble corrosion products in waters kept in equilibrium with known partial pressures of oxygen and carbon dioxide. The dependence of these rates on the partial pressure of each gas at various fixed partial pressures of the other has been completely explored. Dissolved salts commonly found in potable waters, at concentrations at which they are present naturally, exert profound effects on corrosion rates, some of them unexpected and opposed to accepted views.

Abstract No. 75

Tarnishing Reactions of Silver in Iodine Atmospheres

D. M. Smyth and **Marjorie Cutler,** Sprague Electric Co., North Adams, Mass.

The tarnishing of silver in halogen vapors, particularly iodine vapor, has been studied as a function of reaction temperature, halogen pressure, silver purity, and concentration of foreign vapors in the halogen atmosphere. The reaction temperature range studied was 25°–150°C for reactions in iodine and up to 200° in bromine and chlorine. In pure halogen vapor the reactions follow the familiar parabolic rate expression and are proportional to the square root of the halogen pressure. In the presence of small partial pressures of water or carbon tetrachloride vapor, however, the tarnishing rate is suppressed and is independent of the tarnish film thickness.

Abstract No. 75A

Oxidation of Titanium, Zirconium, and Hafnium

G. R. Wallwork and **A. E. Jenkins,** School of Metallurgy, N.S.W. University of Technology, Sydney, Australia

A metallographic study of the high-temperature oxidation of titanium, zirconium, and hafnium has shown that alterations in the rate equations relating to such processes may be associated with the establishment of oxygen diffusion gradients in the surface layers of the metal. The penetration of oxygen to the center of the metal specimens has been used to explain changes in scaling observed to occur after long periods of oxidation at high temperature.

ELECTRODEPOSITION

Abstract No. 76

Deposition of Titanium, Zirconium, Hafnium, Chromium, Vanadium, and Molybdenum from Fused Chloride Baths

R. S. Dean, W. W. Gullett, and **F. X. McCawley,** Chicago Development Corp., 5810 47th Ave., Riverdale, Md.

The electrorefining of titanium as ultrapure crystals from a bath containing lower titanium chloride and dissolved sodium is in commercial operation. This type of bath has been produced for zirconium, hafnium, chromium, vanadium, and molybdenum, and production of ultrapure metals from crude materials including ferrochromium and ferrovanadium has been carried out on a small pilot plant scale. The procedure mechanism of deposition and product are described. The method of producing and maintaining the baths and the methods of determining their composition are discussed, particularly with regard to confirmation of the essential presence of dissolved alkali metal.

Abstract No. 77

The Electrolytic Preparation of Titanium from Fused Salts, II. Design of Laboratory Cells

M. B. Alpert, J. A. Hamilton, F. J. Schultz, and **W. F. Sullivan,** Research Dept., Titanium Div., National Lead Co., Sayreville, N. J.

The design and function of laboratory scale equipment for the reduction of $TiCl_4$ to reduced titanium chlorides dissolved in a fused salt melt and the further reduction of these chlorides to Ti metal are presented. Modifications of a simple diaphragmed cell leading to continuous operation for extended periods, to electrorefining, or to a diaphragmless type are considered.

Abstract No. 78

Electromotive Series of Metals in Fused Salts

S. N. Flengas and **T. R. Ingraham,** Mines Branch, Dept. of Mines and Technical Surveys, Ottawa, Ont., Canada

A simple, thermodynamically reversible Ag/AgCl reference electrode was constructed in silica and used in equimolar KCl-NaCl melts at temperatures between 650° and 900°C to measure the standard electrode potentials of a series of metal-metal chloride systems including $Co/CoCl_2$, $Ni/NiCl_2$, $Pb/PbCl_2$, $Zn/ZnCl_2$, $Cd/CdCl_2$, $Cu/CuCl$, $Cu/CuCl_2$, $Cr/CrCl_2$, $Cr/CrCl_3$, $Mn/MnCl_2$, $Sn/SnCl_2$, etc. The Nernst equation was applicable over the concentration range investigated. The temperature coefficients of the electromotive forces were measured and the heats of the cells reactions were calculated from the data.

Abstract No. 79

A Sodium-Ion-Conductive Porcelain Reference Electrode for Molten Salt Systems

R. J. Labrie and **V. A. Lamb,** Chemistry Div., National Bureau of Standards, Washington 25, D. C.

A reference electrode for use in molten salt systems is described. It consists of a porcelain capsule conductive to sodium ions, in which is contained a silver electrode immersed in a melt of silver chloride and sodium chloride. The electrode is reversible to sodium ions. It is stable, reproducible, and temperature-reversible and can be used at relatively high temperatures. The capsule-type construction prevents the salt inside the electrode from contaminating the melt under study.

Abstract No. 80

Nickel-Aluminum Alloys Formed by Electrodeposition

Dwight Couch and **Jean Connor,** National Bureau of Standards, Washington 25, D. C.

Nickel-aluminum alloy coatings were produced by the electrodeposition of aluminum over electrodeposited nickel. The basis metal was steel. The aluminum was plated from fused salt baths operated from 170° to 1000°C and from an organic bath operated at room temperature. The coatings had a hardness of about 700 Vickers and were much superior to nickel coatings for the protection of steel in salt spray tests. The oxidation of these alloys at 1000°C was much slower than that of pure nickel. Attempts to codeposit nickel and aluminum from an organic type of bath were not successful.

Abstract No. 81

On the Growth and Properties of Electrolytic Whiskers

P. B. Price, D. A. Vermilyea, and **M. B. Webb,** Research Lab., General Electric Co., Schenectady, N. Y.

The electrolytic growth of metal whiskers from solutions containing additives is examined, and a mechanism for their growth is proposed. It is assumed that adsorbed impurity molecules hinder the motion of atomic steps over crystal surfaces, and also that adsorbed molecules are incorporated into a growing crystal. A quantitative theory of the rate of growth of whiskers is in good agreement with experiment. Properties and structures of the whiskers are discussed.

Abstract No. 82

Electrodeposition Behavior of Trace Amounts of Copper

R. C. DeGeiso, Dept. of Chemistry and Lab. for Nuclear Science, Massachusetts Institute of Technology, Cambridge, Mass. (Present address: E. I. du Pont de Nemours and Co., Experimental Station, Wilmington, Del.) and **L. B. Rogers,** Dept. of Chemistry and Lab. for Nuclear Science, Massachusetts Institute of Technology, Cambridge, Mass.

Deposition, onto inert electrodes, of copper in amounts insufficient to form a monolayer takes place more readily than predicted using the Nernst equation. The undervoltage decreases with an increase in lattice mismatch of the copper and the electrode material. The undervoltage is also a function of the acidity, the anion present, and the amount of copper deposited.

Abstract No. 83

The Electrolytic Pointing of Tungsten Whiskers

P. F. Russo, R. B. Soper, and **Pei Wang,** Sylvania Electric Products Inc., Woburn, Mass.

The electrolytic technique for pointing tungsten whisker wires used in the fabrication of semiconductor point contact diodes has been carefully investigated. It is established that the meniscus at the electrolytic-whisker interface and the elimination of gas bubbling are important factors for achieving reproducible results, and the configuration of the points can be varied as desired by controlling the pointing conditions. The effect of the various factors such as the composition and temperature of the electrolyte, the nature of the counter-electrode, the power input, and the diameter of the whiskers is discussed.

Abstract No. 84

A Radioisotopic Study of Leveling in Bright Nickel Electroplating Baths

S. E. Beacom and **B. J. Riley,** Research Staff, General Motors Corp., Box 188, North End Station, Detroit 2, Mich.

A radioisotope-containing addition agent has been synthesized and used as a component in a bright and leveling nickel bath. Investigation by autoradiography and various counting techniques shows that this agent is preferentially deposited at the high points of an irregular surface, thereby substantiating a part of leveling theory. The radioactive addition is also used in an attempt to better understand the mechanism of formation of laminations in this type of nickel deposit.

Abstract No. 85

Electrodeposition of Porous Nickel

J. J. MacDonald, D. G. Gage, and **E. C. Brown,** Dept. of National Defence, Defence Research Board, Naval Research Establishment, Dartmouth, Nova Scotia

In an attempt to simplify nickel-cadmium battery production, studies of the electroforming of porous nickel were undertaken with a view to replacing the normal sintered plaques. Plaques with up to 80% porosity have been electrodeposited reproducibly from a Watts-type bath to which has been added lamp black or graphite. When tested as battery positives, the best plaques showed capacities 70% as high as those of sintered nickel plaques.

Abstract No. 86

Electroplating of Nickel from the Pyrophosphate Bath

S. K. Panikkar and **T. L. Rama Char,** Electrochemistry Lab., Dept. of General Chemistry, Indian Institute of Science, Bangalore-3, India

The pyrophosphate bath has been studied in detail for the electrodeposition of nickel. It gives satisfactory deposits over a wide range of operating conditions. Potential measurements have been made and the throwing power determined. This bath is comparable to the commercial acid baths for nickel plating in respect to current density, current efficiencies, and quality of the deposit. It has a low nickel content, high throwing power, and is suitable for plating on zinc.

Abstract No. 87

Electroplating on Group IVB-VIB Metals

E. B. Saubestre, Central Research Labs., Sylvania Electric Products Inc., Bayside, N. Y.

In a new plating method, the conventional etching step is eliminated. Instead, the substrate is treated cathodically to form a hydride covered surface, which permits good adhesion of thin nickel deposits. The hydride is then removed by a vacuum bake, followed by further plating as desired. It was found possible to plate over oxide-coated Nb and Nb-Ti alloys, without need for activation or post-plating baking operations. The oxide was applied by anodizing.

Abstract No. 88

Novel Nickel Plating Process

J. T. N. Atkinson, Dept. of National Defence, Defence Research Board, Naval Research Establishment, Dartmouth, Nova Scotia

Following earlier work on electroplating on aluminum from strongly acid solutions, a new process for nickel plating aluminum was developed. Adhesion values of about 5000 psi in shear were obtained regularly, and still better adhesion could result from the use of a proper heat treatment. The process for plating nickel on aluminum was found to be surprisingly versatile. It appears to have industrial potentialities for

general electroplating and electroforming operations with nickel.

Abstract No. 89

Electroplating Metal Contacts on Semiconductors

D. R. Turner, Bell Telephone Labs., Inc., Murray Hill, N. J.

Various metals have been plated on germanium, silicon, gallium-arsenide, and titanate semiconducting oxide ceramics. These materials usually have oxide layers on them which could interfere with the intimate contact required between metal and semiconductor for good adhesion and the desired electrical properties. Oxide films and residues from chemical etching on germanium can be removed by cathodic reduction prior to metal deposition in many plating solutions. Sixteen different metals were plated on n- and p-type germanium. Since oxide films on silicon are difficult to reduce cathodically, special techniques are required to produce adherent electrodeposits on silicon. "Electroless" nickel is used to make low-resistance ohmic contacts to silicon, gallium-arsenide, and semiconducting oxides.

Abstract No. 90

Electrodeposition of Aluminum on Uranium*

J. G. Beach and **C. L. Faust,** Battelle Memorial Institute, 505 King Ave., Columbus 1, Ohio

Electroplating of aluminum was studied as an alternate method for aluminum cladding of uranium fuel elements. Uranium electroclad with 12 mils of aluminum over a 0.5-mil nickel or nickel-plus-copper electroplate resisted corrosion for more than 100 hr in boiling water. Hot pressing the electroclad composite improved the corrosion resistance. Many of the results obtained with aluminum electrocladdings paralleled those obtained with wrought aluminum claddings on uranium.

* Work performed under AEC Contract W-7405-eng-92.

Abstract No. 91

Electroplating on Thorium*

J. G. Beach and **G. R. Schaer,** Battelle Memorial Institute, 505 King Ave., Columbus 1, Ohio

A method was developed for treating thorium whereby adherent electroplates of most metals can be applied. The method involves anodic pickling in hydrochloric acid and chemical pickling in sulfuric acid prior to plating. Factors affecting the adherence and protective quality of the electroplated coatings are discussed.

* Work performed under AEC Contract W-7405-eng-92.

Abstract No. 92

Immersion Plating on Zircaloy 2

L. R. Kohan, Armour Research Foundation, 10 W. 35th St., Chicago 16, Ill.

Coatings of such metals as copper, iron, nickel, and tin have been deposited on Zircaloy 2 by chemical displacement from solutions containing low concentrations of hydrofluoric acid. The character of these coatings was suitable for subsequent joining methods. Bath variables were studied and it was found that small changes in agitation, temperature, and HF concentration greatly affected the coating thickness. Coatings up to a thickness of one mil were produced by this technique.

Abstract No. 93

Electrocladding of Zirconium with Platinum*

A. B. Tripler, J. G. Beach, and **C. L. Faust,** Battelle Memorial Institute, 505 King Ave., Columbus 1, Ohio

A method which included the use of periodic reverse plating was developed for electrocladding zirconium with sound, pore-free platinum coatings up to 1.5 mils in thickness. A smoother more protective platinum deposit can be plated over on an intermediate diffusion-bonded nickel electroplate than can be obtained when platinum is plated directly on zirconium. On nickel, platinum thickness of 0.5–0.75 mil appears adequate for corrosion protection in boiling HCl.

* Work performed under AEC Contract W-7405-eng-92.

Abstract No. 94

Chromium Plating on Titanium Alloys

Charles Levy, Watertown Arsenal Labs., Watertown, Mass.

Electrodeposited chromium has been applied to commercially available titanium alloys using conventional plating techniques. Treatments prior to plating involved dry sandblasting and a zinc immersion coating process. The adhesion of the chromium deposits applied by these methods was compared with the adhesion of deposits applied by methods reported in the literature. Microscopic examination of the bond was the principal means of this evaluation.

Abstract No. 95

Plated Coating on Titanium Gears

W. J. Hyink, Research Div., Western Gear Corp., Lynwood, Calif.

The procedures involved in electroless plating a phosphorus-nickel alloy on titanium and titanium alloy gears are discussed. Included are experimental pre-plate preparation methods, the chemistry of the electroless plating method used, and post plating procedures applied to produce a usable titanium gear after the plated coating has been applied. These experimental procedures are in compliance with a contract issued to the Western Gear Corp. in Lynwood, Calif., by the U. S. Air Force.

ELECTRONICS—SEMICONDUCTORS

Abstract No. 96

Design of Thermoelectric Materials for Power Generation and Refrigeration

R. R. Heikes, Research Labs., Westinghouse Electric Corp., Pittsburgh, Pa.

An elementary discussion of a thermoelectric power generator is given in order to determine those physical parameters which enter the materials design problem. The present theoretical understanding of these parameters is then discussed.

Abstract No. 97

Preparation and Thermoelectric Properties of Bi_2Te_3 and Alloys with Bi_2Se_3*

T. C. Harman, M. J. Logan, B. Paris, and **E. H. Lougher,** Battelle Memorial Institute, 505 King Ave., Columbus 1, Ohio

Details are presented on the preparation of Bi_2Te_3 and alloys of the compound with Bi_2Se_3 as carried out by a modified Bridgman technique. Resistivity, thermoelectric power, and thermal conductivity were measured as a function of temperature for various specimens. The data show that the lattice thermal conductivity of Bi_2Te_3 is reduced substantially by introducing the electrically neutral impurity atoms by means of alloying. The other thermoelectric properties are changed only slightly. Effects of special preparation procedures and of specimen fabrication are also discussed.

* Supported by the Office of Naval Research.

Abstract No. 98

Thermoelectric Measurements at Low Temperatures

E. Mooser, W. B. Pearson, and **I. M. Templeton,** Div. of Pure Physics, National Research Council, Ottawa, Ont., Canada

Recent measurements of the thermoelectricity of pure metals down to temperatures as low as perhaps 0.02°K have shown that a pure metal such as gold may have

a surprisingly large absolute thermoelectric power, greater than 4 μv/°C at 0.5°K. It therefore appears interesting to survey the absolute thermoelectric power of "semiconductor-like compounds" of low resistivity down to low temperatures, since, if significantly larger thermoelectric powers are found, there may be some use for such substances in thermoelectric cooling at temperatures lower than those normally considered. Measurements are reported on compounds such as Bi_2Se_3, which are believed to contain intrinsic holes in the valence band and which should therefore have a relatively low resistivity even at very low temperatures.

Abstract No. 99

The Use of Controlled Solidification in Equilibrium Diagram Studies

W. A. Tiller, Westinghouse Electric Corp., Pittsburgh 35, Pa.

It will be shown theoretically how the use of controlled solidification in phase diagram studies enables the determination of liquidus and solidus surfaces plus tie-lines for a polycomponent alloy. The method was tested by determining the liquidus and solidus for the pseudo-binary Bi_2Te_3-Bi_2Se_3 system by both the conventional cooling and heating curve technique and by the controlled solidification technique. Excellent agreement was found between the two methods, and partition coefficients for Bi, Te, and Se were determined.

Abstract No. 100

Crystal Chemistry and Physical Properties of Semiconductors

E. Mooser, Div. of Pure Physics, National Research Council, Ottawa, Ont., Canada

Since Welker's discovery of the semiconducting properties of the III-V compounds, crystal chemistry has repeatedly and successfully been applied in the search for new semiconducting materials and eventually led to the formulation of a "valence bond theory of semiconductors." In this paper the present status of the crystal chemistry of semiconductors is reviewed. Possible new developments are discussed and it will follow from this discussion that in the near future we will be able to predict with some accuracy not only semiconductivity but also the parameters determining the physical properties of a semiconductor. Such predictions will open up new possibilities in the field of semiconductor devices since they allow us to choose the material best suited for any given application.

Abstract No. 101

Inorganic Compounds for Semiconductor Devices

A. J. Cornish, Research Labs., Westinghouse Electric Corp., Pittsburgh 35, Pa.

The most familiar semiconducting compounds possess a large degree of covalent bonding and are composed of nonmetallic Group B elements. As elements from the left side of the periodic table are substituted for some of the Group B elements, the compounds become more metallic and/or ionic. Methods of predicting semiconducting properties become more difficult. By a combination of theoretical and empirical relations and a scheme of cataloging the various compounds, certain trends in structures, melting points, energy gaps, and mobilities can be predicted. Ternary and quaternary compounds are treated as combinations of binaries.

Abstract No. 102

Silicon Carbide Crystal Formation

A. H. Smith, Research Div., Raytheon Manufacturing Co., Waltham, Mass.

An experiment for making silicon carbide crystals of unusually good geometric perfection has been performed using a high-temperature pressure vessel. The reaction involves only semiconductor-grade silicon and carbon-yielding silicon carbide of higher resistivity than any selected crystals of the highest purity commercial material.

Abstract No. 103

Oxidation of Indium Antimonide*

A. J. Rosenberg, M. C. Levine, and **C. S. Martel, Jr.,** Lincoln Lab., Massachusetts Institute of Technology, Lexington, Mass

The reaction of chemically polished, single crystal InSb with oxygen yields uniform oxide films. The oxidation rate is given by

$$X\,dX/dt =$$

$$0.231\,p^{0.188}\exp(-35{,}500/RT)\ \text{cm}^2\text{min}^{-1}\ (p \text{ in atm})$$

for temperatures in the range, 259°-410°C, pressures in the range, 2-4000 microns, and film thicknesses, X, in the range, 180-1700A. The data are discussed in terms of the Wagner oxidation mechanism.

* The research reported in this document was supported jointly by the Army, Navy, and Air Force under contract with M.I.T.

Abstract No. 104

Purification of Semiconductor Materials by Chemical Methods*

J. A. Kafalas and **P. H. Robinson,** Lincoln Lab., Massachusetts Institute of Technology, Lexington, Mass.

The development of intermetallic semiconductors is at present seriously handicapped by the virtual impossibility of obtaining intermetallic compounds of sufficient purity. This paper deals with several of the major obstacles involved in the chemical purification of such materials. Methods are discussed for the purification of gallium and other constituents of intermetallic compounds. Conventional methods of purification, such as solvent extraction and electrolysis, are re-examined, and the purification of reagents is discussed in some detail.

* The research reported in this document was supported jointly by the Army, Navy, and Air Force under contract with M.I.T.

Abstract No. 105

Stability of the Zinc Blende Structure of III-V Compounds*

Carol Kolm, Lincoln Lab., Massachusetts Institute of Technology, Lexington, Mass.

The stability of the zinc blende structure—$A^{III}B^{V}$—intermetallic compounds has been investigated through lattice parameter and energy gap measurements on combinations of InSb with InBi, InSb with TlSb, GaSb with GaBi, and GaSb with TlSb. Results indicate that the instability of certain III-V combinations is due to an unfavorable size factor rather than to an electronic effect.

* The research reported in this document was supported jointly by the Army, Navy, and Air Force under contract with M.I.T.

Abstract No. 106

The Use of Bismuth as a Donor Type Impurity in Germanium Single Crystals

George Mortimer, Clevite Transistor Products, Waltham, Mass.

Bismuth has been studied as an N-type doping impurity for controlling the conductivity of single crystals of germanium. It was found to give extremely reproducible results if uniform conditions of crystal growth are maintained. Bismuth was found to have a segregation coefficient of approximately 5×10^{-5}. The effective segregation coefficient varied with the rate of advance of the solid-liquid interface during growth. The maximum practical concentration of bismuth in germanium as determined from resistivity measurements, is approximately 2×10^{16} at./cm^3 (i.e., —0.00005 at. %) when introduced from the melt during growth. The advantage of bismuth over most doping impurities for germanium is that it can be used reproducibly by direct addition to the melt without the use of a "master alloy." The electrical and structural properties were found to compare favorably with those grown with other Group V impurities by similar techniques.

Abstract No. 107

Simple Method of Determining Crystal Perfection

H. K. Herglotz, Pigments Dept., E. I. du Pont de Nemours & Co., Inc., Newport, Del.

An optical analogy leads to a simple x-ray method of determining crystal perfection. Although furnishing semiquantitative information only, this method can be considered superior to existing ones such as etch pit counts or x-ray rocking curves, because it integrates over a large number of lattice planes; it is combined with the determination of the crystal orientation since it is based upon a slightly modified Laue back-reflection method.

Abstract No. 108

Vapor Deposition of Single-Crystal Ge by the Decomposition of GeI_2

R. C. Sirrine, General Electric Co., Syracuse, N. Y.

(No abstract received)

Abstract No. 109

Analog Computation of Silicon Crystal Profiles with Three Active Impurities

K. M. Kolb, Pigments Dept., E. I. du Pont de Nemours & Co., Inc., Newport, Del.

Analog solutions of the normal freezing equation,

$$C_s = C_o k \left(\frac{M_o}{M_s}\right)^{1-k},$$

for three impurities in silicon crystals grown by the Czochralski technique were calculated. The results were plotted as resistivity profiles for the first 90% of the grown crystal. The impurities considered were boron, $k = 0.9$; phosphorus, $k = 0.35$; and aluminum, $k = 0.003$.

Abstract No. 109A

Imperfections in Silicon

H. L. Taylor, Texas Instruments, Inc., Dallas, Texas

Investigations of the number and types of dislocations and the quantity of oxygen present by the Dash copper precipitation technique and infrared transmission are discussed. Crystals grown from a silica crucible without rotating the seed have fewer dislocations and less oxygen. Growth along different crystallographic axes produces different dislocation densities. Five "types" of precipitated lines in well-defined annular rings have been observed and displayed in three-dimensional models. Oxygen appears to influence diffused copper behavior.

Abstract No. 110

Effects on Concentration Profiles of Variable Diffusion Coefficient and Surface Concentration

Worden Waring, Raytheon Manufacturing Co., Newton, Mass.

When the diffusion coefficient of a doping material varies with distance below the semiconductor surface, or when the diffusion coefficient or surface concentration varies with time, the resulting concentration profile of the doping material may differ considerably from the usual error function complement. Quantitative results for several processes are presented.

Abstract No. 111

Evaluation and Control of Surface Concentration in Diffused Germanium Systems

H. S. Veloric and **W. Greig,** Radio Corp. of America, Somerville, N. J.

Calculations are presented for determination of surface concentrations for diffused impurity layers from measurements of sheet resistance and junction depth. The calculations are for an erfc impurity distribution using mobility values estimated from Hall data and neutron activation analysis. Diffusion of impurities from a solid source is shown to be a reliable technique for predicting and controlling surface concentration. The surface concentration is primarily a function of the impurity concentration in the source and the temperature of diffusion.

Abstract No. 112

Conversion Control during the Diffusion of Impurities into N-Type Germanium

F. Barson, M. J. Dyett, C. Karan, and **W. E. Mutter,** Product Development Lab., International Business Machines Corp., Poughkeepsie, N. Y.

In the diffusion of impurities into wafers of relatively high-resistivity N-type germanium a frequent problem is the thermal conversion of the bulk material. A diffusion process is described wherein a liquid layer of suitable composition on one side of a wafer serves both as a source of the desired diffusant and as a sink for deleterious impurities which contribute to thermal conversion. Details of the process and the control of surface concentration of the diffusant are discussed.

Abstract No. 113

Germanium Diffused Minicrystals and Their Use in Transistors

I. A. Lesk and **R. E. Coffman,** General Electric Co., Syracuse, N. Y.

The diffused minicrystal process involves growing onto a miniature seed a tiny crystal from a small melt containing both donor and acceptor impurities and then heating to cause diffusion of the impurities from the grown crystal into the seed. This yields a germanium drift p-n-p bar-type transistor structure that has no practical limitations on base width for high-frequency use and permits great freedom in choosing emitter, base, and collector impurity concentrations.

Abstract No. 113A

Area Control in Diffused Silicon Devices through Variations in Diffusant Surface Concentrations

L. D. Armstrong, Radio Corp. of America, Somerville, N. J.

This paper describes how diffused junction areas may be controlled by successive diffusions under conditions of controlled surface concentrations of diffusants. The conditions of control are given and typical examples cited. Techniques have been worked out for reproducible fabrication of numerous devices on individual wafers of silicon. Diodes and both p-n-p and n-p-n transistors of the single-diffused and double-diffused types have been successfully processed in this way.

Abstract No. 114

Chemical Etching of Silicon, II. The System HF, HNO_3, H_2O, $HC_2H_3O_2$

H. Robbins and **B. Schwartz,** Semiconductor Engineering, Hughes Products, International Airport Station, Los Angeles 45, Calif.

This paper concerns a study of the etching of silicon in the system HF, HNO_3, H_2O, $HC_2H_3O_2$ as a function of etchant composition. The reaction mechanisms are discussed in relation to the kinetic data, and comparison is made to the etching system HF, HNO_3, H_2O.

Abstract No. 115

Reactions of Silicon with Aqueous Solutions of HF and Various Oxidizing Agents

W. T. Eriksen and **A. E. Baker,** Raytheon Manufacturing Co., Waltham, Mass.

The reaction of silicon with aqueous solutions of HF and the following oxidizing agents have been undertaken: potassium dichromate, ferrous chloride, vanadium oxide, and nitric acid. Analyses of gaseous products, coatings, and soluble products have been made. The results indicate that a rather complicated mechanism governs the reaction. In every case there is evidence that water is not an inert solvent but enters into the reaction. The first attack on the silicon is to

oxidize it to the plus-two state by the added oxidizing agent. Further oxidation to plus four is accomplished by other components of the solution.

It is also shown by an analysis of the reaction products that the mechanism of etching silicon by the standard HF-HNO_3 solutions changes with concentration of the components of the solutions.

Abstract No. 116

New Low-Melting Glasses Potentially Useful as Protective Coatings for Semiconductors

S. S. Flaschen and **A. D. Pearson,** Bell Telephone Labs., Inc., Murray Hill, N. J.

Properties and compositions are given for a series of new inorganic sulfide glasses which are fluid in the temperature range 200°-400°C. They show very low permeability to gases and water vapor, as do the vacuum-tight seals which are formed between the glasses and certain metals. When a germanium or silicon device is coated by dipping in the molten glass no harm is done to the semiconductor, and in many instances improvement in electrical characteristics has been observed. Exposure of glass-coated devices to 100% relative humidity for months causes no deterioration in electrical characteristics.

Abstract No. 117

Selective Deposition of Metals on n- and p-Type Silicon by Electrochemical Displacement

D. R. Turner, Bell Telephone Labs., Inc., Murray Hill, N. J.

Antimony, copper, silver, platinum, and gold can be deposited on lapped or bright etched silicon by electrochemical displacement in solutions containing hydrofluoric acid. On lapped surfaces, a metal will deposit preferentially on the p-side of a p-n junction. If the surface is bright etched, the results are reversed, and metal plates out mostly on the n-side. Metal can be deposited preferentially on the p-side of a bright etched silicon p-n junction if the surface is illuminated with a strong light. The process shows up not only p-n junctions but also any abrupt change in impurity concentration at the surface. The maximum resolution of multiple junctions on bright etched surfaces is better than 10 microns.

Abstract No. 118

Germanium Electrode Behavior*

W. W. Harvey, Lincoln Lab., Massachusetts Institute of Technology, Lexington, Mass.

Steady-state potentials under zero external current have been obtained for germanium electrodes in a number of aqueous electrolytes. For a given solution composition the change in potential upon illumination is determined by the oxygen partial pressure and the bulk electronic properties of the germanium. Observed photoeffects are related to surface recombination velocities measured *in situ*.

* The research reported in this document was supported jointly by the Army, Navy, and Air Force under contract with M.I.T.

Abstract No. 119

An Analysis of Diode Characteristics with Application of Inversion Layer Theory to Forward Bias Conditions

C. D. Root, Raytheon Manufacturing Co., Newton 58, Mass.

Forward and reverse diode characteristics are analyzed in the light of existing inversion layer theory and the space charge generation-recombination theory of Sah, *et al.* Inversion layer effects are analyzed under forward bias conditions and are found capable of producing unusually slow current increases for a given voltage increase in the low-voltage region (0.01-0.2 v). When the inversion layer is stable, a current component is produced in the forward direction which tends to saturate when the forward bias reaches the inversion layer surface potential. It is this component which can create a region in which current increases more slowly than would be explained by $I \propto \exp(qV/2KT)$ —1. Analysis has been applied to alloyed and diffused diodes.

ELECTROTHERMICS AND METALLURGY

Abstract No. 120

High-Temperature Mechanical Properties of Two Commercial Graphites

L. Green, Jr., M. L. Stehsel, and **C. E. Waller,** Aerojet-General Corp., Azusa, Calif.

High-precision tensile measurements of creep behavior, stress-vs-strain properties, and ultimate breaking strength of regular-grade and reimpregnated H4LM graphite at temperatures up to 2400°C are summarized, together with similar data (including stress relaxation) for specimens stressed in torsion at temperatures up to 2800°C. Young's modulus measurements by forced flexural vibration at temperatures up to 2400°C are reported, as well as linear thermal expansion data. Effects of specimen orientation in the molded block and of the reimpregnation treatment are discussed, and the time or strain-rate effects observed are interpreted in terms of thermally activated mechanisms.

Abstract No. 121

Some Physical Properties of a Commercial Graphite from Ambient Temperature to 2500°C

P. N. Wagner, A. R. Driesner, E. A. Kmetko, and **D. P. MacMillan,** University of California, Los Alamos Scientific Lab, Los Alamos, N. Mex.

A study has been made of the properties of a 36 in. O. D. commercial graphite both at a nominal density of 1.74 and using stock reimpregnated to a density of 1.80-1.85. This includes compressive strength, dead load compressive creep, thermal conductivity, coefficient of friction, from ambient temperature to approximately 2500°C. The variation of tensile strength from point to point within the piece has been determined at ambient temperature.

Abstract No. 122

High-Temperature Short-Time Creep of Graphite

H. E. Martens, L. D. Jaffe, and **D. D. Button,** Jet Propulsion Lab., California Institute of Technology, 4800 Oak Grove Drive, Pasadena 3, Calif.

Constant-load creep tests were run at 3500°-5100°F on some commercial graphites. Specimens ¼ in. diameter x 1 in. gauge length were heated in helium by an external heater. The creep rate increased continually with temperature; a minimum corresponding to the peak in tensile strength at 4500°F was not found. No third stage creep was observed. Elongations up to 30% and density decreases up to 16% occurred during creep.

Abstract No. 123

Measurement of Creep in Graphite at 2500°-3000°C

H. C. Stieber and **R. C. Stroup,** Niagara Development Lab., National Carbon Co., Division of Union Carbide Corp., Niagara Falls, N. Y.

Creep data are presented for several commercial grades of graphite which have potential application at very high temperatures. Creep rate is expressed as a function of tensile load, measured at three temperatures: 2500°, 2750°, and 3000°C. Specimen size is somewhat larger (½ in. diameter x 5 in. long) than in previous work and direct readings on the specimen are made of both temperature and elongation. The apparatus and test methods are fully described.

Abstract No. 124

A Comparison of Physical, Electrical, and Thermal Properties of Graphite with Some Common Reference Materials

G. B. Engle and **L. M. Liggett,** Speer Carbon Co., 4861 Packard Rd., Niagara Falls, N. Y.

The physical, electrical, and thermal properties of graphite are reviewed. Properties of graphite are com-

pared with some common ceramics, cermets, metals, and alloys. Certain high-temperature characteristics of graphite and the above materials also are compared. Some typical applications of graphite are discussed.

Abstract No. 125

Photomicrographic Examination of Cokes and Formed Carbon Bodies

E. C. Thomas, Electrode Div., Great Lakes Carbon Corp., P. O. Box 637, Niagara Falls, N. Y.

Photomicroscopy as a research tool has been applied to cokes, carbon aggregates, and solid systems processed therefrom. A technique for conducting photomicroscopic examinations under reflected polarized light is reviewed and photographs at both the micro and macro levels are presented. The influence of structural differences observed in some of the aggregate materials is discussed in terms of some of the properties of formulated solid systems. The latter include many of the standard products of the carbon industry in the United States.

Abstract No. 126

Some Characteristics of Low Permeability Graphite

R. L. Robinson and **R. L. Mansfield,** Niagara Development Lab., National Carbon Co., Division of Union Carbide Corp., Niagara Falls, N. Y.

This paper discusses recently developed types of graphite having low permeability which have been tailor made for applications such as liquid metal and fused salt nuclear reactors and various high-temperature chemical applications. The method of measuring and a means of expressing very low permeability are outlined. The properties of these new graphites are discussed briefly and their permeability characteristics are related to pore size and distribution.

Abstract No. 127

Thermal Conductivity of Pre- and Postirradiated Graphite as a Function of Temperature

R. A. Meyer, Brookhaven National Lab., Upton, N. Y.

An apparatus was developed with which the thermal conductivity of graphite could be measured in the temperature range from 200° to 800°C. The thermal conductivities of special grades of graphite which have been developed for their use in a liquid metal fuel reactor were measured before and after exposure to irradiation. The radiation exposure of 3.6×10^{20} NVT at a temperature from 360° to 390°C has resulted in a decrease of conductivity of approximately 50% at the low temperatures and 10-50% at 600°C. These results and annealing effects are discussed.

Abstract No. 128

Electrical Resistance of Graphite-Graphite Connectors

E. C. Thomas and **J. H. Whitwell,** Electrode Div., Great Lakes Carbon Corp., P. O. Box 637, Niagara Falls, N Y.

The electrical conductivity of graphite-graphite connections has been studied in conjunction with investigations of a number of different types of pin-to-plate connections for mercury cell anodes. Electrical resistance data for both the interference and threaded types of joint assemblies are presented and discussed. The electrical resistance of pressed interference joints is found to decrease within a limited range of interferences beyond which the resistance is found to increase. An explanation for this behavior is postulated. Data showing the change in resistance with tightening torque for threaded joint assemblies are presented.

Abstract No. 129

Typical Distributions of Graphite Properties

N. C. Hodge, Electrode Div., Great Lakes Carbon Corp., P. O. Box 637, Niagara Falls, N. Y.

Graphite is produced in a wide variety of commercial products. The physical properties of these products very often determine their acceptability for a commercial application. The normal physical properties that are measured are: apparent density, electrical resistance, coefficient of thermal expansion, modulus of rupture, and modulus of elasticity. Since one or more of these properties are used to evaluate the quality of each product, it is the purpose of this paper to present the distribution characteristics of these properties as developed from extensive measurements made on standard commercial products.

Abstract No. 130

The Continuous Transfer of Energy to Materials from an Arc Discharge

J. Holmgren, L. Mead, and **C. Sheer,** Vitro Labs., West Orange, N. J.

The general subject of energy transfer to materials from an arc discharge is reviewed from the standpoint of high-temperature chemical processing. A comparison is made of the advantages and limitations of more or less conventional arc furnaces with those of more recent techniques such as the various forms of fluid stabilized arcs and the high-intensity arc. Models of the energy transfer mechanism in each case are described in terms of the energy balance in the arc plasma and at the electrode boundary sheaths. The special problems relating to the treatment of liquids and gases as well as solids are also discussed.

Abstract No. 131

Pressures in and around a High-Current Metallic Arc

F. W. Wood, U. S. Dept. of the Interior, Bureau of Mines, Region 1, Albany, Ore.

In the arc-melting industry there is disagreement concerning the pressures that prevail in the immediate vicinity of a high-current d-c arc discharge. On one hand, it is claimed that high vacuum (below 1 μ) can exist. The opposing view is that minimum pressures in the order of 1 mm Hg or higher are necessary to sustain arc discharge mechanisms, and that superficial pressure measurements in the order of 10^{-4} mm Hg or less reflect only the steepness of the pressure gradient within the arc chamber. This paper advocates and reviews reasons for the latter view. The origin and order-of-magnitude of arc pressures are discussed theoretically in terms of inherent electromagnetic compression and plasma liquid-vapor equilibria resulting from gas and vapor evolution. The theoretical deductions are compared with various experimental measurements. Some consequences of this reasoning are summarized by noting the role of pressure in determining: (*a*) modes of arc operation and discharge stability, (*b*) potential-current relationships, (*c*) cathode-plasma-anode energy partitions, and (*d*) the degassing of molten metal.

Abstract No. 132

Positional Instability Behavior of Low Pressure D-C Arcs

E. W. Johnson and **R. Itoh,** Research Labs., Westinghouse Electric Corp., Pittsburgh 35, Pa.

The positional instability tendency of reduced pressure consumable electrode d-c arcs with iron electrodes was studied as a function of gas pressure, arc length, current, and electrode surface cleanliness and geometry. Results were recorded on motion picture film which will be shown during the presentation of this paper. It was found that arc positional stability is enhanced by decreasing the gas pressure and arc length and increasing the electrode surface cleanliness and current density. Quantitative relationships for these effects are presented.

Abstract No. 133

Crater Resistance of Submerged Arc Smelting Furnaces Simulated by a Simple Model

O. Ch. Böckman, Elektrokemisk A/S, Oslo, Norway

An electrolytic trough technique has been used to study the effect of size and shape of the smelting crater on the ohmic resistance of the crater of submerged arc smelting furnaces. The ohminch rule is demonstrated and the correct use of this rule is discussed.

Abstract No. 134

Arc Behavior in Variable Pressure Systems

R. P. Morgan and **T. E. Butler,** Metals Research Labs., Electro Metallurgical Co., Niagara Falls, N. Y.

Several distinct modes of arc behavior are induced in a-c and d-c systems when the ambient gas pressure is reduced from atmospheric values. General relationships between the various arc modes, the arc current, electrode composition, metal transfer, and the composition of the residual gas have been developed. These factors have a direct bearing on the application of reduced pressure arcs in industrial processes. Color pictures are used to illustrate the effect of specific variables.

Abstract No. 135

Heat Transfer Ratio of the Argon Plasma Jets

C. S. Stokes, W. W. Knipe, and **L. A. Streyg,** Research Institute of Temple University, Philadelphia, Pa.
(No abstract received)

Abstract No. 136

Some Applications of the Carbon Arc Image Furnace

M. R. Null and **W. W. Lozier,** National Carbon Research Labs., Cleveland, Ohio
(No abstract received)

Abstract No. 137

The Carbothermic Reduction of Magnesium Oxide in the High-Intensity Arc*

S. Korman, A. Diniak, and **C. Sheer,** Vitro Labs., West Orange, N. J.

A laboratory investigation of the vapor-phase reduction of magnesium oxide has been carried out in the tail flame of a d-c high intensity arc. Thermodynamic considerations were used to predict an approximate temperature-dependence for the homogeneous reaction, $MgO + C \rightarrow Mg + CO$. Spectrographic correlation of flame composition and temperature was used to position a water-cooled quench plate for product sampling. For ⅝-in. diameter anodes, containing slightly greater than a stoichiometric fraction of carbon, a 7-kw arc operating in 0.1 atm of nitrogen yielded a product representing 64% reduction of the oxide with an equivalent power consumption of 8.2 kwhr/lb of metal.

* This work was sponsored by the Combustion Dynamics Branch of the Air Force Office of Scientific Research.

Abstract No. 138

Arc Decomposition of Rhodonite*

V. Harris, J. Holmgren, S. Korman, and **C. Sheer,** Vitro Labs., West Orange, N. J.

A developmental pilot line for the arc treatment of Colorado rhodonite has been built and operated to investigate the applicability of the high-intensity arc process to the extraction of manganese from siliceous ores. The rhodonite is incorporated into 2 in. diameter electrodes to the extent of 75-85% by weight and vaporized in a d-c high-intensity arc operating in the range 40-60 kw. The arc vaporization is effective in decomposing the manganese silicate content of the rhodonite into a mixture of MnO and SiO_2 from which the manganese content is readily leached. The product is collected as a mixture of the respective oxides in finely particulated form. The effect of variations in significant process variables is discussed, and a film showing the various processing steps is presented.

* This work was sponsored by the General Services Administration of the U. S. Dept. of Interior.

Abstract No. 139

Arc Furnace Preparation of Refractory Compounds

H. A. Johansen, Research Labs., Westinghouse Electric Corp., Pittsburgh 35, Pa.

The development and uses of the laboratory arc furnace are reviewed briefly. The preparation of high-purity borides, carbides, nitrides, and silicides of 4th, 5th, and 6th group transition elements by means of a laboratory arc furnace of recent design is described. Techniques of reacting and fusing the highest melting point materials known are reported. The advantages and limitations of the arc method of preparation of refractory compounds are discussed.

Abstract No. 140

Electron Beam Vacuum Welding—Development of Process

W. L. Wyman and **W. I. Steinkamp,** General Electric Co., Richland, Wash.

Electron beam vacuum welding is a new development for fusion welding in a high vacuum. The process consists of focusing a beam of high velocity electrons which act as a heat source. The equipment required includes a vacuum chamber, an electron gun, and a high voltage power supply. In operation the electrons are accelerated and focused on to the work pieces by a high voltage potential between the work pieces and the gun. Extremely pure atmospheres can be obtained by vacuums and the reactive materials such as zirconium, titanium, columbium, and others can be welded with ease. Consistently high quality welds are obtained. The process has been applied to most of the metals used by industry, including both the common and the rare metals.

Abstract No. 141

Special Optical Techniques for the Direct Observation of Oxidation in Metals

S. J. Majka, Dept. of Engineering and Metallurgy, Ontario Research Foundation, Ottawa, Ont., Canada

The design and operation of equipment in use at the Ontario Research Foundation for direct microscopic observation of the oxidation process are described. The apparatus consists of a small furnace equipped with a vacuum system and fitted to the stage of a microscope. The following points will be discussed: optical factors, thermal factors, and metallographic factors.

Abstract No. 142

The Initial Suggestion of Oxidation and the Problems of Discontinuous Oxidation

U. M. Martius, Dept. of Engineering and Metallurgy, Ontario Research Foundation, Ottawa, Ont., Canada

Studies of the initial oxidation of high-purity nickel were conducted using the equipment described in the preceding paper by S. J. Majka. The experimental conditions under which discontinuous oxidation in nickel is observed are reviewed in the light of the evidence of discontinuous oxidation in other metals (iron, copper, iron-nickel, and nickel-chrome alloys), its relation to purity, dislocation structure, and surface reactions. The problem of the anisotropy of the oxidation rates is discussed and evidence of a strong dependence of this anisotropy on temperature is presented.

Abstract No. 143

High-Temperature Oxidation of Aluminum in Water Vapor

P. E. Blackburn and **E. A. Gulbransen,** Research Labs., Westinghouse Electric Corp., Pittsburgh 35, Pa.

The rate of reaction between water vapor and aluminum is greater than that between the metal and oxygen. Mixtures of water vapor with either oxygen or hydrogen react with the metal at the same rate as does water vapor alone. Hydrogen blisters are formed in the metal in the presence of water vapor, but none is observed when water is absent. Blister formation in water vapor is not detected if the metal is first reacted with HCl acid solution.

Abstract No. 144

Kinetics of the Oxidation of Platinum

G. C. Fryburg and **H. M. Murphy,** NACA Lewis Flight Propulsion Lab., 21000 Brookpark Rd., Cleveland 11, Ohio

The oxidation of platinum has been investigated employing electrically heated ribbons at temperatures from 900° to 1400°C and at pressures from 55 μ to 1 atm. An energy of activation of 40 kcal/mole has been obtained from the temperature dependence of the rate. An unusual pressure dependence has been observed which was found to result from the back reflection of the volatile PtO_2 by the surrounding gas molecules: at 1 atm pressure, only 0.5% of the PtO_2 formed escapes from the platinum.

Abstract No. 145

Kinetics of the Uranium-Steam Reaction

B. E. Hopkinson, Atomic Energy Establishment, Harwell, England (Present address: Research Lab., The International Nickel Co., Inc., Bayonne, N. J.)

Reaction rates of unalloyed uranium with super heated steam at 160°-1400°C and 1 atm pressure have been determined by a thermogravimetric method. Up to 880°C the reaction follows a linear rate law with maximum rates at approximately 300° and 750°C. Above 880°C a parabolic rate law applies for the first 60-120 min, after which corrosion is linear; the oxide formed in the initial period gives protection to the underlying metal, and the subsequent linear rate is as low as that at about 200°C. X-ray diffraction of the reaction product indicated that uranium dioxide was formed over almost the whole temperature range.

Abstract No. 146

Selective Oxidation of Al from an Al-Fe Alloy

R. E. Grace, Dept. of Metallurgical Engineering, Purdue University, Lafayette, Ind., and **A. U. Seybolt,** Research Lab., General Electric Co., Schenectady, N. Y.

The selective oxidation of aluminum from a 4.8 wt % Al-Fe alloy was studied with a microbalance at temperatures of 700°-900°C. The oxidizing gas was damp H_2, with dewpoints ranging from —55° to 0°C. The oxidation product was identified by electron diffraction to be the crystalline spinel, γ-Al_2O_3. At 800°C the parabolic oxidation constant was approximately proportional to the 1/7th power of the H_2O/H_2 gas ratio, and the experimental activation energy for the over-all oxidation reaction with 0°C dewpoint hydrogen gas was 72 kcal/mole.

Abstract No. 147

Selective Oxidation of 3¼% Si-Fe

A. U. Seybolt, Research Lab., General Electric Co., Schenectady, N. Y.

When silicon-iron is heated in hydrogen-water mixtures, only silica is formed as an oxidation product. There is some evidence that in the early stages of oxidation an amorphous (vitreous) SiO_2 film is formed. However, thicker films were found to be either low tridymite or low cristobalite or both. The selective oxidation data of silicon-iron can be rather complicated, and sometimes appears impossible to rationalize. In some temperature regions, notably 800° and 1000°C, the data obeyed the familiar parabolic law. However, at intermediate temperatures, complications were noted, some of which are probably due to the order-disorder reaction in the silicon-iron solid solution.

Abstract No. 148

Oxidation Studies on the Iron-Chromium-Aluminum Heater Alloys

E. A. Gulbransen and **K. F. Andrew,** Research Labs., Westinghouse Electric Corp., Beulah Rd., Churchill Boro., Pittsburgh 35, Pa.

The oxidation behavior of three iron-chromium-aluminum alloys was studied using sensitive weight gain techniques. In addition, x-ray diffraction methods were used to determine the crystal structure and composition of the oxide films. The adhesion characteristics of the oxide film to the metal were tested by introducing strains into the metal oxide system during oxidation.

Abstract No. 149

Experimental Electric Smelting of a Siliceous Iron Ore

G. E. Viens, G. V. Sirianni, and **R. R. Rogers,** Mines Branch, Dept. of Mines and Technical Surveys, Ottawa, Ont., Canada

The production of pig iron from a highly siliceous ore was investigated at the Department of Mines and Technical Surveys, Ottawa. The ore was concentrated by magnetic separation, sintered, and smelted in a 250 kva electric arc furnace. The effect of the CaO/SiO_2 ratio in the slag on pig iron composition, iron losses in the slag, and energy requirement during smelting, was studied in considerable detail.

Abstract No. 150

Iron and Phosphate Slag from Byproduct Ferrophosphorus

J. M. Potts, W. C. Scott, Jr., J. U. Campbell, and **J. A. Wilbanks,** Tennessee Valley Authority, Wilson Dam, Ala.

A process and furnace were developed for converting byproduct ferrophosphorus into high-grade iron for metallurgical purposes and phosphatic slag that might be used as a fertilizer or animal-feed supplement. The process consists in continuously smelting ferrophosphorus with calcined, siliceous iron ore and burnt lime in an electric furnace. The furnace has a two-component lining: walls of graphite, which resist corrosion by molten phosphate slag, and a hearth of magnesite, which resists attack by iron of low phosphorus content. In pilot-plant tests in a 6.5-ft diameter by 5-ft furnace operated at a power input of 350 kw, best results were obtained with about 100 v between the two electrodes. The product iron contained 0.5% P and the slag contained 22% citrate-soluble P_2O_5. The process offers an economical means for utilizing byproduct ferrophosphorus, the production of which greatly exceeds domestic demand.

INDEX TO AUTHORS

(The number in the right hand column is the abstract number used in the Technical Program and in the Abstracts.)

	Abstract No.
Albrecht, W. M.	60
Alpert, M. B.	77
Andrew, K. F.	61, 148
Angstadt, R. T.	14
Armstrong, L. D.	113A
Atkinson, J. T. N.	88
Baker, A. E.	115
Barnartt, S.	47
Barson, F.	112
Bartlett, J. H.	65
Battist, L.	46
Beach, J. G.	90, 91, 93
Beacom, S. E.	84
Beck, W.	39
Bicknell, R. W.	37
Blackburn, P. E.	143
Bloom, M. C.	29, 30
Böckman, O. C.	133
Bockstie, L. G., Jr.	4
Bothwell, M. R.	53
Brown, E. C.	85
Buck, W. R., III	68
Burbank, J.	20, 57
Butler, T. E.	134
Button, D. D.	122
Cahan, B. D.	14, 56
Cahoon, N. C.	16, 25, 26
Campbell, J. U.	150
Campney, K. N.	23
Cartledge, G. H.	72
Casey, E. J.	11, 23
Christensen, C. J.	48
Coffman, R. E.	113
Cohen, M.	55, 64
Connor, J.	80
Consiglio, J. A.	42
Cook, C. F., Jr.	27
Cornish, A. J.	101
Cornish, D. C.	51
Couch, D.	80
Croft, G. T.	12
Cutler, M.	75
Dean, R. S.	76
De Geiso, R. C.	82
De Haan, F.	22
Dibbs, H. P.	51
Dignam, M. J.	59
Diniak, A.	137
Dirkse, T. P.	17, 22
Driesner, A. R.	121
Dyett, M. J.	112
Eilbeck, A. B.	28
Engle, G. B.	124
Eriksen, W. T.	115
Eyring, H.	48
Faust, C. L.	90, 93
Fischer, W. H.	42
Flaschen, S. S.	116
Flengas, S. N.	78
Fryburg, G. C.	144
Funk, A. G.	48
Gage, D. G.	85
Gatos, H. C.	70
Giddings, J. C.	48
Giles, F. H.	65
Glicksman, R.	1, 2, 9, 10, 52
Grace, R. E.	146
Green, L., Jr.	120
Greig, W.	111
Gulbransen, E. A.	61, 143, 148
Gullett, W. W.	76
Hackerman, N.	46
Hamilton, J. A.	77
Harman, T. C.	97
Harris, V.	138
Harvey, W. W.	70, 118
Haycock, E. W.	62, 63
Heikes, R. R.	96
Henderson, I. H. S.	23
Herglotz, H. K.	107
Hodge, N. C.	129
Hoey, G. R.	55
Holmgren, J.	130, 138
Hopkinson, B. E.	145
Hudson, J. C.	58
Hyink, W. J.	95
Ingraham, T. R.	78
Itoh, R.	132
Ives, D. J. G.	51, 74
Jaffe, L. D.	122
Jenkins, A. E.	75A
Johansen, H. A.	139
Johnson, E. W.	132
Kafalas, J. A.	104
Karan, C.	112
Karas, H. R.	24
Keir, D. S.	73
Ketcham, S. J.	39
King, P. F.	44, 54
Kmetko, E. A.	121
Knipe, W. W.	135
Kohan, L. R.	92
Kolb, K. M.	109
Kolm, Carol	105
Korman, S.	137, 138
Korver, M. P.	16, 26
Kozawa, A.	15
Kruger, J.	50
Labrie, R. J.	79
Lake, P. E.	11
Lamb, V. A.	79
Leidheiser, H., Jr.	68
Leonhard, F. W.	27
Lesk, I. A.	113
Levine, M. C.	103
Levy, C.	94
Lewis, J. E.	33, 34
Liggett, L. M.	124
Linnenbom, V. J.	31
Logan, M. J.	97
Lougher, E. H.	97
Lozier, W. W.	136
MacDonald, J. J.	85
MacMillan, D. P.	121
Majka, S. J.	141
Mallett, M. W.	60
Mansfield, R. L.	126
Martel, C. S., Jr.	103
Martens, H. E.	122
Martius, U. M.	142
McCawley, F. X.	76
McGinnis, L. P.	4
McKee, E. S.	4
Mead, L.	130
Meyer, R. A.	127
Mooser, E.	98, 100
Morehouse, C. K.	1, 2, 9, 10
Morgan, R. P.	134
Mortimer, G.	106
Murphy, H. M.	144
Mutter, W. E.	112
Nickols, J. L.	53
Null, M. R.	136
Nye, W. F.	27
Oliver, J. P.	25
Panikkar, S. K.	86
Paris, B.	97
Pearson, A. D.	116
Pearson, W. B.	98
Petrocelli, J. V.	43
Pittman, R. W.	51
Plumb, R. C.	33, 35, 36, 40, 41
Posey, F. A.	71, 72
Potts, J. M.	150

	Abstract No.
Price, P. B.	81
Pryor, M. J.	73
Rama Char, T. L.	86
Rawson, A. E.	74
Riley, B. J.	84
Robbins, H.	114
Robinson, J. L.	53, 54
Robinson, P. H.	104
Robinson, R. L.	126
Rogers, L. B.	82
Rogers, R. R.	69, 149
Root, C. D.	119
Rosenberg, A. J.	103
Ruben, S.	8
Ruetschi, P.	14, 56
Russo, P. F.	83
Sasaki, K.	15
Saubestre, E. B.	87
Schaefer, J. F.	24
Schaer, G. R.	91
Schultz, F. J.	77
Schwartz, B.	114
Scott, W. C., Jr.	150
Selis, S. M.	4
Seybolt, A. U.	146, 147
Shearer, R. E.	5
Sheer, C.	130, 137, 138
Shibasaki, Y.	13
Silvester, D. R.	32
Sirianni, G. V.	149
Sirrine, R. C.	108
Smith, A. H.	102
Smyth, D. M.	7, 75
Soper, R. B.	83
Stanners, J. F.	58
Stern, M.	45
Stehsel, M. L.	120
Steinkamp, W. I.	140
Stieber, H. C.	123
Stirland, D. J.	37
Stokes, C. S.	135
Strauss, M. J.	29, 30
Streicher, M. A.	67
Strevg, L. A.	135
Stroup, R. C.	123
Sullivan, W. F.	77
Taylor, H. L.	109A
Templeton, I. M.	98
Thomas, E. C.	125, 128
Thomas, U. B.	18
Tiller, W. A.	99
Tingley, I. I.	69
Tragert, W. E.	38
Tripler, A. B.	93
Turner, D. R.	89, 117
Uhlig, H. H.	44
Veloric, H. S.	111
Vermilyea, D. A.	49, 81
Viens, G. E.	149
Vosburgh, W. C.	19
Waber, J. T.	66
Wagner, P. N.	121
Waller, C. E.	120
Wallwork, G. R.	75A
Wang, P.	83
Wanklyn, J. N.	32
Ward, J. W.	66
Waring, W.	110
Webb, M. B.	81
Weininger, J. L.	6
Werner, R. C.	5
Whitwell, J. H.	128
Wilbanks, J. A.	150
Willihnganz, E.	21
Wilson, P. R.	60
Wood, F. W.	131
Wood, R. E.	3
Wyman, W. L.	140
Yaffe, R. P.	72
Zavaglia, E. D.	39

December 1958 Discussion Section

A Discussion Section, covering papers published in the January-June 1958 JOURNALS, is scheduled for publication in the December 1958 issue. Any discussion which did not reach the Editor in time for inclusion in the June 1958 Discussion Section will be included in the December 1958 issue.

Those who plan to contribute remarks for this Discussion Section should submit their comments or questions in triplicate to the Managing Editor of the JOURNAL, 1860 Broadway, New York 23, N. Y., *not later than September 1, 1958.* All discussions will be forwarded to the author(s) for reply before being printed in the JOURNAL.

FUTURE MEETINGS OF
The Electrochemical Society

Ottawa, Canada, September 28, 29, 30, October 1, and 2, 1958

Headquarters at the Chateau Laurier

Sessions will be scheduled on

Batteries, Corrosion, Electrodeposition (including symposia on "Electrodeposition on Uncommon Metals" and "Electrodeposition from Fused Salts"

Electronics (Semiconductors),

Electrothermics and Metallurgy,

and a symposium on "Films Formed in Contact with Liquids"

sponsored by Theoretical Electrochemistry, Battery, and Corrosion Divisions

* * *

Philadelphia, Pa., May 3, 4, 5, 6, and 7, 1959

Headquarters at the Sheraton Hotel

Sessions probably will be scheduled on

Electric Insulation, Electronics (including Luminescence and Semiconductors), Electrothermics and Metallurgy (including a Projected Symposium on "Mechanical Properties of Intermetallic Compounds"), Industrial Electrolytics, and Theoretical Electrochemistry

* * *

Columbus, Ohio, October 18, 19, 20, 21, and 22, 1959

Headquarters at the Deshler-Hilton Hotel

* * *

Chicago, Ill., May 1, 2, 3, 4, and 5, 1960

Headquarters at the Lasalle Hotel

* * *

Houston, Texas, October 9, 10, 11, 12, and 13, 1960

Headquarters at the Shamrock Hotel

* * *

Papers are now being solicited for the meeting to be held in Philadelphia, Pa., May 3-7, 1959. Triplicate copies of each abstract (*not exceeding 75 words in length*) are due at Society Headquarters, 1860 Broadway, New York 23, N. Y., *not later than January 2, 1959* in order to be included in the program. *Please indicate on abstract for which Division's symposium the paper is to be scheduled, and underline the name of the author who will present the paper.* Complete manuscripts should be sent in triplicate to the Managing Edittor of the JOURNAL at 1860 Broadway, New York, 23, N. Y.

Current Affairs

Candidates for Society Offices

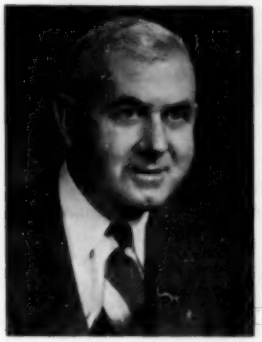

F. L. LaQue

W. J. Hamer

F. W. Koerker

W. C. Gardiner

The Board of Directors of the Society, in accordance with the provisions of our Constitution, has approved the following Report of the Nominating Committee.

Report of Nominating Committee

Your Nominating Committee takes pleasure in submitting the following nominees for election to the offices to be filled for the years 1959-1960 and 1959-1962:

For President to Serve One Year (1959-1960)—
William C. Gardiner
For Vice-President to Serve Three Years (1959-1962)—
Walter J. Hamer
Frederick W. Koerker
Frank L. LaQue
For Secretary to Serve Three Years (1959-1962)—
Ivor E. Campbell
Lee O. Case

Each of the above candidates has been notified of his selection and has expressed his willingness to run for office and to serve if elected.

(Signed) R. M. Hunter, *Chairman*
T. P. May
Hans Neumark
M. F. Quaely
R. A. Schaefer

The two other Vice-Presidents, Ralph A. Schaefer and Henry B. Linford, since they were elected for a three-year term, will automatically become first and second Vice-President, respectively.

The above slate will be voted on in the fall ballot-by-mail election, and the successful candidates will assume office in the spring of 1959.

William C. Gardiner
Presidential Candidate

William C. Gardiner was born in Exeter, Ont., in 1904 and became a citizen of the United States in 1939. While he was an undergraduate at Queen's University, Professor Dorrance persuaded him that power development on the St. Lawrence River would create a great demand for electrochemists. Accordingly, he took a Master's degree working on an electroplating problem. He continued his electrochemical training at Princeton University under Professor G. A. Hulett. His thesis on the Weston Normal Cell was published in the TRANSACTIONS of The Electrochemical Society in 1929 and won for him the Society's first award of the Young Author's Prize.

Dr. Gardiner spent three years as a research chemist for Comstock and Wescott, Inc., in Niagara Falls, working on chlorine metallurgy. Since 1932, he has worked on electrochemical research and development for Mathieson Alkali Works (now Olin Mathieson Chemical Corp.). His present position is manager research engineering, Research and Development Dept., Industrial Chemicals Div.; his work has been with mercury type alkali-chlorine cells. He was active in the design, construction, and initial operation of plants using Mathieson cells at Arvida, Que.; Saltville, Va.; McIntosh, Ala.; Linden, N. J.; and Monterrey, Mexico. He was captain of the U. S. chlorine industry team which toured German chlorine plants after World War II and brought back working drawings and detailed operating instructions of the best practice there. He also worked on the development of a cell to produce magnesium and chlorine from hydrated magnesium chloride feed. These cells were installed at the Mathieson Magnesium Plant in Lake Charles, La., where he was superintendent of the Electrolytic Dept. He holds patents on brine treatment, mercury cells, and magnesium cells, and has published papers of interest to the electrolytic chlorine industry. He acts as consultant on electrochemical problems for several U. S. Government projects.

Dr. Gardiner joined The Electrochemical Society in 1927 and has been active in the Niagara Falls Section, which he has served as Secretary-Treasurer and Chairman. He also served on convention committees when the Society met in the Buffalo-Niagara Falls area. He has been Chairman of the Industrial Electrolytic Division, and Divisional Editor of the JOURNAL since 1950. He also has been a member of the Alkali-Chlorine Committee. Dr. Gardiner has been a Vice-President of the Society for the past two years, serving on the Finance Committee and the Ways and Means Committee. He was Chairman of the latter com-

mittee last year. This year he has been Acting President during the illness of President Swann.

Walter J. Hamer
Vice-Presidential Candidate

Walter J. Hamer is chief of the Electrochemistry Section of the National Bureau of Standards, Washington, D.C. He was born in Altoona, Pa., in 1907. He received his undergraduate training at Juniata College in Huntingdon, Pa., and his graduate training at Yale University, from which he received the Ph.D. degree in physical chemistry in 1932. He then returned to Yale for two years as a U. S. Navy post-doctorate Research Fellow. In July 1934, he accepted a position as research associate in physical chemistry at M.I.T., which position he held until November 1935 when he joined the staff of the National Bureau of Standards.

Dr. Hamer is the author or co-author of a substantial number of articles dealing with various aspects of electrochemistry. He has conducted research on electrolytes, fused salts, primary and secondary batteries, and on standard cells. He has published a series of papers on the lead-acid storage battery and another series on dry cells. He has also published a series of papers on pH standards. At the National Bureau of Standards, one of his main responsibilities is the maintenance of the nation's primary standard of electromotive force.

During the war years, Dr. Hamer worked as an electrochemist first for the Office of Scientific Research and Development and then for the Manhattan Project. He served as battery consultant to the Dept. of Defense in 1952-1954. Dr. Hamer is a member of the Commission on Electrochemistry of The International Union of Pure and Applied Chemistry and is technical advisor on primary batteries to the U. S. National Committee of the International Electrotechnical Committee. He is a fellow of the New York Academy of Science and holds memberships in the American Association for the Advancement of Science, Sigma Xi, Alpha Chi Sigma, the American Institute of Electrical Engineers, the American Physical Society, The Faraday Society, the American Chemical Society, and the Washington Academy of Science.

Dr. Hamer, a member of The Electrochemical Society since 1937, has been active in its affairs. He was Chairman of the Theoretical Electrochemistry Division in 1951-1953 and a member of the Executive Board of the Battery Division in 1954-1956. In 1951, he organized and contributed to the bi-centennial issue of the JOURNAL devoted to the Theoretical Electrochemistry Division; and has conducted a number of Society symposia. He is editor of the Society's monograph on "The Structure of Electrolytic Solutions" now in press. This monograph is an outgrowth of the international symposium held on Washington, D. C., in 1957 and was co-sponsored by the National Science Foundation. At present, Dr. Hamer is a member of the Society's Honors and Awards Committee, and represents the Society on the American Standards Association's Committees Y10 and Y32 which deal with letter symbols and abbreviations and standardization of graphical symbols.

L. O. Case

I. E. Campbell

Frederick W. Koerker
Vice-Presidential Candidate

Frederick W. Koerker, technical expert in the Electrochemical Planning Dept. of the Dow Chemical Co., Midland, Mich., was born in Milwaukee, Wis., June 9, 1913. He received his B.S. and M.S. degrees in chemistry from the University of Wisconsin in 1934 and 1936, respectively, serving as a teaching assistant and lecture assistant under a former President of The Electrochemical Society, Dr. Louis Kahlenberg.

Mr. Koerker started work for the Dow Chemical Co. in the Main Lab. in 1936, and after one year entered research and, later, supervisory duties in the Chlorine Dept. under another former President of the Society, Dr. Ralph M. Hunter. He was appointed to his present position in 1953. He is the author of numerous papers presented in annual conferences of the various Dow divisions, and presented the paper "Materials of Construction for Chlor-Alkali Plants" at the Philadelphia Meeting of the Society in 1949.

Mr. Koerker joined The Electrochemical Society in 1944. He served in all the offices of the Midland Local Section (Chairman 1950), and as Secretary, Vice-Chairman, and Chairman (1953) of the Industrial Electrolytic Division. While Chairman of the Division, he organized the symposium on "Molten Bath Electrolysis" for the 1954 Chicago convention, and earlier was head of the committee which arranged the trip to Midland during the 1951 Detroit convention of the Society. Mr Koerker was Secretary of the former Local Section Advisory Committee of the Society. He was instrumental in the formation of the new Council of Local Sections, Chairman of the Bylaws Committee for this group, and, later, Chairman of the Council of Local Sections and Director of the Society representing the Council for two years. He has been Chairman of the Society Membership Committee since 1956.

His other professional associations are the American Chemical Society, Alpha Chi Sigma, and Phi Lambda Upsilon.

Frank L. LaQue
Vice-Presidential Candidate

F. L. LaQue has been a vice-president of the International Nickel Co., Inc., and manager of its Development and Research Div. since June 1954. He previously had been head of the Corrosion Engineering Section of that division since 1945.

A native of Gananoque, Ont., Canada, Mr. LaQue received his degree of Bachelor of Science in chemical and metallurgical engineering from Queen's University, Kingston, Ont., in 1927.

He joined the International Nickel Co.'s Development and Research Div. that year and, since, has devoted his activities to the field of corrosion and corrosion-resisting materials. He was assistant director of Technical Service on Mill Products from 1937 until April 1940, when he became engaged in development activities on all applications of both ferrous and nonferrous nickel-contain-

ing alloys. Under his leadership, the well-known corrosion testing stations of the company at Kure Beach and Harbor Island, N. C., were established.

He has been a member of the American Society for Testing Materials since 1935. In 1951, he delivered the Edgar Marburg Memorial Lecture on "Corrosion Testing." Mr. LaQue is a vice-president of the American Society for Testing Materials, and also serves on the following committees: Technical Committee Activities, Development Activities, Finance Committee, and the Administrative Committee on Papers and Publications.

In 1949, Mr. LaQue was the recipient of the F. N. Speller Award in Corrosion Engineering of the National Association of Corrosion Engineers, of which he is past president. Mr. LaQue is also a member of the American Chemical Society, American Society for Metals, American Association for the Advancement of Science, National Association of Corrosion Engineers, and serves on the Visiting Committees of the Massachusetts Institute of Technology and Case Institute of Technology.

As a member of The Electrochemical Society, Mr. LaQue has served as Business Manager of the JOURNAL, and Chairman of the Sustaining Membership Committee.

Mr. LaQue is the author of numerous articles and papers on corrosion.

Ivor E. Campbell

Secretarial Candidate

Ivor E. Campbell is chief of the Div. of Inorganic Chemistry and Chemical Engineering of the Battelle Memorial Institute in Columbus, Ohio. He was born in Kenton, Ohio, in 1919, and received his undergraduate training in chemistry and mathematics at Evansville College in Evansville, Ind., and his graduate training at the Ohio State University, from which he received the Ph.D. degree in inorganic chemistry in 1943.

Dr. Campbell joined the Battelle staff as a research chemist in 1943. He was made assistant supervisor of the Div. of Nonferrous Metallurgy in 1948 and was named to his present position in 1950.

He is the author of over 30 papers in various scientific and trade journals. These papers deal principally with vapor plating and with the properties of high-purity metals. He is coauthor of The Electrochemical Society's monograph "Vapor Plating" published in 1955, and editor of "High Temperature Technology" published by John Wiley, as part of the Society's monograph series, in 1956.

Dr. Campbell's major present interests, as indicated by his publications, have been in the development of improved processes for the preparation of high-purity metals and in the formation of refractory coatings by vapor-deposition techniques. He has worked extensively with iodide-refining processes for metals, and has presented at Society meetings a number of papers on the preparation of high-purity metals by the iodide process.

Dr. Campbell joined The Electrochemical Society in 1944. He served as Secretary-Treasurer of the Electrothermics Division from 1949 to 1953, Chairman of the Division from 1953 to 1955, and as a member of the Executive Committee of the Division from 1955 to 1957. He was Chairman of the Bylaws Committee of the Society in 1954 and 1955, and Chairman of the Becket Memorial Award Committee in 1956.

During Dr. Campbell's term as Chairman, the Electrothermics Division merged with the Rare Metals Group of the Electronics Division to form the Electrothermics and Metallurgy Division. The establishment of the Becket Memorial Award for undergraduate students demonstrating proficiency in the field of electrothermics was initiated by the Electrothermics and Metallurgy Division during his term as Chairman.

Lee O. Case

Secretarial Candidate

Lee O. Case, associate professor of chemistry at the University of Michigan, Ann Arbor, was born in Marshall, Mich., in 1895. He received all his professional training at the University of Michigan, his B.S. degree in chemical engineering and his M.S. and Ph.D. in physical chemistry, the latter in electrochemistry under Dr. A. L. Ferguson, former President of The Electrochemical Society. He has served continuously on the faculty of the University of Michigan since 1922, his particular interests being in the fields of thermodynamics, phase equilibrium, and electrochemistry.

He is a member of the Detroit Section of The Electrochemical Society and has represented this Section as Councilor for several consecutive terms. During this period, he was active in the organization of the Council of Local Sections, of which he has been Secretary, Vice-Chairman, and Chairman, and is at present one of the representatives of the Council of Local Sections on the Board of Directors of the Society.

Division News

E & M Symposium on Mechanical Properties of Intermetallic Compounds

The Electrothermics and Metallurgy Division announces a Projected Symposium on "Mechanical Properties of Intermetallic Compounds" to be held during the 115th Meeting of The Electrochemical Society in Philadelphia, Pa., May 3-7, 1959.

For the purposes of this Symposium, intermetallic compounds will be held to comprise all intermediate phases in binary or higher order systems of true metals, including superlattices. Interstitial compounds of metals and nonmetals, such as the carbides, nitrides, borides, etc., will *not* be considered.

It is hoped to include papers covering the following topics:

Mechanical Properties of Intermetallic Compounds

Fundamental Behaviors: Deformation Modes; Initiation and Propagation of Fracture; Effects of Crystal Structure; Dislocations in Intermetallic Compounds; Influence of Point Defects; Radiation Damage.

Phenomenology: Effects of Processing Variables; Temperature Dependence of Mechanical Properties; Effects of Impurities; Effects of Alloying; Effects of Stress State and Strain Rate.

Experimental Techniques: Testing Techniques Applicable to Brittle Compounds; Preparation of Intermetallic Compounds with Reference to Mechanical Property Studies, e.g., Single Crystal, and High-Purity Samples.

Titles and authors of proposed papers should be sent immediately, and triplicate copies of 75-word abstracts by January 2, 1959, to the Secretary-Treasurer of the Electrothermics and Metallurgy Division (please underline the name of the author who will present the paper):

Dr. J. H. Westbrook
Research Lab.
General Electric Co.
P.O. Box 1088
Schenectady, N. Y.

Arrangements can be made for authors residing outside the United States who wish to have papers presented *in absentia*.

William J. Kroll Chosen Acheson Medalist

William J. Kroll, scientist-electrochemist-metallurgist, has been selected as the 15th recipient of the Edward Goodrich Acheson Medal and Prize of The Electrochemical Society. The presentation will be made at the banquet to be held in Dr. Kroll's honor on September 30, 1958, during the 114th Meeting of the Society at the Chateau Laurier in Ottawa, Ont.

The award, a gold medal and $1000 prize, is conferred biennially by The Electrochemical Society for the most outstanding contribution to those fields of activity fostered by the Society. It was founded by Dr. Edward Goodrich Acheson in August 1928 as a means of promoting the science and technology of electrochemistry. By unanimous decision, in 1929 Dr. Acheson himself was the first recipient of the medal for his contributions to electronics.

Dr. Kroll is a graduate of the Technische Hochschule, Charlottenburg, Germany, from which he received the degree of Doctor of Engineering in 1917 under Professor K. A. Hofmann. For several years following this, Dr. Kroll traveled about, working in Germany, Austria, and Hungary. In 1923 he returned to Luxembourg, the place of his birth, where he set up his own laboratory, Bel'air. The work he did there had an effect on the entire field of metallurgy. In 1940 he left Luxembourg ahead of the Nazi invasion and came to the United States, becoming an American citizen in 1952.

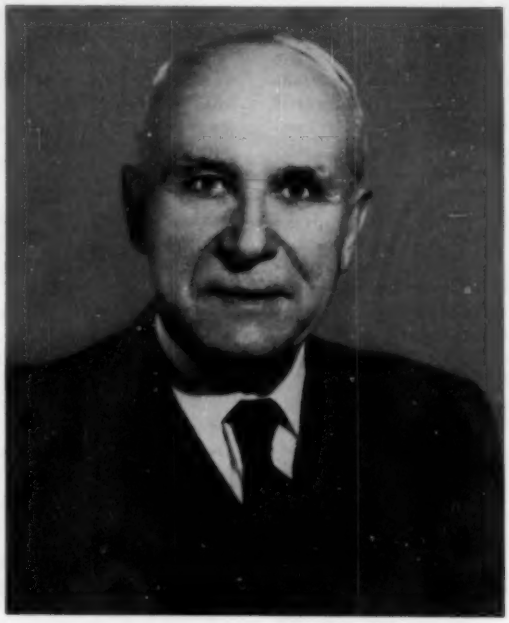

W. J. Kroll, 1958 Acheson Medalist

He was a consultant for the Union Carbide Research Labs. in Niagara Falls, N. Y., during 1940-1945. For the next five years he was in charge of the zirconium project of the U. S. Bureau of Mines in Albany, Ore. Since 1950 he has been doing private consulting work in Corvallis, Ore., where he makes his home.

Many honors and awards have been conferred on Dr. Kroll, including the Francis J. Clamer Medal, 1954; the James Douglas Medal, 1954; the Heyn Award; the Albert J. Sauveur Award, 1955; Honorary Degree, University of Grenoble, 1955. In January of this year, he was presented with the 1958 Perkin Medal for his achievement in applied chemistry (*see* March JOURNAL, p. 58C).

His numerous publications, patents, and technical developments, the best-known of which is the Kroll titanium process, constitute an impressive list.

News Items

New Sustaining Members

The Schering Foundation, Inc., Bloomfield, N. J., recently became a Sustaining Member of The Electrochemical Society.

C.I.T.C.E. Meeting

The tenth meeting of the International Committee of Electrochemical Thermodynamics and Kinetics (C.I.T.C.E.) will be held in Amsterdam, Holland, September 15-18, 1958.

Sessions of the following commissions are scheduled: 1. Tension—pH diagrams; 2. Electrochemical definitions and nomenclature; 3. Experimental methods in electrochemistry; 4. Batteries; 5. Corrosion

Communications regarding attendance at the meeting can be addressed to: N. Ibl, Physical Sciences Div., Stanford Research Institute, Menlo Park, Calif.

Noted Chemical Engineers Receive A.I.Ch.E Founder Awards

Five of the nation's leading chemical engineers were presented with Founders Awards on June 23, 1958 during the Golden Jubilee Meeting of the American Institute of Chemical Engineers in Philadelphia.

Among those honored were Sidney D. Kirkpatrick, editorial director and vice-president, McGraw-Hill Book Co., New York City; and John V. N. Dorr, founder and chairman of the board, Dorr-Oliver Co., New York City.

The awards are given to members of the A.I.Ch.E. who have extraordinary impact on chemical engineering and whose achievements have advanced the profession in any of its aspects. They consist of pins in the shape of the Institute shield, and a lifetime invitation to attend annual meetings with special registration privileges.

Dr. Kirkpatrick has been active in industry, education, technical literature, public service, and professional societies since his graduation from the University of Illinois in 1916. He is a Past President of The Electrochemical Society (1945).

Mr. Dorr is a pioneer in the application of chemical engineering principles and techniques to extractive metallurgy, and in other branches of chemical engineering, for which he has received many honors. He has been a member of The Electrochemical Society since 1913.

William Blum Awarded Highest Honor of American Electroplaters' Society

Dr. William Blum, noted scientist of Washington, D. C., has been announced as winner of the first annual "AES Scientific Achievement Award," the American Electroplaters' Society's recently created, highest honor.

William Blum

Chosen unanimously for that summit award by a six-man "Scientific Achievement Award Committee" headed by Dr. Russel E. Harr of Chicago, from a panel of nine distinguished AES members nominated by the society's Branches for outstanding, decade-or-more accomplishment in advancement of electroplating, metal finishing, and allied arts, Dr. Blum will consequently deliver the first "William Blum Lecture" at the society's Golden Jubilee Convention and Industrial Finishing Exposition in Detroit in June 1959, which international event will climax the AES's 50th Anniversary observance. Aside from a scroll and other material recognition, he will receive a $500 honorarium at that assembly.

A native Philadelphian, educated at the University of Pennsylvania where he received his degrees, including the Ph.D. in 1908, Dr. Blum, from 1913 to his retirement in 1951, headed, with conspicuous distinction, the Electrodeposition Section of the National Bureau of Standards. He since has been a prominent consultant.

His rich record includes service as President of The Electrochemical Society (1926). Among a wealth of honors bestowed on him here and abroad, he received the Hothersall Medal of the Institute of Metal Finishing in London in 1954; the Award of Merit of the ASTM; the Cresson Medal of the Franklin Institute of Philadelphia in 1953; the "Distinguished Governmental Service" medal of the American Institute of Chemists in 1926; the Edward Goodrich Acheson Medal and Prize of The Electrochemical Society in 1944. His Alma Mater conferred the honorary degree of Doctor of Science on him in 1953. And, that same year, the American Chemical Society awarded him a certificate for a half-century's outstanding service, and made him an "Emeritus Member."

Paul Ruetschi

Young Author's Prize for 1957

At the Annual Banquet held on Tuesday, April 29, during the New York Meeting of The Electrochemical Society, the Young Author's Prize of $100 was presented to Paul Ruetschi of the Electric Storage Battery Co. His prize-winning paper, "The Galvani Electrode Potential," was published in the March 1957 issue of the JOURNAL.

Dr. Ruetschi was educated in Switzerland and received his Ph.D. degree from the Federal Institute of Technology, Zurich, in 1953. Subsequently, he taught practical courses in physical chemistry at the same school. In 1954 he accepted an invitation to work for one year with Professor Paul Delahay at Louisiana State University on a Naval Research contract. Dr. Ruetschi came to this country on a permanent basis in the fall of 1955, joining the Research Dept. of the Electric Storage Battery Co. in Philadelphia, where at present he is head of the Electrochemistry Div.

Dr. Ruetschi was the recipient of the Medal of the Federal Institute of Technology in Zurich in 1953. He has already published about 20 papers in various scientific journals here and abroad. His scientific interests are in the physics and chemistry of surfaces, in particular, theory of electrode potentials and electrode kinetics, and heterogeneous catalysis.

In addition to The Electrochemical Society, Dr. Ruetschi holds memberships in the Faraday Society, the American Chemical Society, and the Franklin Institute. He is also a member of the International Committee of Electrochemical Kinetics and Thermodynamics.

Turner Memorial Award for 1957

The Society's Francis Mills Turner Memorial Award, Sponsored by the Reinhold Publishing Corp., consisting of $100 worth of books, went

A. C. Makrides

to A. C. Makrides for his paper, "Stoichiometric Numbers and Hydrogen Overpotential," which appeared in the November 1957 issue of the JOURNAL. Announcement of the award was made during the New York Meeting of The Electrochemical Society at the Annual Banquet on April 29, 1958. Dr. Makrides' paper was prepared while he was with the Dept. of Chemistry at the University of Texas.

Dr. Makrides was awarded B.A. and Ph.D. degrees from the University of Texas, Austin. During 1954-1955 he was a Union Carbide Research Fellow and Instructor at the Institute for the Study of Metals at the University of Chicago, and from 1955 to 1958 he was research chemist with the American Petroleum Institute, Project 47d, at the Dept. of Chemistry, University of Texas. He joined the Metals Research Labs. of the Electro Metallurgical Co., Div. of Union Carbide Corp., Niagara Falls, N. Y., in April 1958.

Dr. Makrides' research has been concerned with dissolution of metals in aqueous acid solutions, hydrogen overpotential, and corrosion inhibition. He has also worked in microcalorimetric studies of heats of wetting of solids by liquids and on surface properties of silicon dioxide.

He is a member of The Electrochemical Society, as well as of Phi Beta Kappa, Tau Beta Pi, and Sigma Xi.

Latest Nuclear Research in Chemistry Available

The latest research in the application of atomic energy to the chemical industry will be presented at the 1958 International Conference on the Peaceful Uses of Atomic Energy to be held in Geneva, September 1-13, 1958.

The Document Service of The Chronicle of United Nations Activities has inaugurated a complete service to supply the chemical industry with materials of the Conference. Available immediately are the lists of papers to be presented, including several hundred papers dealing with chemical research throughout the world.

Topics covered include reactor technology and chemistry, including compatibility studies and corrosion phenomena; basic application of chemistry in atomic energy, with discussions on basic chemistry of materials such as individual fission products, transuranic elements, and analytical procedures, including activation analysis and fundamental radiation chemistry of organic and inorganic systems.

The lists may be obtained free by writing to: Chemical Document Service, The Chronicle of United Nations Activities, 234 W. 26th St., New York 1, N. Y.

New Members

In June 1958, the following were elected to membership in The Electrochemical Society by the Admissions Committee:

Active Members

Maire S. Blomgren, Philco Corp.; Mail add: 214 So. 39 St., Philadelphia 4, Pa. (Electronics, Theoretical Electrochemistry)

Henry E. Bridgers, Bell Telephone Labs., Inc., 555 Union Blvd., Allentown, Pa. (Electronics)

Robert G. Carlson, General Electric Co., 21800 Tungsten Rd., Cleveland 17, Ohio (Electrothermics & Metallurgy)

Hugh M. Cleveland, Bell Telephone Labs., Inc., Murray Hill, N. J. (Electronics)

John J. Darcy, Jr., Mellon Institute; Mail add: 543 Oxford Blvd., Pittsburgh 16, Pa. (Electronics, Electro-Organic)

Albert W. Dauer, Dow Chemical Co.; Mail add: 514 Wisteria, Lake Jackson, Texas (Industrial Electrolytic)

Robert E. Davis, Westinghouse Electric Corp.; Mail add: Box 366, Murrysville, Pa. (Electronics)

ECS Membership Statistics

The following three tables give breakdown of membership as of July 1, 1958. The Secretary's Office feels that a regular accounting of membership will be very stimulating to membership committee activities. In Table I it should be noted that the totals appearing in the right-hand column are *not* the sums of the figures in that line since members belong to more than one Division and, also, because Sustaining Members are not assigned to Divisions. But the totals listed are the total membership in each Section. In Table I, Sustaining Members have been credited to the various Sections.

Table I. *ECS Membership by Sections and Divisions*

Section	Division: Battery	Corrosion	Electric Insulation	Electro-deposition	Electronics	Electro-Organic	Electrothermics & Met.	Industrial Electrolytic	Theoretical Electrochem.	No Division	Total as of 1/1/58	Total as of 7/1/58	Net Change
Boston	13	26	7	35	54	8	20	13	23	6	131	134	+ 3
Chicago	16	35	4	46	23	11	13	14	23	12	111	127	+16
Cleveland	59	37	2	51	41	10	27	34	39	15	203	209	+ 6
Columbus, Ohio	1	12	0	13	4	2	22	3	8	5	45	44	— 1
Detroit	8	21	5	48	8	7	7	6	20	20	84	88	+ 4
India	7	6	3	17	8	6	9	13	13	3	36	33	— 3
Indianapolis	11	7	3	11	10	4	6	3	6	2	40	41	+ 1
Midland	9	15	0	5	2	2	7	16	11	2	45	43	— 2
Mohawk-Hudson	5	15	13	9	12	1	7	3	12	4	51	53	+ 2
New York	82	103	23	137	133	32	65	67	96	43	482	503	+21
Niagara Falls	16	24	1	22	8	5	74	66	31	22	175	183	+ 8
Ontario-Quebec	12	24	1	17	4	3	36	26	8	14	75	78	+ 3
Pacific Northwest	5	10	0	8	3	1	9	10	9	10	47	42	— 5
Philadelphia	24	33	3	38	62	12	23	19	50	29	174	180	+ 6
Pittsburgh	4	47	3	27	29	5	37	16	34	9	130	131	+ 1
San Francisco	6	14	2	22	16	4	14	22	22	4	64	70	+ 6
S. Calif.-Nevada	15	20	2	26	27	3	15	16	22	10	95	99	+ 4
Washington-Baltimore	34	39	7	39	22	3	11	9	30	6	128	129	+ 1
U. S. Non-Section	54	89	13	85	73	43	62	76	114	32	395	399	+ 4
Foreign Non-Section	42	59	5	61	30	29	37	60	73	89	224	259	+35
Total as of Jan. 1, 1958	409	638	100	705	518	193	479	485	620	313	2735		
Total as of July 1, 1958	423	636	97	717	569	191	501	492	644	337		2845	

Table II. *ECS Membership by Grade*

	Total as of 1/1/58	Total as of 7/1/58	Net Change
Active	2448	2486	+ 38
Faraday (Active)	—	30	+ 30
Deutsche Bunsen Gesellschaft (Active)	—	14	+ 14
Delinquent	61	77	+ 16
Active Representative Patron Members	8	10	+ 2
Active Representative Sustaining Members	70	83	+ 13
Total Active Members	2587	2700	+113
Life	16	16	0
Emeritus	54	51	— 3
Associate	31	32	+ 1
Student	42	42	0
Honorary	5	4	— 1
	2735	2845	+110

The figures pertaining to Patron and Sustaining Member Representatives, and Faraday and Deutsche Bunsen Gesellschaft members subscribing to the JOURNAL, have been added to reflect reclassifications and changes in membership status.

Table III. *ECS Patron and Sustaining Membership*

	Total as of 1/1/58	Total as of 7/1/58	Net Change
Patron Member Companies	4	5	+ 1
Sustaining Member Companies	127	138	+ 2

Blanton C. Duncan, National Bureau of Standards; Mail add: 3550 Valley Dr., Alexandria, Va. (Theoretical Electrochemistry)

Robert M. Folsom, I.B.M. Corp.; Mail add: 33 Kinry Rd., Poughkeepsie, N. Y. (Electronics)

Howard A. Froot, International Nickel Co.; Mail add: 33-25 90th St., Jackson Heights 72, N. Y. (Corrosion)

Sol Gilman, I.B.M. Corp.; Mail add: Meier Rd., R.D. 2, Poughkeepsie, N. Y. (Electronics, Theoretical Electrochemistry)

Nicholas Glyptis, Multi-Tron Lab., Inc.; Mail add: 9818 W. Drury Lane, Westchester, Ill. (Electronics, Electrothermics & Metallurgy, Theoretical Electrochemistry)

Wiley W. Greer, E. I. du Pont de Nemours & Co., Inc., Technical Service Lab., Pigments Dept., Chestnut Run, Wilmington, Del. (Electronics)

David K. Hartman, General Electric Co.; Mail add: 113 Huntleich Ave., Fayetteville, N. Y. (Electronics)

Charles W. Henson, Norton Co., Worcester 6, Mass. (Electrothermics & Metallurgy)

Heribert K. Herglotz, E. I. du Pont de Nemours & Co., Inc.; Mail add: 2904 Newport Gap Pike, Wilmington 8, Del. (Electronics)

Mary S. Jaffe, General Electric Co.; Mail add: 3590 Woodridge Rd., Cleveland Heights 21, Ohio (Electronics)

Kenneth M. Kolb, E. I. du Pont de Nemours and Co., Inc.; Mail add: Apt. 6, Texas Bldg., Parklynn Apts., Wilmington 5, Del. (Corrosion, Electrodeposition, Electronics, Electrothermics & Metallurgy, Industrial Electrolytic)

Solomon Levinson, General Precision Lab.; Mail add: 700 Cleveland St., Brooklyn 8, N. Y. (Electronics, Theoretical Electrochemistry)

Seymour Z. Lewin, New York University, Chemistry Dept., Washington Square, New York 3, N. Y. (Theoretical Electrochemistry)

Alberto Loro, Northern Electric Co., Dept. 4854, 1401 St. Patrick St., Montreal, Que., Canada (Electrodeposition, Electronics, Electrothermics & Metallurgy)

Ian M. Mackintosh, Bell Telephone Labs., Inc., Murray Hill, N. J. (Electronics)

John A. Poole, Electralab, Inc.; Mail add: 31 Locust Ave., Lexington 73, Mass. (Corrosion, Electric Insulation, Electrodeposition, Electronics, Theoretical Electrochemistry)

Francis X. Rizzo, Brookhaven National Lab., 31 Herschal Pl., Upton, N. Y. (Electronics)

Donald G. Rogers, Sprague Electric Co., North Adams, Mass. (Electrothermics & Metallurgy)

Harry Sello, Shockley Semiconductor Lab., 391 San Antonio Rd., Mountain View, Calif. (Electronics)

Lloyd H. Shaffer, American Machine & Foundry Co., Central Research Lab., P. O. Box 889, Stamford, Conn. (Battery, Electronics, Theoretical Electrochemistry)

Stanley L. Siegel, Enequist Chemical Co.; Mail add: 131 Bennett Ave., New York 33, N. Y. (Electrodeposition)

Morris N. Slater, Radio Corp. of America, Lancaster, Pa. (Electronics)

Bjarne B. Smith, Elektrokemisk A.S., 101 Park Ave., New York 17, N. Y. (Electrothermics & Metallurgy)

Harris M. Sullivan, General Electric Co., Semiconductor Products Dept., Electronics Park, Bldg. 3, Rm. 202, Syracuse, N. Y. (Electronics)

Earl Q. Teaford, Battelle Memorial Institute, 505 King Ave., Columbus 1, Ohio (Electrothermics & Metallurgy)

Harold A. Tubbesing, Trojan Battery Co.; Mail add: 2053 Empress Ave., South Pasadena, Calif. (Battery)

Herman B. Urbach, Olin Mathieson Corp.; Mail add: 45 Dexter Terrace, Tonawanda, N. Y. (Industrial Electrolytic, Theoretical Electrochemistry)

Harold S. Veloric, Radio Corp. of America, Semiconductor Div., Somerville, N. J. (Electronics)

William R. Von Tress, Dow Chemical Co., B 1404, Freeport, Texas (Theoretical Electrochemistry)

Mieczyslaw Wojciechowski, General Motors Corp.; Mail add: 9319 St. Cyril St., Detroit 13, Mich.

Associate Member

Nicola A. Calandrello, Raytheon Manufacturing Co.; Mail add: 77 Robbins St., Waltham 54, Mass. (Corrosion, Electrodeposition)

Reinstatements to Active Membership

William C. Davis, C.B.S. Hytron; Mail add: 12 Pearson St., Chelmsford, Mass. (Electronics)

Deane O. Hubbard, Food Machinery & Chemical Corp.; Mail add: 30603 Winston Dr., Bay Village, Ohio (Industrial Electrolytic)

By action of the Board of Directors of the Society, all prospective members must include first year's dues with their applications for membership.

Also, please note that, if sponsors sign the application form itself, processing can be expedited considerably.

Section News

Philadelphia Section

The May "Ladies' Day" meeting of the Philadelphia Section was held on the beautiful Princeton University Campus. Following a tour of the campus, cocktails and dinner were enjoyed by the large group in attendance. The evening meeting then was held at the RCA Labs. nearby.

In the business meeting, the 1958-1959 officers were elected:

Chairman—George W. Bodamer
Vice-Chairman—Knut Krieger
Treasurer—Albert A. Ware
Secretary—Harry C. Mandell, Jr., Pennsalt Chemicals Corp., P. O. Box 4388, Philadelphia 18, Pa.

Thanks were voted to the retiring officers.

Mr. Cyril N. Hoyler, manager of technical relations, David Sarnoff Research Center, presented a fascinating demonstration-lecture on "New Adventures in Electronics." Mr. Hoyler had impressive demonstrations and stimulating comments on such subjects as light amplification, electrostatic photography, miniaturized television, and electronically produced music. The imaginations of all present were excited by this glimpse of activities at the forefront of electronic science.

H. C. Mandell, Jr., *Secretary*

Personals

William D. Robertson has been appointed chairman of the Dept. of Metallurgy at Yale University, succeeding Professor Arthur Phillips who will be on leave of absence preceding his retirement in June 1959.

Douglas S. Keir, formerly of Spokane, Wash., recently accepted a position as research engineer at the Aluminum Technical Center, Olin Mathieson Chemical Corp., New Haven, Conn.

1957 Bound Volume Available

A limited number of the bound volume of 1957 JOURNALS (Vol. 104) are available from Society Headquarters, 1860 Broadway, New York 23, N. Y., at $18.00 per copy to nonmembers, including subscribers, and $12.00 per copy to ECS members, subject to prior acceptance.

Lepel
HIGH FREQUENCY
INDUCTION
HEATING
UNITS
BOMBARDING
SOLDERING
MELTING
HARDENING
ANNEALING
The Lepel line of induction heating equipment represents the most advanced thought in the field of electronics as well as the most practical and efficient source of heat yet developed for industrial heating.
If you are interested in induction heating you are invited to send samples of the work with specifications. Our engineers will process and return the completed job with full data and recommendations without any cost or obligations.

TYPICAL INDUCTION HEATING APPLICATIONS IN THE MANUFACTURE OF TRANSISTORS

SOLDERING TRANSISTOR ASSEMBLIES BY INDUCTION HEATING

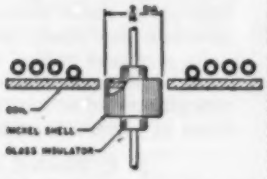

Concentrator-type coil creates high intensity, restricted heating at joint of nickel shell and tinned glass, thus causing solder to flow for permanent seal.

SINGLE CRYSTAL PULLER

General arrangement for pulling single crystals. Induction heating coil is shown surrounding quartz tube containing crucible with molten germanium in suitable atmosphere.

MULTIPLE ZONE REFINING

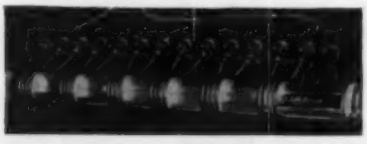

Induction heating apparatus used in zone refining. The six coils shown provide simultaneous molten zones in the ingot as it passes through the tube containing the protective atmosphere.

Electronic Tube Generators from 1 kw to 100 kw.
Spark Gap Converters from 2 kw to 30 kw.
WRITE FOR THE NEW LEPEL CATALOG . . . 36 illustrated pages packed with valuable information.

All Lepel equipment is certified to comply with the requirements of the Federal Communications Commission.
LEPEL HIGH FREQUENCY LABORATORIES, INC.
55th STREET and 37th AVENUE WOODSIDE 77 NEW YORK CITY N Y

P. S. Rajasekhar, who had been with the Textilana Corp. in Hawthorne, Calif., has joined Hughes Products in Los Angeles.

Peter A. Loughlin, formerly with Raytheon Manufacturing Co., Quincy, Mass., is now with the Canadian Westinghouse Works, Cathode Ray Tube Dept., Hamilton, Ont., Canada.

T. G. Edgeworth, of the Aluminum Co. of Canada, has transferred from Shawinigan Falls, Que., to the company's General Technical Dept., Smelter-Chemical Div., in Montreal.

Irwin Goldman has been named associate director of research, Chemistry and Metallurgy, by Sylvania Research Labs., a division of Sylvania Electric Products Inc., Bayside, N. Y. In his new assignment, Mr. Goldman will be responsible for the direction of the division's Chemistry Lab. and Metallurgy Lab. He had been manager of technical planning.

Donato J. Bracco, formerly manager of the Chemistry Lab. of Sylvania Research Labs., a division of Sylvania Electric Products Inc., Bayside, N. Y., has been appointed manager of planning with responsibility for the planning of the division's research program, economic analyses, market surveys, and similar programs.

John A. Upper

John Alden Upper, resident manager of the Chippawa plant of the Electro-Chemical Div. of the Norton Co., Niagara Falls, Canada, died suddenly on May 27, 1958. He was 47 years old.

Mr. Upper was a graduate in electrical engineering of the University of Toronto. On graduation in 1934, he began work in the research department of the Norton Co. at Chippawa. He acquired wide experience and eventually was appointed development engineer in charge of the research plant.

He contributed heavily to the design of the Norton Co. plants for casting various types of Alundum® and held a number of patents on developments made in connection with this work.

In 1946-1947, he was engineer in charge of the construction of the present Chippawa research laboratory which was completed late in 1947. About that time, he was appointed research engineer and section head. Mr. Upper contributed many technical publications on the subject of arc furnace practice in the manufacture of abrasives and refractories. Two of his papers ap-

peared in the JOURNAL of The Electrochemical Society.

In May 1956, Mr. Upper transferred from the research to the production department. Later in the same year, he was appointed resident manager and a member of the operating board of the Electro-Chemical Div. of the Norton Co.

Mr. Upper was also active in professional and community affairs. In addition to The Electrochemical Society, he was a member of the Association of Professional Engineers and The Chemical Institute of Canada.

He is survived by his wife, Madge; two daughters, Joy and Marnie; and one son, Randall.

Letters to the Editor

Dear Sir:

After reading a review of the book "Organic Electrode Processes" in the July issue of the JOURNAL, I could not help but feel that the reviewer had scanned rather than thoroughly read this monograph. His opening statement is presumptuous in that he, a nonelectro-organic chemist, assumes the information contained in the book to be of no interest to members of the Electro-Organic Division when he himself shows little knowledge of the subject. He is correct, however, in mentioning the fact that this book is aimed at the synthetic organic chemist. In the author's preface, which the reviewer may or may not have read, is the statement to the effect that this book was written with the object of imparting information which would enable the organic chemist, who may be a novice in the field of synthetic electrochemical techniques, to obtain a complete picture of these techniques and the results he might anticipate in performing such reactions on the various types of organic compounds. Furthermore, it was also noted in this preface that there are many subjects, especially those involving the theoretical aspects, which could have been presented in a more elaborate form, but the author felt this complexity might discourage those desirous of exploring this technique.

In the second paragraph of the review, the reviewer claims he is unable to distinguish between chemical reversibility and thermodynamic reversibility. It is indeed unfortunate that this difference escapes the reviewer. Furthermore, the reviewer claims the author to be in the gaslight era of bubble overpotential and "decomposition potential." If this be the case, the author has excellent company, for example, E. C. Potter whose volume on Electrochemistry was published in 1956. I should like to bring to the attention of the reviewer that the use of the word depolarizer to describe the reactant is common in this field. An excellent justification for this can be found in the section on Polarization.

In the third paragraph of the review, lines 1 to 5, the reviewer gives a misleading impression by lifting a few scattered words out of context. Further along in this paragraph, the reviewer mentions that the author's recommended power supply instrumentation is far too complex. Since when is a battery or a variable voltage rectifier unit which can be purchased in kit form and used in conjunction with a voltmeter and ammeter too complex and expensive? The reviewer accuses the author of recommending an elaborate device, consisting of a 440-volt, 60-cycle, 3-phase, 5-hp induction motor to drive the d-c generator, as part of the apparatus. This was incorporated in the book by way of illustrating an instrument designed essentially for semiproduction scale electrochemical preparations in which controlled potential and/or high currents and voltages are desired. Although the reviewer seems concerned about the coding of a particular British circuit, the American reader, if interested, could go to the original article. Had the reviewer studied the manuscript carefully, he would have realized that this book was initially published in England and, as a result, there may be a few items described primarily for the Continental investigators.

In the fifth paragraph, the reviewer attributes a statement to the author which cannot be found in the text. From the reviewer's closing comments, it is obvious that he is unaware of the prime purpose of this book, "to give organic chemists the fundamental information necessary to start investigatory work," and as such it cannot be compared to another work of similar title but different purpose.

In closing, I am certain that the author appreciates the reviewer's correction of a typographical error; he refers to page 124 of the book in which the quaternary ammonium nitrogens have one more covalent bond than necessary. Future editions will take note of this with thanks.

M. J. Allen

Dear Sir:

I was happy enough with Dr. Allen's "Organic Electrode Processes" to write an introductory note to the book. Judge my surprise on reading Mr. H. W. Salzberg's review in the July number of the JOURNAL.

Mr. Salzberg is unknown to me in either organic or electro-organic chemistry, yet he is brave enough to speak for both: misusing the nomenclature of one and misquoting a book about the other. His comments will help to popularize what I believe to be an earnest contribution to an interesting field.

Christopher L. Wilson
Phillips-Foscue Corp.
High Point, N. C.

JOURNAL ELECTROCHEMICAL SOCIETY

Wanted to Buy.
Back sets, volumes, and issues of this JOURNAL and TRANSACTIONS.
Especially volumes 1, 3 and from volume 60 to date.
We pay good prices.
Buy also Technical and Scientific Periodicals.
E. O. ASHLEY, 27 E. 21 St., N. Y. 10, N. Y.

Advertiser's Index

E. I. du Pont de Nemours & Company, Inc. 144C
Enthone, Incorporated ..... Cover 4
Great Lakes Carbon Corporation ..... Cover 2
Lepel High Frequency Laboratories, Inc. 178C
E. H. Sargent & Company 142C

Employment Situation

Please address replies to box shown, c/o The Electrochemical Society, Inc., 1860 Broadway, New York 23, N. Y.

Position Wanted

Chemist-Electrochemist. Situation wanted—Age 36, B.S. degree. Experienced in plating and finishing processes, development-research, process design, production, and control. Extensive experience in metallizing and plating on plastics, printed circuitry, automatic plating, electroless plating, noble metals, cleaning. *Reply to Box 364.*

The Electrochemical Society

Patron Members

Aluminum Company of Canada, Ltd., Montreal, Que., Canada
International Nickel Company, Inc., New York, N. Y.
Olin Mathieson Chemical Corporation, Niagara Falls, N. Y.
  Industrial Chemicals Division, Research and Development Department
Union Carbide Corporation
  Divisions:
    Electro Metallurgical Company, New York, N. Y.
    National Carbon Company, New York, N. Y.
Westinghouse Electric Corporation, Pittsburgh, Pa.

Sustaining Members

Air Reduction Company, Inc., New York, N. Y.
Ajax Electro Metallurgical Corporation, Philadelphia, Pa.
Allied Chemical & Dye Corporation
  General Chemical Division, Morristown, N. J.
  Solvay Process Division, Syracuse, N. Y. (3 memberships)
Alloy Steel Products Company, Inc., Linden, N. J.
Aluminum Company of America, New Kensington, Pa.
American Machine & Foundry Company, Raleigh, N. C.
American Metal Company, Ltd., New York, N. Y.
American Platinum Works, Newark, N. J. (2 memberships)
American Potash & Chemical Corporation, Los Angeles, Calif. (2 memberships)
American Zinc Company of Illinois, East St. Louis, Ill.
American Zinc, Lead & Smelting Company, St. Louis, Mo.
American Zinc Oxide Company, Columbus, Ohio
M. Ames Chemical Works, Inc., Glens Falls, N. Y.
Auto City Plating Company Foundation, Detroit, Mich.
Bart Manufacturing Company, Bellville, N. J.
Bell Telephone Laboratories, Inc., New York, N. Y. (2 memberships)
Bethlehem Steel Company, Bethlehem, Pa. (2 memberships)
Boeing Airplane Company, Seattle, Wash.
Burgess Battery Company, Freeport, Ill. (4 memberships)
C & D Batteries, Inc., Conshohocken, Pa.
Canadian Industries Ltd., Montreal, Que., Canada
Carborundum Company, Niagara Falls, N. Y.
Catalyst Research Corporation, Baltimore, Md.
Chrysler Corporation, Detroit, Mich.
Ciba Pharmaceutical Products, Inc., Summit, N. J.
Columbian Carbon Company, New York, N. Y.
Columbia-Southern Chemical Corporation, Pittsburgh, Pa.
Consolidated Mining & Smelting Company of Canada, Ltd., Trail, B. C., Canada (2 memberships)
Continental Can Company, Inc., Chicago, Ill.
Cooper Metallurgical Associates, Cleveland, Ohio
Corning Glass Works, Corning, N. Y.
Crane Company, Chicago, Ill.
Diamond Alkali Company, Painesville, Ohio (2 memberships)
Dow Chemical Company, Midland, Mich.
Wilbur B. Driver Company, Newark, N. J. (2 memberships)
E. I. du Pont de Nemours & Company, Inc., Wilmington, Del.
Eagle-Picher Company, Chemical Division, Joplin, Mo.
Eastman Kodak Company, Rochester, N. Y.
Eaton Manufacturing Company, Stamping Division, Cleveland, Ohio
Electric Auto-Lite Company, Toledo, Ohio
Electric Storage Battery Company, Philadelphia, Pa.
The Eppley Laboratory, Inc., Newport, R. I. (2 memberships)
Federal Telecommunication Laboratories, Nutley, N. J.
Food Machinery & Chemical Corporation
  Becco Chemical Division, Buffalo, N. Y.
  Westvaco Chlor-Alkali Division, South Charleston, W. Va.
Ford Motor Company, Dearborn, Mich.
General Electric Company, Schenectady, N. Y.
  Chemistry & Chemical Engineering Component, General Engineering Laboratory
  Chemistry Research Department

(Sustaining Members cont'd)

General Electric Company (cont'd)
Metallurgy & Ceramics Research Department
General Motors Corporation
Brown-Lipe-Chapin Division, Syracuse, N. Y. (2 memberships)
Guide Lamp Division, Anderson, Ind.
Research Laboratories Division, Detroit, Mich.
Gillette Safety Razor Company, Boston, Mass.
Gould-National Batteries, Inc., Depew, N. Y.
Graham, Savage & Associates, Inc., Jenkintown, Pa.
Great Lakes Carbon Corporation, New York, N. Y.
Hanson-Van Winkle-Munning Company, Matawan, N. J. (3 memberships)
Harshaw Chemical Company, Cleveland, Ohio (2 memberships)
Hercules Powder Company, Wilmington, Del.
Hooker Electrochemical Company, Niagara Falls, N. Y. (3 memberships)
Houdaille-Hershey Corporation, Detroit, Mich.
Hughes Aircraft Company, Culver City, Calif.
International Business Machines Corporation, Poughkeepsie, N. Y.
International Minerals & Chemical Corporation, Chicago, Ill.
Jones & Laughlin Steel Corporation, Pittsburgh, Pa.
K. W. Battery Company, Skokie, Ill.
Kaiser Aluminum & Chemical Corporation
Chemical Research Department, Permanente, Calif.
Division of Metallurgical Research, Spokane, Wash.
Keokuk Electro-Metals Company, Keokuk, Iowa
Libbey-Owens-Ford Glass Company, Toledo, Ohio
P. R. Mallory & Company, Indianapolis, Ind.
McGean Chemical Company, Cleveland, Ohio
Merck & Company, Inc., Rahway, N. J.
Metal & Thermit Corporation, Detroit, Mich.
Minnesota Mining & Manufacturing Company, St. Paul, Minn.
Monsanto Chemical Company, St. Louis, Mo.
Motorola, Inc., Chicago, Ill.
National Cash Register Company, Dayton, Ohio
National Lead Company, New York, N. Y.
National Research Corporation, Cambridge, Mass.
Norton Company, Worcester, Mass.
Olin Mathieson Chemical Corporation, Niagara Falls, N. Y.
High Energy Fuels Organization (2 memberships)
Pennsalt Chemicals Corporation, Philadelphia, Pa.
Philips Laboratories, Inc., Irvington-on-Hudson, N. Y.
Pittsburgh Metallurgical Company, Inc., Niagara Falls, N. Y.
Poor & Company, Promat Division, Waukegan, Ill.
Potash Company of America, Carlsbad, N. Mex.
Radio Corporation of America, Harrison, N. J.
Ray-O-Vac Company, Madison, Wis.
Raytheon Manufacturing Company, Waltham, Mass.
Reynolds Metals Company, Richmond, Va. (2 memberships)
Schering Foundation, Inc., Bloomfield, N. J.
Shawinigan Chemicals Ltd., Montreal, Que., Canada
Speer Carbon Company
International Graphite & Electrode Division, St. Marys, Pa. (2 memberships)
Sprague Electric Company, North Adams, Mass.
Stackpole Carbon Company, St. Marys, Pa. (2 memberships)
Stauffer Chemical Company, Henderson, Nev., and New York, N. Y. (2 memberships)
Sumner Chemical Company, Division of Miles Laboratories, Inc., Elkhart, Ind.
Superior Tube Company, Norristown, Pa.
Sylvania Electric Products Inc., Bayside, N. Y. (2 memberships)
Sarkes Tarzian, Inc., Bloomington, Ind.
Tennessee Products & Chemical Corporation, Nashville, Tenn.
Texas Instruments, Inc., Dallas, Texas
Titanium Metals Corporation of America, Henderson, Nev.
Udylite Corporation, Detroit, Mich. (4 memberships)
Upjohn Company, Kalamazoo, Mich.
Victor Chemical Works, Chicago, Ill.
Wagner Brothers, Inc., Detroit, Mich.
Weirton Steel Company, Weirton, W. Va.
Western Electric Company, Inc., Chicago, Ill.
Wyandotte Chemicals Corporation, Wyandotte, Mich.
Yardney Electric Corporation, New York, N. Y.

How to make metal cleaning an exact science: Enthone's broad range of cleaning and degreasing compounds are the end result of more than 20 years of applied research in the laboratory and in the field on metal finishing problems. These compounds include emulsifiable and solvent cleaners, alkaline cleaners for soak or electrolytic cleaning of iron, steel, copper, brass, zinc and zinc base die castings. And if there's no Enthone stock cleaner that meets your requirements, Enthone will develop a special one that does. Write us about it. Enthone, Inc., 442 Elm St., New Haven 11, Conn.

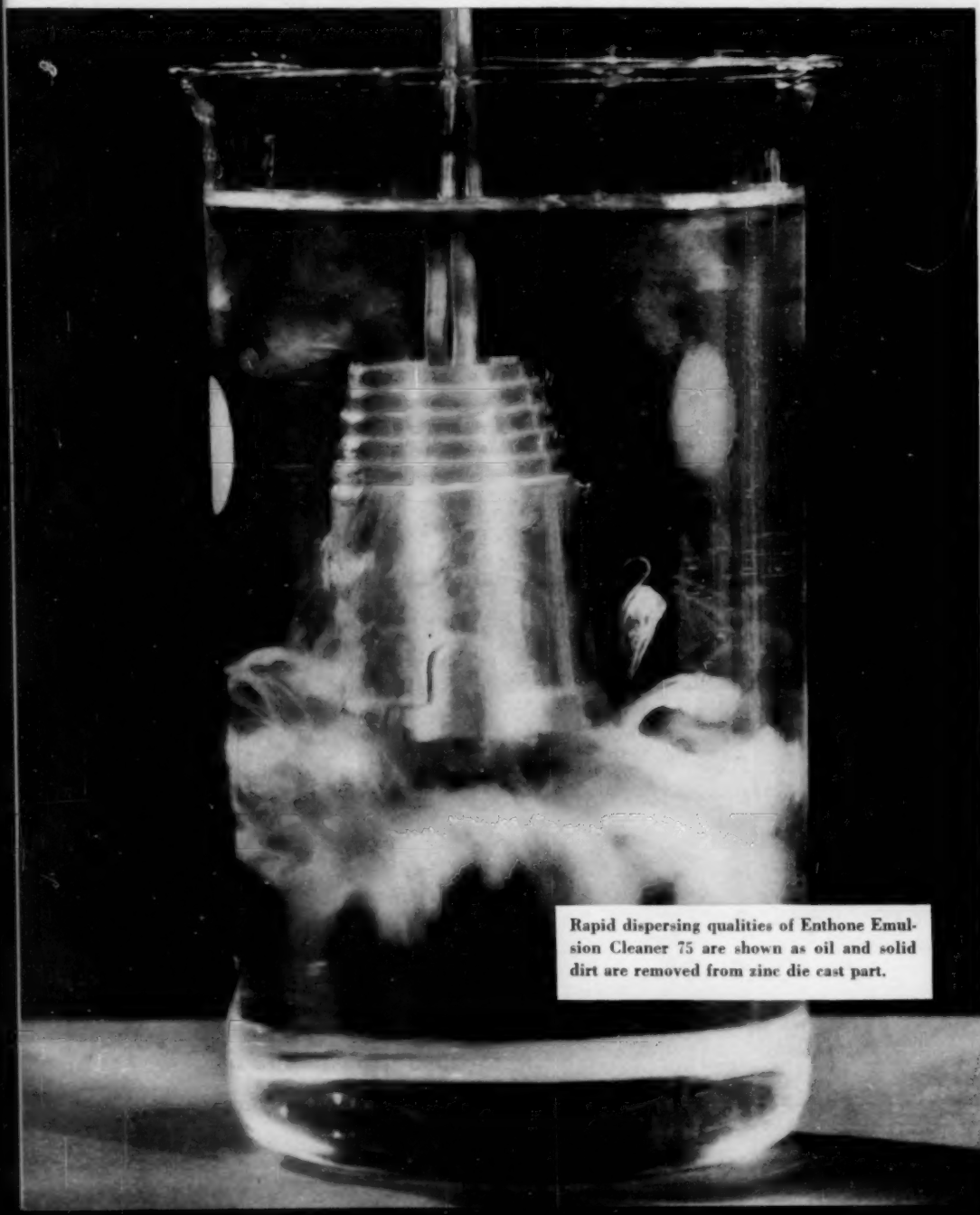

Rapid dispersing qualities of Enthone Emulsion Cleaner 75 are shown as oil and solid dirt are removed from zinc die cast part.

ENTHONE

ENTHONE, INC. IS A SUBSIDIARY OF AMERICAN SMELTING AND REFINING COMPANY